

Washington University in St. Louis
Washington University Open Scholarship

All Theses and Dissertations (ETDs)

10-8-2013

The Mechanism of the Gastric Epithelial Stem Cell Response to Metaplastic Injury

Shradha Sachin Khurana
Washington University in St. Louis

Follow this and additional works at: <https://openscholarship.wustl.edu/etd>

 Part of the [Cell and Developmental Biology Commons](#)

Recommended Citation

Khurana, Shradha Sachin, "The Mechanism of the Gastric Epithelial Stem Cell Response to Metaplastic Injury" (2013). *All Theses and Dissertations (ETDs)*. 1199.

<https://openscholarship.wustl.edu/etd/1199>

This Dissertation is brought to you for free and open access by Washington University Open Scholarship. It has been accepted for inclusion in All Theses and Dissertations (ETDs) by an authorized administrator of Washington University Open Scholarship. For more information, please contact digital@wumail.wustl.edu.

WASHINGTON UNIVERSITY IN ST. LOUIS

Division of Biology and Biomedical Sciences
Developmental, Regenerative, and Stem Cell Biology

Dissertation Examination Committee:

Jason C. Mills, Chair

Richard J. DiPaolo

Fanxin Long

Deborah V. Novack

Deborah C. Rubin

William F. Stenson

The Mechanism of the Gastric Epithelial Stem Cell Response to Metaplastic Injury

by

Shradha Sachin Khurana

A dissertation presented to the
Graduate School of Arts and Sciences
of Washington University in
partial fulfillment of the
requirements for the degree
of Doctor of Philosophy

December 2013

St. Louis, Missouri

© Copyright 2013 by Shradha Sachin Khurana.

All rights reserved.

TABLE OF CONTENTS

LIST OF FIGURES	vi
LIST OF ABBREVIATIONS	ix
ACKNOWLEDGEMENTS	x
DEDICATION	xiv
ABSTRACT OF THE DISSERTATION	xv
CHAPTER 1: Introduction to biology and pathophysiology of the gastric epithelial stem cell and models to study its activation and homeostasis	1
I. The Stomach	2
a. Development	2
b. Structure and Organization	
II. The Gastric Epithelial Stem Cell	6
a. Salient Features of the Stem Cell	9
b. Response of the Stem Cell to Different kinds of Gastric Injuries	10
1. Spasmolytic Polypeptide Expressing Metaplasia	11
ii. Genetic Ablation of Parietal Cells	12
iii. Treatment with DMP-777	12
iv. Treatment with Tamoxifen	12
2. Intestinal Metaplasia	14
III. Conclusions	16
IV. References	18
CHAPTER 2: Tamoxifen induces rapid, reversible atrophy, and metaplasia in mouse stomach	22
I. Abstract	23
II. Introduction	24
III. Materials and Methods	24
IV. Results and Discussion	29
V. Acknowledgements	40
VI. References	41

CHAPTER 3: The hyaluronic acid receptor CD44 coordinates normal and metaplastic gastric epithelial progenitor cell proliferation	43
I. Abstract	45
II. Introduction	46
III. Materials and Methods	48
IV. Results	53
a. CD44 is expressed in isthmal cells and regulates normal baseline proliferation	53
b. Infection with <i>Helicobacter pylori</i> causes parietal cell atrophy and expansion of CD44 into the base of gastric units	59
c. Tamoxifen induced parietal cell atrophy causes a burst of CD44 ⁺ progenitor cell proliferation	61
d. CD44 regulates gastric progenitor cell proliferation through STAT3	69
e. ERK signaling regulates progenitor cell proliferation through CD44	71
f. ERK signaling is increased in multiple models of gastric metaplasia and labels isthmal cells	74
V. Discussion	80
VI. Acknowledgements	85
VII. References	85
 CHAPTER 4: Metaplasia in the stomach is induced by cytokines produced by macrophages	 90
I. Abstract	91
II. Introduction	92
III. Materials and Methods	93
IV. Results	97
a. IL-6 is produced and secreted into the serum immediately after treatment with tamoxifen	97
b. Macrophages secrete IL-6 when treated with tamoxifen <i>ex vivo</i> and are necessary for developing metaplasia	98
c. Macrophages induce ERK activation and iNOS expression following treatment with tamoxifen	101
d. iNOS is expressed in damaged parietal cells of mice and humans	102
e. Nitric oxide signaling is necessary and sufficient for inducing parietal cell death and expansion of proliferation	105
V. Discussion	107
VI. References	109
 CHAPTER 5: Conclusions and future directions	 111
I. Conclusions	112
II. Future Directions	116

a.	Determining the role of the CD44 ligand, hyaluronan, in regulating CD44 expression and proliferation of isthmal cells	116
b.	Determining the factors secreted by activated macrophages that lead to parietal cell atrophy and proliferation expansion	120
c.	Determining the mechanism by which zymogenic cells undergo dedifferentiation following parietal cell atrophy	121
d.	Determining the role of CD44 in <i>Helicobacter pylori</i> niche establishment	126
III.	References	129

APPENDIX 1: The gastric mucosa: Development and Differentiation 131

I.	Abstract	132
II.	Introduction	133
III.	Early foregut development	133
IV.	Specification of the stomach as a separate organ: an overview	134
V.	Morphogenetic codes involved in stomach specification	135
a.	The Hedgehog signaling pathway: early events	136
i.	Left-right axis formation	
ii.	Anterior-posterior endodermal patterning in the gut	
iii.	Hedgehog in stomach development	
b.	The Wnt signaling pathway	138
c.	The FGF pathway	140
d.	The BMP/TGF signaling pathway	141
e.	The Retinoic Acid signaling pathway	142
f.	The Notch signaling system	143
VI.	Transcription Factors	143
a.	The <i>Hox</i> genes	144
b.	COUP-TFII	145
c.	SOX2	145
d.	BARX1	146
e.	BAPX1	146
f.	Forkhead-box (FOX) family	147
VII.	Postnatal gastric development	149
VIII.	Adult gastric homeostasis	150
IX.	Morphogenetic pathways in maintaining adult gastric homeostasis	154
a.	The Hedgehog pathway	154
b.	The BMP signaling system	155
X.	Conclusion	156
XI.	References	157

APPENDIX 2: Autoimmune gastritis mediated by CD4 ⁺ T cells promotes the development of gastric cancer	163
I. Abstract	164
II. Introduction	165
III. Materials and Methods	167
IV. Results	171
a. Inflammation in TxA23 mice is characterized by CD4 ⁺ T cells secreting IFN- γ and IL-17	171
b. TxA23 progress through a series of pathological changes associated with the development of gastric cancer	173
c. Increased epithelial cell proliferation, phosphorylated STAT3, IL-6, and expression of gastric cancer-associated biomarkers in TxA23 mice	175
d. SPEM is present in the gastric mucosa of TxA23 mice	179
e. TxA23 Mice Develop Gastric Intraepithelial Neoplasia (GIN)	181
V. Discussion	183
VI. References	185
CURRICULUM VITAE	188

LIST OF FIGURES

CHAPTER 1: Introduction to biology and pathophysiology of the gastric epithelial stem cell and models to study its activation and homeostasis

- Figure 1.1: Typical anatomy and histology of a mammalian stomach
- Figure 1.2: Origins of principal corpus epithelial lineages
- Figure 1.3: Current model for the origin and progression of gastric metaplasias
- Figure 1.4: Cellular mechanisms of SPEM

CHAPTER 2: Tamoxifen induces rapid, reversible atrophy, and metaplasia in mouse stomach

- Figure 2.1: Tamoxifen causes rapid, reversible gastric metaplasia in mice, which is highlighted by parietal cell death, concomitant increase in proliferation and loss of differentiated cell markers
- Figure 2.2: Other organs are not affected by tamoxifen as severely as the stomach
- Figure 2.3: Tamoxifen induced SPEM is dose dependent
- Figure 2.4: Tamoxifen results in SPEM by causing death of parietal cells
- Figure 2.5: SPEM induction by tamoxifen is not estrogen receptor (ER) or sex dependent
- Figure 2.6: SPEM induction by tamoxifen is ameliorated by omeprazole treatment

CHAPTER 3: The hyaluronic acid receptor CD44 coordinates normal and metaplastic gastric epithelial progenitor cell proliferation

- Figure 3.1: The CD44⁺ cells expanding from the isthmus upon tamoxifen induced parietal cell atrophy were epithelial
- Figure 3.2: CD44 labels undifferentiated cells in the normal stem cell zone, i.e. the isthmus, of the gastric unit, and its loss stunts basal rates of proliferation
- Figure 3.3: Loss of functional CD44 caused abbreviated pit/foveolar regions
- Figure 3.4: Helicobacter pylori infection causes parietal cell atrophy and expansion of CD44 expression
- Figure 3.5: CD44 expands and labels proliferating cells upon parietal cell atrophy and is required for this injury induced expansion of progenitor cells
- Figure 3.6: CD44⁺ epithelial cells expand 5-7 fold upon parietal cell atrophy as quantified by FACS
- Figure 3.7: Hyaluronic acid (HA), a ligand of CD44, was increased upon atrophic injury with tamoxifen
- Figure 3.8: *Cd44*^{-/-} mice have compensatory mechanisms for increasing proliferation following tamoxifen induced atrophy
- Figure 3.9: CD44 is necessary for elevating the rate of progenitor cell proliferation upon induction of atrophy
- Figure 3.10: CD44 regulates gastric progenitor cell proliferation through STAT3
- Figure 3.11: ERK signaling is activated early upon induction of injury and is required to induce CD44

- Figure 3.12: pERK labels metaplasia-associated cells in mice and humans
Figure 3.13: CD44 and pERK label the same population of cells as they start expanding from the isthmus during tamoxifen induced metaplasia
Figure 3.14: ERK signaling is activated after parietal cell atrophy in both, humans and mice
Figure 3.15: Model for stem/progenitor cell renewal during normal and atrophic injury conditions

CHAPTER 4: Cytokine signaling from macrophages provides the upstream signal for inducing gastric metaplasia

- Figure 4.1: Tamoxifen increases IL-6 secretion by macrophages
Figure 4.2: Depletion of macrophages by treatment with clodronate rescues SPEM development induced by tamoxifen
Figure 4.3: Clodronate blocks ERK activation and iNOS expression in tamoxifen induced SPEM
Figure 4.4: iNOS labels parietal cells in tamoxifen treated mice
Figure 4.5: iNOS is expressed in pre-parietal cells of tox176 mice and in PCs of humans with gastric metaplasia
Figure 4.6: Effect of nitric oxide donors on epithelial proliferation
Figure 4.7: Blocking iNOS activity and scavenging nitric oxide inhibits the expansion of proliferation during metaplasia
Figure 4.8: *iNOS*^{-/-} mice treated with tamoxifen display a threshold phenomenon whereby they either lose all their parietal cells or none.

CHAPTER 5: Conclusions and future directions

- Figure 5.1: Hyaluronic acid (HA), a ligand of CD44, was increased upon atrophic injury with tamoxifen
Figure 5.2: Hyaluronic acid (HA) is increased in human patients with gastritis and intestinal metaplasia
Figure 5.3: HA is sufficient to induce expansion of stem cell proliferation
Figure 5.4: HA is necessary for normal and injury induced expansion of proliferation
Figure 5.5: Tamoxifen induces spasmodic polypeptide-expressing metaplasia (SPEM)
Figure 5.6: YAP1 is activated upon treatment with tamoxifen

APPENDIX 1: The gastric mucosa: Development and Differentiation

- Figure A1.1: Epithelial-mesenchymal interactions during early foregut/stomach development in the embryo
Figure A1.2: Normal architecture and organization of different cell types in the gastric unit of the adult mouse

Figure A1.3: Interplay between developmental signaling pathways coordinating differentiation and maintenance of different cell lineages within the gastric unit

APPENDIX 2: Autoimmune gastritis mediated by CD4⁺ T cells promotes the development of gastric cancer

Figure A2.1: Inflammation in TxA23 mice

Figure A2.2: Preneoplastic lesions in TxA23 mice

Figure A2.3: Increased epithelial cell proliferation in the gastric mucosa of TxA23 mice

Figure A2.4: Increased levels of cancer associated markers in TxA23 mice

Figure A2.5: TxA23 mice have distinct regions of parietal cell loss coupled with the emergence SPEM

Figure A2.6: TxA23 mice develop masses with dysplastic foci as they age

LIST OF ABBREVIATIONS

WT – wildtype
KO – knockout
GIF – gastric intrinsic factor
GSII – lectin from *Griffonia simplicifolia*
SC – stem cell
PC – parietal cell
ZC – zymogenic cell
NC – neck cell
ERK – extracellular signal-regulated kinase
STAT - signal transducer and activator of transcription
IL – interleukin
FGF – fibroblast growth factor
EGF – epidermal growth factor
Tam – tamoxifen
Hh – hedgehog
PBS – phosphate buffered saline
PCR – polymerase chain reaction
IP – intraperitoneal
qPCR – quantitative PCR
TGF – transforming growth factor
iNOS – inducible nitric oxide synthase
HA – hyaluronic acid
HAS – hyaluronan synthase
TLR – toll-like receptor
BMP – bone morphogenetic protein
ER – estrogen receptor
SERM – selective estrogen receptor modulator
BrdU – bromo deoxyuridine
AAA – lectin from *Anguilla anguilla* agglutinin
Cre – cre recombinase
SPEM – spasmodic polypeptide expressing metaplasia
IM – Intestinal metaplasia
GIN – gastric intraepithelial neoplasia
GC – gastric cancer
OLFM – olfactomedin

ACKNOWLEDGEMENTS

The Ph.D. journey is full of undiscovered turns, excitement and frequent disappointment. I could not have asked for a better mentor than Dr. Jason Mills to guide me through this journey. Jason is the kind of person who will go out of his way to make you feel welcome and comfortable. It is through his efforts that I have grown in the last five years from a shy, confused foreigner to a confident, creative and independently thinking individual. Jason has given me the freedom to pursue various projects without objection and been genuinely excited about my findings. I am sincerely thankful for having such a kind and motivating mentor as Jason and for providing me with an extended family – the Mills Lab. I appreciate all of our Rasoi lab lunches together and summer barbecue parties at Jason and Indira’s home. I would especially like to thank Won Jae Huh for training me when I first started out in lab and molding me to think like a scientist. I am grateful for all the constructive discussions with Greg Sibbel, even though most of them end with Greg saying, “Silly Shradha”. I’m thankful for Ben Moore’s infectious optimism for the numerous times that I’ve need a pick-me-up. I am grateful for Ben Capoccia’s leadership as a postdoc and for being a vital part of the lab’s Pink Floyd fan club. Ray Jin, thank you for teaching me to be meticulous about my experiments and answering all my petty questions. Jessie Geahlen, thank you for driving me around and taking me out for Indian food when I was new and lost in this country. I am thankful for Ed Oates’ vast sea of experience and knowledge. I have been blessed in having talented and efficient summer students whom I have had the opportunity to train and go shopping with! Lydia Espinoza and Min Jung, I hope you are successful in all your future endeavors.

I would like to thank my thesis committee members – Deb Rubin, Bill Stenson, Fanxin Long, Deb Novack, Rich DiPaulo - for their support, collaboration, ideas and excellent feedback. Dr. Stenson and Terry Riehl, thank you for the fruitful collaboration and critical input for completing our project. I appreciate my collaborative studies with Rich DiPaulo and Long Nguyen from the Saint Louis University as well as Rick Peek from Vanderbilt University, which have enabled me to broaden my areas of expertise. I would like to thank the Siteman Cancer Center for selecting me into the Cancer Biology Pathway, so I could learn more about clinical research in cancer biology and have first-hand experience in seeing the daily lives of oncologists. A special note of thanks to Theresa Waldhoff for accommodating my numerous scheduling requests and for being interested in my well-being even after completing the pathway. I would also like to thank Jim Skeath and Stacy Kiel for being a sounding board for us and for persuading me to present my work at times when I would be too shy to volunteer.

The Mills lab has excelled at producing beautiful images that have adorned multiple journal covers. I was fortunate to have learned the art of making pretty images while working here and this would have been impossible without the support of our very capable histology cores – the Developmental Biology core (Bill Coleman and Marlene Scott) and the DDRCC Morphology core (Kymberli Carter and Angela Hamer). I would also like to thank Linda Otero-Garcia in the Division of Gastroenterology for sorting out all my purchasing issues, initiating me into yoga and being the single largest admirer and patron of my handmade jewelry.

It is never easy to leave our motherland and travel thousands of miles away from home in pursuit of knowledge. I greatly appreciate the amazing friends I have made in St. Louis who have helped me stay afloat. Emel Esen and Kristi Stemler have been my pillars of support and I can never thank them enough for always being there. My Indian family at WashU. has

helped me stay connected to my roots and shared my passion for Bollywood films. I would especially like to thank Phani and Soumya Chavali, Adhira Sunkara, Karthik Omanakuttan, Ayesha Gonsalves, Kshamata Shah, Rahul Desai, Vivek Shah, Piyush Karande, Venkat R. and Geetanjali Chugh for maintaining my emotional equilibrium, the awesome potluck parties and the much needed gossip sessions.

I must also thank my inspirations back home in India who molded my scientific curiosity and made me believe in myself. Meghana Kanitkar and Kaustubh Gokhale, you taught me to never give up even when things seem impossible. Dr. Joshi, Dr. Acharya, Dr. Momin and Dr. Korad from Fergusson College, thank you for instilling in me an enthusiasm for biology. Dr. Partha Roy from IIT Roorkee, I will always be grateful to you for teaching us to think outside the box and making learning fun.

I owe my achievements to my family, for without their support, I would not have reached this milestone. I thank my parents for raising me right, for pushing me to the limit and being there to hold me when I fell. I wish my father were here today as this was his dream more than mine. I love and miss you, dad, and dedicate this thesis to you. I thank my brother, Karan, for toughening me up through all our childhood fights and squabbles and for loving me unconditionally. I would like to thank my grandmother, Chacha and Chachi for all the care and nurturing; and Maanvi, for letting me cling on to my childhood while I am with her. I love you all dearly and even though you are not with me physically, I know you will continue to support me through life's rain and shine. I am grateful for having inherited another loving family in Maa, Papa, Kakooa, Debangana di, Rahul da and Vyom, who have accepted me wholeheartedly and are genuinely proud of my accomplishments. I would also like to thank my closest friends, Prachi, Pooja, Anand and Pravesh for growing up with me and sharing some of my most

wonderful experiences. You understand my troubles even when I don't say a word and travel across the country to be with me. You are my family and I am grateful for having you in my life.

I cannot find a way to thank my fiancé, Rohit, without a lump in my throat. You held my hand and motivated me when I was most vulnerable. Thank you for always being just a phone call away and patiently listening to all my complaining. You are my closest friend, my fellow Mark Knopfler and Pink Floyd fan and the love of my life. There is no better way to show you how much you mean to me than by sharing the lyrics of our favorite Mark Knopfler song:

I can't do the talk like they talk on the TV

And I can't do a love song like the way it's meant to be

I can't do everything but I'd do anything for you

I can't do anything except be in love with you".

DEDICATION

I would like to dedicate this thesis to my wonderful family. Dad and Mom, thank you for always pushing me to the limit and supporting me every time I felt overwhelmed. I would not have been able to reach this milestone had it not been for your constant motivation and teaching me the importance of focus and perseverance. I owe my education and thirst for knowledge to you. Dad, I know this thesis means the world to you and this accomplishment is as much yours as it is mine. Karan, thank you for all your love and support through the years. You have always been there for me during times of happiness and sorrow. I am blessed to have an encouraging and loving family and I dedicate this thesis to them.

ABSTRACT OF THE DISSERTATION

The Mechanism of the Gastric Epithelial Stem Cell Response to Metaplastic Injury

by

Shradha Sachin Khurana

Doctor of Philosophy in Developmental, Regenerative and Stem Cell Biology

Washington University in St. Louis, 2013

Professor Jason C. Mills, Chair

Almost nothing is known about the identity of the epithelial stem cell of the gastric corpus, either during normal turnover or in response to injury. Our lab has shown that injection of the selective estrogen receptor modulator tamoxifen leads to near complete atrophy of parietal cells by 3 days and induces expansion of an undifferentiated cell population within the normal stem cell niche in the isthmus of the gastric unit. Here we show that CD44 labels the membranes of such undifferentiated isthmal cells, both in the normal gastric epithelium and when those cells expand fourfold upon injury with tamoxifen. Loss of CD44, either in knockout mice or by blocking its interaction with its ligand, leads to reduced proliferation. We found CD44 regulates proliferation by binding to active STAT3 and occupying the *CyclinD1* promoter; accordingly, blocking STAT3 activity completely abrogates atrophy induced proliferation. We screened for signaling kinases potentially responsible for increased CD44 and/or proliferation and found only ERK MAPK was activated during early stages following injury (as few as 6 hours following tamoxifen injection). This burst of ERK activation is localized to non-differentiated cells of the

isthmus, and blocking ERK activation with the inhibitor U0126 blocked the expansion of CD44-positive cells.

To determine which cytokines induced ERK in progenitor cells, we assayed sera of mice treated with tamoxifen for 6h. Compared to control injected mice, tamoxifen treated mice have a significant increase in the STAT3-inducing cytokine IL-6 levels, correlating with increased F4/80⁺ macrophages in the gastric mesenchyme. Isolated peritoneal macrophages treated ex vivo with tamoxifen showed significantly increased IL-6 expression, and depletion of bone-marrow derived macrophages in vivo blocks tamoxifen induced metaplasia and increased progenitor cell proliferation. Depletion of macrophages also blocks activation of ERK and expression of the stress signal, iNOS, in parietal cells. Inhibition of iNOS and scavenging of nitric oxide blocks parietal cell atrophy and stem cell expansion. Taken together, our data suggest that CD44 marks a population of undifferentiated epithelial cells within the stem-cell niche of the gastric unit, which greatly expands on injury and is regulated by ERK-MAPK signaling. ERK, in turn, is potentially regulated by cytokines like IL-6 secreted by peritoneal and resident macrophages. Once induced, CD44 associates with pSTAT3 to increase Cyclin D1 expression and consequent stem/progenitor cell proliferation. In conclusion, this thesis identifies a marker and pathway for the presumptive stem cell of the gastric epithelium during response to atrophy and during normal homeostasis.

CHAPTER 1: Introduction

I. The Stomach

a. Development

The source of nutrients for an embryo is obviously different from that of a neonate. Until birth, the developing embryo procures its nourishment from the placenta and from substances in the swallowed amniotic fluid, which might also contain factors that aid in development. As the newborn develops, maturation and gland formation in the gastrointestinal tract continue, with the rate of growth peaking at around three weeks in rodents. The stomach grows at a more rapid rate just after birth as compared to the rest of the body. At birth, gastric acid secretion capacity is low, but it rapidly increases by about threefold during the first 3 days post-partum. The gastric epithelium undergoes continuous renewal throughout the life of the animal.

b. Structure and organization

The mouse stomach is divided into four regions from the proximal to distal end: forestomach, corpus, antrum, and pylorus. The forestomach is lined by squamous epithelium and is absent in humans. Mature, differentiated cells that aid in digestion of food are situated in the glandular, columnar epithelium of the corpus, which is found in all mammals. A schematic of the architecture of a typical mammalian stomach is shown in Fig.1. The corpus epithelium is comprised of gastric units which are tubular invaginations that extend into the lamina propria. Each gastric unit can be divided into four different regions depending upon the cell types occupying each region. The region closest to the gastric lumen is the pit where surface mucous pit cells reside. The next is the isthmus where gastric stem/progenitor cells reside, followed by the neck which is populated by mucous neck cells. The deepest region is the base which is mainly occupied by zymogenic or chief cells. Parietal cells (acid-secreting) and endocrine cells are dispersed in all four regions (Fig. 1). The antrum is the distal part of the stomach adjacent to

the duodenum and lacks parietal cells and differentiated zymogenic cells. Gastrin secreting G-cells are found in the antrum. Gastrin stimulates release of histamine and acid in the corpus. The pylorus is the distal muscular sphincter that connects the antrum to the duodenum and regulates flow of gastric chyme into the intestine.

In constantly renewing tissues such as the stomach and intestine, mechanisms must exist to balance stem cell division and cell lineage allocation, so that the correct number of cells of each lineage is constantly generated. This renewal occurs due to the proliferation and differentiation of the multipotent stem cells that are present in the isthmus region of the adult gastric unit. The stem cells give rise to precursors that move bi-directionally (toward the lumen and toward the base) in the unit, giving rise to three main lineages with 11 cell types, that is:

1. Pit (also known as surface-associated/foveolar) cell lineage: Pre-pit cell precursors, pre-pit cells, pit cells [marked by AAA lectin and TFF1]
2. Zymogenic Cell (ZC) lineage: Pre-neck cell precursors, pre-neck cells, neck cells [marked by GSII lectin and TFF2], pre-ZCs, and ZCs [marked by intrinsic factor (GIF), pepsinogen (PGC), Mist1]
3. Parietal Cell (PC) lineage: Pre-PC precursors, pre-PCs, and PCs [marked by H/K-ATPase and VEGF-B]

Secretory granule-free pre-pit cells within the isthmus give rise to mucous secreting pit cells when they enter the pit region by upward migration in the gastric unit. 87% of pit cells differentiate from pre-pit cells, while the remaining 13% come from their own mitoses [1]. The process of pit cell migration to the surface takes 3 days [1]. On the other hand, cells of the

zymogenic lineage migrate in the opposite direction from the isthmus, down towards the base of the unit.

Members of the zymogenic lineage differentiate during a downward migration from the isthmus. A granule-free pre-neck cell precursor produces pre-neck cells, which are transformed to neck cells as they migrate from the isthmus to the neck. Neck cells complete their journey through the neck region in 14 days [1]. Upon arrival at the upper portion of the base of gastric units, they become pre-zymogenic cells. Terminal differentiation to zymogenic cells occurs during a continued downward descent to the lower portion of the base of gastric units. Zymogenic cells die by necrosis or apoptosis. The sequence is completed in 190 days [1]. Conversion of undifferentiated granule-free cells to pre-parietal cells occurs in the isthmus and takes 1 day [1]. Differentiation of pre-parietal to parietal cells also takes place in the isthmus. Parietal cells subsequently undergo a bipolar migration to both the pit and base. Death ensues and cells are disposed of by extrusion or phagocytosis. The overall turnover time for parietal cells is 54 days [1].

In addition to these lineages, endocrine cells are also scattered throughout the gastric unit. Even though there is emerging literature on the mechanisms by which the different cell types are formed, many gaps remain. For example, even though the location of the stem cell within the isthmus region of the gastric corpus has been well established by ultrastructure and turnover analysis, its molecular identity has not been well characterized [2].

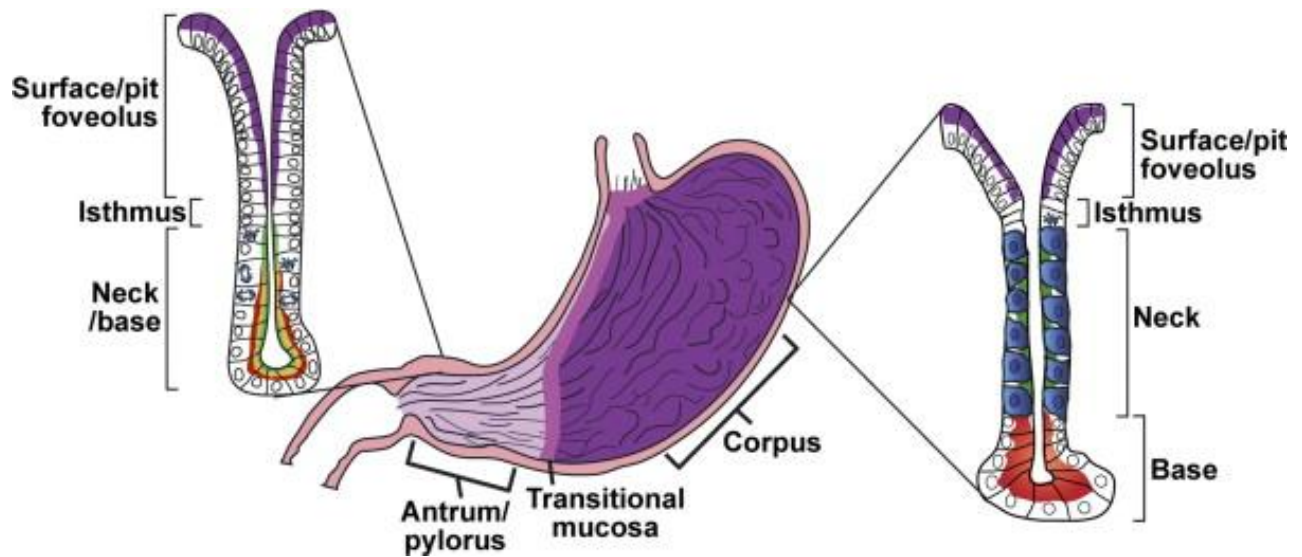


Figure 1.1: Typical anatomy and histology of a mammalian stomach. There are a number of variations in mammalian gastric anatomy. For example, mice have a forestomach with keratinized squamous epithelium, whereas humans have a pronounced cardiac region with simpler mucous glands that mark the transition region between the esophagus and corpus. However, the most prominent regions in most mammals are a proximal corpus, encompassing most of the stomach volume, and a distal antrum or pylorus. The corpus epithelium is organized into repeating gastric units that are invaginations from the surface and contain multiple cell lineages in 4 distinct zones. In the diagram, acid-secreting parietal cells are blue, digestive enzyme secreting zymogenic (chief) cells are red, mucous neck cells are green, and the mucus-secreting pit cells nearest the surface are purple. In the antrum, the gastric units are simpler, with few parietal or zymogenic cells. Antral units contain 2 distinct types of mucous cells: those lining the surface (purple) are similar to the surface cells of the corpus, and those nearer to the base have properties intermediate between zymogenic cells and mucous neck cells of the corpus (red-yellow). The interfaces between esophagus and corpus and between corpus and antrum are

not abrupt but marked by transitional mucosae. Endocrine cells (not depicted) are also present throughout the corpus and antrum epithelium. (Adapted from [3])

II. The Gastric Epithelial Stem Cell

It is believed that all gastric mucosal cells originate from stem cells that reside in the isthmus region of the gastric unit [4, [5], because ^{32}P -radiolabeled cycling cells appeared in this region. Studies by Leblond in the 1940s showed that one or a few cells in the isthmus constantly regenerate cells that migrate bi-directionally, up to the mucosal surface and down to the gland base, as they differentiate into mature cells of the gastric unit [6] (Fig. 1.2).

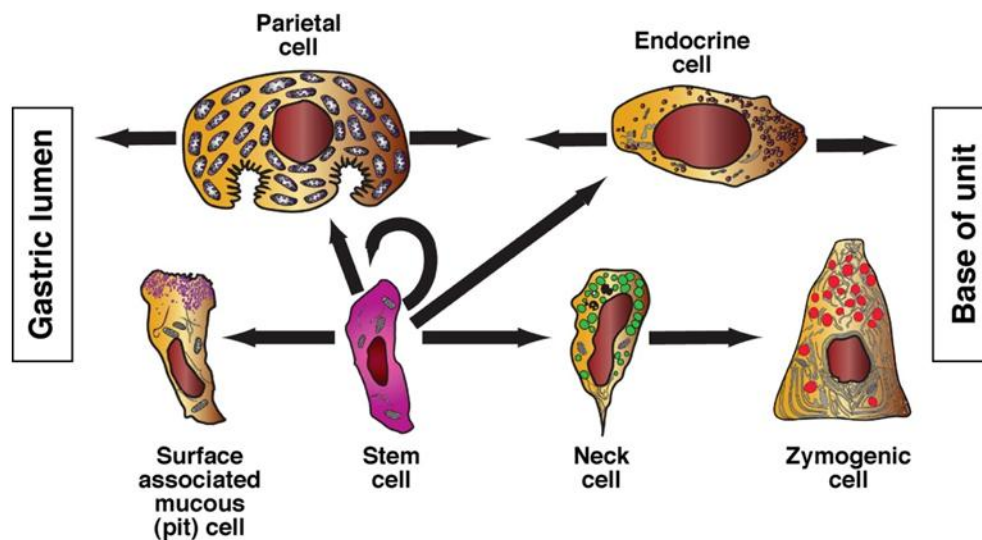


Figure 1.2: Origins of principal corpus epithelial lineages. The self-renewing stem cell gives rise to each of the principal epithelial lineages of the corpus. There is ultrastructural evidence for the transient intermediates for each lineage; however, available evidence indicates greater complexity in the zymogenic lineage, which arises from a long-lived (≥ 1 week in mice) intermediate, the mucous neck cell, with its own distinct ultrastructure and probable function. (Adapted from [3]).

In 1966, Robert Corpron identified small, undifferentiated cells, with high nucleus:cytoplasm ratio, open chromatin and lack of granules in the isthmus of the gastric units of rats [7], which repopulated the entire unit. Karam et al. were able to identify a similar subset of cells in the isthmi of human gastric units [8]. In 2002, Bjerknes and Cheng demonstrated that the entire gastric unit, corporal and antral, could arise from a single cell, i.e. the stem cell [5]. They utilized lineage tracing to identify clones that had lost LacZ expression in the mutagenized ROSA26 reporter mouse. They found clones that spanned entire gastric units and ones that were long lived (48 weeks), confirming that the mutagen hit the stem cell in these instances. Over time, many putative stem cell markers have emerged, but none has satisfied the gold standard requirements of tracing of all lineages and in vitro gland formation for the gastric corpus. The different putative stem cell markers are listed below (adapted from [9]):

Table 1: Putative stem cell markers of the gastrointestinal tract

Marker	Location	Lineage tracing	Life span	Response to pathogenic stimuli	Ref.
Villin promoter	Mainly antral; below isthmus, but mobile in gland base after IFN γ	Give rise to all cell types	>1 year	Increased proliferation and gland replacement after IFN γ	[10]
Lgr5	Mainly antral; gland base	Give rise to all cell types	>638 days	Can give rise to tumors after conditional Apc deletion	[11]
Mist1	Mature chief cells of corpus gland	Give rise to SPEM	As chief cells	Lost during metaplasia, dysplasia, and carcinoma	[12, [13]

Marker	Location	Lineage tracing	Life span	Response to pathogenic stimuli	Ref.
	base	lineage			
Tff2	Corpus, isthmus zone (mRNA)	Give rise to mucous neck cells, chief cells, parietal cells only	>200 days	Amplified by DMP-777	[14, [15]
BMDSC	Do not normally engraft in the absence of injury		>52 weeks	Widespread in epithelial engraftment after extensive chronic injury and Helicobacter infection	[16]
Prominin 1 (CD133)	Base of gastric glands	N/D	N/D	Highly expressed in gastric carcinomas	[17, [18, [19]
Dclk1 (DCAM KL1)	Corpus, one cell per gland (at isthmus)	N/D	N/D	Amplify in a Kras environment	[20, [21]
CD44	Corpus/antrum; gland base	N/D	N/D	Increased in tumors. Isolated cells give rise to tumors in xenograft model	[22, [23, [24]

N/D not done, IFN γ interferon gamma, BMDSC bone marrow derived stem cells.

In spite of identifying the location of the gastric epithelial stem cell within the unit, little is known about its niche or markers that label this population specifically.

a. Salient features of the stem cell

The gastric stem cell is different when compared to stem cells of other regions of the digestive tract. For one, the gastric stem cell is located much higher in the glandular unit than the intestinal stem cell, which is located in the base of the crypt [3]. Due to its location, it is more likely to come in contact with external stimuli and react to them. Second, its progeny undergo bidirectional migration to fuel the turnover of cells in the gastric unit [3]. Third, life-spans of different gastric epithelial lineages are very diverse, ranging from ~3 days for pit cells to several months for ZCs, compared to 3-5 days for enterocytes or 2 weeks for paneth cells in the intestine [3]. This forces the gastric stem cell to generate different numbers of precursors for each lineage in each differentiation cycle. Fourth, the steady-state gastric corpus does not rely on Wnt signaling for maintaining homeostasis, like the intestine [3]. However, the antrum or pylorus of the stomach might be considered a hybrid between the gastric corpus and intestine, since antral stem cells label with LGR5, the Wnt-responsive, intestinal stem cell marker, and depend on Wnt signaling for homeostasis [3]. Moreover, *Apc^{Min}* and *Apc^{I322T}* mice, which develop intestinal polyps due to inactivation of the Wnt-regulatory gene *Apc*, develop adenomas in the gastric antrum but not in the corpus [3]. Loss of *Apc* in *Lgr5⁺* cells rapidly results in formation of antral but not corpus adenomas [3]. These observations indicate that the antrum has Wnt-responsive stem cells that are distinct from those that mediate corpus mucosal self-renewal. Also, antral stem cells rarely generate PCs or ZCs [3]. Gastric corpus stem cells do not stain with markers of intestinal stem cells. While there has been significant advancement in identification of intestinal stem cell markers by virtue of lineage tracing, the promoters have failed to trace any of the gastric lineages. For example, *Lgr5* [25], *Bmi1* [26], *Prom1/CD133* [27, [28], *Sox9* [29] label stem cells in the intestine but fail to do so in the gastric corpus. *Lgr5* is expressed in antral stem

cells, but is conspicuous by its absence in the adult corpus [11]. Identification of a marker to trace corpus stem cells will enable us to understand signaling pathways that maintain stem cell homeostasis as well as those that respond to external stimuli and injuries.

b. Response of the gastric epithelial stem cell to injury:

Although gastric cancer is the second leading cause of cancer related deaths worldwide [30], little is known about its cause, pathophysiology and treatment strategies. According to the gastric carcinogenesis model proposed by Correa [31], cancer occurs by serial progression from superficial gastritis, atrophic gastritis, intestinal metaplasia, finally culminating into gastric cancer. Chronic infection of the stomach with the gram-negative bacterium *Helicobacter pylori* is a major risk factor for developing gastric cancer. Infection with *H. pylori* causes inflammation along with dramatic reorganization of the epithelium by directly or indirectly causing PC death, dedifferentiation of ZCs and activation of stem cells. Whether PC death is the causative agent for affecting the differentiation state of ZCs and stem cell proliferation remains to be determined.

Metaplasia is defined as a potentially reversible change from a fully differentiated cell type to another. Human gastric metaplasias are of two main types: Intestinal Metaplasia (IM) and Spasmolytic Polypeptide Expressing Metaplasia (SPEM). The presence of intestinal goblet cells in the gastric epithelium is the hallmark of IM, since goblet cells are not normally present in the stomach. Goblet cells in IM are positive for markers such as Muc2 and Trefoil Factor 3 (TFF3) [32]. Evidence shows that IM in the stomach has a high risk of developing into cancer and is, therefore, defined as a precancerous condition [33]. Epidemiological studies have linked *H. pylori* infection with IM [34] and hence, *H. pylori* has been implicated as a major cause of IM. A second, possibly preneoplastic metaplasia has been identified in the presence of parietal cell atrophy, which is known as SPEM (Spasmolytic Polypeptide Expressing Metaplasia). SPEM is

characterized by glands that resemble antral glands rather than those of the corpus, and express high amounts of Muc6 and TFF2 (Trefoil Factor 2 or Spasmolytic Polypeptide) [35]. SPEM is associated with 90% of all resected gastric cancers [36, [37, [38]. Therefore, both, IM and SPEM are precancerous gastric lesions and the signaling intermediates that cause the progression from metaplasia to cancer remain to be elucidated.

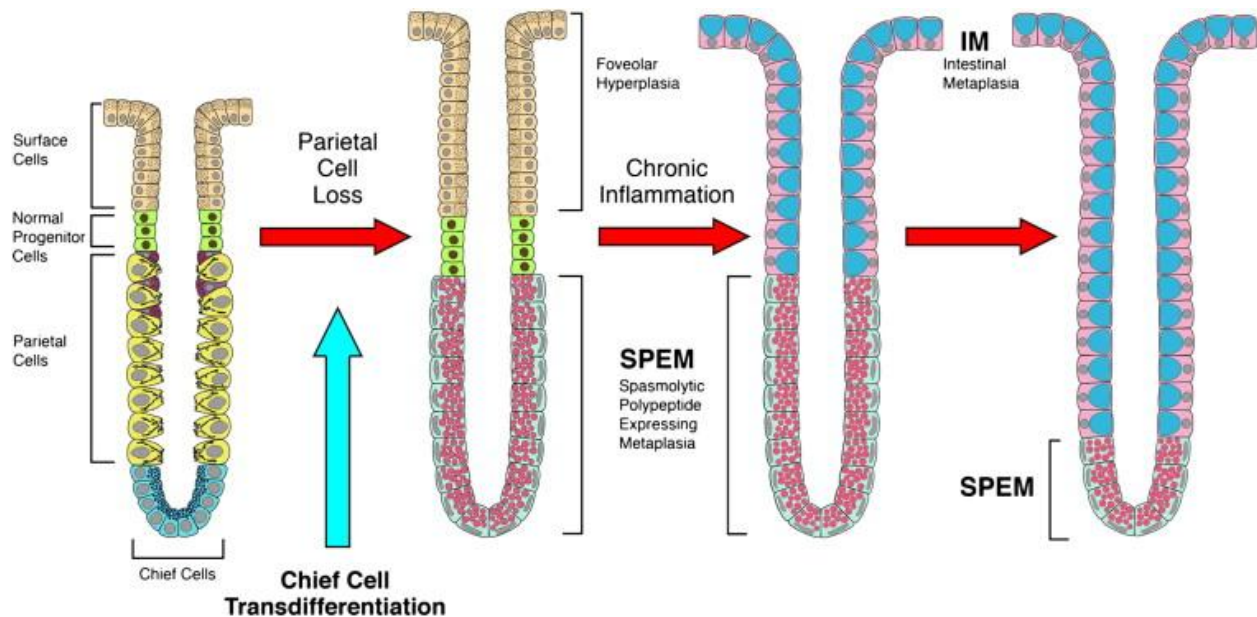


*Figure 1.3: Current model for the origin and progression of gastric metaplasias. Chief cell transdifferentiation into SPEM is triggered by loss of parietal cells in the corpus mucosa. In the presence of inflammation, such as during *H. pylori* infection, SPEM can expand into a proliferative metaplasia. With continued chronic inflammation, intestinal metaplasia (IM) evolves in the setting of pre-existing SPEM and can come to dominate the entirety of the glands. (Adapted from [39])*

1. Spasmolytic Polypeptide Expressing Metaplasia (SPEM):

While infection of human stomachs with *H. pylori* leads to the development of IM, those of mice fail to develop IM when infected with the mouse adapted strain, *H. felis*. Chronic infection of

mice with *H. plori* or *H. felis* leads to loss of parietal cells and inflammation throughout the mucosa [40, [41, [42]. Mice infected with *H. felis* develop SPEM after 6 months of infection [43] which eventually progresses to dysplasia, without ever developing IM. Since inflammation is a confounding factor in *Helicobacter* dependent development of SPEM, various other non-pathogenic models have been developed to assess the contribution of PC death alone in SPEM development.

- i. Genetic ablation of PCs: In 1996, Li et. al [44] generated a transgenic mouse line containing a fragment of the attenuated diphtheria toxin (DT-A *tox176*) driven off the H^+/K^+ -ATPase β -subunit promoter, which is specifically expressed in PCs. Expression of *tox176* led to ablation of PCs and development of metaplasia, characterized by a 4-5 fold increase in proliferation extending into the base of the gastric unit and dedifferentiated zymogenic cells in adult transgenic mice [44]. These mice also showed a twofold increase in pit cell number and a modest increase in pre-pit cells [44]. These data confirm the point of view of PCs being the differentiation signaling hub of the gastric unit.
- ii. DMP-777: In 2000, Goldenring et. al [45] identified that DMP-777, a cell-permeant inhibitor of neutrophil elastase that caused specific PC death when rats were gavaged with 200mg/kg /day of the drug for 3 months. PC atrophy was unaccompanied by inflammation. Mice treated with DMP-777 developed SPEM 10-14 days after administration, with PC atrophy around day 3, without developing dysplasia even a year after administration [45, [46]. This suggests that inflammation might be a key determinant of development of neoplasia.
- iii. Tamoxifen: In 2012, Huh et. al [47] identified a tamoxifen induced mechanism for

causing PC death and associated metaplasia. Tamoxifen is a selective estrogen-receptor modulator frequently used in humans for the treatment of breast cancer and in mice for spatiotemporally deleting genes using the Cre-ERT/loxP system [47]. Mice treated with a single injection of 5mg/20g body weight of tamoxifen undergo PC atrophy, expansion of proliferating progenitor cells and dedifferentiation of zymogenic cells within 3 days of treatment [47]. This method of SPEM induction is completely reversible within two weeks of tamoxifen administration [47]. The mechanism by which tamoxifen induces PC atrophy is uncertain, although, the proton pump inhibitor, omeprazole, partially rescues the effects of tamoxifen like DMP-777 [47]. Therefore, it is believed that the mode of action of tamoxifen is similar to DMP-777 [47].

Figure 1.4 demonstrates the epithelial changes characteristic of SPEM caused by the above mentioned methods.

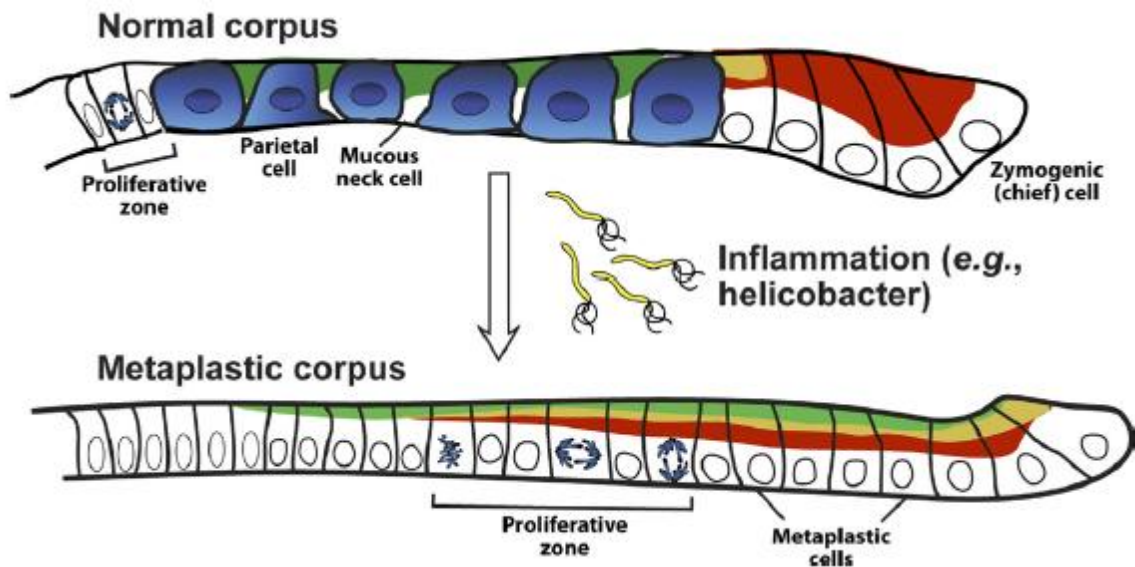


Figure 1.4: Cellular mechanisms of SPEM. Chronic inflammation of the corpus in mammals leads to characteristic changes in differentiation in the gastric unit. Parietal cells are lost

(atrophy), and the zymogenic chief cell lineage is reprogrammed so that genes that are normally expressed only in mucous neck cells, such as spasmodic polypeptide/TFF2 (shown in green), are expressed at high levels in cells at the base. Zymogenic cell markers (such as pepsinogen C; red) are co-expressed with neck cell markers. Proliferation is increased and occurs more basally in the unit. The pattern of basal proliferation and coexpression of neck and zymogenic cell genes is similar to the histologic pattern in the normal antrum and pylorus, which is why it is called pseudopyloric metaplasia. The most common metaplasia-inducing inflammation is caused by H pylori infection, although autoimmune gastritis (in which autoantibodies target parietal cells) can cause the same metaplasia pattern.

2. Intestinal Metaplasia

Intestinal metaplasia (IM) is considered a preneoplastic lesion of the stomach in which the normal gastric mucosa is replaced by mucosa which resembles the intestine. Morphologically, IM can be identified by the presence of goblet cells, which are normally absent in the stomach. Although IM is considered to be a risk factor for developing gastric cancer, it is unclear whether IM causes gastric cancer or is a marker for increased cancer risk [48]. Since infection with *H. pylori* is the greatest predisposing factor for developing gastric cancer, early investigations studied the association of infection with presence of IM. However, it was found that IM occurred at an equal frequency in patients with dysplasia and gastric cancer regardless of their *H. pylori* status [48]. Also, eradication of *H. pylori* did not benefit patients whose mucosa had already progressed to IM, suggesting that development of IM marks a point of no return in the progression to cancer [49].

The genetic events in IM are not well understood. According to published data, some genetic markers that change during progression to IM and cancer are listed below in Table 2.

Table 2: Expression of genes during normal turnover, IM and gastric cancer (Adapted from [48]).

Gene	Normal Mucosa	Intestinal Metaplasia	Gastric Cancer
CDX1	-	↑↑↑↑	↑↑
CDX2	-	↑↑↑↑↑	↑
TFF1	↑↑↑↑↑	↑↑↑	ND
TFF2	-	↑↑	ND
TFF3	ND	↑↑↑↑↑	ND
Villin	-	↑↑↑	ND
Sox2	↑↑↑	↑↑	-
Pdx1	↑	↑↑	↑↑↑
OCT-1	↑	↑↑↑	↑↑↑
RUNX3	↑↑	↑	-
Shh	↑↑↑	-	ND

↑ : relative degree of upregulation, ND: Not Defined, -: Absent

CDX, caudal type homeobox; OCT, octamer binding transcription factor; PDX, pancreatic and duodenal homeobox; RUNX3, runt related transcription factor; shh, sonic hedgehog; TFF, trefoil factor.

Since IM is the conversion of normal gastric mucosa to a more intestinal type, it is expected to find upregulation of intestinal genes during IM. Accordingly, the homeobox developmental genes, *Cdx1* and *Cdx2*, which confer intestinal identity, are upregulated in IM. Interestingly, their expression is decreased during the progression of IM to cancer [50]. Liu et. al. [50] suggest that a sufficiently high expression of *Cdx* genes converts gastric epithelium to a terminally differentiated intestinal epithelium. In order to further progress to gastric cancer, the level of *Cdx* must be decreased to cause sufficient dedifferentiation and proliferation. Another homeobox gene, *Sox2*, is expressed in the gastric mucosa but is almost absent in the intestinal epithelium during development. However, during IM development, *Sox2* levels decrease while *Cdx2* levels increase. While ectopic expression of *Cdx2* in gastric tissue leads to the appearance of goblet cells [51], ectopic expression of *Sox2* in prospective intestinal tissues leads to a more gastric phenotype [52].

The function of the gastric stem cell during development of IM is unknown. Since *Helicobacter* infected mice do not develop IM prior to dysplasia like humans do, they do not serve as ideal model organisms for studying IM progression. Other models such as *Cdx2* expressing transgenic mice or Mongolian gerbils infected with *Helicobacter* have been used to determine the mechanisms responsible for the conversion of the epithelium from gastric to intestinal [48] and the response of the stem cell.

Conclusions

Most gastric injuries, such as SPEM, IM and cancer, depend on the response of the stem cell to external stimuli. Therefore, it is imperative to understand mechanisms that lead to stem cell

homeostasis during normal turnover and those that lead to stem cell activation during injury. The above mentioned models of metaplasia help in determining signaling pathways that regulate stem cell proliferation. We have utilized a number of models of metaplasia to understand mechanisms that lead to parietal cell atrophy, stem cell activation and entry of cells into the cell cycle. In Chapter 2, we have described, in detail, the tamoxifen induced model of metaplasia and its advantages over other chronic models of metaplasia. In Chapter 3, we utilize tamoxifen induced atrophy in identifying CD44 as a marker of gastric epithelial stem cells, the role of CD44 in expansion of stem cell proliferation during metaplasia and the signaling pathways that regulate proliferation downstream of CD44. In Chapter 4, we explore the role of circulating factors and cytokines that are upstream modulators of parietal cell atrophy, which transduces the first signal to stem cells to start proliferating.

Therefore, in this thesis, we have:

- i. Established a new model for studying parietal cell atrophy and stem cell activation – Tamoxifen treatment of mice;
- ii. Determined the signaling cascade by which stem cell proliferation is regulated during normal turnover and tamoxifen induced atrophy;
- iii. Determined potential mechanisms by which parietal cells are damaged in different models of SPEM;
- iv. Identified potential circulating factors secreted by the innate immune system in regulating parietal cell atrophy and subsequent stem cell activation

References

1. Karam, S.M. and C.P. Leblond, *Dynamics of epithelial cells in the corpus of the mouse stomach. II. Outward migration of pit cells*. Anat Rec, 1993. **236**(2): p. 280-96.
2. Huh, W.J., et al., *Location, allocation, relocation: isolating adult tissue stem cells in three dimensions*. Curr Opin Biotechnol, 2006. **17**(5): p. 511-7.
3. Mills, J.C. and R.A. Shivdasani, *Gastric epithelial stem cells*. Gastroenterology, 2011. **140**(2): p. 412-24.
4. Thompson, M., et al., *Gastric endocrine cells share a clonal origin with other gut cell lineages*. Development, 1990. **110**(2): p. 477-81.
5. Bjerknes, M. and H. Cheng, *Multipotential stem cells in adult mouse gastric epithelium*. Am J Physiol Gastrointest Liver Physiol, 2002. **283**(3): p. G767-77.
6. Leblond, C.P., C.E. Stevens, and R. Bogoroch, *Histological Localization of Newly-formed Desoxyribonucleic Acid*. Science, 1948. **108**(2811): p. 531-3.
7. Corpron, R.E., *The ultrastructure of the gastric mucosa in normal and hypophysectomized rats*. Am J Anat, 1966. **118**(1): p. 53-90.
8. Karam, S.M., et al., *Defining epithelial cell progenitors in the human oxyntic mucosa*. Stem Cells, 2003. **21**(3): p. 322-36.
9. Qiao, X.T. and D.L. Gumucio, *Current molecular markers for gastric progenitor cells and gastric cancer stem cells*. J Gastroenterol, 2011. **46**(7): p. 855-65.
10. Qiao, X.T., et al., *Prospective identification of a multilineage progenitor in murine stomach epithelium*. Gastroenterology, 2007. **133**(6): p. 1989-98.
11. Barker, N., et al., *Lgr5(+ve) stem cells drive self-renewal in the stomach and build long-lived gastric units in vitro*. Cell Stem Cell, 2010. **6**(1): p. 25-36.
12. Nam, K.T., et al., *Mature chief cells are cryptic progenitors for metaplasia in the stomach*. Gastroenterology, 2010. **139**(6): p. 2028-2037 e9.
13. Ramsey, V.G., et al., *The maturation of mucus-secreting gastric epithelial progenitors into digestive-enzyme secreting zymogenic cells requires Mist1*. Development, 2007. **134**(1): p. 211-22.
14. Quante, M., et al., *TFF2 mRNA transcript expression marks a gland progenitor cell of the gastric oxyntic mucosa*. Gastroenterology, 2010. **139**(6): p. 2018-2027 e2.

15. Peterson, A.J., et al., *Helicobacter pylori* infection promotes methylation and silencing of trefoil factor 2, leading to gastric tumor development in mice and humans. *Gastroenterology*, 2010. **139**(6): p. 2005-17.
16. Houghton, J., et al., *Gastric cancer originating from bone marrow-derived cells*. *Science*, 2004. **306**(5701): p. 1568-71.
17. Zhao, P., Y. Li, and Y. Lu, *Aberrant expression of CD133 protein correlates with Ki-67 expression and is a prognostic marker in gastric adenocarcinoma*. *BMC Cancer*, 2010. **10**: p. 218.
18. Ishigami, S., et al., *Prognostic impact of CD133 expression in gastric carcinoma*. *Anticancer Res*, 2010. **30**(6): p. 2453-7.
19. Futagami, S., et al., *Celecoxib inhibits CD133-positive cell migration via reduction of CCR2 in Helicobacter pylori-infected Mongolian gerbils*. *Digestion*, 2010. **81**(3): p. 193-203.
20. Okumura, T., et al., *K-ras mutation targeted to gastric tissue progenitor cells results in chronic inflammation, an altered microenvironment, and progression to intraepithelial neoplasia*. *Cancer Res*, 2010. **70**(21): p. 8435-45.
21. Giannakis, M., et al., *Molecular properties of adult mouse gastric and intestinal epithelial progenitors in their niches*. *J Biol Chem*, 2006. **281**(16): p. 11292-300.
22. Takaishi, S., et al., *Identification of gastric cancer stem cells using the cell surface marker CD44*. *Stem Cells*, 2009. **27**(5): p. 1006-20.
23. Ghaffarzadehgan, K., et al., *Expression of cell adhesion molecule CD44 in gastric adenocarcinoma and its prognostic importance*. *World J Gastroenterol*, 2008. **14**(41): p. 6376-81.
24. da Cunha, C.B., et al., *De novo expression of CD44 variants in sporadic and hereditary gastric cancer*. *Lab Invest*, 2010. **90**(11): p. 1604-14.
25. Barker, N., et al., *Identification of stem cells in small intestine and colon by marker gene Lgr5*. *Nature*, 2007. **449**(7165): p. 1003-7.
26. Sangiorgi, E. and M.R. Capecchi, *Bmi1 is expressed in vivo in intestinal stem cells*. *Nat Genet*, 2008. **40**(7): p. 915-20.
27. Zhu, L., et al., *Prominin 1 marks intestinal stem cells that are susceptible to neoplastic transformation*. *Nature*, 2009. **457**(7229): p. 603-7.

28. Snippert, H.J., et al., *Prominin-1/CD133 marks stem cells and early progenitors in mouse small intestine*. *Gastroenterology*, 2009. **136**(7): p. 2187-2194 e1.
29. Furuyama, K., et al., *Continuous cell supply from a Sox9-expressing progenitor zone in adult liver, exocrine pancreas and intestine*. *Nat Genet*, 2011. **43**(1): p. 34-41.
30. Lozano, R., et al., *Global and regional mortality from 235 causes of death for 20 age groups in 1990 and 2010: a systematic analysis for the Global Burden of Disease Study 2010*. *Lancet*, 2012. **380**(9859): p. 2095-128.
31. Correa, P., *Human gastric carcinogenesis: a multistep and multifactorial process--First American Cancer Society Award Lecture on Cancer Epidemiology and Prevention*. *Cancer Res*, 1992. **52**(24): p. 6735-40.
32. Ectors, N. and M.F. Dixon, *The prognostic value of sulphomucin positive intestinal metaplasia in the development of gastric cancer*. *Histopathology*, 1986. **10**(12): p. 1271-7.
33. Walker, M.M., *Is intestinal metaplasia of the stomach reversible?* *Gut*, 2003. **52**(1): p. 1-4.
34. Sakaki, N., et al., *Ten-year prospective follow-up study on the relationship between Helicobacter pylori infection and progression of atrophic gastritis, particularly assessed by endoscopic findings*. *Aliment Pharmacol Ther*, 2002. **16 Suppl 2**: p. 198-203.
35. Goldenring, J.R., et al., *Spasmolytic polypeptide-expressing metaplasia and intestinal metaplasia: time for reevaluation of metaplasias and the origins of gastric cancer*. *Gastroenterology*, 2010. **138**(7): p. 2207-10, 2210 e1.
36. Schmidt, P.H., et al., *Identification of a metaplastic cell lineage associated with human gastric adenocarcinoma*. *Lab Invest*, 1999. **79**(6): p. 639-46.
37. Halldorsdottir, A.M., et al., *Spasmolytic polypeptide-expressing metaplasia (SPEM) associated with gastric cancer in Iceland*. *Dig Dis Sci*, 2003. **48**(3): p. 431-41.
38. Yamaguchi, H., et al., *Identification of spasmolytic polypeptide expressing metaplasia (SPEM) in remnant gastric cancer and surveillance postgastrectomy biopsies*. *Dig Dis Sci*, 2002. **47**(3): p. 573-8.
39. Goldenring, J.R., K.T. Nam, and J.C. Mills, *The origin of pre-neoplastic metaplasia in the stomach: chief cells emerge from the Mist*. *Exp Cell Res*, 2011. **317**(19): p. 2759-64.
40. Wang, T.C., et al., *Mice lacking secretory phospholipase A2 show altered apoptosis and differentiation with Helicobacter felis infection*. *Gastroenterology*, 1998. **114**(4): p. 675-89.

41. Fox, J.G., et al., *Hypertrophic gastropathy in Helicobacter felis-infected wild-type C57BL/6 mice and p53 hemizygous transgenic mice*. Gastroenterology, 1996. **110**(1): p. 155-66.
42. Fox, J.G., et al., *Host and microbial constituents influence Helicobacter pylori-induced cancer in a murine model of hypergastrinemia*. Gastroenterology, 2003. **124**(7): p. 1879-90.
43. Nomura, S., et al., *Spasmolytic polypeptide expressing metaplasia to preneoplasia in H. felis-infected mice*. Gastroenterology, 2004. **127**(2): p. 582-94.
44. Li, Q., S.M. Karam, and J.I. Gordon, *Diphtheria toxin-mediated ablation of parietal cells in the stomach of transgenic mice*. J Biol Chem, 1996. **271**(7): p. 3671-6.
45. Goldenring, J.R., et al., *Reversible drug-induced oxyntic atrophy in rats*. Gastroenterology, 2000. **118**(6): p. 1080-93.
46. Nomura, S., et al., *Alterations in gastric mucosal lineages induced by acute oxyntic atrophy in wild-type and gastrin-deficient mice*. Am J Physiol Gastrointest Liver Physiol, 2005. **288**(2): p. G362-75.
47. Huh, W.J., I.U. Mysorekar, and J.C. Mills, *Inducible activation of Cre recombinase in adult mice causes gastric epithelial atrophy, metaplasia and regenerative changes in the absence of "floxed" alleles*. Am J Physiol Gastrointest Liver Physiol, 2010. **299**(2): p. G368-380.
48. Busuttill, R.A. and A. Boussioutas, *Intestinal metaplasia: a premalignant lesion involved in gastric carcinogenesis*. J Gastroenterol Hepatol, 2009. **24**(2): p. 193-201.
49. Leung, W.K., et al., *Factors predicting progression of gastric intestinal metaplasia: results of a randomised trial on Helicobacter pylori eradication*. Gut, 2004. **53**(9): p. 1244-9.
50. Liu, Q., et al., *CDX2 expression is progressively decreased in human gastric intestinal metaplasia, dysplasia and cancer*. Mod Pathol, 2007. **20**(12): p. 1286-97.
51. Silberg, D.G., et al., *Cdx2 ectopic expression induces gastric intestinal metaplasia in transgenic mice*. Gastroenterology, 2002. **122**(3): p. 689-96.
52. Raghoebir, L., et al., *Disturbed balance between SOX2 and CDX2 in human vitelline duct anomalies and intestinal duplications*. Virchows Arch, 2013. **462**(5): p. 515-22.

CHAPTER 2: Tamoxifen induces rapid, reversible atrophy, and metaplasia in mouse stomach

This chapter was published in Gastroenterology

Tamoxifen induces rapid, reversible atrophy, and metaplasia in mouse stomach

Huh WJ, Khurana SS, Geahlen JH, Kohli K, Waller RA, Mills JC.

Gastroenterology. 2012 Jan;142(1):21-24.e7. DOI: 10.1053/j.gastro.2011.09.050. Epub 2011 Oct 14.

PMID: 22001866

WJH and SSK contributed equally to this manuscript.

Unless otherwise noted, SSK and WJH performed all the experiments in this chapter.

Abstract

Tamoxifen, a selective estrogen receptor modulator, is widely used in research and clinically in patients. We find that treatment of normal mice with a single $\geq 3\text{mg}/20\text{g}$ body weight dose of tamoxifen leads to apoptosis of $> 90\%$ of all gastric parietal cells and metaplasia of zymogenic chief cells within 3 days. Remarkably, gastric histology returns to nearly normal by 3 weeks. Tamoxifen toxicity occurs by oral and intraperitoneal administration, in both sexes, in multiple strains, and does not depend on estrogen, though acid secretion inhibition is partially protective. Thus, substantial gastric toxicity is a heretofore unappreciated tamoxifen side effect.

Introduction

Tamoxifen is widely used to spatio-temporally delete mouse genes using the CreERT/loxP system [1]. Tamoxifen is also used clinically as a selective estrogen receptor (ER) modulator, in chemotherapeutic, anti-osteoporotic, and several other therapeutic regimens [2, [3] . Some reports suggest tamoxifen also increases risk for subsequent gastric cancer [4, [5]. Most gastric cancers occur in stomachs colonized by *Helicobacter pylori* [6]. Precancerous effects of bacterial colonization include: death (atrophy) of acid-secreting gastric parietal cells (PCs), differentiation changes (metaplasia) in the digestive-enzyme secreting zymogenic (chief) cell lineage (ZC) and increased stem cell proliferation [7, [8].

Materials and Methods

Animals and injections- All experiments involving animals were performed according to protocols approved by the Washington University School of Medicine Animal Studies Committee. Mice were maintained in a specified-pathogen-free barrier facility under a 12 hour light cycle. Wild type *C57BL/6*, *BALB/c* and *FVB/N* mice were purchased from The Jackson Laboratory. To trace parietal cells (PCs), *H⁺/K⁺ATPase-Cre* mice [9] were crossed with a reporter line, *B6.129-Gt(ROSA)26Sor^{tm1Joe}/J* (The Jackson Laboratory) [10], which expresses floxed β -galactosidase in the nucleus under the control of the Rosa26 promoter. Tamoxifen (1-5mg/20g body weight, Sigma, St. Louis, MO; and in 1 experiment, 5mg/20g, Cayman Chemical Company, MI) was injected intraperitoneally for one or three days to induce SPEM and mice were dissected at 12 hours, 3 days, 7 days, 14 days, 21 days and 28 days after treatment. Tamoxifen was dissolved in a vehicle of 10% ethanol and 90% sunflower seed oil (Sigma). Tamoxifen stock concentrations ranged from 5mg/ml to 2mg/ml; 200 μ l/20g body weight was injected intraperitoneally. Each mouse was orally gavaged with 4mg tamoxifen, prepared in the

same vehicle described above, for 3 days and dissected at day 3. Fulvestrant (Sigma; 3mg/20g body weight, dissolved in the same vehicle as tamoxifen) and 17β -estradiol (Sigma; 50 μ g /20g body weight, dissolved in the same vehicle as tamoxifen to stock concentration of 100ng/100 μ l) were injected subcutaneously every day for three days, with or without one injection of 5mg/20g tamoxifen on the first day; stomachs were harvested 3 days after the first injection. Omeprazole (Sigma; 1.5mg/20g body weight) was dissolved in 100 μ l DMSO (Sigma) in 90 μ l 1% methyl cellulose (Sigma) and orally gavaged every day for four days, with or without one injection of 5mg/20g tamoxifen on the second day of gavaging, with harvesting at 3 days after tamoxifen injection. Raloxifene (Sigma; 5mg/20g body weight) was dissolved in 10% DMSO and 90% sunflower seed oil and injected into wildtype mice for 3 days and dissected on day 3. To evaluate efficiency of recombination, *R26CreERT* [11] mice were crossed with *B6.129-Gt(ROSA)26Sor^{tm1Joe}/J* (The Jackson Laboratory) [10] and injected with 2mg/20g body weight raloxifene for 5 days, dissected at day 14 and stained for LacZ.

Immunofluorescence- Stomachs were prepared, and stained, and imaged using methods modified from Ramsey et al [12]. Primary antibodies used for immunostaining were: rabbit (1:10,000), goat (1:2000) anti-human gastric intrinsic factor (gifts of Dr. David Alpers, Washington University), rabbit anti-H⁺/K⁺ ATPase α subunit (1:10,000, Dr. Michael Caplan, Yale University), goat anti-BrdU (1:20,000, Jeffrey Gordon, Washington University), rabbit anti-Cytochrome C (1:100, Cell Signaling Technology). Secondary antibodies, GSII lectin and BrdU labeling were as described [12].

Genotyping- For PCR, tissue was lysed with 25mM sodium hydroxide (pH 12.0) at 95°C for 25 minute and neutralized with the same volume of 40mM Tris buffer (pH 5.0) For Cre, PCR was

with RedTaq (Sigma), and KlenTaq (DNA Polymerase Facility, Washington University, St. Louis, MO) was used for LacZ PCR. Primers: Cre forward: AGG GAT CGC CAG GCG TTT TC and reverse: GTT TTC TTT TCG GAT CCG CC, LacZ forward: GTT GCA GTG CAC GGC AGA TAC ACT TGC TGA and reverse: GCC ACT GGT GTG GGC CAT AAT TCA ATT CGC.

LacZ staining- LacZ staining was modified from Lobe, et al, 1999 [13]. Tissue was fixed in LacZ fix for 4 hours at 4°C and washed in LacZ wash buffer three times. Tissue was equilibrated in 30% sucrose/PBS overnight at 4°C, was embedded in O.C.T. (Sakura, Torrance, CA) and was frozen in dry ice. The frozen block was cryosectioned at 14 µm thickness. The section was fixed again for 10 minutes in LacZ fix and washed in LacZ wash buffer three times. Then the section was incubated in LacZ stain 6 hours at 30°C and washed in PBS three times. The section was post-fixed in LacZ fix at room temperature for ten minutes, dehydrated through ethanol and xylene, counter stained with nuclear fast red (Vector Laboratories Inc., Burlingame, CA) and then mounted in Cytoseal XYL (Richard-Allan Scientific, Kalamazoo, MI).

Tunel Staining - Stomachs were inflated with freshly prepared formalin and suspended in fixative overnight at 4°C, followed by multiple rinses in 70% Ethanol, arrangement in 2% agar in a tissue cassette, and routine paraffin processing. Sections (5 µm) were deparaffinized and rehydrated, and Terminal deoxynucleotidyl transferase dUTP nick end labeling (TUNEL) staining was performed using the 'In Situ Cell Death Detection Kit, Fluorescein' (Roche) according to the manufacturer's instructions. Sections were counter-stained with GS-II at 594nm (1:2000, Invitrogen)

Quantitative RT-PCR - For quantitative RT-PCR (qRT-PCR) analysis, total RNAs from stomach tissue were extracted by RNAeasy Midi Kit (Qiagen, Valencia, CA). cDNA was synthesized with Superscript III (Invitrogen) and random primers. qRT-PCR was performed with SYBR Advantage qPCR Mix (Clontech, Mountain View, CA) and gene-specific primers (see table) on an Mx3000P (Stratagene, La Jolla, CA). qRT-PCR analysis and standardization was as described [14], every run was standardized to 18s rRNA primers: forward CAT TCG AAC GTC TGC CCT ATC, reverse CCT GTG CCT TCC TTG GA.

Gene-specific primers used were as follows:

Sr. No.	Gene	Forward Primer 5'→3'	Reverse Primer 5'→3'	Ref.
1.	Tff1	AGCACAAGGTGATCTGTGTCC	GGAAGCCACAATTTATCCTCTCC	[14]
2.	Atp4a	TCTGCTTTGCGGGACTTGTA	CGGCATTTGAGCACAGCAT	[14]
3.	Tff2	TGCTCTGGTAGAGGGCGAG	CGACGCTAGAGTCAAAGCAG	[14]
4.	Pgc	ATGAAGAGTATCCGGGAGACC	TGGGCTCATAGAGTACACTGTAG	[14]
5.	GIF	CCCTCTACCTCCTAAGTGTTCTC	CTGAGTCAGTCACCGAGTTCT	[14]
6.	Gast	ACACAACAGCCAACACTATTC	CAAAGTCCATCCATCCGTAG	[15]
7.	Mist1	GCTGACCGCCACCATACTTAC	TGTGTAGAGTAGCGTTGCAGG	[14]
8.	He4	AACCAATTACGGACTGTGTGTT	TCGCTCGGTCCATTAGGCT	[16]
9.	Lyz	GAGACCGAAGCACCGACTATG	CGGTTTTGACATTGTGTTTCGC	[16]

Western blot - For Western blot analysis, stomach tissue was frozen in liquid nitrogen and ground in urea buffer (8 M urea, 0.19 M Tris-HCl pH 6.8, 1% SDS) using PowerGen 700 homogenizer (Fischer Scientific). Proteins were separated on a 10% polyacrylamide gel

(Invitrogen) and transferred to Nitrocellulose membrane (Amersham Hybond ECL). Primary antibodies used for blotting were rabbit anti- H^+/K^+ ATPase α subunit (1:1000, gift from Dr. Michael Caplan), rabbit anti-Gastric Intrinsic Factor (1:10,000 gift from Dr. David Alpers), rabbit- anti-Chromogranin A (1:1000, DiaSorin, Stillwater, MN), rabbit anti-Cleaved Caspase 3 (1:1000, Cell Signaling Technology) and rabbit anti- α -tubulin (1:2,000, Cell Signaling Technology). Secondary antibody was horseradish peroxidase (HRP)-conjugated donkey anti-rabbit IgG (1:2,000, Santacruz Biotenchnology, Inc.). Immobilon Western Chemiluminescent HRP Substrate (Millipore) was used for detection.

Parietal cell ($Atp4a^+$) and proliferating cell ($BrdU^+$) counts – Cell counts were either by immunofluorescence or from H&E. For immunofluorescence, stomach sections were costained with GS-II, bisbenzimidazole, and either anti- H^+/K^+ ATPase or anti-BrdU antibody. The numbers of PCs or BrdU positive (proliferating) cells in every field were scored for five randomly selected fields in the corpus of a single mouse, with three mice in every experimental set. PCs were also counted in H&E-stained sections for every mouse used in the study. Fifty well aligned corpus gastric units were selected at random from every mouse under study, the total number of PCs determined and average PC/unit calculated. H&E counts were indistinguishable from immunofluorescence-based counts.

Microscopy - Light and transmission electron photomicrographs were taken as described [17]

Graphing and statistics - All graphs and statistics were performed in GraphPad Prism, using one-way ANOVA with either Dunnett's or Tukey's post-hoc multiple comparison tests for cell count data. qRT-PCR data significance was assessed by Student's t test followed by Bonferroni post hoc analysis to ensure against multiple comparison bias. Quantification of GSII and GIF

immunofluorescent staining was performed using ImageJ software (<http://rsbweb.nih.gov/ij/>). The GSII/GIF positive region of each unit was divided lengthwise into 10 equal sections. The images were then thresholded (GSII 4-6 MFI; GIF 10-17 MFI) to subtract background. The mean fluorescent intensities (MFI) above the threshold was multiplied by the area of pixels above the threshold for both the GSII and GIF channel for each section. For tamoxifen treated day 3 and day 21, the data from 20 units from 2 mice were quantified; in untreated mice, data from 15 units from one mouse was quantified. The data for each section was averaged and plotted.

Results and Discussion

In control experiments for tamoxifen induction of Cre-recombinase activity [14], we noticed that tamoxifen injection (3 consecutive days, intraperitoneal, 5mg/20g mouse body weight) caused dramatic rearrangement of the gastric mucosa with loss of > 90% of PCs, a 6-fold increase in proliferation in stem/progenitor cells, and morphological changes in the ZCs in the bases of gastric-units (Fig. 2.1A-D). By 14-21 days, the epithelium recovered (Fig. 2.1A).

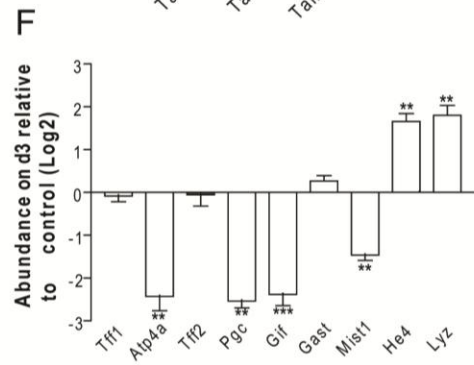
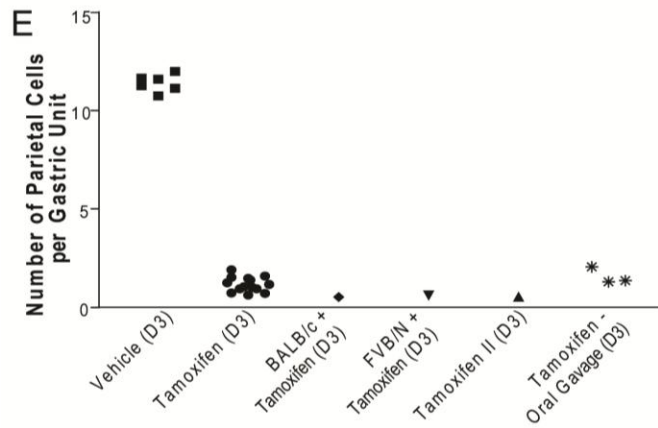
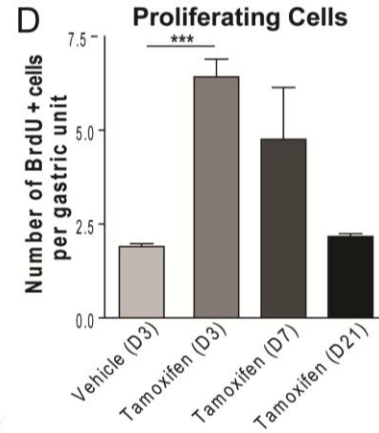
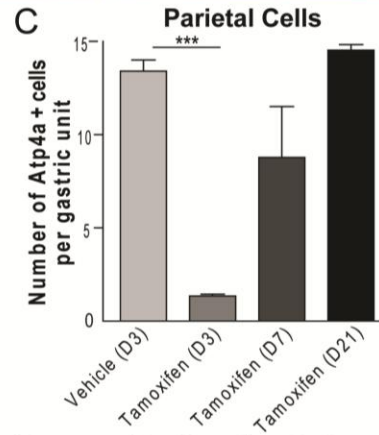
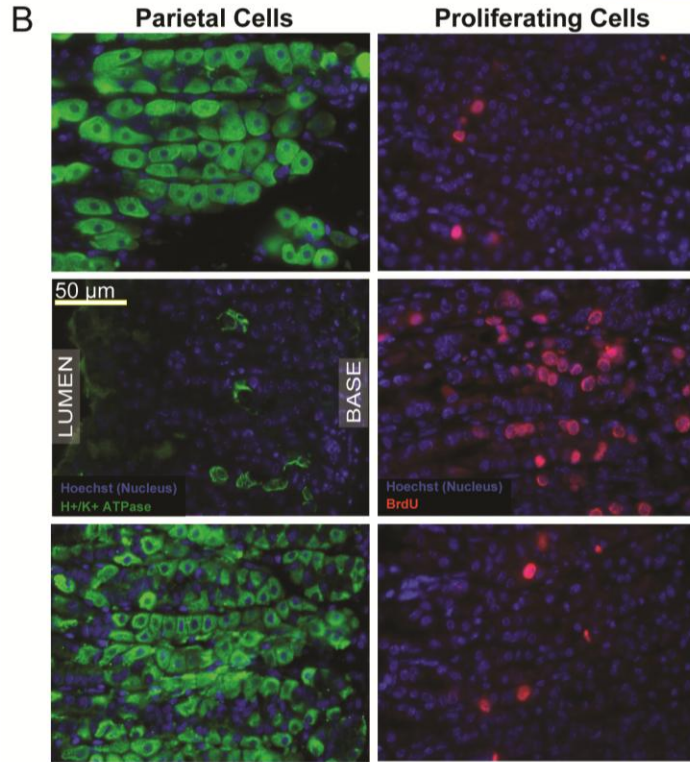
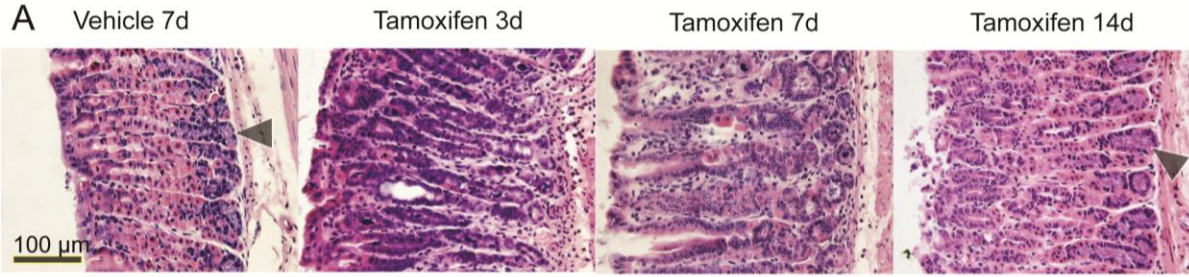


Fig. 2.1. Tamoxifen causes rapid, reversible gastric metaplasia in mice, which is highlighted by parietal cell death, concomitant increase in proliferation and loss of differentiated cell

*markers. A) H&E of wild-type mice following intraperitoneal (i.p.) injection of vehicle at day 7 or 5mg/20g body weight tamoxifen at 3, 7, and 14 days following injection. B) Immunofluorescence (green: anti-ATP4A; red:anti-BrdU) at d3, quantified in C,D. E) Quantification of mean PCs/unit/individual mouse by H&E; unless otherwise indicated, mice were C57/B6 strain; "Tamoxifen II": tamoxifen from another supplier. F) Whole stomach qRT-PCR (expressed as Log₂ scale. *P<0.05;**P<0.01;***P<0.001)*

No other organs had marked phenotypes at this dose or time-schedule (Fig. 2.2). Even a single dose of tamoxifen, by intraperitoneal injection or oral gavage, from two different commercial suppliers in three different strains of mice caused similar effects in n>63 mice (Fig. 2.1E, 2.3A-F). By qRT-PCR, PC-specific transcripts (*Atp4a*) and markers of ZC maturation (*Mist1* aka *Bhlha15*, *Pgc*, *GIF*) [17] were significantly reduced by d3, whereas the surface/foveolar lineage marker (*Tff1*) and transcripts for gastrin were unchanged (Fig. 2.1F, see Fig. 2.3G for western blots of GIF and ATP4A).

Increased progenitor cell proliferation and changes in ZC differentiation are characteristic of spasmolytic polypeptide expressing metaplasia (SPEM) [14, [18]. In SPEM, expression of mucous neck cell markers (like spasmolytic polypeptide, aka TFF2) occurs in the base of glands, where ZCs normally reside [17, [18]. Tamoxifen increased two SPEM-specific transcripts, *He4* and *Lyz* [8]; however, transcript levels for spasmolytic polypeptide(*Tff2*) itself were unchanged (Fig. 2.1F). SPEM is usually diagnosed by histopathological criteria and not transcriptionally [7, [8, [17, [18, [19], but we cannot rule out the possibility that the lack of increased *Tff2* indicates that tamoxifen-induced metaplasia is a SPEM variant.

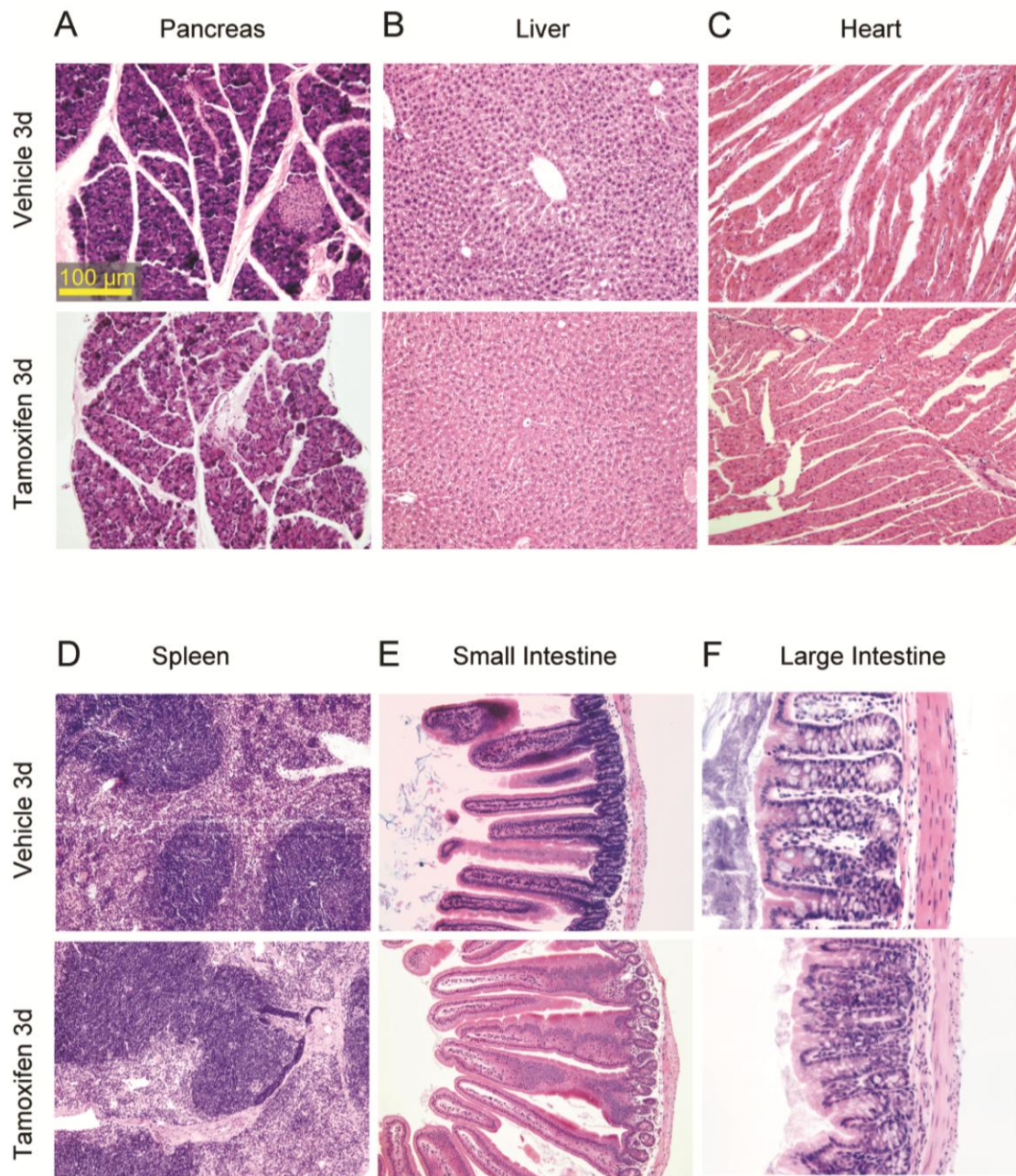


Fig. 2.2. Other organs are not affected by tamoxifen as severely as the stomach. Pancreas (A), Liver (B), Heart (C), Spleen (D), Small Intestine (E) and Large Intestine (F) from vehicle treated (top) and tamoxifen treated (bottom) wild-type mice 3 days following injection. Note that organs exposed to tamoxifen do not differ substantially from those of control mice.

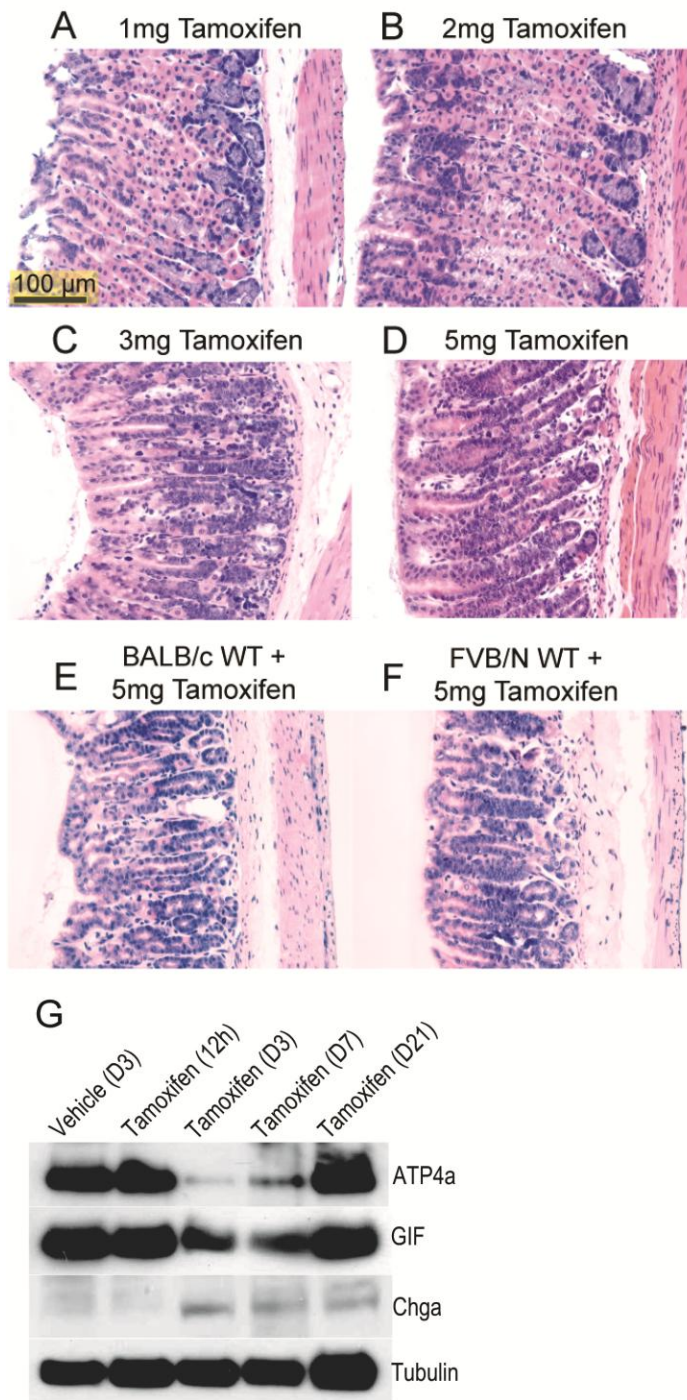


Fig. 2.3. Tamoxifen induced SPEM is dose dependent. Wild type mice injected with 1mg/20g body weight (A), or 2mg/20g body weight (B) tamoxifen for 3 days did not show parietal cell death or features of SPEM, whereas, mice treated with 3mg/30g body weight (C) for 3 days or a single injection of 5mg/20g body weight (D) tamoxifen show complete atrophy of parietal cells and SPEM histology. Other strains of mice develop SPEM equivalently on tamoxifen treatment as shown in BALB/c (E) and FVB/N (F) strains after 3 days of injection of 5mg/20g tamoxifen. G: Western blot showing decrease in H^+/K^+ ATPase and Intrinsic Factor (GIF, zymogenic cell marker) protein levels 3 days after tamoxifen treatment in mice,

when compared with controls. Chromogranin A levels are slightly higher post tamoxifen treatment, which is consistent with previous reports of spasmolytic polypeptide expressing metaplasia (SPEM).

In humans and mice, metaplasia always occurs in the setting of PC atrophy [8, [17]. To assess PC death, we crossed *Atp4b-Cre* mice, whose PCs constitutively express Cre [9], to nuclear lacZ-R26R mice. In these mice, all mature PCs had, as expected, nuclear lacZ expression (Fig. 2.4A). Tamoxifen caused near complete loss of lacZ, indicating that PCs died and did not give rise to other cells with different morphological or molecular characteristics. TUNEL-positive PCs were not observed in the vehicle treated controls, whereas they were common within 12 hours after a single injection of 5mg/20g tamoxifen (Fig. 2.4B). By 12h, cytochrome C staining could now be found leaked into the cytoplasm of the majority of PCs, consistent with early apoptosis; in controls, distribution was still punctate, consistent with retention in the mitochondria (Fig. 2.4B). By transmission electron microscopy, PCs showed neither vacuolization nor organellar swelling, characteristics of necrotic death, but had apoptotic features like electron-dense inclusions in mitochondria and peripheral chromatin condensation (Fig. 2.4D, E). Finally, only tamoxifen-treated stomachs showed Caspase 3 cleavage (Fig. 2.4C).

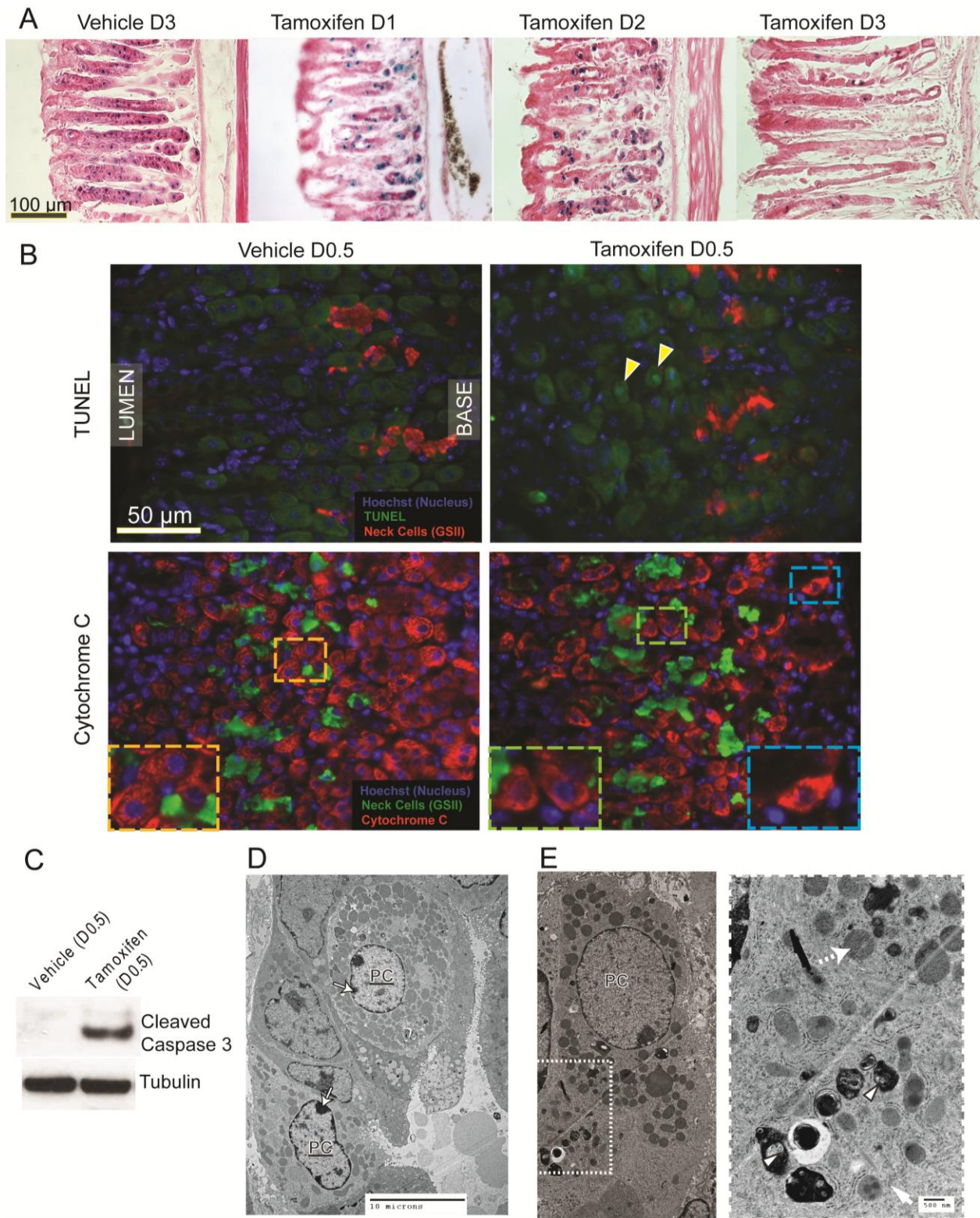
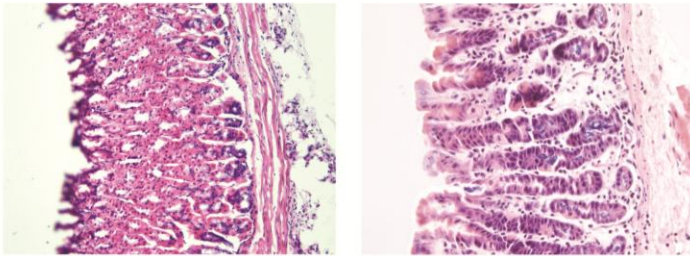


Fig. 2.4. Tamoxifen results in SPEM by causing death of parietal cells. A) Nuclear LacZ labeled PCs following tamoxifen treatment. **B)** Top: TdT-mediated dUTP nick-end labeling

shows dying PCs (arrowheads). Below: Cytochrome C staining is punctate, consistent with mitochondrial localization in vehicle-treated (below left) and dispersed throughout the cytoplasm tamoxifen-treated PCs (below right) C) Cleaved caspase 3 western blot with tubulin loading control. D) At 2.5d following tamoxifen, PCs show chromatin condensation (arrows with black outline), consistent with early apoptosis. E) Another degenerating PC exhibits mitochondria ranging in morphology from normal (dashed arrow) to electron-dense-inclusion-containing (white solid arrow) to electron-dense and degenerating (arrowheads).

Tamoxifen can function as both an estrogen receptor (ER) agonist and antagonist depending on tissue type; however, neither treatment with the pure ER agonist 17- β -estradiol nor the specific antagonist fulvestrant induced atrophy/metaplasia. And neither blocked tamoxifen effects (Fig. 2.5A, B). The sex of the mice also did not affect tamoxifen effects (Fig. 2.5C), nor did ovariectomy of females to block endogenous estrogen production (Fig. 2.5C; data not shown).

A Estradiol 3d Tamoxifen + Estradiol 3d



B Fulvestrant 3d Tamoxifen + Fulvestrant 3d

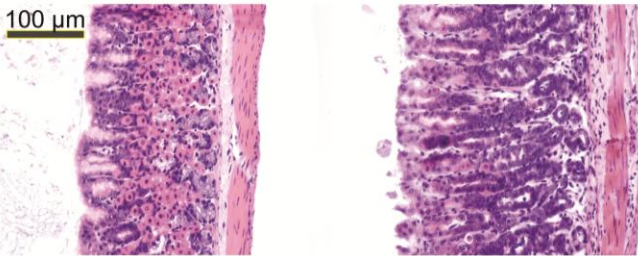
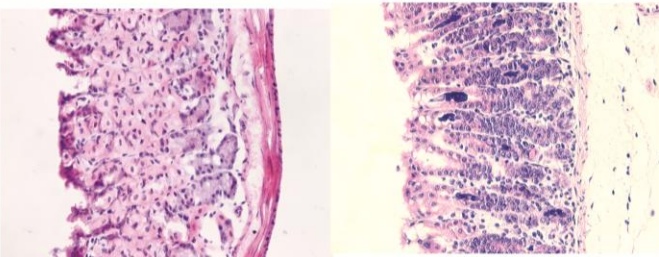


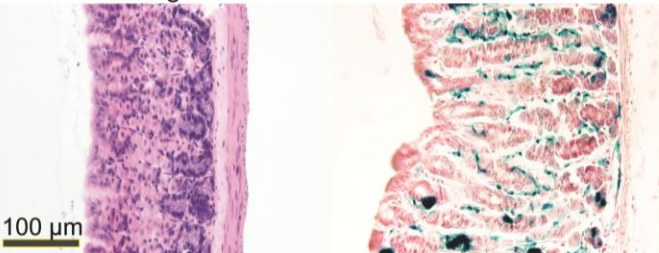
Fig. 2.5. SPEM induction by tamoxifen is not estrogen receptor (ER) or sex dependent. Mice treated with ER agonist, 17- β -estradiol did not develop SPEM (A) and neither did estradiol rescue SPEM induced by tamoxifen (right). Similarly, mice treated with ER antagonist, Fulvestrant did not develop SPEM (B)

and neither did it rescue SPEM induced by Tamoxifen (right).

C Ovariectomized Female Tamoxifen 3d - Female



D Raloxifene 3d 5mg **E** R26Cre-R26R + Raloxifene 14d



Ovariectomized (C) and female (right) mice also developed SPEM like their male counterparts (male mice used for all other experiments in the current study) on injection with tamoxifen. D: Raloxifene does not show toxicity, like tamoxifen, at the same dose and time course. E: Cre-recombinase driven by the R26 promoter, in a R26-Reporter

background, is induced by Raloxifene. Blue depicts LacZ staining in cells with Cre-recombinase activity. The staining pattern is similar to what we see with tamoxifen in other experiments (not shown) using R26-Cre: nearly all mesenchymal cells and many ZCs show induced.

However, tamoxifen effects could largely be reversed by blocking the PC proton pump with omeprazole (Fig. 2.6), suggesting a role for active acid secretion in tamoxifen toxicity to PCs. Finally, another SERM family member, raloxifene, which also has both pro and anti-estrogenic effects, did not cause atrophy up to a dose of 5mg/20g (Fig. 2.5D), indicating toxicity is not a general feature of SERMs. On the other hand, intraperitoneal injection of raloxifene induced Cre recombinase-mediated lacZ activation in mice expressing Rosa26-Cre fused with a modified ER (Fig. 2.5E), indicating that raloxifene can be used to induce Cre recombinase activity to obviate the off-target toxicity of tamoxifen in Cre-loxP inducible systems.

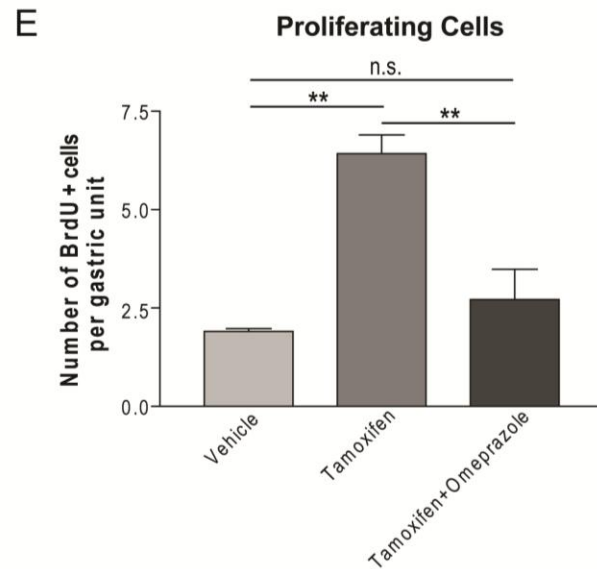
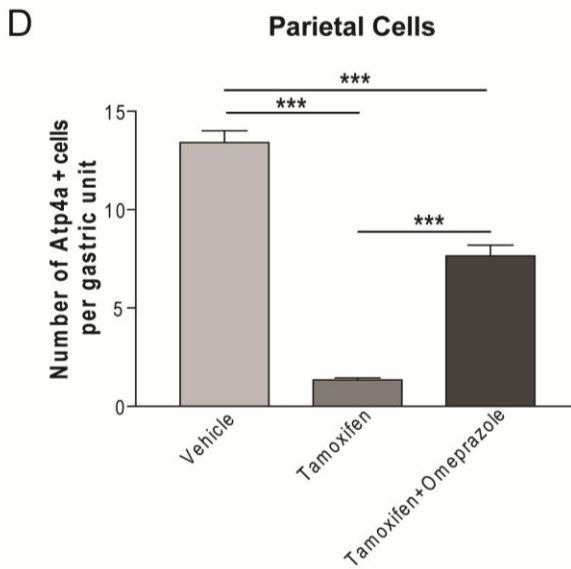
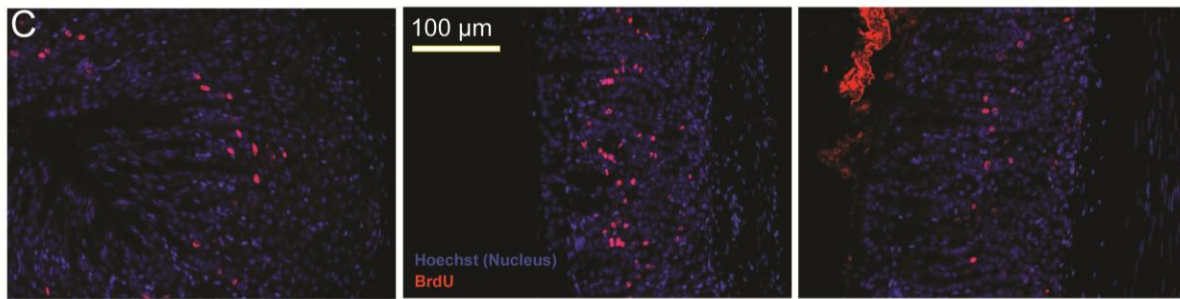
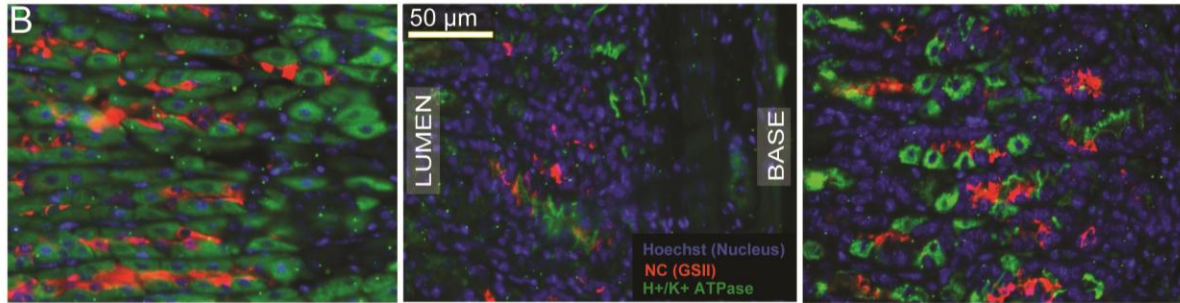
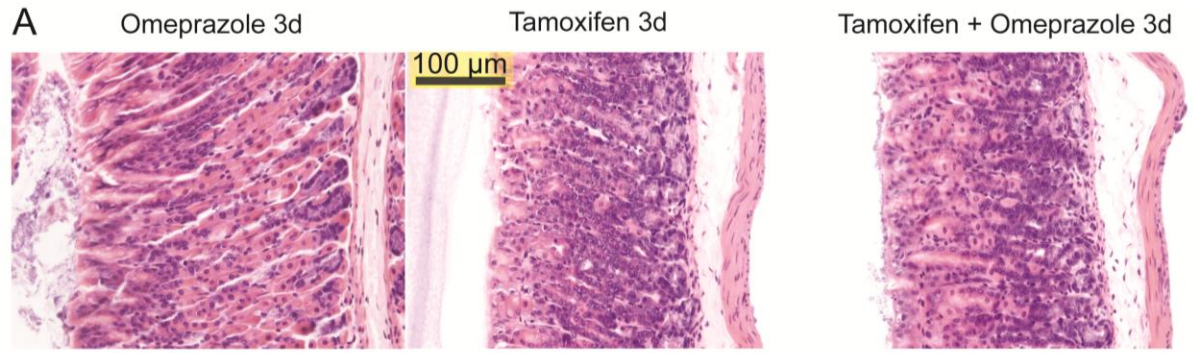


Fig. 2.6. SPEM induction by tamoxifen is ameliorated by omeprazole treatment. **A:** Wild-type mice injected with the proton pump inhibitor, omeprazole, in conjunction with tamoxifen (right) are partially protected from SPEM induced by tamoxifen alone (center). Omeprazole, by itself, does not have any effect on the stomach mucosa (left). **B:** Tamoxifen and omeprazole co-treated mice show higher numbers of H^+/K^+ ATPase expressing parietal cells (right) when compared to those treated with only tamoxifen (center). Omeprazole alone does not alter the number of H^+/K^+ ATPase (*Atp4*) expressing parietal cells (left). These results are quantified in (**D**). **C:** Tamoxifen and omeprazole co-treated mice show lower numbers of BrdU positive proliferating cells (right) when compared to those treated with only tamoxifen (center). Omeprazole alone does not alter the number of BrdU positive proliferating cells (left). These results are quantified in (**E**).

Tamoxifen is a chemotherapeutic drug that has toxic effects on cancer cells from diverse tissues. In osteoclasts (which, like PCs, are large, mitochondria- and proton pump-rich cells), toxicity is caused by disrupting proton gradients and, thereby intracellular pH [20]. The drug DMP-777 causes PC death the same way [19]. Omeprazole is partially protective against both DMP-777 and tamoxifen toxicity, suggesting a similar mode of action [19]. The minimal dosing that causes metaplasia in the current study is an order of magnitude more than the equivalent (40 mg/day) used therapeutically in humans [21]. Acute loss of PCs in patients taking tamoxifen might be beneficial for acid-reflux associated illness but could also predispose, long-term to gastric cancer. Further experiments are clearly needed to address effects of tamoxifen on the human stomach.

Acknowledgements

Authors WJH and SSK contributed equally to this work.

References

1. Feil, R., et al., *Ligand-activated site-specific recombination in mice*. Proc Natl Acad Sci U S A, 1996. **93**(20): p. 10887-90.
2. Jordan, V.C., *The strategic use of antiestrogens to control the development and growth of breast cancer*. Cancer, 1992. **70**(4 Suppl): p. 977-82.
3. Love, R.R., et al., *Effects of tamoxifen on bone mineral density in postmenopausal women with breast cancer*. N Engl J Med, 1992. **326**(13): p. 852-6.
4. Chandanos, E., et al., *Tamoxifen exposure and risk of oesophageal and gastric adenocarcinoma: a population-based cohort study of breast cancer patients in Sweden*. Br J Cancer, 2006. **95**(1): p. 118-22.
5. Matsuyama, Y., et al., *Second cancers after adjuvant tamoxifen therapy for breast cancer in Japan*. Ann Oncol, 2000. **11**(12): p. 1537-43.
6. Helicobacter and G. Cancer Collaborative, *Gastric cancer and Helicobacter pylori: a combined analysis of 12 case control studies nested within prospective cohorts*. Gut, 2001. **49**(3): p. 347-53.
7. Lennerz, J.K., et al., *The Transcription Factor MIST1 Is a Novel Human Gastric Chief Cell Marker Whose Expression Is Lost in Metaplasia, Dysplasia, and Carcinoma*. Am J Pathol, 2010. **177**: p. 1514-1533.
8. Lee, H.J., et al., *Gene expression profiling of metaplastic lineages identifies CDH17 as a prognostic marker in early stage gastric cancer*. Gastroenterology, 2010. **139**(1): p. 213-25 e3.
9. Syder, A.J., et al., *A transgenic mouse model of metastatic carcinoma involving transdifferentiation of a gastric epithelial lineage progenitor to a neuroendocrine phenotype*. Proc Natl Acad Sci U S A, 2004. **101**(13): p. 4471-6.
10. Stoller, J.Z., et al., *Cre reporter mouse expressing a nuclear localized fusion of GFP and beta-galactosidase reveals new derivatives of Pax3-expressing precursors*. Genesis, 2008. **46**(4): p. 200-4.
11. Huh, W.J., I.U. Mysorekar, and J.C. Mills, *Inducible activation of Cre recombinase in adult mice causes gastric epithelial atrophy, metaplasia and regenerative changes in the absence of "floxed" alleles*. Am J Physiol Gastrointest Liver Physiol, 2010. **299**(2): p. G368-380.

12. Ramsey, V.G., et al., *The maturation of mucus-secreting gastric epithelial progenitors into digestive-enzyme secreting zymogenic cells requires Mist1*. Development, 2007. **134**(1): p. 211-22.
13. Lobe, C.G., et al., *Z/AP, a double reporter for cre-mediated recombination*. Dev Biol, 1999. **208**(2): p. 281-92.
14. Huh, W.J., et al., *XBPI controls maturation of gastric zymogenic cells by induction of MIST1 and expansion of the rough endoplasmic reticulum*. Gastroenterology, 2010. **139**(6): p. 2038-49.
15. Jain, R.N., et al., *Hip1r is expressed in gastric parietal cells and is required for tubulovesicle formation and cell survival in mice*. J Clin Invest, 2008. **118**(7): p. 2459-70.
16. Nam, K.T., et al., *Mature chief cells are cryptic progenitors for metaplasia in the stomach*. Gastroenterology, 2010. **139**(6): p. 2028-2037 e9.
17. Bredemeyer, A.J., et al., *The gastric epithelial progenitor cell niche and differentiation of the zymogenic (chief) cell lineage*. Dev Biol, 2009. **325**(1): p. 211-24.
18. Quante, M., et al., *TFF2 mRNA transcript expression marks a gland progenitor cell of the gastric oxyntic mucosa*. Gastroenterology, 2010. **139**(6): p. 2018-2027 e2.
19. Ogawa, M., et al., *Omeprazole treatment ameliorates oxyntic atrophy induced by DMP-777*. Dig Dis Sci, 2006. **51**(3): p. 431-9.
20. Lehenkari, P., et al., *The effects of tamoxifen and toremifene on bone cells involve changes in plasma membrane ion conductance*. J Bone Miner Res, 2003. **18**(3): p. 473-81.
21. Reagan-Shaw, S., M. Nihal, and N. Ahmad, *Dose translation from animal to human studies revisited*. FASEB J, 2008. **22**(3): p. 659-61.

CHAPTER 3: The hyaluronic acid receptor CD44 coordinates normal and metaplastic gastric epithelial progenitor cell proliferation

This chapter was published in The Journal of Biological Chemistry

The hyaluronic acid receptor CD44 coordinates normal and metaplastic gastric epithelial progenitor cell proliferation

Khurana SS, Riehl TE, Moore BD, Fassan M, Ruge M, Romero-Gallo J, Noto J, Peek RM Jr, Stenson WF, Mills JC.

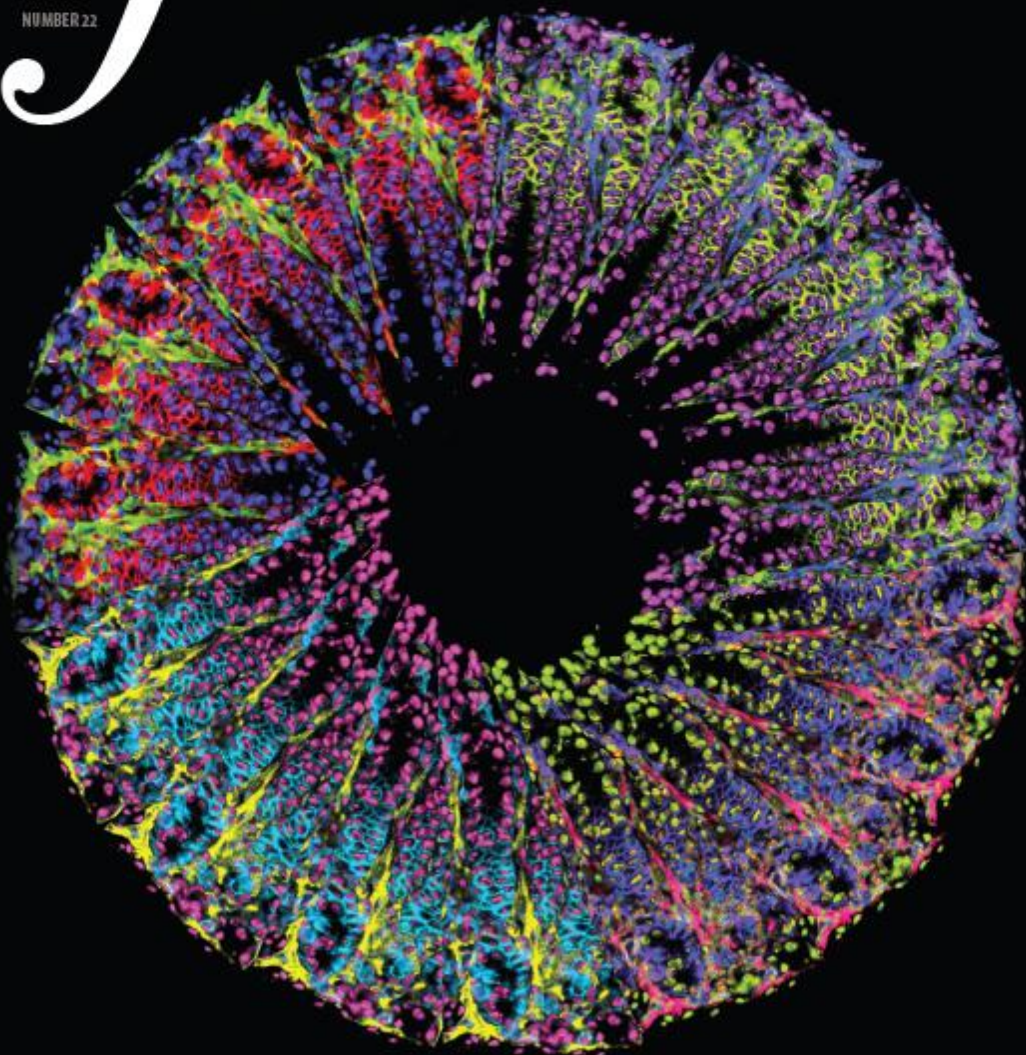
J Biol Chem. 2013 May 31;288(22):16085-97. doi: 10.1074/jbc.M112.445551. Epub 2013 Apr 15.

PMID: 23589310

Unless otherwise noted, SSK performed all the experiments in this chapter.

the journal of biological chemistry
jbc

MAY 31, 2013
VOLUME 288
NUMBER 22



 AMERICAN SOCIETY FOR BIOCHEMISTRY AND MOLECULAR BIOLOGY

Abstract

The stem cell in the isthmus of gastric units continually replenishes the epithelium. Atrophy of acid-secreting parietal cells (PCs) frequently occurs during infection with *Helicobacter pylori*, predisposing patients to cancer. Atrophy causes increased proliferation of stem cells, yet little is known about how this process is regulated. Here we show that CD44 labels a population of small, undifferentiated cells in the gastric unit isthmus where stem cells are known to reside. Loss of CD44 *in vivo* results in decreased proliferation of the gastric epithelium. When we induce PC atrophy, by *Helicobacter* infection or tamoxifen treatment, this CD44⁺ population expands from the isthmus towards the base of the unit. CD44 blockade during PC atrophy abrogates the expansion. We find that CD44 binds STAT3, and inhibition of either CD44 or STAT3 signaling causes decreased proliferation. Atrophy-induced CD44 expansion depends on pERK, which labels isthmal cells in mice and humans. Our studies delineate an *in vivo* signaling pathway, ERK→CD44→STAT3, that regulates normal and atrophy-induced gastric stem/progenitor-cell proliferation. We further show that we can intervene pharmacologically at each signaling step *in vivo* to modulate proliferation.

Introduction

Tumors of the stomach are the second leading cause of cancer-related death worldwide [1, [2]. Most of these tumors occur in the setting of chronic infection with the bacterium *Helicobacter pylori*, which causes atrophy (death) of the acid-secreting parietal cells (PC). PC atrophy, in turn, causes precancerous, metaplastic changes in other epithelial cells [3, [4, [5, [6]. In normal corpus gastric units, PCs concentrate in the middle (neck) portion amongst mucous neck cells (NCs) [7] and below the isthmus that houses the stem cell. Classical ³²P-radiolabeling studies indicate that one or a few cells in the isthmus constantly regenerate cells that undergo bidirectional migration, up to the mucosal surface and down to the gland base, as they differentiate into mature cells of the gastric unit [4, [8]. NCs migrate slowly from their birth into the base, where they rapidly transition into digestive enzyme-secreting zymogenic cells (ZCs).

PC atrophy in humans, mice and other model animals causes existing ZCs to re-express NC markers [6, [9, [10, [11]. This aberrant ZC differentiation pattern is known as Spasmolytic Polypeptide Expressing Metaplasia (SPEM) due to greatly increased expression of the NC marker Spasmolytic Polypeptide (TFF2). PC atrophy also causes increased proliferation of normal stem/progenitor cells in the isthmus [6, [7]. The pattern of chronic PC atrophy and SPEM has been associated with 90% of resected gastric cancers and is thought to be a key predisposing factor, but the molecular mechanisms causing SPEM as well as progenitor expansion have not been elucidated [12, [13, [14]. Given that eradication of *H. pylori* seems to cause only partial reversion of metaplasia and risk for cancer [15, [16, [17, [18], developing additional treatment strategies that would encourage reversion of these lesions can potentially greatly decrease the risk for gastric cancers worldwide.

Our understanding of the molecular regulation of gastric corpus isthmal stem cell proliferation, even under normal homeostasis, is still rudimentary despite considerable recent work having elucidated gene products marking stem cells in the intestines (e.g. LGR5 [19], LRIG1 [20], BMI [21]) and even in the more distal gastric antrum [19, [22]. A handful of molecular pathways and markers [23, [24, [25] have been proposed for the gastric epithelium, but no mechanistic studies revealing molecules that regulate proliferation of the canonical isthmal stem cell either under normal conditions or in response to injury have been reported [4]. Furthermore, the mechanisms underlying altered patterns of stem cell behavior during precancerous conditions in any tissue are only beginning to be explored.

We have recently shown that a $\geq 3\text{mg}/20\text{g}$ body weight dose of tamoxifen is toxic specifically to PCs, in an estrogen receptor independent manner, within the mouse stomach [26]. Nearly all PCs atrophy by 3 days after a single intraperitoneal injection of tamoxifen, and death begins within hours, leading to SPEM [26] that eventually reverses several weeks later if no more tamoxifen is injected. PC death is accompanied by a rapid activation of stem and progenitor cells in the isthmus region [26]. Thus, tamoxifen causes PC atrophy and isthmal stem cell activation that is rapid, synchronous, and robust, affording us a novel tool to study the induction of stem cell activity in response to PC atrophy within an animal model. Here, we report the signaling mechanisms by which gastric corpus epithelial stem cells maintain homeostasis. We find that CD44 labels undifferentiated, proliferating cells within the isthmus, which expand dramatically during atrophy induced by *Helicobacter* infection and tamoxifen. Baseline isthmal progenitor proliferation is reduced in *Cd44*^{-/-} mice. Moreover, wild-type (WT) mice treated with PEP-1, a peptide that blocks the interaction between hyaluronic acid (HA) and CD44, also show both inhibited normal proliferation as well as blocked expansion during atrophy. We next show that,

along with CD44, STAT3 phosphorylation is critical for isthmal cell proliferation in response to injury and that STAT3 activation depends on CD44. We find ERK signaling is activated almost immediately following PC damage and acts as the upstream modulator of *Cd44* and the atrophy induced proliferative response, as determined by a kinase activation screen. Finally, we show that cells expressing pERK in their nuclei expand in the isthmus of mice during PC atrophy and in atrophic and metaplastic lesions in human patients. Our results identify for the first time an *in vivo* signaling pathway that mediates the response of the normal stem/progenitor cell compartment to a metaplasia inducing injury.

Materials and Methods

Animals and injections- All experiments involving animals were performed according to protocols approved by the Washington University School of Medicine Animal Studies Committee. Mice were maintained in a specified-pathogen-free barrier facility under a 12 hour light cycle. Wild-type C57BL/6 and CD44^{-/-} mice were purchased from The Jackson Laboratory. Mice from all treatment groups were given an i.p. injection of a mixture of 5-bromo-2'-deoxyuridine (BrdU, 120 mg/kg) and 5-fluoro-2'-deoxyuridine (12 mg/kg) 90 minutes before sacrifice to label S-phase cells. Vehicles used for all injections are: sterile water, sterile saline, ethanol in sunflower seed oil, or DMSO in sunflower seed oil; no phenotypes were induced by injection of any of the vehicles alone.

Table 3.1: Mice treatments and injections

Treatment	Dose (body weight)	Vehicle	Injection Scheme	Source
Tamoxifen	5mg/20g	10% ethanol + 90% sunflower seed oil	i.p. one day, sacrificed as indicated	Sigma
U-0126	50mg/kg	10% DMSO (Sigma) + 90%	i.p. one hour before and	Sigma

		sunflower seed oil	every two hours after tamoxifen	
WP1066	2mg/20g	20% DMSO + 80% sunflower seed oil.	i.p. one hour before and every 12 hours after tamoxifen	EMD Millipore
Hyaluronan (HA)	30mg/kg	0.9% sterile saline	i.p. twice a week since weaning, for 5 weeks	Sigma
PEP-1 (5 week)	40mg/kg	Sterile water	i.p. twice a week since weaning, for 5 weeks	New England Peptide, Gardner, MA
PEP-1 (3 days)	40mg/kg	Sterile water	i.p. once a day for 3 days, starting one day before tamoxifen injection	New England Peptide, Gardner, MA

H. pylori growth conditions and murine infection- The wild-type rodent-adapted *cag*⁺ *H. pylori* strain PMSS1 was cultured on trypticase soy agar with 5% sheep blood agar plates (BD Biosciences) for in vitro passage, as previously described [27]. It was then cultured in Brucella broth (BB, BD Biosciences) supplemented with 10% fetal bovine serum (FBS, Atlanta Biologicals) for 16 to 18 hours at 37°C with 5% CO₂. Male C57BL/6 mice were purchased from Jackson Laboratories and housed in the Vanderbilt University Animal Care Facilities in a room with a 12-hour light-dark cycle at 21°C to 22°C. Mice were orogastrically challenged with either Brucella broth (BB), as an uninfected (UI) control, or with the mouse-adapted wild-type *cag*⁺ *H. pylori* strain PMSS1. Mice were euthanized at 4 and 8 weeks post-challenge and gastric tissue was harvested for immunohistochemistry.

Human Tissues- Examination of human gastric pathological tissue specimens was approved by the Institutional Review Board of Washington University School of Medicine, the Comité de

Bioetica of Nicaragua for Universidad Nacional Autonoma De Nicaragua – Facultad De Ceincias Medicas Managua, and the Research Ethics Board Manager for Health Sciences at the University of Toronto. Serial sections (4–6 μm thick) obtained from paraffin-embedded tissue samples (H&E and alcian blue–periodic acid–Schiff stains) were reviewed by two pathologists in Italy (M.F., and M.R.) with specific expertise in gastrointestinal diseases, and a consensus on the score for each pertinent histologic variable was reached. Diagnoses and selection of specific regions of transitions among normal stomach, atrophic stomach, and intestinal metaplasia was performed by a third pathologist in the US (JCM).

Immunofluorescence and Immunohistochemistry- Stomachs were prepared, and stained, and imaged using methods modified from Ramsey et al [28]. Immunohistochemistry was performed using ABC reagent and DAB substrate kits (Vector Labs) as per the manufacturer’s instructions. For BrdU/Ki67 quantifications, positive cells were counted in >50 gastric units per mouse and >3 mice per experiment. Total number of positive cells was divided by the total number of gastric units for each mouse. Stomachs were prepared, and stained, and imaged using methods modified from Ramsey et al [28]. Primary antibodies used for immunostaining are listed in

Table 3.2: Primary antibodies used for immunostaining

Serial No.	Antibody	Dilution	Source
1	Goat α -BrdU	1:20,000	Jeffrey Gordon, Washington University
2	Rabbit α -pERK1/2	1:100	Cell Signaling Technology, Danvers, MA
3	Rabbit α -Ki67	1:100	Abcam, Cambridge, MA
4	Rat α -CD44	1:50	BD Biosciences, San Jose, CA
5	Mouse α -E-cadherin	1:200	BD Biosciences, San Jose, CA
6	Rabbit α -Atp4a	1:10,000	Dr. Michael Caplan, Yale University

Hyaluronan-binding protein staining was performed as described [29]. Secondary antibodies, lectins and BrdU labeling were as described [28].

Western Blotting – Western Blotting –Western blot analysis was performed as described [26]. Antibodies used for blotting are listed in Table 3.3. Immobilon Western Chemiluminescent HRP Substrate (Millipore) was used for detection.

Table 3.3: Primary antibodies used for Western blotting

Serial No.	Antibody	Dilution	Source
1	Rabbit α -Cyclin D1	1:1,000	Cell Signaling Technology, Danvers, MA
2	Rabbit α -pERK1/2	1:1000	Cell Signaling Technology, Danvers, MA
3	Rabbit α -p-p38MAPK	1:1000	Cell Signaling Technology, Danvers, MA
4	Rabbit α -SAPK/JNK	1:1000	Cell Signaling Technology, Danvers, MA
5	Rabbit α -pAKT	1:1000	Cell Signaling Technology, Danvers, MA
6	Rabbit α -PLC γ	1:1000	Cell Signaling Technology, Danvers, MA
7	Rabbit α -Egr1	1:1000	Cell Signaling Technology, Danvers, MA
8	Rabbit α -pSTAT3	1:1000	Cell Signaling Technology, Danvers, MA
9	Rabbit α -STAT3	1:2000	Cell Signaling Technology, Danvers, MA
10	Rat α -CD44	1:500	BD Biosciences, San Jose, CA
11	Goat α -HAS1	1:1000	Santacruz Biotechnology Inc., CA
12	Goat α -HAS2	1:1000	Santacruz Biotechnology Inc., CA

Secondary antibodies were horseradish peroxidase (HRP)-conjugated donkey anti-rabbit IgG (1:2,000, Santa Cruz Biotenchnology, Inc.), goat anti-rat IgG (1:1000, Santa Cruz Biotechnology,

Inc.) and donkey anti-goat IgG (1:1000, Santa Cruz Biotechnology, Inc.).

Flourescence Activated Cell Sorting - Gastric corpora were collected, washed in PBS, dissected into $\sim 1\text{mm}^2$ pieces, suspended in 1mL HBSS, and mechanically disaggregated with two 20 second pulses in a Medimachine (BD). Tissue was incubated for 1h with vigorous shaking at 37° C in 10mL HBSS supplemented with 1mM DTT and 5mM EDTA. The cell suspension was filtered (50 μm filter, Partek) and the filtrate incubated at 37° C, 5% CO₂ until staining. The remaining mucosa/tissue left on the filter was rinsed in 10mL RPMI, then incubated at 37° C with vigorous shaking in 10mL RPMI containing 5% BSA and 1.5mg/mL Dispase II (Stem Cell Technologies) for 1.5 h. This cell suspension was filtered, and the second filtrate pooled with the first, washed, and surfaced labeled for flow cytometry. Cells were stained with Alexa Fluor™ 647-conjugated with either anti-mouse Epcam (Cell signaling) or Alexa Fluor™ 647-conjugated anti-mouse E-cadherin (for some experiments), and APC-Cy™7-conjugated anti-mouse CD44. Labeled cells were analyzed with a FACScan (BD) flow cytometer. The use of high wavelength fluorophores avoided considerable autofluorescence of living gastric epithelial cells.

Immunoprecipitation – Immunoprecipitation was performed using the Pierce Crosslink IP Kit (Thermo Scientific, Rockford, IL) using the manufacturer's instructions. Rabbit anti-Stat3 (1:200, Cell Signaling Technology) was used for pull down and western blots analysis was done as described above.

Microscopy - Light and epifluorescence micrographs were taken as described [7].

Graphing and statistics - All graphs and statistics were performed in GraphPad Prism, using Student's t test (one-tailed or two-tailed, as appropriate) for comparison of two groups of data and one-way ANOVA with either Dunnett's or Tukey's for multiple comparison tests.

Results

CD44 is expressed in isthmal cells and regulates normal baseline proliferation

CD44 is a cell-surface adhesion molecule, widely described as a marker of cells with highest proliferative capacity in cancers of the breast [30, [31], colon [32, [33], and stomach [34]. CD44 is highly expressed in gastric cancer cell lines [34], *Helicobacter pylori* infected human patient epithelia [34, [35], gastric carcinomas [36, [37], intestinal metaplasia [37, [38] and dysplasia [39]. Though CD44 is expressed in gastric tumors [34, [35, [40], its expression has not been characterized in normal mouse corpus gastric epithelial tissue [41], but it has been observed in the antral epithelium [34] and at the squamous-corpus junction [42]. We found that CD44 was expressed throughout the scant interglandular mesenchymal cells (Fig. 3.1A), but CD44⁺ epithelial cells could also be found in epithelial cells within the isthmus (Fig. 3.2A) and in the foveolar/pit region of wild-type mice (Fig. 3.1A, white bracket).

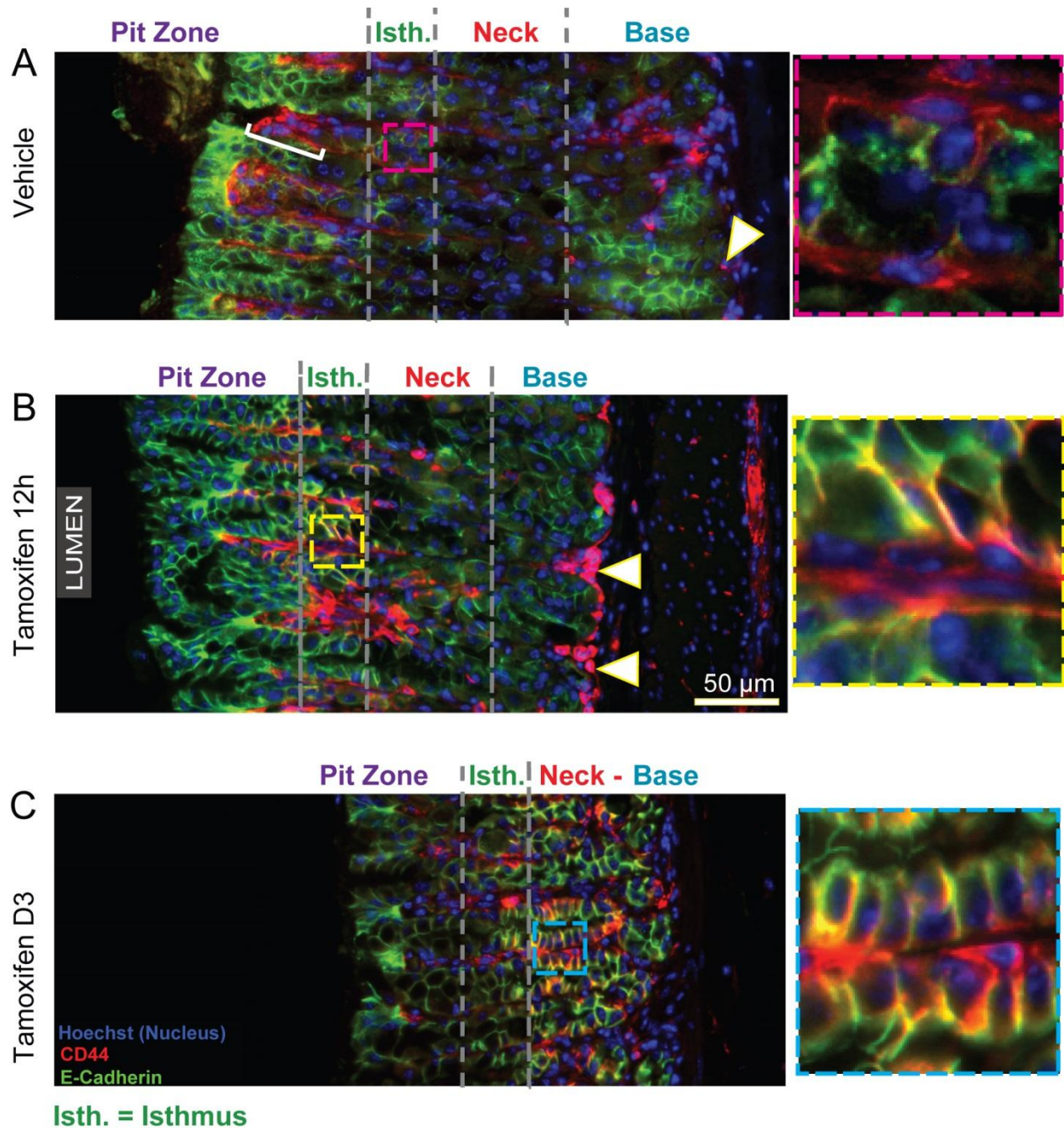


Fig. 3.1: The CD44⁺ cells expanding from the isthmus upon tamoxifen induced parietal cell atrophy were epithelial. In vehicle treated mice, there was little overlap between CD44 (red) and the epithelial marker, E-cadherin (green) (A, note only one isthmal cell with partial CD44-partial E-cadherin label in magnified box at right), but this population expanded gradually over 3 days after tamoxifen treatment (B, C). Mesenchymal CD44⁺ cells are labeled with a white

bracket, and CD44⁺ immune cells are marked by white arrowheads. Insets show magnified images of the cells showing overlap between CD44 and E-cadherin (yellow).

CD44⁺ isthmal epithelial cells were small and undifferentiated, as they did not co-stain with markers of differentiated cells, such as AAA and GSII (Fig. 3.2A). Since CD44 is known to affect proliferation [43], we next investigated the requirement for CD44 signaling in gastric epithelial stem cell proliferation. In mice lacking *Cd44*, the basal rate of proliferation was half of the wild type (WT) controls (Fig. 3.2B, C; n=10), suggesting a role for CD44 in normal stem cell homeostasis. CD44 can interact with multiple ligands in the extracellular matrix such as osteopontin, collagen, fibronectin, laminin, and chondroitin sulfate, but its principal ligand is hyaluronan (HA) [44]. HA activates CD44 by binding to its N-terminal functional domain [45]. To determine whether direct CD44 activation was required for isthmal cell proliferation, we next treated adult mice with PEP-1 twice a week for 5 weeks. PEP-1 inhibits CD44-mediated signaling by blocking the binding of its ligand, HA. Blocking the CD44-HA interaction with PEP-1 caused statistically significant decrease in proliferation of normal stem cells to levels phenocopying *Cd44*^{-/-} mice (Fig. 3.2D n= 12 mice total, 3 mice per experiment, 50 gastric units analyzed per mouse).

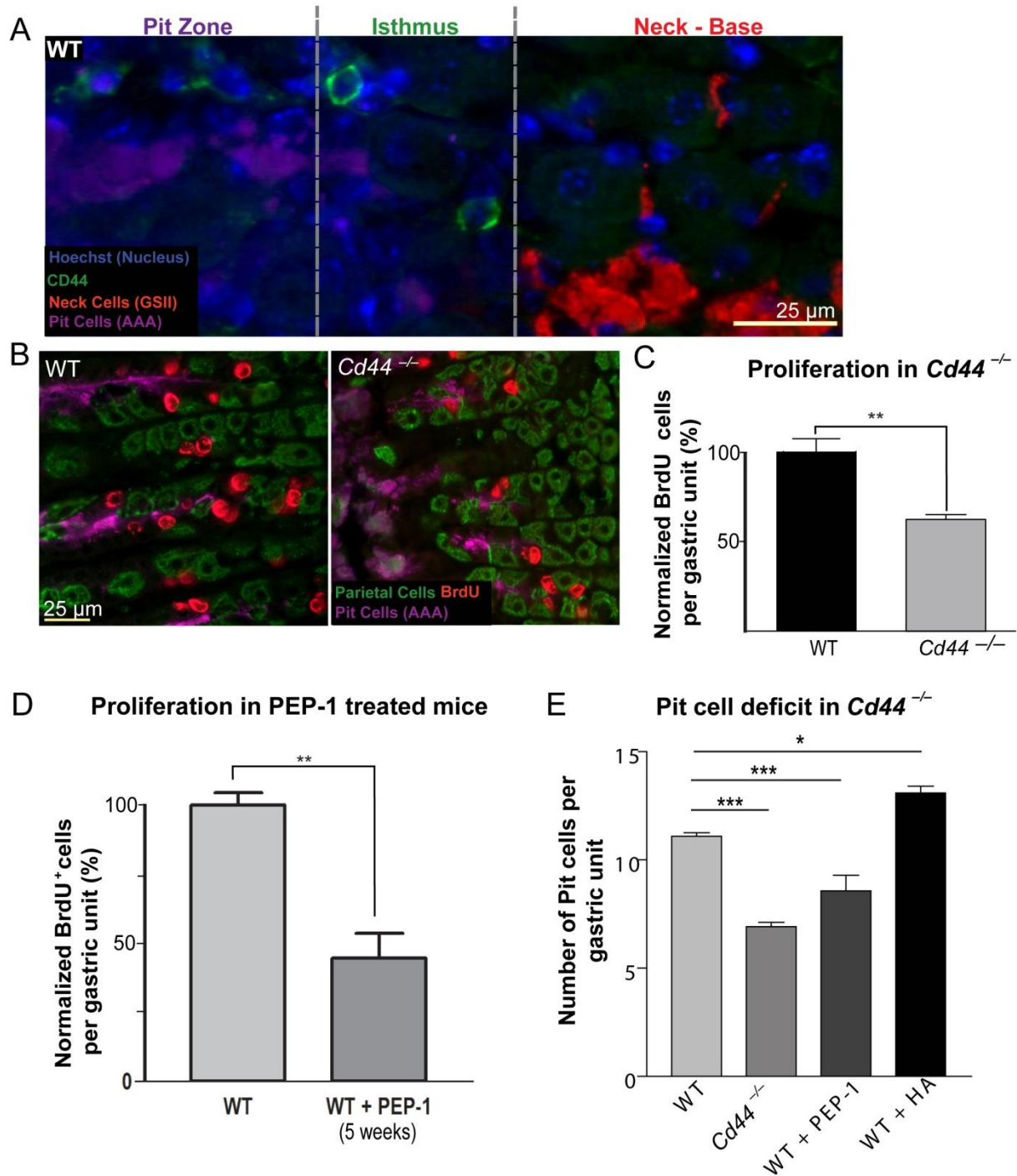


Fig. 3.2: CD44 labels undifferentiated cells in the normal stem cell zone, i.e. the isthmus, of the gastric unit, and its loss stunts basal rates of proliferation. In the normal mouse gastric unit, CD44 labeled small, distinct cells in the isthmus region (A). Mice lacking the Cd44 gene have about half the number of proliferating cells per gastric unit compared to WT controls (B,

C). PEP-1 is a peptide inhibitor which blocks the interaction between hyaluronic acid and CD44. Treatment with PEP-1 for 5 weeks reduces basal rates of proliferation (D), and results in lower numbers of pit cells (E), similar to the $Cd44^{-/-}$ animals (E). In all figures: * $P < 0.05$, ** $P < 0.01$, *** $P < 0.001$.

$Cd44^{-/-}$ gastric units also showed stunting of the gastric unit zone between the gastric lumen and the isthmus, the pit/foveolar zone (Fig. 3.3A,B) and overall decreased census of pit cells (Fig. 3.2E), a phenotype that was recapitulated by 5-week treatment of WT mice with PEP-1 (Fig. 3.2E, 3.3C). Pit cells slough rapidly after emergence from the isthmal stem cell zone (half-life of ~3 days [46]) and would be expected to be most affected by decreased stem cell proliferation due to their high turnover rate. We also treated mice for 5 weeks with HA, which caused statistically significant increased isthmal cell proliferation (Fig. 3.3E, n=7) and pit/foveolar zones relative to wild type (Fig. 3.2E), showing that injection of the CD44 activating ligand was sufficient to induce increased proliferation and further confirming a direct role of CD44 signaling in regulating isthmal stem cell proliferation. PCs and other non-pit cell epithelial lineages did not differ in their baseline census whether CD44 was activated, inhibited or deleted (Fig. 3.3F). Taken together, our data indicate that CD44 is expressed in undifferentiated epithelial cells within the isthmus and regulates normal rates of gastric epithelial stem cell proliferation.

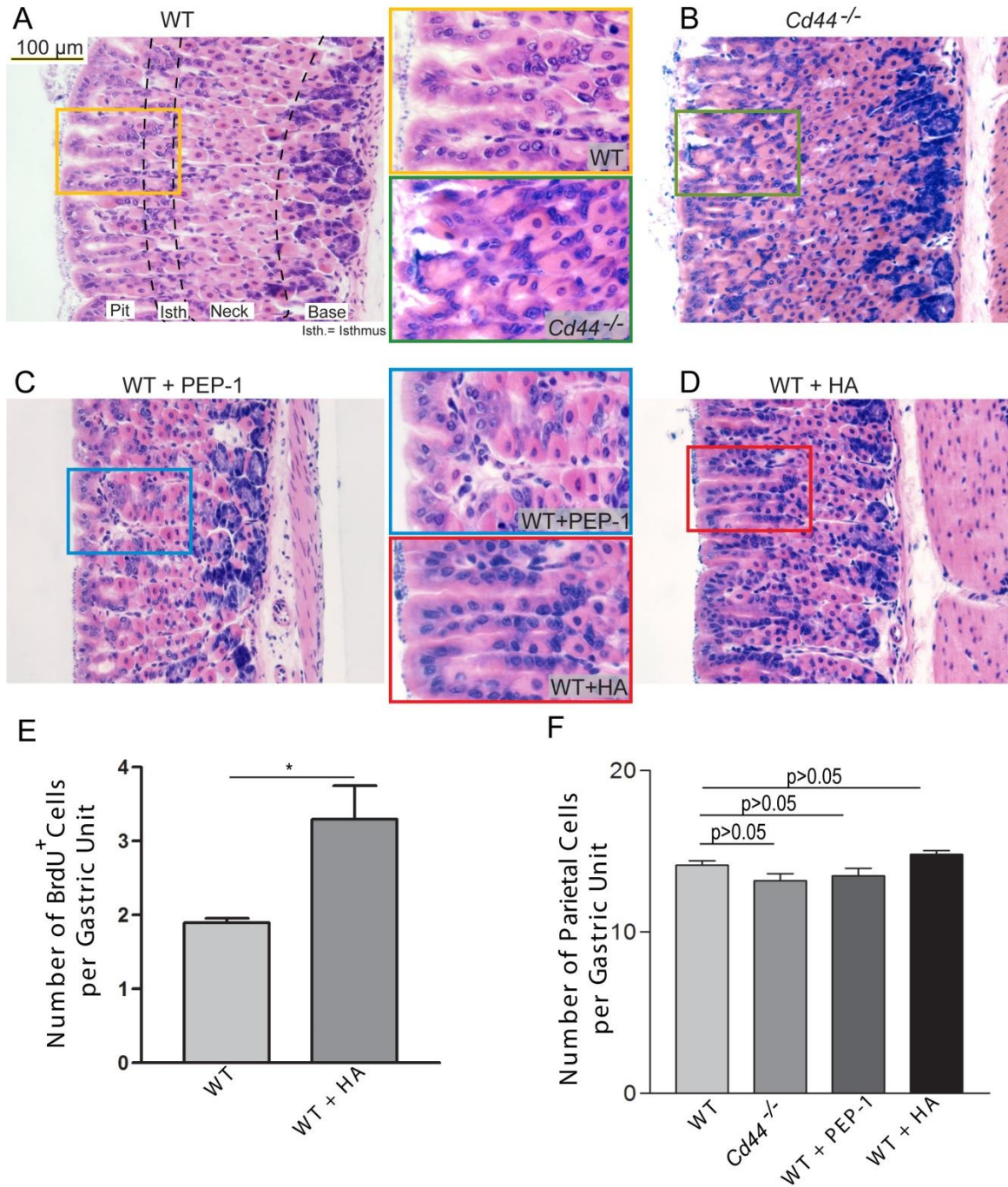


Fig. 3.3: Loss of functional CD44 caused abbreviated pit/foveolar regions. While wildtype mice showed long pit regions (A) with ~11 pit cells per unit (Fig. 1D), $Cd44^{-/-}$ mice showed shorter pits with almost 2-fold reduced number of normal foveolar cells per unit (B, Fig. 1D). Mice treated with PEP-1, showed a similar foveolar phenotype as $Cd44^{-/-}$ (C), whereas, those treated

with the CD44 ligand HA showed longer pit regions (D) with an average of ~13 foveolar cells per unit (Fig. 3.2D) and almost twice the rate of proliferation of WT mice (E). None of the conditions changed the parietal census significantly (F). In all figures: * $P < 0.05$, ** $P < 0.01$, *** $P < 0.001$.

Infection with Helicobacter pylori causes PC atrophy and expansion of CD44 into the base of gastric units

We sought to determine whether CD44 expression in gastric epithelial cells was affected by PC atrophy, which induces proliferation in mice and humans. Infection of humans with CagA⁺ strains of *H. pylori* is a major predisposing factor for the development of gastric adenocarcinoma [47]. We infected WT mice with a CagA⁺ strain of *H. pylori*, PMSS1, for 8 weeks (n=5 mice). As expected, in uninfected mice, there was no parietal cell death (Fig. 3.4A, left green arrowhead indicates a PC), and CD44 was expressed in the epithelium in the isthmus (Fig. 3.4B, C, left; orange arrowhead). In contrast, 8 weeks after *H. pylori* infection, most PCs were atrophic (Fig. 3.4A, right, note only rare residual PCs in a section of the gastric corpus, green arrowheads), and CD44 expression was found diffusely in the base of gastric units (Fig. 3.4B, C) in zymogenic cells which co-expressed the neck cell marker, GSII (yellow arrowheads), indicating they were metaplastic.

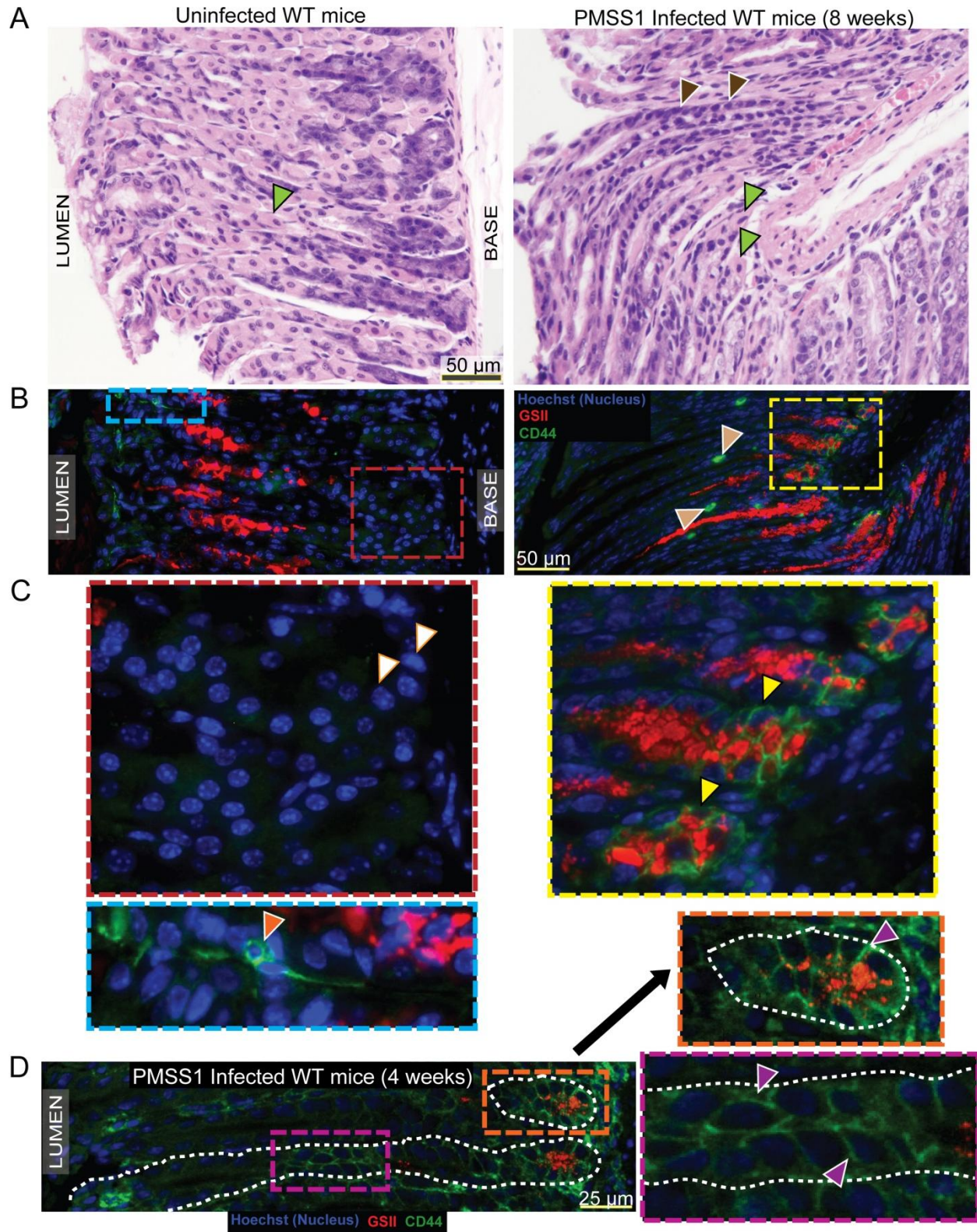


Fig. 3.4: Helicobacter pylori infection causes parietal cell atrophy and expansion of CD44

expression. Hematoxylin and eosin stained sections of wild-type, uninfected mice show healthy parietal cells (A, left, green arrowhead), whereas, those infected for 8 weeks with the *cag+* PMSS1 strain of *H. pylori* show diffuse loss of parietal cells (A, right). The gastric unit is largely replaced with metaplastic cells (A, right; brown arrowheads), and only a few parietal cells remain (A, right; green arrowheads). CD44 also labels occasional immune cells infiltrating interglandular regions (B, right; beige arrowheads). CD44 is expressed in the uninfected gastric epithelium in the isthmus (B,C blue box; orange arrowheads) but expands to the base of the unit upon infection with *H. pylori* (B, right, yellow box). In uninfected mice, the zymogenic cells do not express CD44 (C, left, white arrowheads), however, upon infection, they become metaplastic and express neck cell markers such as GSII (red) as well as CD44 (C, right, yellow arrowheads). In mice infected with *H. pylori* for a shorter time period of 4 weeks, (D), CD44 expansion can be seen to extend from the isthmus (purple box) and into the base (orange box) in some gastric units. Exemplar CD44⁺ cells are marked with purple arrowheads (D, insets); gastric units are outlined by dashed white line.

Tamoxifen induced parietal cell atrophy causes a burst of CD44+ progenitor cell proliferation

H. pylori infection in mice and humans is chronic and often focal and asynchronous across the stomach. Elucidation of the molecular mechanisms underlying atrophy-induced proliferation in the stomach requires a system for inducing atrophy that is synchronous, rapid, and global throughout the whole stomach. We have shown that a single injection of 5mg/20g body weight of tamoxifen causes dramatic rearrangement of the gastric mucosa, an effect that does not depend on the estrogenic or anti-estrogenic effects of tamoxifen but instead causes direct PC toxicity [26]. Fig 3.5 shows how within 3 days, over 90% of PCs atrophied, yet complete recovery of PC

census occurred by 21 days (Fig. 3.5A and [26]). As PCs atrophied, proliferation accelerated in the normal stem cell region, the isthmus, reaching 6-fold baseline levels by day 3 (Fig. 3.5B, C and ref [26]). Even by 12h, almost half of the PCs had atrophied, and isthmal progenitor cells could be seen expanding towards the base of the unit, the region vacated by dying PCs (Fig. 3.5B, C). Western blots showed that CD44 and the proliferation markers, PCNA and cyclin D1, increased throughout the gastric corpus (Fig. 3.5D).

In short, tamoxifen causes PC atrophy, increased CD44 expression, and proliferation, similar to infection with *Helicobacter* but has a rapid and synchronous timeframe for atrophy and injury response across the whole stomach allowing for biochemical analysis of the process. Furthermore, we have shown previously that tamoxifen treatment does not cause substantial inflammatory cell infiltrate [26]. Unlike infection with CagA⁺ *Helicobacter*; the changes are almost wholly confined to the mucosal cells already present at time of treatment, reducing confounding variables in analyzing differences in global analysis of changes in signaling pathways and gene expression.

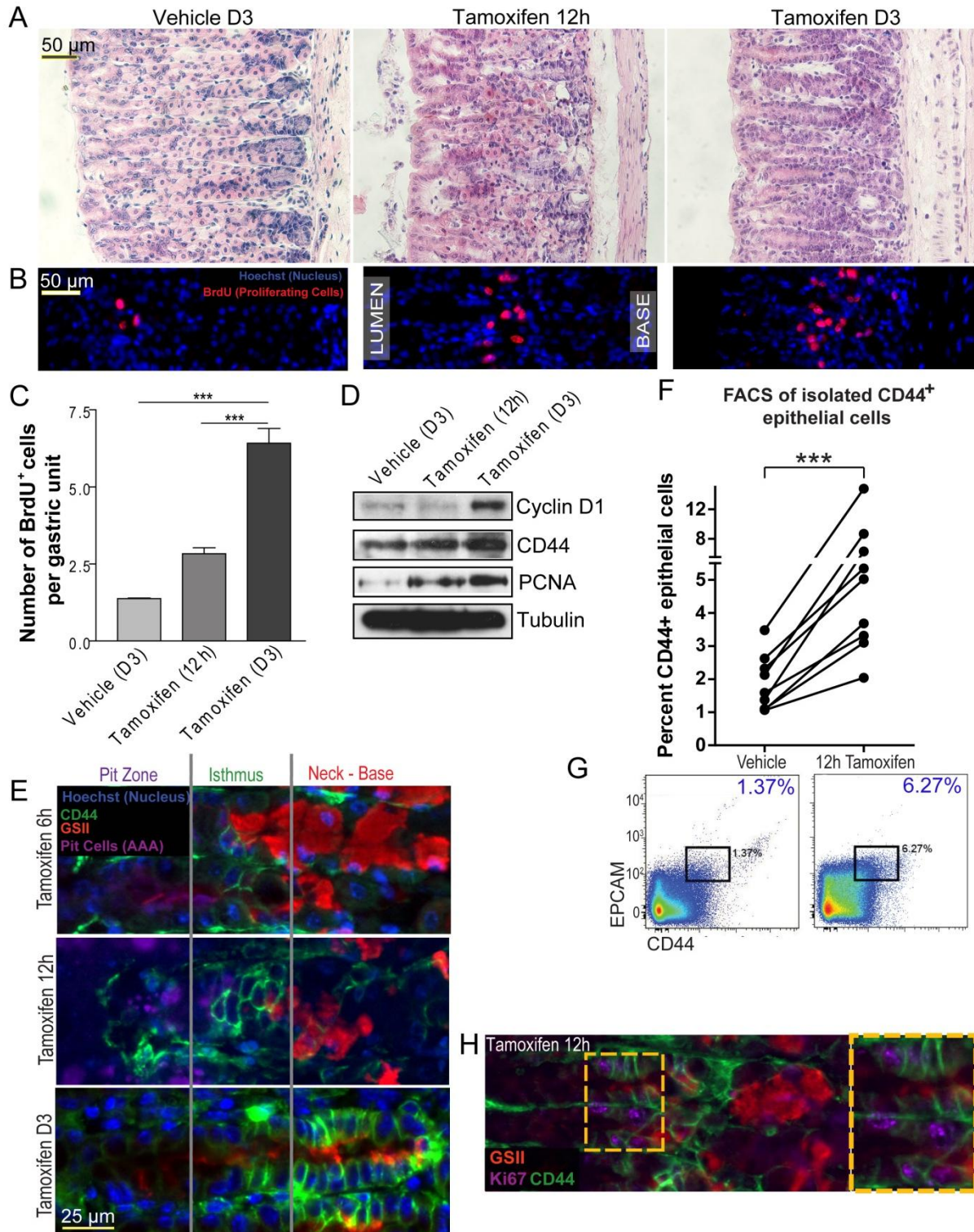


Fig. 3.5: CD44 expands and labels proliferating cells upon parietal cell atrophy and is required for this injury induced expansion of progenitor cells. Hematoxylin and eosin stained

sections of wild-type mice at 3 days (A, left) following intraperitoneal (i.p.) injection of vehicle, and, at 12 hours (A, middle) and 3 days (A, right) following i.p. injection of 5mg/20g body weight of tamoxifen. Wild-type mouse stomach treated with vehicle shows normal stomach epithelium, whereas, those injected with tamoxifen show a progressive loss of PCs. PC loss is coupled with an expansion in proliferation, measured by BrdU incorporation (stained in red), at 12 hours (B, middle; C) and 3 days (B, right; C) after tamoxifen treatment, compared to vehicle controls (B, left; C). Cyclin D1 and PCNA, which are markers of proliferation, are also increased on PC atrophy at 12h and day 3 by western blot of whole corpus stomach regions (D). The blot also shows that CD44 expression increases upon atrophy. A CD44⁺ epithelial population starts expanding from the time-point (6h) when PCs first begin to die (E) and reaches the base of the unit by day 3 (E). The number of CD44⁺ epithelial cells expands ~3-5 fold during this time, as shown by multiple FACS experiments (F). One of the FACS plots graphed in F is shown in G. Many CD44 expressing cells co-stain with Ki67 after treatment with tamoxifen (H, yellow box is magnified in inset at right).

We next set out to use tamoxifen-induced atrophy as a tool to determine the origin of CD44⁺ cells following PC atrophy. CD44⁺ isthmal cells began to expand as early as 6h after tamoxifen injection (Fig. 3.5E). The initial increase in CD44-positive epithelial cells occurred in the isthmal progenitor zone, from which they expanded into the base until there were CD44 and E-cadherin double positive epithelial cells from isthmus to base by D3 (Fig. 3.5E, Fig. 3.1B,C). This pattern was similar to the chronic CD44 labeling that occurred in the base of Helicobacter-infected corpus units. By day 3, many of the CD44⁺ cells in the base labeled SPEM-type metaplastic cells, co-labeling with GSII (Fig. 3.5E). We next decided to look at an earlier time point in our

Helicobacter infected mice (4 weeks post infection) to determine whether, in certain units, CD44⁺ cells could also be identified expanding from the isthmus as occurred shortly after tamoxifen-induced atrophy. Fig. 3.4D shows that, whereas many units already show full metaplasia with GS-II⁺/CD44⁺ cells only at the base, as in the 8-week post-infection animals, some units showed CD44 extending from isthmus to the base.

We next quantified the expansion of CD44⁺ epithelial cells. Their census increased ~3 to 5-fold over the course of the three day tamoxifen treatment, as determined by flow cytometry (n= 18 mice across 9 experiments) (Fig. 3.5F, G, Fig. 3.6).

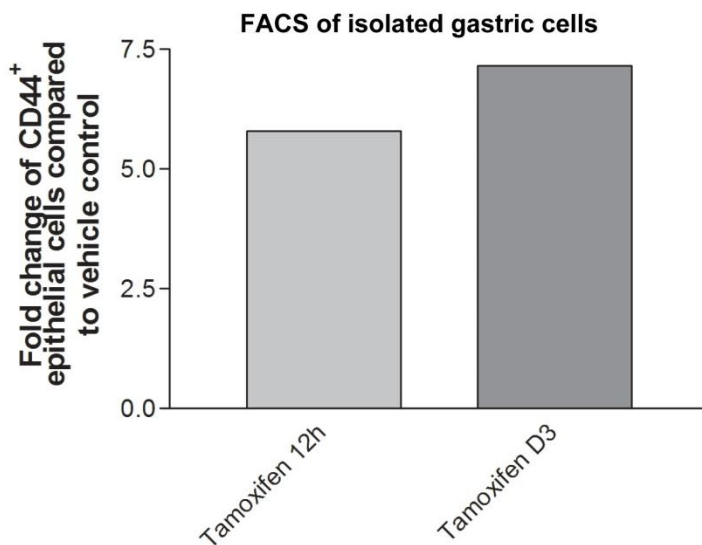


Fig. 3.6: CD44⁺ epithelial cells expand 5-7 fold upon parietal cell atrophy as quantified by FACS. A representative FACS graph from an experiment shows that CD44⁺ epithelial cells increase ~5-7 fold upon treatment with tamoxifen for 12h and day 3 compared to vehicle

controls.

Furthermore, there was extensive co-labeling of the CD44⁺ population (at 12h) with the proliferation marker Ki67 (Fig. 3.5H). CD44's activating ligand, HA, was found in the mesenchyme between gastric glands (Fig. 3.7A) and increased following atrophy, as did the enzymes that synthesize it, HAS1 and HAS2 (Fig. 3.7B).

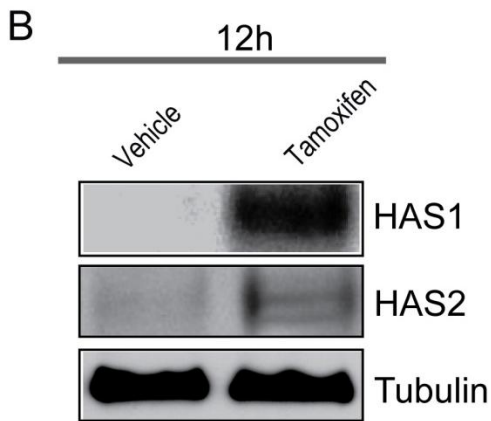
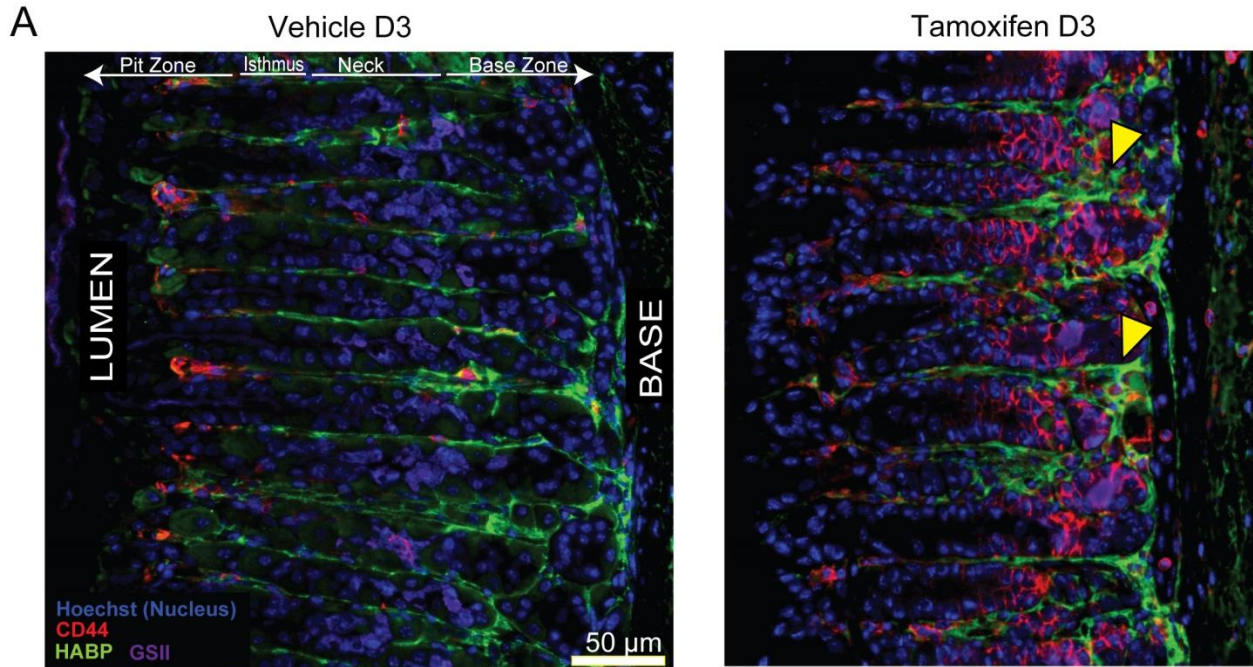


Fig. 3.7: Hyaluronic acid (HA), a ligand of CD44, was increased upon atrophic injury with tamoxifen. HA (stained using Hyaluronan-binding protein; in green) and CD44 (red) were increased in expression towards the base of the gastric unit during tamoxifen induced metaplasia (A, arrowheads). HAS1 and HAS2, enzymes that synthesizes HA, were also increased by 12h of tamoxifen treatment (B).

Thus, both CD44 and HA were increased in expression in tandem, following atrophy, with HA present in the region of the basement membrane of the epithelial cells expressing CD44. During response to PC atrophy, *Cd44*^{-/-} mice showed a statistically significant reduction in isthmal proliferation compared to controls (n=6 mice, 2 experiments) (Fig. 3.8A), and a short, 3 day pretreatment with PEP-1 was sufficient to nearly completely abrogate the proliferative response

induced by PC atrophy (Fig. 3.9; n=5, 2 experiments).

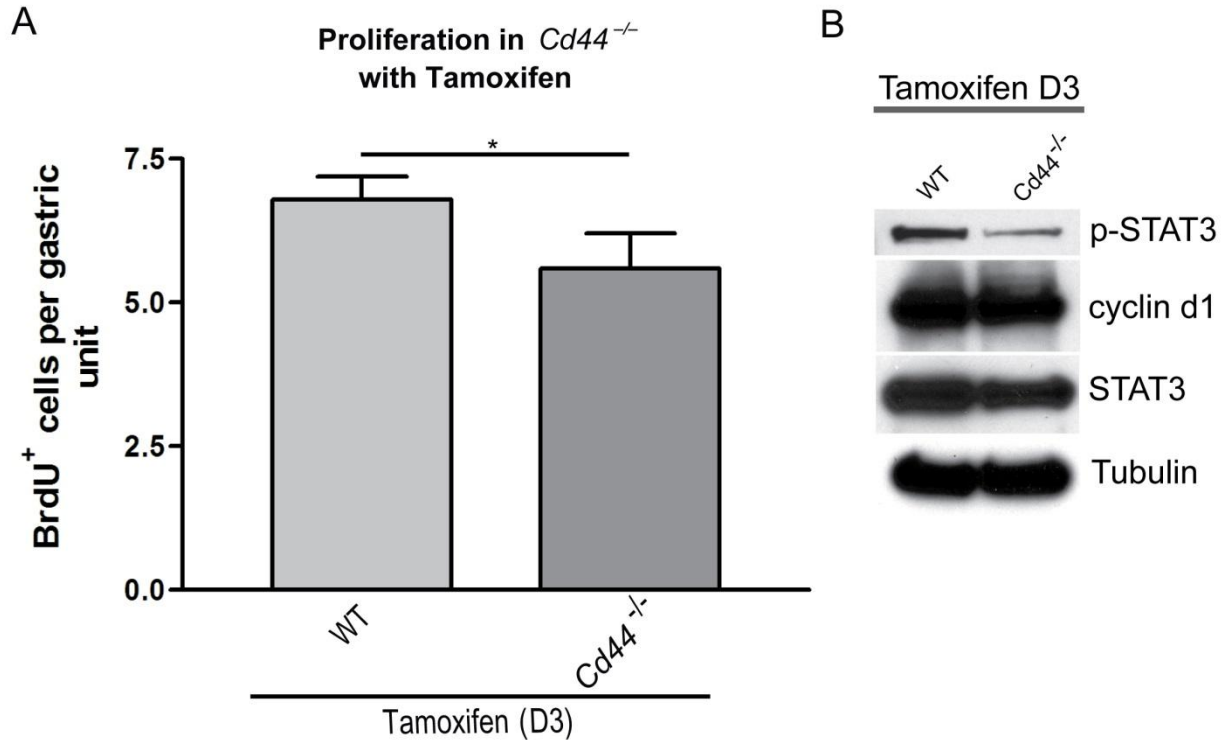


Fig. 3.8: $Cd44^{-/-}$ mice have compensatory mechanisms for increasing proliferation following tamoxifen induced atrophy. When treated with tamoxifen, $Cd44^{-/-}$ mice were able to increase proliferation to almost normal levels (A; one-tailed, paired Student's *t* test), despite the defect in basal levels of proliferation. Although there was a decrease in pSTAT3 in the $Cd44^{-/-}$ mice (B), similar to PEP-1 treatment (Fig. 6E), Cyclin D1 levels did not change in the $Cd44^{-/-}$ mice (B), suggesting that there might be a CD44-STAT3 independent compensatory mechanism in these mice that regulates proliferation in the face of atrophy.

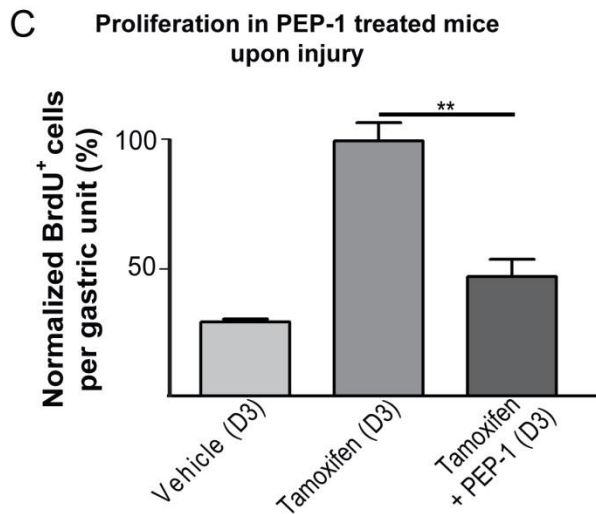
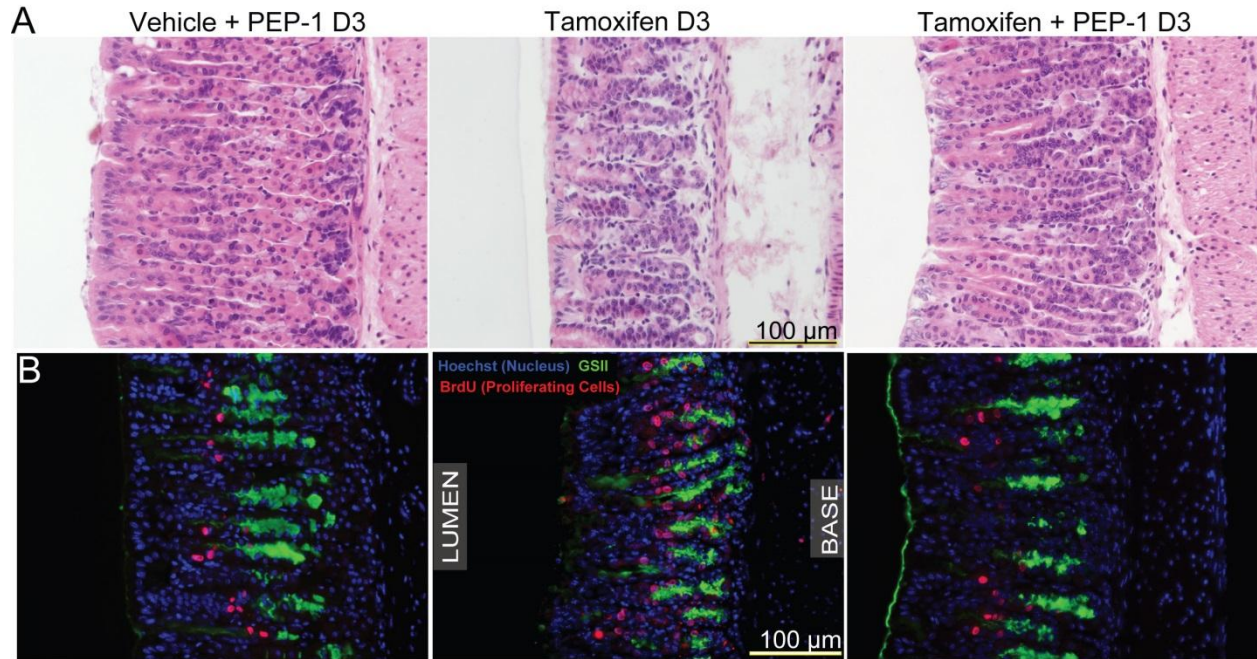


Fig. 3.9: CD44 is necessary for elevating the rate of progenitor cell proliferation upon induction of atrophy. PEP-1 blockade of CD44 activation halves atrophy induced proliferation (B, C), measured by BrdU incorporation (red, B), whereas parietal cells still die upon PEP-1 inhibition of CD44 (A).

Thus, both stem cell normal homeostasis and response to PC atrophy are mediated by HA-CD44 interactions, though in mice null for Cd44 from conception, compensatory mechanisms allow for some degree of non-CD44-mediated proliferation increase (note in Fig. 3.8B that atrophy still caused an increase in cyclin D1 expression in *Cd44*^{-/-} mice).

Therefore, our data show that CD44: (a) is expressed by cells in the normal stem cell compartment; (b) marks proliferating progenitor cells during injury, and; (c) is necessary for

maintaining the normal and injury-responsive proliferative capacity of the gastric units. We next sought to determine the mechanism by which CD44 regulates progenitor cell proliferation.

CD44 regulates gastric progenitor cell proliferation through STAT3

Signal transducer and activator of transcription 3 (STAT3) controls diverse cellular functions, such as growth, differentiation and apoptosis [48]. When activated by cytokines and growth factors, STAT3 localizes to the nucleus and regulates transcription of target genes that control proliferation and apoptosis [34, [48, [49]. STAT3 increases normal and cancer stem cell proliferation [50] by inducing its targets survivin and cyclin D1 [51, [52] and is activated by *cagA*⁺ strains of *H. pylori* in host cells, *in vitro* and *in vivo* [53]. CD44 increases cyclin D1 expression by directly interacting with active STAT3 [54]. As we observed increased proliferation and cyclin D1 expression in the CD44-dependent response of the gastric unit to PC atrophy, we hypothesized that the mechanism of CD44 action might be via STAT3-cyclin D1. Consistent with our hypothesis, we found that while activated STAT3 (STAT3 phosphorylated on Tyr 705) was at low levels in normal mucosa, there was abundant p-STAT3 during atrophy (Fig. 3.10A). We then checked whether STAT3 bound CD44 by co-immunoprecipitation and found indeed that there was more CD44 associated with STAT3 in response to atrophy (Fig. 3.10B) when compared to controls. Immunoprecipitated STAT3 was phosphorylated only in tamoxifen treated samples and not in control or *Cd44*^{-/-} stomachs (Fig. 3.10B). STAT3 phosphorylation was also decreased in the absence of CD44 or when CD44-HA interactions were blocked by PEP-1 (Fig. 3.10C, 3.8B). CD44 expression was also reduced by PEP-1 blockade of its HA ligand (Fig. 3.10C). When we blocked STAT3 activation by injecting its specific inhibitor, WP1066 [55], with and without tamoxifen, we found that STAT3 inhibition greatly reduced

atrophy-induced cyclin D1 expression and stem cell proliferation (Fig. 3.10D,E), without affecting CD44 expression (Fig. 3.10E). Hence, we conclude that STAT3 is activated upon injury in the gastric epithelium, and CD44 binds to STAT3 to regulate the injury-induced burst of proliferation of progenitor cells.

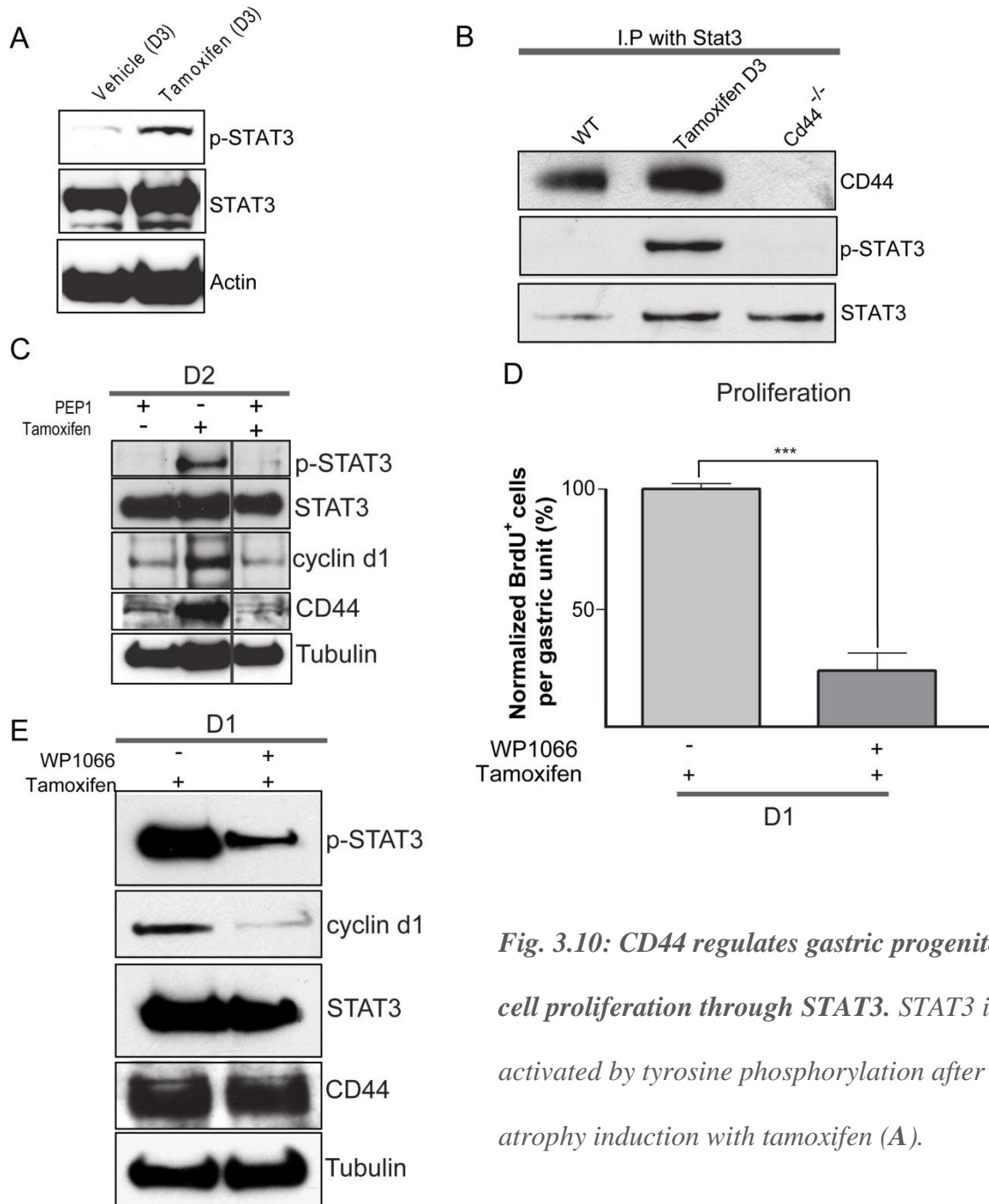


Fig. 3.10: CD44 regulates gastric progenitor cell proliferation through STAT3. STAT3 is activated by tyrosine phosphorylation after atrophy induction with tamoxifen (A).

IP with antibody against STAT3 followed by Western blot for CD44 shows increased association between CD44 and STAT3 during tamoxifen-induced atrophy, compared to controls; also phosphorylated STAT3 was pulled down only during tamoxifen induced atrophy (B). Inhibition of STAT3 and CD44 functions (using WP1066 and PEP-1 respectively) causes decreased Cyclin D1 expression (C, E) and proliferation as quantified in tissue using BrdU (D); “D1”= 1 day post tamoxifen; “D2” = 2 days. CD44 levels were not affected by STAT3 inhibition, whereas, pSTAT3 was significantly reduced upon CD44 inhibition with PEP-1 (C, E). CD44 expression is reduced upon blocking interaction with its HA ligand by PEP-1 (C).

ERK signaling regulates progenitor cell proliferation through CD44

To determine the upstream signal causing CD44 expansion and increased proliferation, we surveyed multiple signaling pathways known to affect proliferation, such as the MAP kinases (p38MAPK, ERK, and JNK), AKT, and PLC γ in tamoxifen-induced atrophy. Whereas most proliferation mediators were either not substantially or only marginally increased, there was a dramatic increase in active ERK at the time of peak atrophy (Fig. 3.11A). ERK is known to increase proliferation in normal [56] as well as neoplastic cells [56, [57], though its role in gastric stem cell homeostasis has not previously been assessed. Accordingly, ERK was strongly activated as early as 6 hours after treatment with tamoxifen (Fig. 3.11B), which was further confirmed by the concomitant increase in expression of its downstream target, EGR1 as well as CD44 (Fig. 3.11B) [58]. If ERK signaling was indeed involved in regulating proliferation in the gastric epithelium following PC atrophy, blocking it should block atrophy-induced proliferation. ERK phosphorylation can be blocked with the kinase-specific inhibitor of MEK, U-0126 [59]. We co-injected mice intraperitoneally with U-0126 along with tamoxifen. Fig. 3.11C shows that

U-0126 successfully blocked ERK phosphorylation in the stomach during tamoxifen-induced atrophy and prevented a downstream increase in ERK's transcriptional target EGR1 [60, [61]. Confirming our hypothesis that pERK mediates PC-atrophy induced CD44, U-0126 injection into mice blocked the increase in CD44 (n= 10 mice across 3 experiments) (Fig. 3.11C). We observed similar results with another inhibitor of ERK activation, PD 98059 [62] (unpublished data; n= 3 mice, two experiments). As expected, ERK inhibition also blocked the proliferative response to atrophy (Fig. 3.11D, E), much like loss or inhibition of CD44. BrdU incorporation per gastric unit, at 12h post tamoxifen treatment, was reduced by $56 \pm 5\%$ (n=3 mice; 50 gastric units counted per mouse) in mice treated with U-0126 compared to those receiving tamoxifen and vehicle.

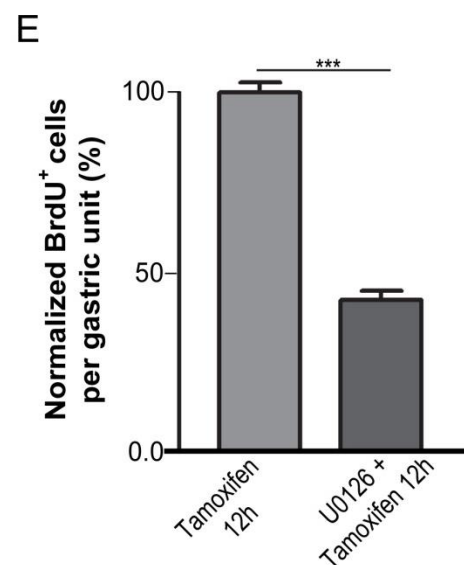
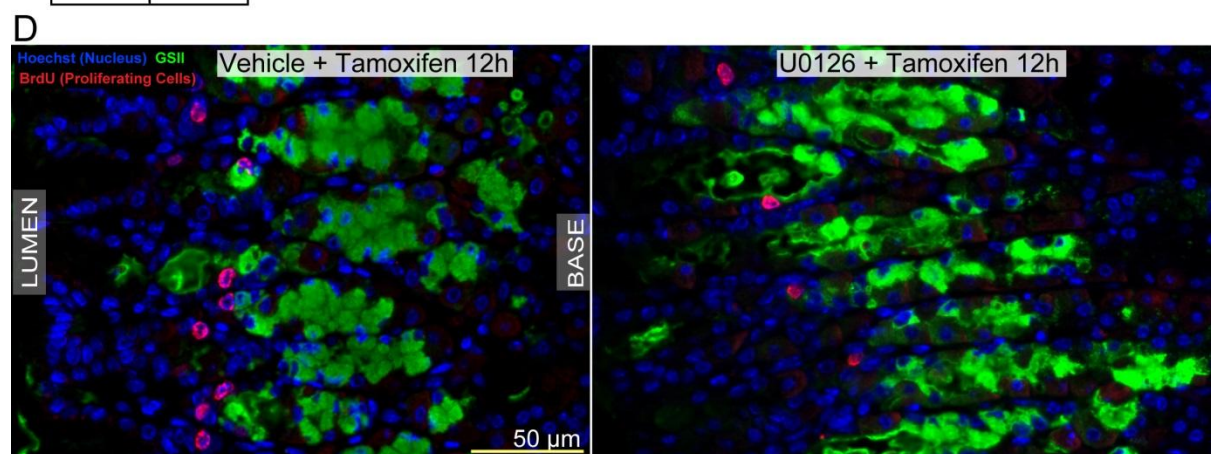
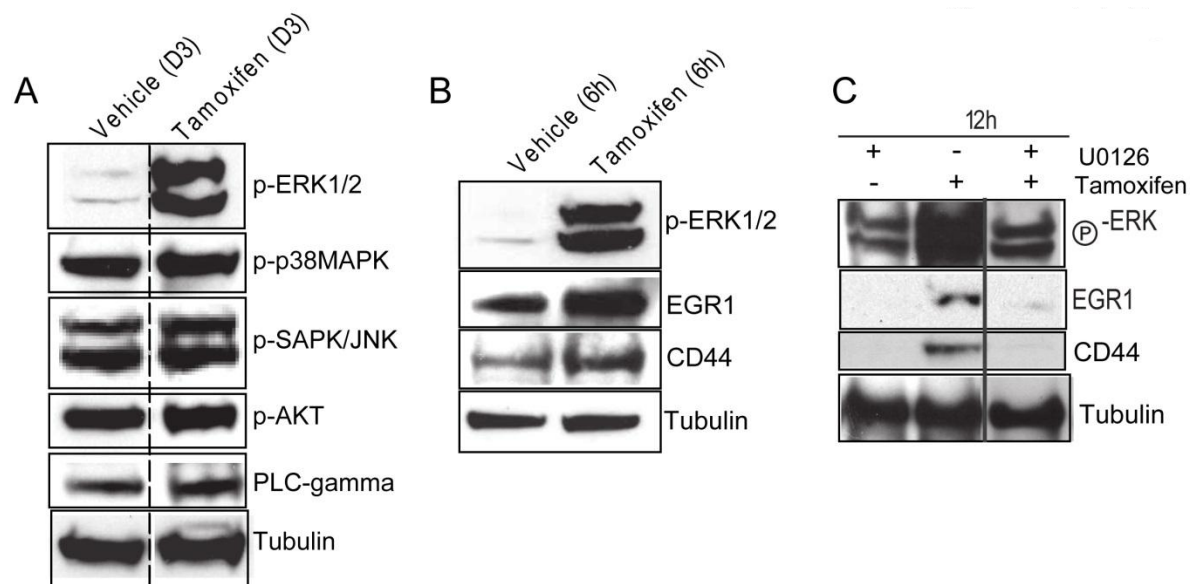


Fig. 3.11: ERK signaling is activated early upon

induction of injury and is required to induce CD44.

Western blots of candidate signaling pathways that might be involved in increasing the proliferative response after PC atrophy by tamoxifen (A). Of the pathways analyzed, only ERK signaling shows a dramatic increase in activation after tamoxifen, compared to vehicle controls. ERK1/2 are tyrosine phosphorylated soon after PC damage ensues (6 hours after tamoxifen treatment);

EGR1 and CD44, downstream targets of ERK signaling, are already increased in expression at this early time point (B). Co-injection of tamoxifen with U-0126, a specific inhibitor of ERK phosphorylation, mutes the metaplastic induction of pERK along with downstream targets, EGR1 and CD44 by western blot (C), and mutes the proliferative response shown by BrdU immunostaining in red (D), quantified in (E).

ERK signaling is increased in multiple models of gastric metaplasia and labels isthmal cells

If ERK activation mediates the expansion of stem/progenitor cells, then phosphorylated ERK should be identifiable within those cells. In agreement, Fig. 3.12A, B show that, whereas control mice showed no detectable pERK, 6 hours following induction of atrophy, we identified 2-3 undifferentiated cells per unit with nuclear pERK within the canonical isthmal stem cell zone (Fig. 3.12A, B). pERK could also be detected in multiple cell nuclei per unit in *tox176* mice [63] that show constitutive PC atrophy due to PC-specific expression of attenuated diphtheria toxin (unpublished data) and in mice 8 weeks after infection with *Helicobacter* (Fig. 3.14A, right panels) whereas pERK was completely absent in uninfected controls (Fig. 3.14A, left panels).

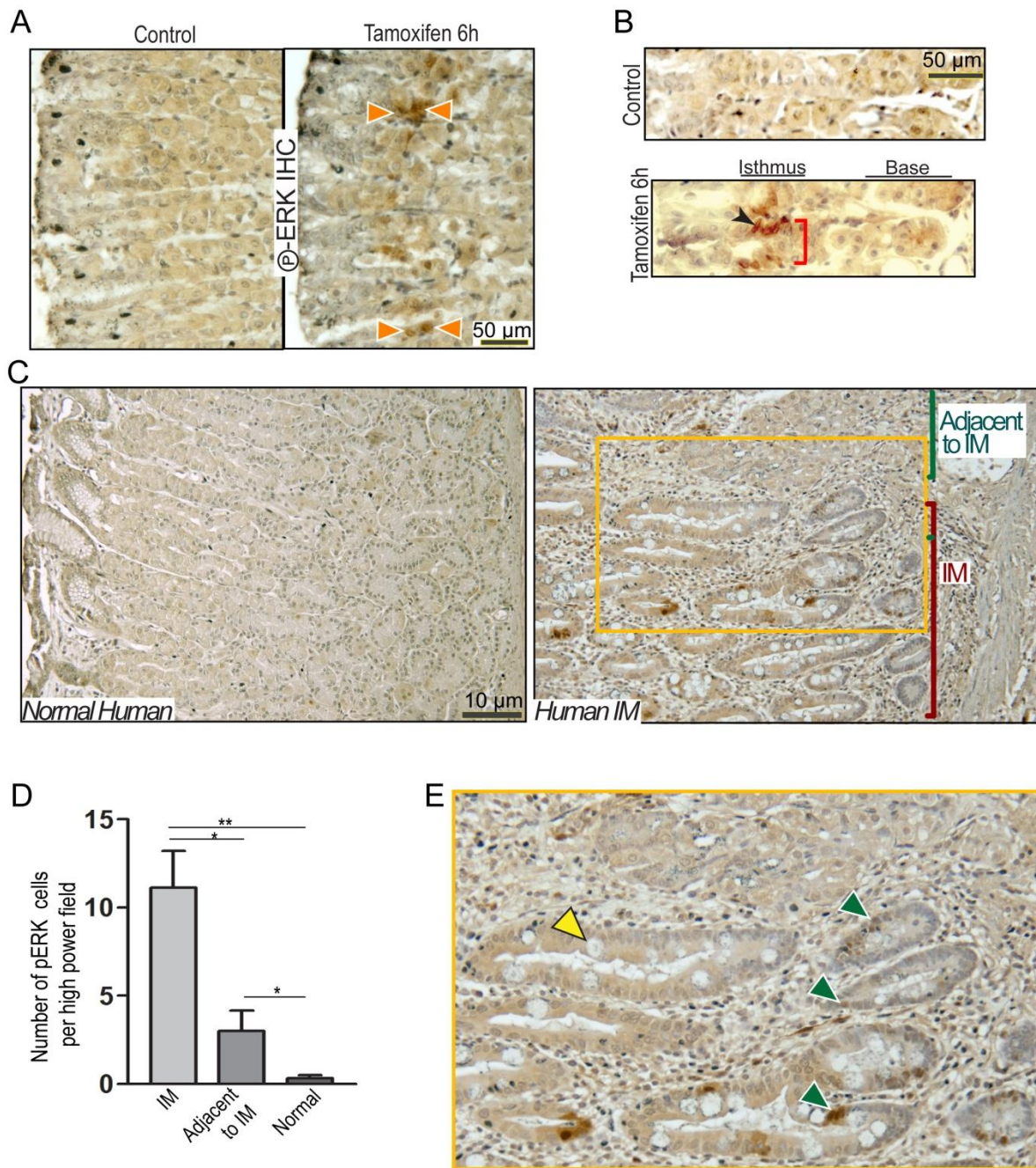


Fig. 3.12: pERK labels metaplasia-associated cells in mice and humans. pERK labels nuclei of isthmal progenitor cells (orange arrowheads) at 6 hours of tamoxifen treatment (A, B), whereas, there is no pERK signal in vehicle treated controls. PCs do not stain positive for pERK in either vehicle or tamoxifen treated mice. Gastric units of human patients showing focal intestinal metaplasia (C, right) in a region with mixed gastric and intestinal differentiation (magnified in

E), indicating transitional/early metaplasia (goblet cell is marked with a yellow arrowhead) stain positive for pERK (green arrowheads). Quantification of pERK expression in human IM patients (n=3) displaying such a transitional epithelium by counting the number of pERK⁺ cells in the 'intestinal metaplasia (IM)' regions and in residual gastric-differentiation regions 'adjacent to IM' epithelium vs. those in normal humans, shows a dramatic increase in pERK⁺ cells in IM regions, with a significant increase in pERK⁺ cells even in gastric regions adjacent to IM when compared to normal human patients (D).

Serial histological sections immunostained with anti-pERK and anti-CD44 from mice injected with tamoxifen for 12h showed a population of positive cells in the same location in the isthmus (Fig. 3.13).

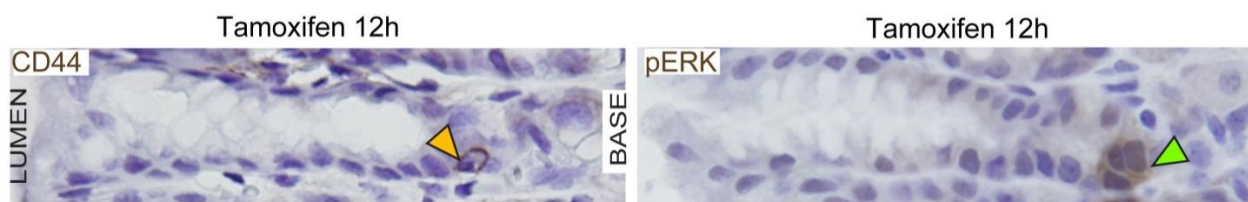
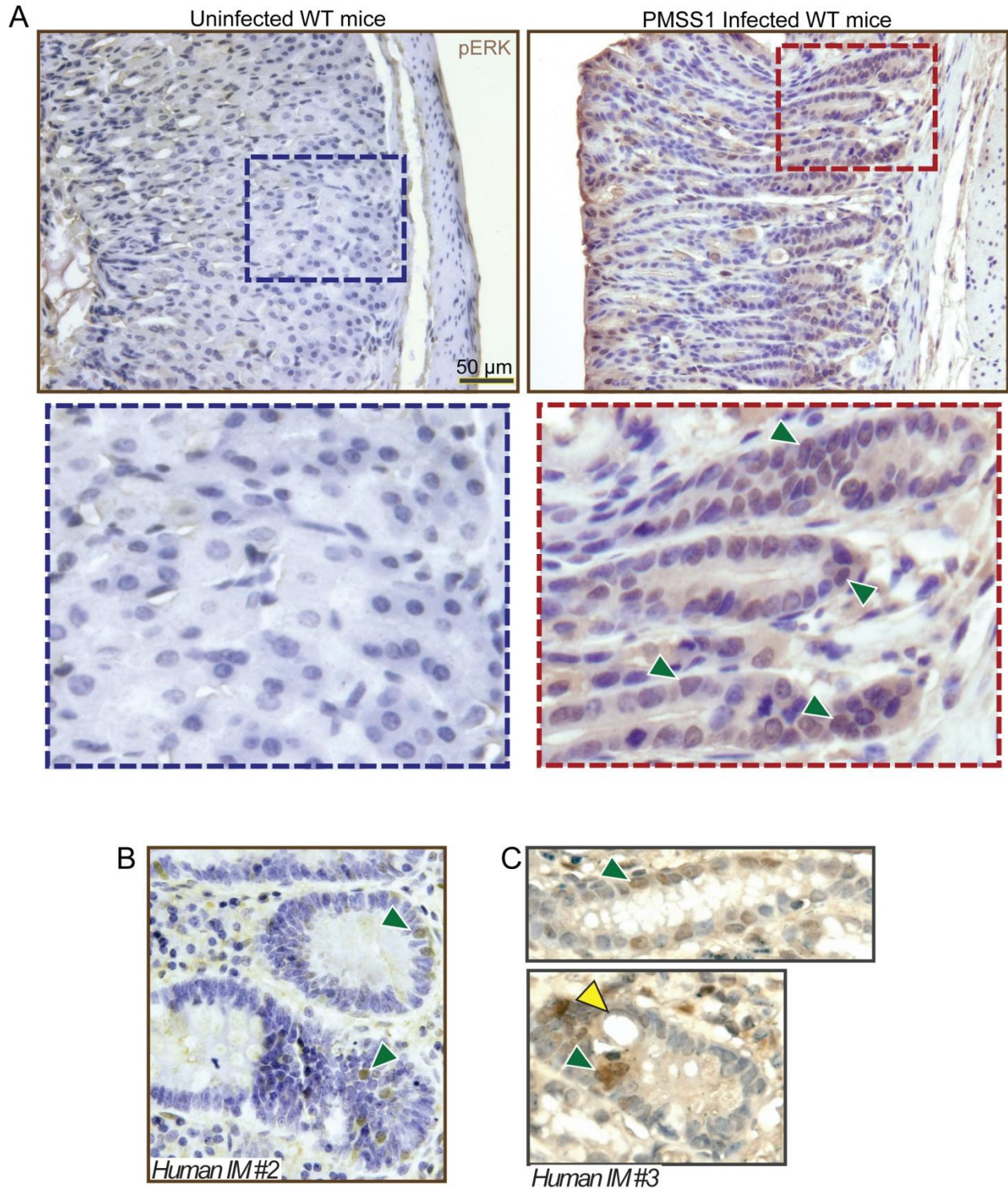


Fig. 3.13: CD44 and pERK label the same population of cells as they start expanding from the isthmus during tamoxifen induced metaplasia. Immunohistochemical staining of serial sections of mouse stomachs treated for 12h with tamoxifen show that CD44 (yellow arrowhead) and pERK (green arrowheads) label a similar, overlapping population of isthmal cells during atrophy.

Finally, we examined a small cohort (n=3) of human gastric resection specimens for pERK staining [10]. pERK⁺ cells were almost never observed in normal control stomach specimens (Fig. 3.12C) or in regions without atrophy. However, pERK⁺ epithelial cells could be found in regions of gastric differentiation neighboring or contiguous with intestinal metaplasia (Fig. 3.12C, magnified in 3.12E). pERK⁺ cells were also particularly prominent in intestinal

metaplasia lesions that neighbored regions of gastric differentiation. To test this pattern of pERK staining in regions of transition between normal and metaplastic differentiation in a broader cohort of samples, we extended our study to include ten more gastric specimens with chronic parietal cell atrophy and inflammation caused by infection with *Helicobacter pylori*.

The specimens were acquired in collaboration with an international consortium studying gastric carcinogenesis in Nicaragua (<http://gcbiomarkers.org/>). 8/10 of these specimens showed the same pattern of pERK staining, with high pERK staining in transition regions adjacent to metaplastic tissue. One specimen did not display metaplasia nor did it stain with pERK. The remaining sample did not stain with pERK even though it displayed intestinal metaplasia. We took 3 random pERK stained patient slides and quantified regions showing transitions between gastric and intestinal differentiation. In regions of intestinal metaplasia with residual gastric epithelium, there were 11 ± 3.46 pERK⁺ cells per high power field of 60X magnification (quantification from n=3 different patient specimens, representative of staining patterns observed in 9/11 specimens; $p < 0.01$). In the gastric epithelium adjacent to intestinal metaplasia, pERK-positive cells were also increased significantly (3.67 ± 1.15 per hpf, $p < 0.05$) compared to regions in the same specimens that had residual normal differentiation patterns with preserved parietal cells (~ 0.33 pERK⁺ cells per hpf) (Fig. 3.12D; Fig. 3.14B,C).



*Fig. 3.14: ERK signaling is activated after parietal cell atrophy in both, humans and mice. Immunohistochemical staining for pERK showed numerous positive nuclei of metaplastic cells in mice infected with the PMSS1 strain of *H. pylori* (A; green arrowheads), whereas uninfected*

controls did not stain positive for pERK (A). pERK staining was also observed in gastric tissues of human patients undergoing intestinal metaplasia (B, C; green arrowheads) in regions of transition between normal gastric tissue and glands developing early intestinal metaplasia with appearance of goblet cells (yellow arrowhead).

Given the data in humans and mice, we posit that activation of ERK signaling plays a key role in the cell proliferative response to PC atrophy and is the upstream regulator of the CD44-STAT3 proliferation axis.

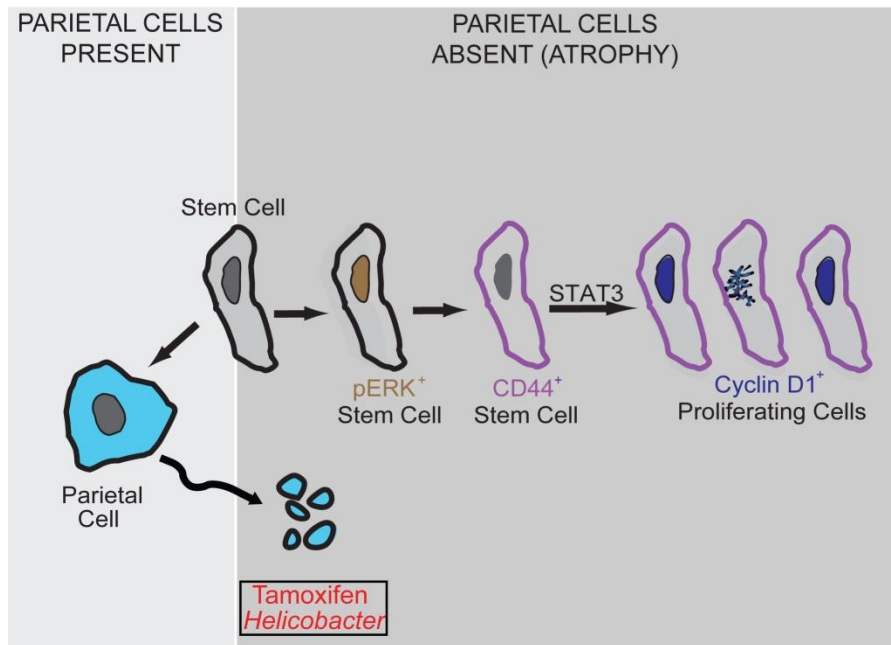


Fig. 3.15: Model for stem/progenitor cell renewal during normal and atrophic injury conditions. The isthmal stem cell (SC) is self-renewing and also gives rise to acid-secreting parietal cells (PCs), among other cell-types within the stomach. Upon atrophy of PCs, by toxins or *H. pylori* infection, the SCs activate ERK to ramp up proliferation. ERK activation is required for expanded CD44 expression and the association between CD44 and pSTAT3, which in turn, upregulates Cyclin D1 to drive proliferation.

Discussion

Here we demonstrate that parietal cell atrophy, which increases the risk for gastric cancer [64], causes increased isthmal stem/progenitor cell proliferation, which depends on activation of ERK. ERK induces CD44, which is critical for both normal proliferation and the atrophy-induced expansion. CD44 signaling maintains normal proliferation and increases proliferation following PC atrophy via interaction with its ligand HA. STAT3 binds CD44 and is phosphorylated only when CD44 is present and can interact with its ligand HA. Inhibition of STAT3 phosphorylation inhibits atrophy-induced stem cell proliferation but does not affect increased expression of CD44. Thus, we conclude that atrophy-induced proliferation depends on an ERK→CD44→STAT3 axis.

To our knowledge, this is the first report delineating an *in vivo* mechanism for isthmal cell expansion almost immediately after PC damage and atrophy. We utilize tamoxifen treatment as a rapid, synchronous, and inducible model for PC atrophy that recapitulates what we observe in mice in chronic *Helicobacter pylori* infection. Soon after PC atrophy begins, there is a dramatic increase in activation of ERK in isthmal cells, possibly due to release of a damage-induced pro-proliferative signal or loss of a proliferation-inhibiting signal from the surrounding PCs. Our finding that ERK is critical for inducing stem cell proliferation is consistent with other reports. In the juvenile rat, premature weaning also induces isthmal proliferation that depends on ERK signaling [65]. In patients infected with *H. pylori*, it has been proposed that bacterial CagA activates the ERK cascade in gastric epithelial cells, which initiates the development of gastric cancer [66]. It has also been shown that systemic constitutive activation of the K-ras oncogene, which is upstream of ERK in the ERK-MAPK pathway, causes gastric hyperplasia and increased proliferation [67]. It appears that ERK is a consistent injury-induced proliferative signal in

precancerous lesions of the gastrointestinal tract, such as esophageal dysplasia [68], Barrett's adenocarcinoma cells [69] and pancreatic ductal adenocarcinoma [70].

Once active, ERK increases the expression of its target CD44. CD44 expression expands from the isthmus soon after PC damage. CD44 is a well-known cancer stem cell marker and co-labels proliferating cells in the gastric epithelium upon injury. CD44 labels a population of cells that includes the LGR5⁺ population in the bases of the pyloric glands [19] (unpublished data); however, we show here it also labels occasional, small epithelial cells in the corpus gastric unit isthmus. Lack of CD44 signaling, in *Cd44*^{-/-} mice and in mice treated with PEP-1, stunts stem cell proliferation. *Cd44*^{-/-} mice display a defect in the numbers of pit cells possibly due to faster turnover rate of these cells compared to parietal and other epithelial cells, which leads to an accumulation of the deficit over time. Another explanation for this observation could be that CD44 might regulate pit cell progenitor proliferation selectively, since we do observe mesenchymal CD44 accumulation adjacent to pit cells. When subjected to PC injury by tamoxifen, the PEP-1 mice are unable to elicit the same proliferative response as control mice, whereas *Cd44* nulls are better at coping with PC atrophy, probably due to compensatory mechanisms established during lifelong lack of CD44. This is confirmed by the fact that while PEP-1 treated mice do not show an expansion in cyclin D1 expression following injury, the *Cd44*^{-/-} mice are still able to elevate cyclin D1 to control levels, suggesting they have developed other ways of responding to injury that are independent of the normal CD44-dependent mechanism. Both PEP-1 treated and *Cd44*^{-/-} mice, when injured with tamoxifen, undergo PC atrophy, establishing that the proliferative response is downstream of the initial attack of tamoxifen, i.e. the ablation of PCs (note in Fig. 3.9C, PEP-1 treated mice have lower proliferation, even though there are almost no PCs remaining). It will be interesting to see

whether loss of CD44 in *Cd44*^{-/-} or PEP-1 inhibited mice affects the course of *H. pylori* infection. In addition to its role in proliferation, CD44 has recently been shown to impart cells with resistance against reactive oxygen species (ROS) [71]. As most gastric pathology involves inflammatory responses, and inflammation induces the release of ROS, CD44 might play a dual role in overcoming such injurious stimuli – by increasing proliferation and protecting the dividing cells from the surrounding toxicity, thereby increasing their lifespan.

CD44 induces cyclin D1 by associating with active STAT3 [54]. Abolishing STAT3 activity decreases proliferation in spite of PC atrophy, without affecting Cd44 expression. Tamoxifen treated *Cd44*^{-/-} and PEP-1 injected mice show reduced pSTAT3, establishing a role for CD44 in STAT3 activation in a feed-forward proliferation circuit. Interestingly, *Cd44*^{-/-} mice are able to increase cyclin D1 without the presence of active STAT3, confirming that the CD44-independent mechanism regulating proliferation in cases of acute PC injury is also STAT3-independent. As PEP-1 has a more dramatic effect on atrophy induced proliferation than loss of CD44, it is possible that HA signaling through its other receptors, such as TLR4 [72], which would be blocked by PEP-1 but would still function in *Cd44*^{-/-} mice, might compensate loss of CD44. However, treating *Cd44*^{-/-} mice with PEP-1 does not further reduce the rate of proliferation in uninjured mice (unpublished data), suggesting that HA receptors other than CD44 might not play key roles in maintaining normal stem cell turnover. Taken together, it appears that the ERK→CD44→STAT3 axis is involved in expansion of proliferating isthmal stem/progenitor cells under conditions of acute injury.

There is only a scant literature on the intracellular signaling pathways that regulate non-neoplastic turnover of progenitor cells in the corpus [4]. On the other hand, some of the signals regulating stem cell response extrinsically have been identified. For example, Sonic hedgehog

and BMP2/4/7 are critical for regulation of normal stem cell turnover because deficiencies in those factors cause increased isthmal proliferation [73, [74], though those effects might be indirect via loss of PCs causing decreased acid and increased gastrin, which is a known corpus stem cell mitogen [75, [76]. Gastrin works in part by stimulating histamine release by enterochromaffin cells, which also regulates proliferation of isthmal stem cells [77, [78, [79]. EGFR stimulating factors like EGF, TGF α , and Amphiregulin work through ERK and other downstream signaling pathways; all cause increased proliferation [80, [81].

It is unclear which ligand stimulates activation of ERK in the responsive isthmal cells. It might be derived from neighboring dying PCs. We do not believe the early stem cell response to atrophy we observe depends on gastrin, as gastrin transcript levels are unchanged until at least 3 days following tamoxifen treatment [26]. Signaling through the EGFR receptor tends to cause pit/foveolar cell specific proliferation as opposed to stimulation of the multipotent, isthmal stem cell [82]. Thus, EGF family ligands are less likely candidates.

Inhibition of the ERK pathway decreases proliferation and CD44 expression. Though regulation of biological processes like proliferative response to injury in vivo is undoubtedly complex, we posit three possible, non-mutually exclusive mechanisms by which ERK could mediate increase in CD44. First, ERK activation could increase CD44 transcriptionally leading to an increase in CD44⁺ cell proliferation. Second, ERK could increase proliferation of CD44⁺ isthmal cells, without increasing CD44 expression directly. Third, ERK signaling could increase HA in the basement membrane/mesenchyme by directly activating HAS, which in turn would increase CD44-dependent proliferation. Our data support the first interpretation. The second mechanism does not seem plausible because if it were true, then blocking CD44 action would not affect proliferation, yet our data show that CD44 is necessary for atrophy-induced increase in

proliferation. The third interpretation seems less likely because we observe pERK in isthmal cells in the epithelium as early as 6h after atrophy induction, just before CD44⁺ cells start expanding from the same region. We do not observe pERK in the mesenchyme, so there are likely to be other mechanisms leading to upregulation of HAS.

It is intriguing to speculate that the resident CD44⁺ epithelial population in wild-type mice might mark a normal corpus stem cell, as these cells are isthmal, occasional, have high N:C ratio under normal conditions and expand greatly upon injury. CD44⁺ cells also co-label with LGR5⁺ cells in the antrum/pyloric region of the stomach, which can regenerate the entire pyloric unit, consistent with multipotency.

One seeming paradox in our CD44 data is that loss of CD44 under homeostatic conditions decreases census of surface/pit cells, whereas, during response to parietal cell atrophy, it affects proliferation of cells expanding away from the pit zone and into the base. One explanation is that in homeostasis, pit cells turnover far more rapidly than any other cells in the gastric unit, so defective CD44 signaling manifests as decreased census of those cells. During parietal cell atrophy, there is rapid turnover of parietal cells, deeper in the unit, so CD44 mediates expansion of cells towards the base of the unit to replace the lost parietal cells.

Lifetime risk for development of gastric cancer has been reported to be decreased only partially by eradication of *Helicobacter pylori* [15, [16, [17]. It is likely that aberrant epithelial differentiation patterns, such as atrophy, metaplasia and increased proliferation, persist after treatment and must also be treated to reduce cancer risk substantially. The experiments in the current study identify both the novel role of a specific signaling pathway involved in the proliferative response to PC atrophy and show, as a proof of principle, that those pathways can be pharmacologically inhibited at multiple steps. Ultimately, the identification of clear

pharmaceutical targets in the metaplasia/atrophy sequence might be critical for reversing the risk for cancer progression from precursor lesions.

Acknowledgements

We thank the Washington University Digestive Diseases Research Core Center (DDRCC), DDRCC Biobank, and Morphology Core, Developmental Biology Histology and Morphology Core (Washington University), the Digestive Diseases Center of Texas Medical Center, and the Vanderbilt University Digestive Disease Research Center. We also thank Vincenza Guzzardo (University of Padua) for technical support, Drs. Reyna Victoria Palacios Gonzalez (Managua, Nicaragua) and Hala El-Zimaity (University Health Network, Toronto) for pathological diagnoses, and Dr. Lawrence Paszat for funding and coordinating acquisition of Nicaraguan samples.

Funding: DK079798-3-42P30 DK052574–12DK33165DK55753R01 DK58587R01 CA 77955P01 116037F32 CA 153539P30 DK 508404 National Institutes of Health

References

1. Ferlay, J., et al., *Estimates of worldwide burden of cancer in 2008: GLOBOCAN 2008*. Int J Cancer, 2010. **127**(12): p. 2893-917.
2. Roder, D.M., *The epidemiology of gastric cancer*. Gastric Cancer, 2002. **5 Suppl 1**: p. 5-11.
3. Correa, P. and J. Houghton, *Carcinogenesis of Helicobacter pylori*. Gastroenterology, 2007. **133**(2): p. 659-72.
4. Mills, J.C. and R.A. Shivdasani, *Gastric epithelial stem cells*. Gastroenterology, 2011. **140**(2): p. 412-24.
5. Nomura, S., et al., *Spasmolytic polypeptide expressing metaplasia to preneoplasia in H. felis-infected mice*. Gastroenterology, 2004. **127**(2): p. 582-94.
6. Nozaki, K., et al., *A molecular signature of gastric metaplasia arising in response to acute parietal cell loss*. Gastroenterology, 2008. **134**(2): p. 511-22.
7. Bredemeyer, A.J., et al., *The gastric epithelial progenitor cell niche and differentiation of the zymogenic (chief) cell lineage*. Dev Biol, 2009. **325**(1): p. 211-24.

8. Karam, S.M. and C.P. Leblond, *Dynamics of epithelial cells in the corpus of the mouse stomach. I. Identification of proliferative cell types and pinpointing of the stem cell*. Anat Rec, 1993. **236**(2): p. 259-79.
9. El-Zimaity, H.M., et al., *Patterns of gastric atrophy in intestinal type gastric carcinoma*. Cancer, 2002. **94**(5): p. 1428-36.
10. Lennerz, J.K., et al., *The transcription factor MIST1 is a novel human gastric chief cell marker whose expression is lost in metaplasia, dysplasia, and carcinoma*. Am J Pathol, 2010. **177**(3): p. 1514-33.
11. Nam, K.T., et al., *Mature chief cells are cryptic progenitors for metaplasia in the stomach*. Gastroenterology, 2010. **139**(6): p. 2028-2037 e9.
12. Goldenring, J.R. and K.T. Nam, *Oxyntic atrophy, metaplasia, and gastric cancer*. Prog Mol Biol Transl Sci, 2010. **96**: p. 117-31.
13. Lee, H.J., et al., *Gene expression profiling of metaplastic lineages identifies CDH17 as a prognostic marker in early stage gastric cancer*. Gastroenterology, 2010. **139**(1): p. 213-25 e3.
14. Goldenring, J.R., et al., *Spasmolytic polypeptide-expressing metaplasia and intestinal metaplasia: time for reevaluation of metaplasias and the origins of gastric cancer*. Gastroenterology, 2010. **138**(7): p. 2207-10, 2210 e1.
15. Romero-Gallo, J., et al., *Effect of Helicobacter pylori eradication on gastric carcinogenesis*. Lab Invest, 2008. **88**(3): p. 328-36.
16. de Vries, A.C., E.J. Kuipers, and E.A. Rauws, *Helicobacter pylori eradication and gastric cancer: when is the horse out of the barn?* Am J Gastroenterol, 2009. **104**(6): p. 1342-5.
17. Graham, D.Y. and N. Uemura, *Natural history of gastric cancer after Helicobacter pylori eradication in Japan: after endoscopic resection, after treatment of the general population, and naturally*. Helicobacter, 2006. **11**(3): p. 139-43.
18. Niv, Y. and R. Hazazi, *Helicobacter pylori recurrence in developed and developing countries: meta-analysis of 13C-urea breath test follow-up after eradication*. Helicobacter, 2008. **13**(1): p. 56-61.
19. Barker, N., et al., *Lgr5(+ve) stem cells drive self-renewal in the stomach and build long-lived gastric units in vitro*. Cell Stem Cell, 2010. **6**(1): p. 25-36.
20. Powell, A.E., et al., *The pan-ErbB negative regulator Lrig1 is an intestinal stem cell marker that functions as a tumor suppressor*. Cell, 2012. **149**(1): p. 146-58.
21. Sangiorgi, E. and M.R. Capecchi, *Bmi1 is expressed in vivo in intestinal stem cells*. Nat Genet, 2008. **40**(7): p. 915-20.
22. Qiao, X.T. and D.L. Gumucio, *Current molecular markers for gastric progenitor cells and gastric cancer stem cells*. J Gastroenterol, 2011. **46**(7): p. 855-65.
23. Mills, J.C., et al., *Molecular characterization of mouse gastric epithelial progenitor cells*. Proc Natl Acad Sci U S A, 2002. **99**(23): p. 14819-24.
24. Kikuchi, M., et al., *Altered expression of a putative progenitor cell marker DCAMKL1 in the rat gastric mucosa in regeneration, metaplasia and dysplasia*. BMC Gastroenterol, 2010. **10**: p. 65.
25. Modlin, I.M., et al., *Gastric stem cells: an update*. Keio J Med, 2003. **52**(2): p. 134-7.
26. Huh, W.J., et al., *Tamoxifen induces rapid, reversible atrophy, and metaplasia in mouse stomach*. Gastroenterology, 2012. **142**(1): p. 21-24 e7.
27. Nagy, T.A., et al., *Helicobacter pylori regulates cellular migration and apoptosis by*

- activation of phosphatidylinositol 3-kinase signaling. *J Infect Dis*, 2009. **199**(5): p. 641-51.
28. Ramsey, V.G., et al., *The maturation of mucus-secreting gastric epithelial progenitors into digestive-enzyme secreting zymogenic cells requires Mist1*. *Development*, 2007. **134**(1): p. 211-22.
 29. Zheng, L., T.E. Riehl, and W.F. Stenson, *Regulation of colonic epithelial repair in mice by Toll-like receptors and hyaluronic acid*. *Gastroenterology*, 2009. **137**(6): p. 2041-51.
 30. Sheridan, C., et al., *CD44+/CD24- breast cancer cells exhibit enhanced invasive properties: an early step necessary for metastasis*. *Breast Cancer Res*, 2006. **8**(5): p. R59.
 31. Ricardo, S., et al., *Breast cancer stem cell markers CD44, CD24 and ALDH1: expression distribution within intrinsic molecular subtype*. *J Clin Pathol*, 2011. **64**(11): p. 937-46.
 32. Du, L., et al., *CD44 is of functional importance for colorectal cancer stem cells*. *Clin Cancer Res*, 2008. **14**(21): p. 6751-60.
 33. Horst, D., et al., *Prognostic significance of the cancer stem cell markers CD133, CD44, and CD166 in colorectal cancer*. *Cancer Invest*, 2009. **27**(8): p. 844-50.
 34. Takaishi, S., et al., *Identification of gastric cancer stem cells using the cell surface marker CD44*. *Stem Cells*, 2009. **27**(5): p. 1006-20.
 35. Fan, X., et al., *Expression of CD44 and its variants on gastric epithelial cells of patients with Helicobacter pylori colonisation*. *Gut*, 1996. **38**(4): p. 507-12.
 36. Chong, J.M., et al., *Expression of CD44 variants in gastric carcinoma with or without Epstein-Barr virus*. *Int J Cancer*, 1997. **74**(4): p. 450-4.
 37. Higashikawa, K., et al., *Evaluation of CD44 transcription variants in human digestive tract carcinomas and normal tissues*. *Int J Cancer*, 1996. **66**(1): p. 11-7.
 38. Dhingra, S., et al., *Clinicopathologic significance of putative stem cell markers, CD44 and nestin, in gastric adenocarcinoma*. *Int J Clin Exp Pathol*, 2011. **4**(8): p. 733-41.
 39. Washington, K., M.R. Gottfried, and M.J. Telen, *Expression of the cell adhesion molecule CD44 in gastric adenocarcinomas*. *Hum Pathol*, 1994. **25**(10): p. 1043-9.
 40. Mayer, B., et al., *De-novo expression of CD44 and survival in gastric cancer*. *Lancet*, 1993. **342**(8878): p. 1019-22.
 41. Ghaffarzadehgan, K., et al., *Expression of cell adhesion molecule CD44 in gastric adenocarcinoma and its prognostic importance*. *World J Gastroenterol*, 2008. **14**(41): p. 6376-81.
 42. Ishimoto, T., et al., *CD44+ slow-cycling tumor cell expansion is triggered by cooperative actions of Wnt and prostaglandin E2 in gastric tumorigenesis*. *Cancer Sci*, 2010. **101**(3): p. 673-8.
 43. Gotte, M. and G.W. Yip, *Heparanase, hyaluronan, and CD44 in cancers: a breast carcinoma perspective*. *Cancer Res*, 2006. **66**(21): p. 10233-7.
 44. Naor, D., R.V. Sionov, and D. Ish-Shalom, *CD44: structure, function, and association with the malignant process*. *Adv Cancer Res*, 1997. **71**: p. 241-319.
 45. Lesley, J. and R. Hyman, *CD44 can be activated to function as an hyaluronic acid receptor in normal murine T cells*. *Eur J Immunol*, 1992. **22**(10): p. 2719-23.
 46. Karam, S.M. and C.P. Leblond, *Dynamics of epithelial cells in the corpus of the mouse stomach. II. Outward migration of pit cells*. *Anat Rec*, 1993. **236**(2): p. 280-96.
 47. Herrera, V. and J. Parsonnet, *Helicobacter pylori and gastric adenocarcinoma*. *Clin Microbiol Infect*, 2009. **15**(11): p. 971-6.
 48. Sherry, M.M., et al., *STAT3 is required for proliferation and maintenance of multipotency*

- in glioblastoma stem cells*. Stem Cells, 2009. **27**(10): p. 2383-92.
49. Li, G.H., et al., *Knockdown of STAT3 expression by RNAi suppresses growth and induces apoptosis and differentiation in glioblastoma stem cells*. Int J Oncol, 2010. **37**(1): p. 103-10.
 50. Ho, P.L., et al., *Stat3 activation in urothelial stem cells leads to direct progression to invasive bladder cancer*. Cancer Res, 2012.
 51. Kanda, N., et al., *STAT3 is constitutively activated and supports cell survival in association with survivin expression in gastric cancer cells*. Oncogene, 2004. **23**(28): p. 4921-9.
 52. Leslie, K., et al., *Cyclin D1 is transcriptionally regulated by and required for transformation by activated signal transducer and activator of transcription 3*. Cancer Res, 2006. **66**(5): p. 2544-52.
 53. Bronte-Tinkew, D.M., et al., *Helicobacter pylori cytotoxin-associated gene A activates the signal transducer and activator of transcription 3 pathway in vitro and in vivo*. Cancer Res, 2009. **69**(2): p. 632-9.
 54. Lee, J.L., M.J. Wang, and J.Y. Chen, *Acetylation and activation of STAT3 mediated by nuclear translocation of CD44*. J Cell Biol, 2009. **185**(6): p. 949-57.
 55. Iwamaru, A., et al., *A novel inhibitor of the STAT3 pathway induces apoptosis in malignant glioma cells both in vitro and in vivo*. Oncogene, 2007. **26**(17): p. 2435-44.
 56. Khavari, T.A. and J. Rinn, *Ras/Erk MAPK signaling in epidermal homeostasis and neoplasia*. Cell Cycle, 2007. **6**(23): p. 2928-31.
 57. Fritz, J.M., L.D. Dwyer-Nield, and A.M. Malkinson, *Stimulation of neoplastic mouse lung cell proliferation by alveolar macrophage-derived, insulin-like growth factor-1 can be blocked by inhibiting MEK and PI3K activation*. Mol Cancer, 2011. **10**: p. 76.
 58. Maegawa, M., et al., *EGFR mutation up-regulates EGR1 expression through the ERK pathway*. Anticancer Res, 2009. **29**(4): p. 1111-7.
 59. Marampon, F., et al., *MEK/ERK inhibitor U0126 affects in vitro and in vivo growth of embryonal rhabdomyosarcoma*. Mol Cancer Ther, 2009. **8**(3): p. 543-51.
 60. Murai, T., et al., *Epidermal growth factor-regulated activation of Rac GTPase enhances CD44 cleavage by metalloproteinase disintegrin ADAM10*. Biochem J, 2006. **395**(1): p. 65-71.
 61. Bourguignon, L.Y., E. Gilad, and K. Peyrollier, *Heregulin-mediated ErbB2-ERK signaling activates hyaluronan synthases leading to CD44-dependent ovarian tumor cell growth and migration*. J Biol Chem, 2007. **282**(27): p. 19426-41.
 62. Baines, P., et al., *The MEK inhibitor, PD98059, reduces survival but does not block acute myeloid leukemia blast maturation in vitro*. Eur J Haematol, 2000. **64**(4): p. 211-8.
 63. Syder, A.J., et al., *Helicobacter pylori attaches to NeuAc alpha 2,3Gal beta 1,4 glycoconjugates produced in the stomach of transgenic mice lacking parietal cells*. Mol Cell, 1999. **3**(3): p. 263-74.
 64. Fox, J.G. and T.C. Wang, *Inflammation, atrophy, and gastric cancer*. J Clin Invest, 2007. **117**(1): p. 60-9.
 65. Osaki, L.H., et al., *EGFR is involved in control of gastric cell proliferation through activation of MAPK and Src signalling pathways in early-weaned rats*. Cell Prolif, 2011. **44**(2): p. 174-82.
 66. Yang, J.J., et al., *Oncogenic CagA promotes gastric cancer risk via activating ERK signaling pathways: a nested case-control study*. PLoS One, 2011. **6**(6): p. e21155.

67. Matkar, S.S., et al., *Systemic activation of K-ras rapidly induces gastric hyperplasia and metaplasia in mice*. Am J Cancer Res, 2011. **1**(4): p. 432-445.
68. Quante, M., et al., *Bile acid and inflammation activate gastric cardia stem cells in a mouse model of Barrett-like metaplasia*. Cancer Cell, 2012. **21**(1): p. 36-51.
69. Souza, R.F., et al., *Acid increases proliferation via ERK and p38 MAPK-mediated increases in cyclooxygenase-2 in Barrett's adenocarcinoma cells*. Am J Physiol Gastrointest Liver Physiol, 2004. **287**(4): p. G743-8.
70. Collisson, E.A., et al., *A Central Role for RAF->MEK->ERK Signaling in the Genesis of Pancreatic Ductal Adenocarcinoma*. Cancer Discov, 2012. **2**(8): p. 685-693.
71. Ishimoto, T., et al., *CD44 variant regulates redox status in cancer cells by stabilizing the xCT subunit of system xc(-) and thereby promotes tumor growth*. Cancer Cell, 2011. **19**(3): p. 387-400.
72. Riehl, T.E., X. Ee, and W.F. Stenson, *Hyaluronic acid regulates normal intestinal and colonic growth in mice*. Am J Physiol Gastrointest Liver Physiol, 2012. **303**(3): p. G377-88.
73. Xiao, C., et al., *Loss of parietal cell expression of Sonic hedgehog induces hypergastrinemia and hyperproliferation of surface mucous cells*. Gastroenterology, 2010. **138**(2): p. 550-61, 561 e1-8.
74. Shinohara, M., et al., *Bone morphogenetic protein signaling regulates gastric epithelial cell development and proliferation in mice*. Gastroenterology, 2010. **139**(6): p. 2050-2060 e2.
75. Jain, R.N. and L.C. Samuelson, *Differentiation of the gastric mucosa. II. Role of gastrin in gastric epithelial cell proliferation and maturation*. Am J Physiol Gastrointest Liver Physiol, 2006. **291**(5): p. G762-5.
76. Wang, T.C., et al., *Synergistic interaction between hypergastrinemia and Helicobacter infection in a mouse model of gastric cancer*. Gastroenterology, 2000. **118**(1): p. 36-47.
77. Grandi, D., W. Schunack, and G. Morini, *Epithelial cell proliferation is promoted by the histamine H(3) receptor agonist (R)-alpha-methylhistamine throughout the rat gastrointestinal tract*. Eur J Pharmacol, 2006. **538**(1-3): p. 141-7.
78. Nakamura, E., et al., *Lack of histamine alters gastric mucosal morphology: comparison of histidine decarboxylase-deficient and mast cell-deficient mice*. Am J Physiol Gastrointest Liver Physiol, 2004. **287**(5): p. G1053-61.
79. Kobayashi, T., et al., *Abnormal functional and morphological regulation of the gastric mucosa in histamine H2 receptor-deficient mice*. J Clin Invest, 2000. **105**(12): p. 1741-9.
80. Tremblay, E., S. Monfils, and D. Menard, *Epidermal growth factor influences cell proliferation, glycoproteins, and lipase activity in human fetal stomach*. Gastroenterology, 1997. **112**(4): p. 1188-96.
81. Goldenring, J.R., et al., *Overexpression of transforming growth factor-alpha alters differentiation of gastric cell lineages*. Dig Dis Sci, 1996. **41**(4): p. 773-84.
82. Coffey, R.J., et al., *Menetrier disease and gastrointestinal stromal tumors: hyperproliferative disorders of the stomach*. J Clin Invest, 2007. **117**(1): p. 70-80.

CHAPTER 4: Metaplasia in the stomach is induced by cytokines produced by macrophages

Abstract

Atrophy of acid secreting parietal cells in the stomach is the first step towards developing metaplasia, which eventually progresses to gastric cancer. Gastric cancer is the second largest cause of cancer related deaths worldwide. Parietal cell death is accompanied by a rapid remodeling of the gastric epithelium, characterized by stem cell activation, dedifferentiation of post-mitotic zymogenic cells and their re-entry into the cell cycle. However, the origin of parietal cell atrophy and metaplasia remain obscure.

We have previously established that the breast cancer treatment drug, tamoxifen, causes prompt parietal cell death within 3 days of administration. Atrophy is accompanied by an increase in stem cell proliferation by activation of the ERK→CD44→STAT3 signaling cascade. Nevertheless, the upstream signal that leads to parietal cell death and the communication between damaged parietal cells and the neighboring stem cells that lead to their activation are unknown. Here we find that, within a few hours, there is a dramatic increase in the levels of circulating IL-6 in the sera of mice treated with tamoxifen. Although inflammation is absent, there is an increase in F4/80⁺ macrophages in the mesenchymes of tamoxifen treated mice. When challenged with tamoxifen *ex vivo*, primary macrophages secrete IL-6. Depletion of macrophages in tamoxifen treated mice blocks parietal cell atrophy and associated expansion in stem cell proliferation. Factors secreted by macrophages lead to the activation of ERK in stem cells and increase in iNOS in parietal cells. ERK causes a burst of stem cell proliferation, whereas, iNOS activates the parietal cell death cascade. When iNOS signaling is blocked, parietal cell atrophy and proliferation expansion are rescued. In conclusion, we propose a mechanism by which the innate immune system signals to the gastric epithelium to initiate parietal cell death and metaplasia.

Introduction

When acid-secreting parietal cells (PCs) in the gastric epithelium atrophy (die) by genetic ablation [1], infection with *Helicobacter pylori* [2] or by chemical means such as treatment with tamoxifen [3], it causes a stereotypic response in the remaining epithelial cells known as spasmolytic polypeptide expressing metaplasia (SPEM). SPEM is characterized by expanded stem cell proliferation and dedifferentiation of enzyme secreting zymogenic cell (ZCs)s. The ZC dedifferentiation is characterized by re-expression of markers like TFF2 (spasmolytic polypeptide) that are usually expressed only during the ZC precursor stage [4]. Healthy PCs secrete a number of factors, such as amphiregulin, transforming growth factor α (TGF- α), heparin binding-epidermal growth factor-like growth factor (HB-EGF), Sonic hedgehog (Shh), that aid in differentiation of other mucosal lineages [4]. It is not clear which, if any, of the known growth factors normally elaborated by PCs might regulate the dedifferentiation of ZCs into SPEM cells. Presumably, loss of the PC-elaborated signal might affect ZC differentiation either directly or via an intermediary cell type. Alternatively, injured or dying PCs might elaborate a stress signal that causes metaplasia of ZCs.

H. pylori infection related PC atrophy is associated with inflammation, which makes mesenchyme to epithelial signaling fairly complicated. Hence, we utilize the tamoxifen induced PC atrophy model to determine signals from them mesenchyme to the epithelium that cause PC stress and eventual death. Tamoxifen does not cause inflammation, but displays all the epithelial changes of *H. pylori* SPEM. Therefore, we analyzed circulating cytokines that were elevated upon tamoxifen treatment that could signal to the epithelium and lead to PC atrophy and stem cell expansion.

Several cytokines are implicated in mediating PC death upon infection with *H. pylori*.

Interleukin-1 β (IL-1 β), IL-6, tumor necrosis factor alpha (TNF- α), IL-8, IL-21, gamma interferon (IFN- γ), and transforming growth factor β (TGF- β) are found at increased levels in the gastric mucosa of patients with *H. pylori*-associated gastritis compared with levels in healthy controls [5]. Antigen presenting cells (APCs) such as dendritic cells and macrophages are present in *H. pylori* infected mucosa and are likely involved in secreting some of the above mentioned cytokines [5]. Along with the function of eradicating the bacterial infection, these APCs might release cytokines that lead to epithelial remodeling and metaplasia. Most studies focus on the role of immune cells and cytokines in eliminating *H. pylori*. Here we are interested in determining the effect of these cytokines on PC death and stem cell expansion.

Our study shows that macrophages are increased in the mesenchymes of tamoxifen treated mouse stomachs and these macrophages secrete IL-6 when challenged *in vivo* and *ex vivo* with tamoxifen. We also find that depletion of macrophages rescues tamoxifen induced PC death and stem cell expansion and this occurs by blocking iNOS expression and ERK activation respectively. Increasing nitric oxide (NO) by injecting NO donors increases proliferation, whereas blocking NO with scavengers reduces PC death and proliferation.

Materials and Methods

Animals and injections- All experiments involving animals were performed according to protocols approved by the Washington University School of Medicine Animal Studies Committee. Mice were maintained in a specified-pathogen-free barrier facility under a 12 hour light cycle. Wild-type C57BL/6 and *iNOS*^{-/-} mice were purchased from The Jackson Laboratory. Mice from all treatment groups were given an i.p. injection of a mixture of 5-bromo-2'-deoxyuridine (BrdU, 120 mg/kg) and 5-fluoro-2'-deoxyuridine (12 mg/kg) 90 minutes before sacrifice to label S-phase cells. Vehicles used for all injections are: sterile saline, ethanol in

sunflower seed oil, or DMSO; no phenotypes were induced by injection of any of the vehicles alone. Table 1 enumerates the treatments given to mice.

Table 4.1: Mice treatments and injections-

Treatment	Dose (body weight)	Vehicle	Injection Scheme	Source
Tamoxifen	5mg/20g	10% ethanol + 90% sunflower seed oil	i.p. once a day, sacrificed as indicated	Sigma
Clodronate	100µL	Solution from manufacturer	i.p. twice a day until sacrifice	Encapsula, Nano Sciences
Control Liposomes	100µL	Solution from manufacturer	i.p. twice a day until sacrifice	Encapsula, Nano Sciences
Aminoguanidine	400mg/kg	0.9% saline	s.c. once a day until sacrifice	Sigma
SNAP	20mg/kg	20% ethanol + 80% sunflower seed oil	i.p. 3 times a day until sacrifice	Sigma
DetaNONOate	0.4mg/kg	0.9% saline	i.p. once a day until sacrifice	Sigma
Curcumin	100mg/kg	25% ethanol + 75% sunflower seed oil	i.p. 3 times a day until sacrifice	Sigma

Human Tissues- Examination of human gastric pathological tissue specimens was approved by the Institutional Review Board of Washington University School of Medicine, the Comité de Bioética of Nicaragua for Universidad Nacional Autónoma De Nicaragua – Facultad De Ciencias Médicas Managua, and the Research Ethics Board Manager for Health Sciences at the University of Toronto. Serial sections (4–6 µm thick) obtained from paraffin-embedded tissue samples (H&E and alcian blue–periodic acid–Schiff stains) were reviewed by two pathologists in Italy (M.F., and M.R.) with specific expertise in gastrointestinal diseases, and a consensus on the score for each pertinent histologic variable was reached. Diagnoses and selection of specific regions of transitions among normal stomach, atrophic stomach, and intestinal metaplasia was performed by a third pathologist in the US (JCM).

IL-6 ELISA- Wildtype mice were injected i.p. with either vehicle (10% ethanol + 90% oil; n=3) or tamoxifen (n=3) and blood was collected by retro-orbital bleeding. Blood was allowed to clot at 37°C for 30 minutes, centrifuged at 2000g for 10 minutes at 4°C and aliquoted and stored at -20°C. Aliquots were shipped to the Cytokine Core Laboratory of the University of Maryland for performing IL-6 ELISAs.

Macrophage collection and culture- Peritoneal macrophages were isolated and cultured as per [6]. Briefly, wildtype mice were each injected with 4mL thioglycollate medium 5 days prior to sacrifice. 10mL of ice cold DMEM was injected into the peritoneal cavity immediately after sacrifice, and collected into the same syringe. Media along with suspended macrophages were centrifuged at 1200 rpm for 10 minutes at 4°C. Supernatant was discarded and the pellet was suspended in DMEM/F12-10 media and plated into a 6-well plate at the concentration of 2×10^6 cells per well. Cells were allowed to adhere to the plate overnight at 37°C, 5% CO₂ in an incubator. Media was changed the following day to discard dead cells and debris. The wells were treated with either DMSO alone or tamoxifen in DMSO (2mg/mL) for 1hr. at 37°C.

IL-6 RT-PCR- Cultured and treated macrophages were washed with PBS and mRNA was extracted using the Qiagen RNeasy Mini Kit using the manufacturer's instructions. RNA was quantified using Biotek ELISA plate reader and Gen5 software. 1µg RNA was synthesized to cDNA using the protocol described in [3] and PCR was performed using the primers for IL-6 (Forward Primer 5'→3' CCAAGAGGTGAGTGCTTCCC; Reverse Primer 5'→3' CTGTTGTTTCAGACTCTCTCCCT) and 18S (Forward Primer 5'→3' CATTCGAACGTCTGCCCTATC; Reverse Primer 5'→3' CCTGTGCCTTCCTTGGA [3]).

Immunofluorescence and Immunohistochemistry- Stomachs were prepared, and stained, and imaged using methods modified from Ramsey et al [7]. For BrdU/Ki67 quantifications, positive

cells were counted in >50 gastric units per mouse and >3 mice per experiment. Total number of positive cells was divided by the total number of gastric units for each mouse. Stomachs were prepared, and stained, and imaged using methods modified from Ramsey et. al. [7]. Primary antibodies used for immunostaining are listed in Table 4.2:

Table 4.2: Antibodies used for immunostaining

Serial No.	Antibody	Dilution	Source
1	Goat α -BrdU	1:20,000	Jeffrey Gordon, Washington University
2	Rabbit α -pERK1/2	1:100	Cell Signaling Technology, Danvers, MA
3	F4/80	1:100	BD Biosciences, San Jose, CA
4	Rabbit α -GIF	1:20,000	David Alpers, Washington University
5	Rabbit α -iNOS	1:100	Abcam, Cambridge, MA

Secondary antibodies, lectins and BrdU labeling were as described [7].

Western Blotting – Western Blotting –Western blot analysis was performed as described [3].

Antibodies used for blotting are listed in Table 4.3. Immobilon Western Chemiluminescent HRP Substrate (Millipore) was used for detection.

Table 4.3: Primary antibodies used for Western blotting

Serial No.	Antibody	Dilution	Source
1	Rabbit α -pERK1/2	1:1000	Cell Signaling Technology, Danvers, MA
2	Rabbit α -Tubulin	1:2000	Cell Signaling Technology, Danvers, MA
3	Goat α -HAS2	1:1000	Santacruz Biotechnology Inc., CA

Secondary antibodies were horseradish peroxidase (HRP)-conjugated donkey anti-rabbit IgG (1:2,000, Santa Cruz Biotenchnology, Inc.), goat anti-rat IgG (1:1000, Santa Cruz Biotechnology, Inc.) and donkey anti-goat IgG (1:1000, Santa Cruz Biotechnology, Inc.).

Microscopy - Light and epifluorescence micrographs were taken as described [8].

Graphing and statistics - All graphs and statistics were performed in GraphPad Prism, using Student's t test (one-tailed or two-tailed, as appropriate) for comparison of two groups of data and one-way ANOVA with either Dunnett's or Tukey's for multiple comparison tests.

Results

IL-6 is produced and secreted into the serum immediately after treatment with tamoxifen

High levels of circulating IL-6 are associated with advanced gastric cancer [9]. IL-6 is a major mediator of inflammation and activator of STAT3, which enhances proliferation and helps cells progressing towards neoplastic growth [10]. In chapter 3, we have shown increased STAT3 activation associated with increased stem cell proliferation following treatment with tamoxifen. Accordingly, we find an increase in circulating IL-6 in sera of mice treated with tamoxifen within 6 hours of injection (Fig. 4.1A). Activated peritoneal macrophages frequently secrete IL-6 in other disease models such as endometriosis [11], stress [12], treatment with LPS [13], and so on. Therefore, we isolated peritoneal macrophages from mice, cultured and treated them with tamoxifen *ex vivo*. While IL-6 transcripts were absent in mice treated with DMSO control, we found IL-6 mRNA expression in macrophages treated with tamoxifen for 1h (Fig. 4.1C). In inflammatory diseases of the gastrointestinal tract, such as ulcerative colitis and Crohn's disease, there is enhanced secretion of IL-6 by mononuclear cells of the lamina propria [14]. Although tamoxifen does not produce classical inflammation in our model of gastric metaplasia, we observed an increase in F4/80⁺ macrophages in the mesenchyme adjacent to the base of the gastric units (Fig. 4.1B). These macrophages presumably secrete IL-6, along with other cytokines and factors that increase STAT3 activation and proliferation of cells at the base of the unit.

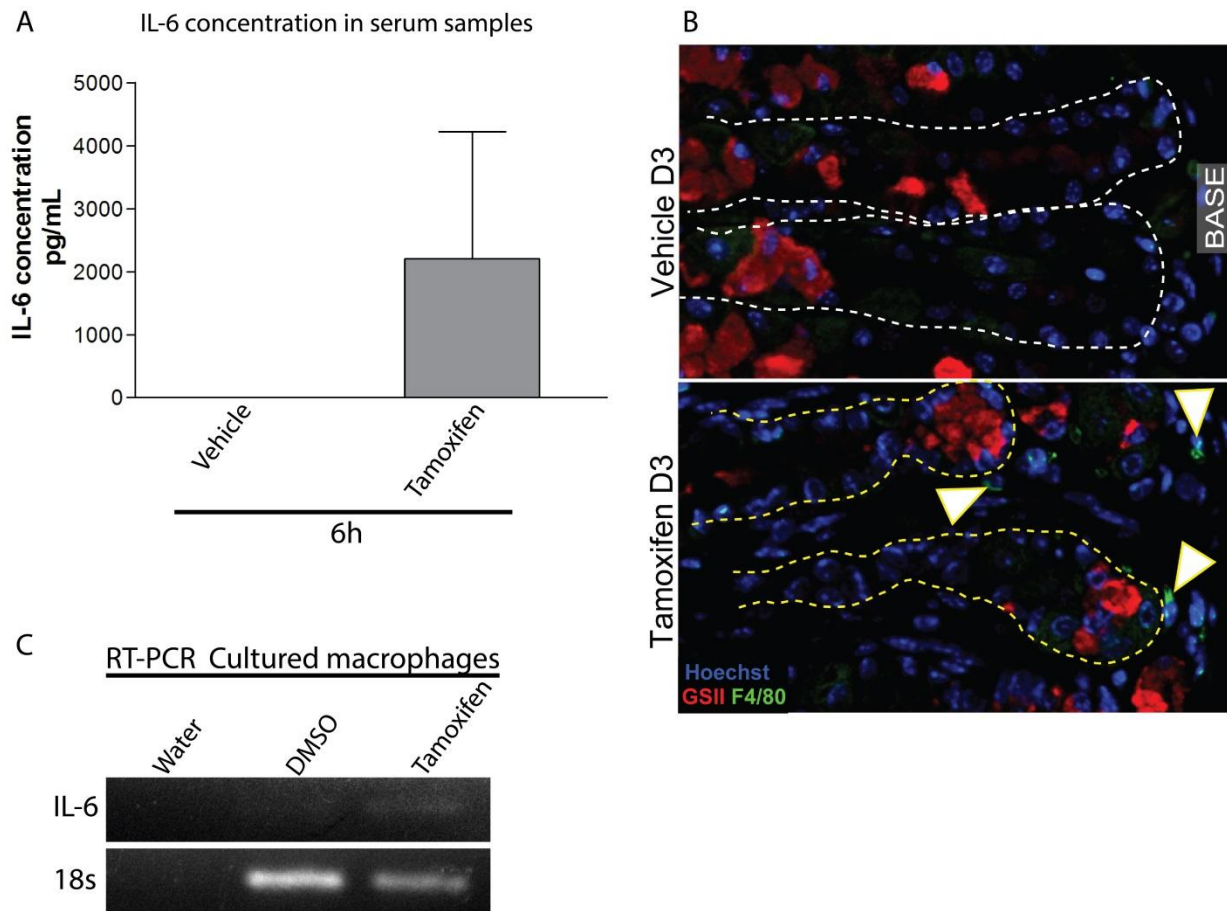


Fig. 4.1 Tamoxifen increases IL-6 secretion by macrophages. In mice treated with vehicle, there was undetectable IL-6 in the sera, whereas tamoxifen treated mice showed a dramatic increase in IL-6 concentration in their sera (A). Macrophages are important secretors of IL-6 and are increased in the mesenchymes of tamoxifen treated mouse stomachs, labeled in green with F4/80 (B). Arrowheads point to green macrophages in the mesenchyme and dashed lines outline gastric units (B). When cultured peritoneal macrophages are treated with tamoxifen, they increase their expression of Il-6 transcripts, shown in (C) by RT-PCR, when compared to DMSO treated controls.

Macrophages secrete IL-6 when treated with tamoxifen *ex vivo* and are necessary for developing metaplasia

IL-6 is typically secreted by either T-cells or macrophages. To rule out the possibility of the involvement of T-cells, we treated *Rag1*^{-/-} mice with tamoxifen and found that they developed metaplasia like the wildtype controls (data not shown). Therefore, we focused our next experiments on macrophages. In order to determine the role of macrophages in inducing metaplasia, we depleted macrophages using clodronate before treating mice with tamoxifen. Mice that received clodronate in addition to tamoxifen had a blunted proliferative response when compared with those that received tamoxifen alone (Fig. 4.2A). Moreover, clodronate also blocked PC death and dedifferentiation of ZCs at the base of the unit (Fig. 4.2B). In Fig. 4.2B, the orange bracket shows dedifferentiated ZCs expressing both neck and ZC markers (purple and red overlap) in the tamoxifen treated mice whereas the clodronate + tamoxifen treated mice show distinct regions of neck cells (white bracket) and ZCs (yellow bracket).

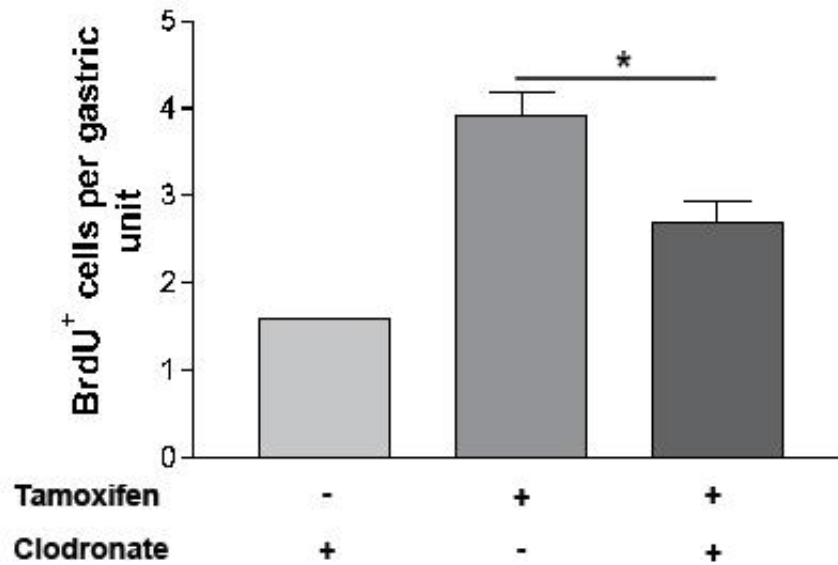
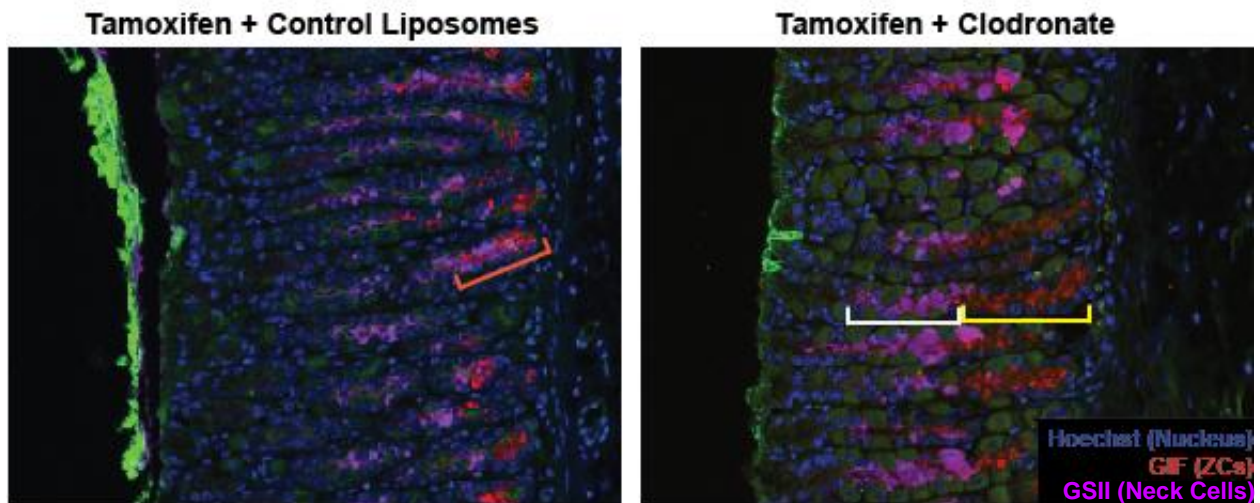
A**B**

Fig. 4.2 Depletion of macrophages by treatment with clodronate rescues SPEM development induced by tamoxifen. Pre-treatment of mice with clodronate before inducing atrophy with tamoxifen blocks the proliferative expansion of stem cells (A) as measured by counting BrdU⁺ proliferating cells per gastric unit. Clodronate pretreated mice also show lower degree of GSII (neck cell marker) and GIF (zymogenic cell marker) overlap signifying lesser dedifferentiation of zymogenic cells in these mice compared to tamoxifen treated positive controls (B).

Macrophages induce ERK activation and iNOS expression following treatment with tamoxifen

We next determined at what stage clodronate affected the ERK-CD44-STAT3 proliferation cascade outlined in Chapter 3. We performed western blots for each signaling intermediate and found that ERK activation was affected by macrophage depletion by clodronate (Fig. 4.3). Clodronate treatment did not affect HA production as its synthesizing enzyme HAS2 remained unchanged (Fig. 4.3). Since we have shown earlier that macrophages secrete IL-6 upon treatment with tamoxifen (Fig. 4.1) and IL-6 is known to activate STAT3, we expected a block in STAT3 phosphorylation in presence of clodronate. However, pSTAT3 levels remained unchanged (Fig. 4.3) suggesting that there might be IL-6 independent methods of activating STAT3. Another possible explanation is that IL-6 might activate STAT3 by phosphorylating Ser727 [15] while we have analyzed phosphorylation at the Tyr705 residue.

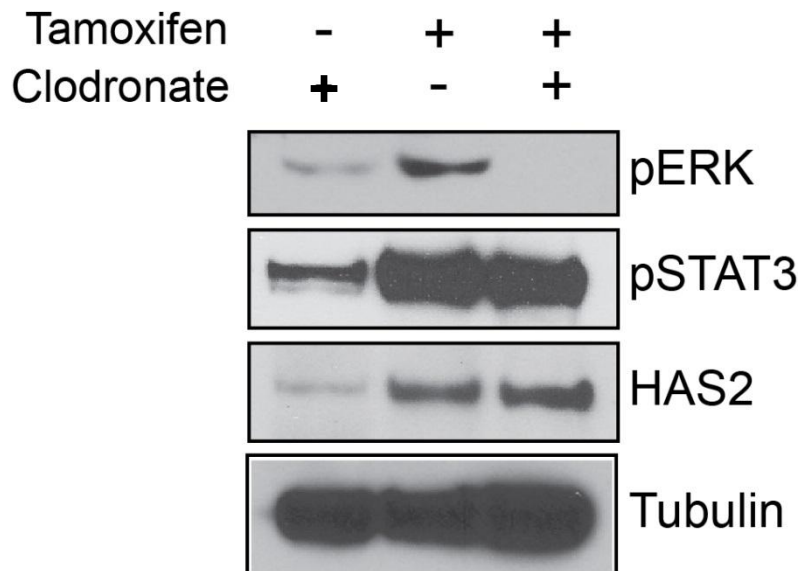


Fig. 4.3: Clodronate blocks ERK

activation and iNOS expression

in tamoxifen induced SPEM.

Western blots show that while

STAT3 activation and HAS2

expression are unchanged upon

clodronate treatment, pERK and

iNOS expressions are blocked by

depletion of macrophages.

These data show that depletion of macrophages blocks ERK activation, which explains the decrease in proliferation. However, we also observe a decrease in PC death with clodronate treatment. Therefore, we assayed for the stress signal, i.e. expression of iNOS and found that while iNOS was increased in tamoxifen treated mice, clodronate inhibited the expression of iNOS (Figure 4.3). Expression of iNOS could be the source of the parietal cell atrophy signal downstream of factors secreted by macrophages.

iNOS is expressed in damaged parietal cells of mice and humans

Nitric oxide (NO) is an endogenous mediator of a number of physiological functions and stress responses. It is a vasodilator that protects gastric mucosa by reducing acid secretion and increasing blood flow and epithelial alkaline secretion [16]. NO is a short-lived molecule that can cause local effects in cells, including proliferation, apoptosis, migration, invasion and angiogenesis [17]. The literature on the role of NO in cancer tumorigenesis is dichotomous, with some reports arguing about its pro-tumorigenic functions and others suggesting that it is anti-tumorigenic [17]. NO is generated by three isoforms of NOS (nitric oxide synthase) enzymes: neuronal NOS (nNOS), endothelial NOS (eNOS) and inducible NOS (iNOS) [17]. eNOS and nNOS produce low concentrations (nanomolar) of NO for short durations, whereas iNOS is capable of producing large amounts (micromolar) of NO over hours or days [17]. At low concentrations, NO acts as a signal transmitter and aids maintenance of homeostasis; whereas, at higher concentrations, such as those produced during injury by iNOS, it is cytoprotective against pathogens and tumors [17]. In humans, *H. pylori* infection is associated with higher levels of iNOS and NO [18]. Moreover, increased risk of developing gastric cancer has been reported in populations with higher consumption of nitrate and nitrite from animal sources, which

decompose in the stomach to give rise to reactive nitrogen species such as NO [19]. Furthermore, tamoxifen increases iNOS expression and NO production by myoepithelial cells when they are co-cultured with conditioned media from or breast carcinoma cells [20]. Therefore, we tried to elucidate the role of iNOS and NO in parietal cell death and stem cell proliferation upon induction of metaplasia by tamoxifen.

While iNOS is normally absent in the gastric mucosa, we found an increase in iNOS expression in PCs of mice injected with tamoxifen (Fig. 4.4). iNOS labeled individual PCs which is in accordance with the trend of asynchronous PC death.

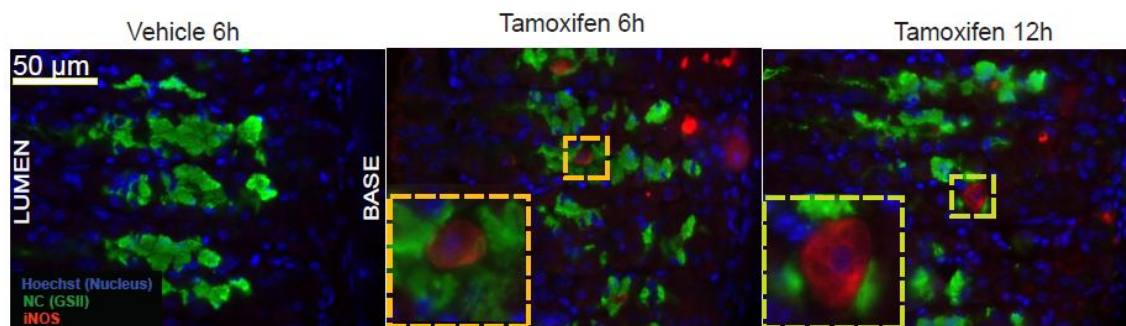


Figure 4.4: iNOS labels parietal cells in tamoxifen treated mice. While vehicle control stomachs do not show any iNOS expression (red; left panel), mice treated with tamoxifen start expressing iNOS as early as 6 hours after treatment with tamoxifen (middle panel) and continue expressing iNOS at 12 hours of treatment (right panel). The expression of iNOS is limited to parietal cells, shown in insets.

We also observed an increase in iNOS staining in human gastrectomy samples that exhibited SPEM (Fig. 4.5A, right). In *tox176* mice, where PCs are killed by diphtheria toxin as soon as they differentiate, we saw rare iNOS staining in pre-parietal cells (Fig. 4.5A, left). iNOS staining by immunohistochemistry was prominent in parietal cells of metaplastic human stomachs (Fig. 4.5B).

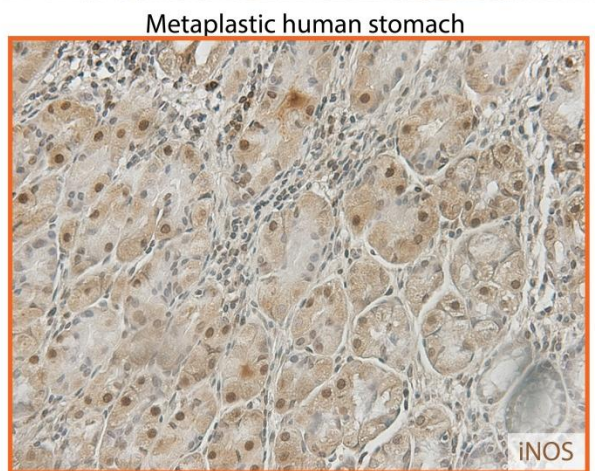
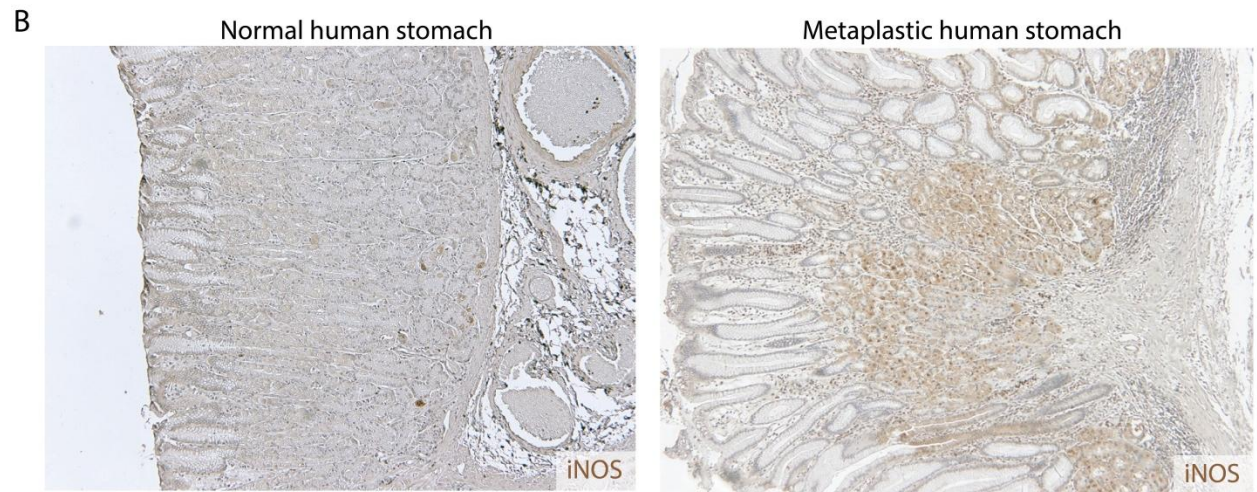
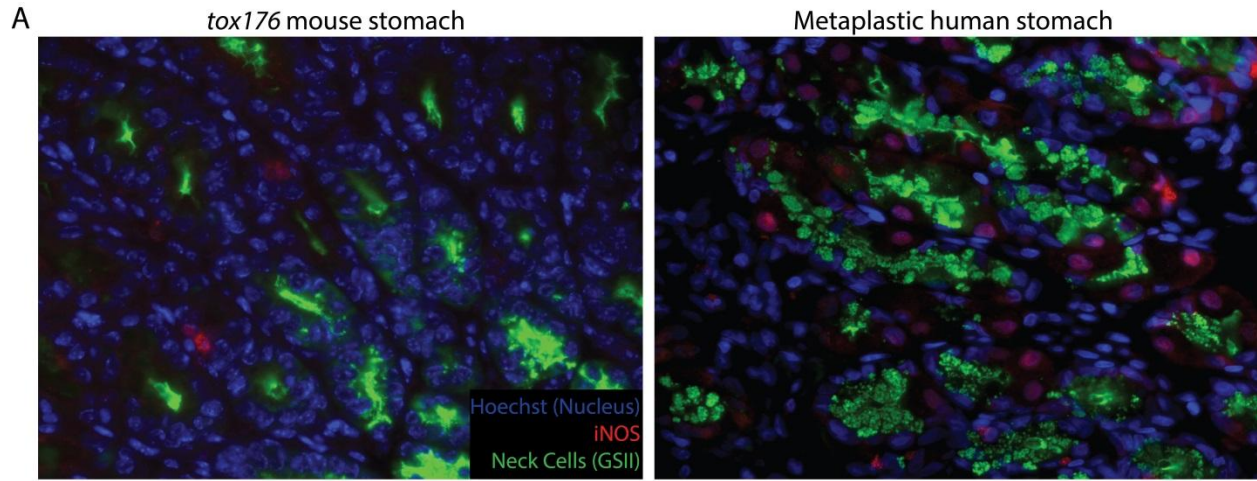


Fig. 4.5: iNOS is expressed in pre-parietal cells of *tox176* mice and in PCs of humans with gastric metaplasia. Pre-parietal cells of *tox76* mice express iNOS (A, left), as do parietal cells of humans with metaplasia (A, right; B, right and below). Normal human stomachs do not express iNOS (B, left)

Nitric oxide signaling is necessary and sufficient for inducing parietal cell death and expansion of proliferation

In order to delineate the role of NO in inducing or protecting from PC atrophy and stem cell expansion, we performed loss of function and gain of function experiments, using NO donor and NO scavenger injections in mice. We injected SNAP (S-Nitroso-N-acetyl-DL-penicillamine) and DetaNONOate NO donors into mice and observed a slight increase in proliferation at Days 1 and 3 respectively (Fig. 4.6A, B).

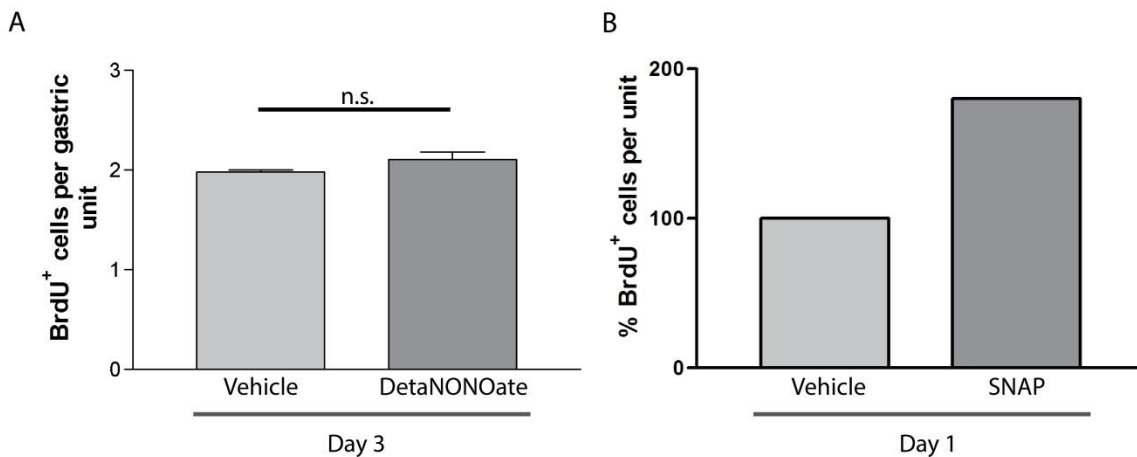


Figure 4.6: Effect of nitric oxide donors on epithelial proliferation. While administration of the NO donor, DetaNONOate, for 3 days did not significantly increase proliferation (A), treatment with another NO donor, SNAP, caused a doubling of proliferating cells within a day of treatment (B).

We then injected mice with tamoxifen in the presence of an iNOS specific inhibitor, Aminoguanidine, and found a decrease in the expansion of proliferation induced by tamoxifen alone (Fig. 4.7A). When treated with an NO scavenger, curcumin, we observed a more substantial decrease in proliferation compared to tamoxifen alone (Fig. 4.4B).

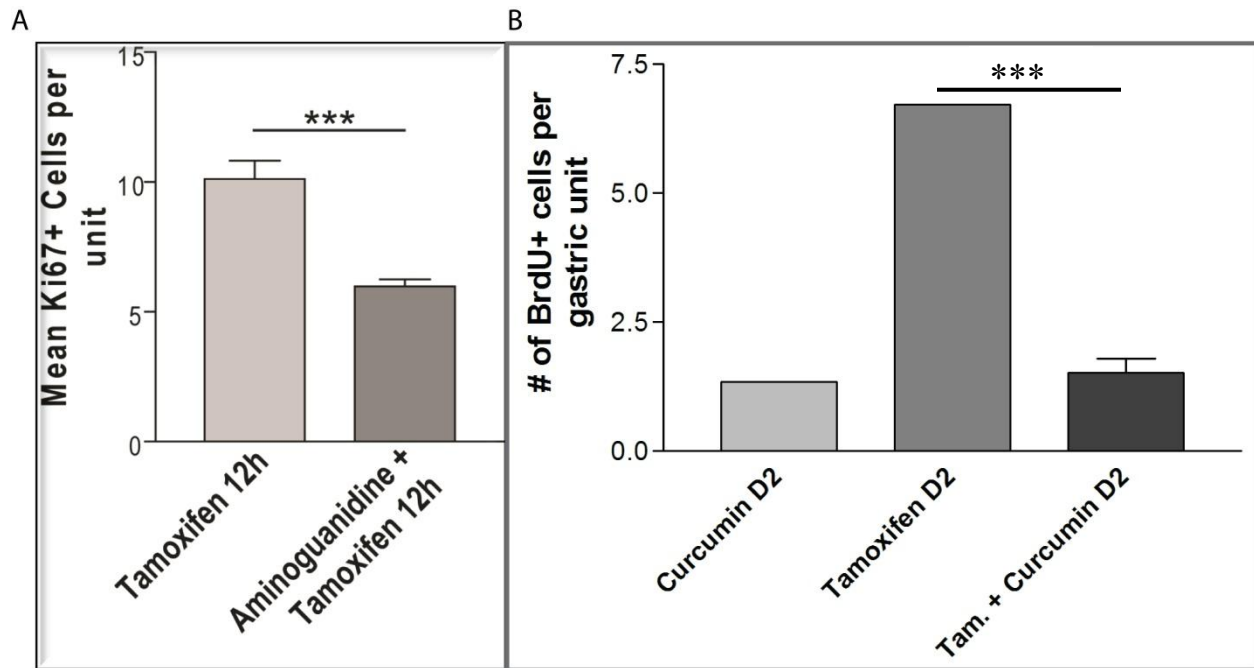


Figure 4.7: Blocking iNOS activity and scavenging nitric oxide inhibits the expansion of proliferation during metaplasia. Mice pre-treated with the iNOS inhibitor, aminoguanidine, before injury with tamoxifen showed a blunting of the proliferative response (A), as did mice pre-treated with the NO scavenger, curcumin (B).

However, multiple experiments with treatment of $iNOS^{-/-}$ mice with tamoxifen did not consistently show a decrease in proliferation or parietal cell protection compared to WT mice treated with tamoxifen (Fig. 4.8) and we reckon this defect is due to compensation by other NOS enzymes (eNOS and nNOS) in these mice. Also, since curcumin affects multiple signaling pathways, including ERK, we believe that part of the proliferation dampening effect of curcumin might be due to blocking of ERK signaling, which we have proved earlier to be involved in stem cell proliferation (Chapter 3). In conclusion, NO produced by iNOS in parietal cells might be necessary and sufficient in causing stem cell expansion upon metaplasia.

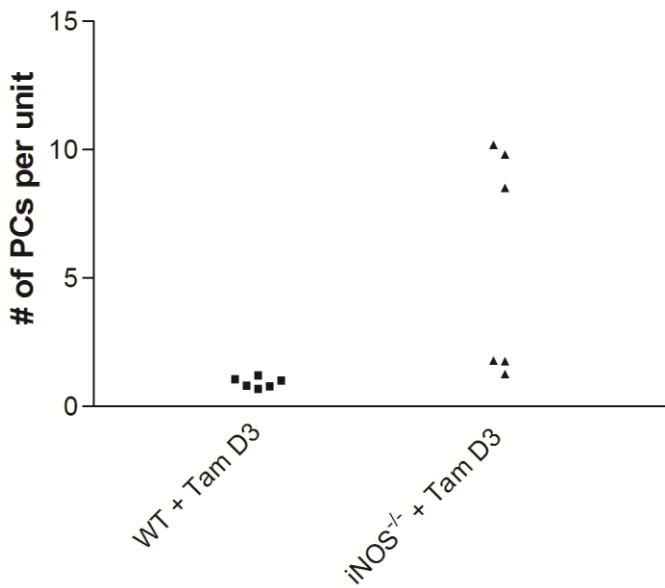


Fig. 4.8: iNOS^{-/-} mice treated with tamoxifen display a threshold phenomenon whereby they either lose all their parietal cells or none. Parietal cell counts show that wildtype mice lose all their PCs upon tamoxifen treatment, whereas iNOS^{-/-} mice either lose PCs or completely rescue their loss.

Discussion

Here we demonstrate that signaling initiated by macrophages leads to parietal cell death and development of metaplasia, which is a known precancerous lesion [4]. In the presence of tamoxifen, macrophages secrete IL-6 and other factors which begin the cascade of parietal cell death and expansion of proliferation. Parietal cell death is mediated by the expression of iNOS. Inhibition of macrophages and iNOS decrease parietal cell death, stem cell proliferation and associated metaplasia. Hence, we conclude that the initiation of metaplastic changes in the gastric epithelium is brought about by factors released by elicited macrophages.

Infection with *Helicobacter pylori*, which is the main predisposing factor for developing gastric cancer, results in inflammatory infiltration in the gastric mesenchyme [5]. Patients with *H. pylori* infection show myeloid antigen presenting cells, such as macrophages and dendritic cells, in their gastric mucosa [5]. *H. pylori* infected monocytes *in vitro* secreted more proinflammatory cytokines such as IL-12p40, IL-23, IL-1 β , IL-6, and IL-10 compared to uninfected controls [5].

Our model of tamoxifen induced parietal cell atrophy displays all the hallmarks of metaplasia associated with *H. pylori* infection, except the development of classical inflammation [3]. However, we do observe the presence of CD45⁺/F4/80⁺ myeloid cells in the mesenchymes of mice treated with tamoxifen, while these cells are absent in vehicle treated samples (Fig. 4.1). Moreover, of all the cytokines assayed, we observe an increase in circulating levels of IL-6 in tamoxifen treated mice compared to controls (Fig. 4.1). Isolated and cultured macrophages express IL-6 when treated with tamoxifen, whereas vehicle treated macrophages fail to do so (Fig. 4.1). Therefore, even in the absence of inflammation, factors secreted by macrophages, including IL-6, are increased in the sera of mice treated with tamoxifen.

Macrophages regulate injury induced stem cell proliferation by modulating the activation of ERK. We have shown in Chapter 3 that ERK activation initiates a CD44-STAT3 proliferation signaling cascade. Loss of ERK activation in mice lacking functional macrophages is responsible for the inhibition of stem cell proliferation and we predict that this is accomplished by a block in the CD44-STAT3 signaling downstream of pERK. We do not observe any change in the expression of HAS2, an enzyme that synthesizes hyaluronic acid, upon macrophage depletion. Therefore, hyaluronic acid activated CD44 is not a critical modulator of proliferation downstream of macrophage signaling. It is intriguing that even though macrophages secrete IL-6 ex vivo and in vivo, and that IL-6 is the main upstream activator of STAT3, we do not find deactivation of STAT3 upon macrophage depletion. This could either be due to an IL-6 and macrophage independent mechanism of STAT3 activation or due to its activation via phosphorylation or acetylation of a different amino acid residue of STAT3 that we did not test for.

Another very interesting observation is that macrophage depletion blocks parietal cell death, which is the first response of the gastric mucosa to injury. Our data show that this blockage

occurs by inhibition of iNOS signaling by clodronate. iNOS is expressed in parietal cells of mice treated with tamoxifen and humans with gastric metaplasia. Nitric oxide release is necessary and sufficient to cause PC death and expansion of proliferation as shown by NO donors and scavengers. *iNOS*^{-/-} mice showed variability in loss of PCs upon tamoxifen treatment, perhaps due to a threshold effect of NO concentration on PC loss or due to compensation by eNOS and nNOS in producing sufficient amounts of NO to cause PC atrophy.

Our observations delineate an interplay between circulating factors, mesenchymal signals and epithelial responders that lead to all aspects of metaplasia development, i.e. parietal cell loss, expansion of proliferation and dedifferentiation of ZCs. Future studies identifying the specific factors that cross talk from the mesenchyme to the epithelium to initiate the metaplastic cascade will prove critical in understanding the source of stem cell activation in the stomach.

References

1. Li, Q., S.M. Karam, and J.I. Gordon, *Diphtheria toxin-mediated ablation of parietal cells in the stomach of transgenic mice*. J Biol Chem, 1996. **271**(7): p. 3671-6.
2. Herrera, V. and J. Parsonnet, *Helicobacter pylori and gastric adenocarcinoma*. Clin Microbiol Infect, 2009. **15**(11): p. 971-6.
3. Huh, W.J., et al., *Tamoxifen induces rapid, reversible atrophy, and metaplasia in mouse stomach*. Gastroenterology, 2012. **142**(1): p. 21-24 e7.
4. Weis, V.G. and J.R. Goldenring, *Current understanding of SPEM and its standing in the preneoplastic process*. Gastric Cancer, 2009. **12**(4): p. 189-97.
5. Fehlings, M., et al., *Comparative analysis of the interaction of Helicobacter pylori with human dendritic cells, macrophages, and monocytes*. Infect Immun, 2012. **80**(8): p. 2724-34.
6. Zhang, X., R. Goncalves, and D.M. Mosser, *The isolation and characterization of murine macrophages*. Curr Protoc Immunol, 2008. **Chapter 14**: p. Unit 14 1.
7. Ramsey, V.G., et al., *The maturation of mucus-secreting gastric epithelial progenitors into digestive-enzyme secreting zymogenic cells requires Mist1*. Development, 2007. **134**(1): p. 211-22.
8. Bredemeyer, A.J., et al., *The gastric epithelial progenitor cell niche and differentiation of the zymogenic (chief) cell lineage*. Dev Biol, 2009. **325**(1): p. 211-24.
9. Kim, H.K., et al., *Elevated levels of circulating platelet microparticles, VEGF, IL-6 and RANTES in patients with gastric cancer: possible role of a metastasis predictor*. Eur J Cancer, 2003. **39**(2): p. 184-91.

10. Hodge, D.R., E.M. Hurt, and W.L. Farrar, *The role of IL-6 and STAT3 in inflammation and cancer*. Eur J Cancer, 2005. **41**(16): p. 2502-12.
11. Keenan, J.A., et al., *Interferon-gamma (IFN-gamma) and interleukin-6 (IL-6) in peritoneal fluid and macrophage-conditioned media of women with endometriosis*. Am J Reprod Immunol, 1994. **32**(3): p. 180-3.
12. Zhu, G.F., et al., *Endogenous substance P mediates cold water stress-induced increase in interleukin-6 secretion from peritoneal macrophages*. J Neurosci, 1996. **16**(11): p. 3745-52.
13. Engelberts, I., et al., *The interrelation between TNF, IL-6, and PAF secretion induced by LPS in an in vivo and in vitro murine model*. Lymphokine Cytokine Res, 1991. **10**(1-2): p. 127-31.
14. Reinecker, H.C., et al., *Enhanced secretion of tumour necrosis factor-alpha, IL-6, and IL-1 beta by isolated lamina propria mononuclear cells from patients with ulcerative colitis and Crohn's disease*. Clin Exp Immunol, 1993. **94**(1): p. 174-81.
15. Schuringa, J.J., et al., *Ser727-dependent transcriptional activation by association of p300 with STAT3 upon IL-6 stimulation*. FEBS Lett, 2001. **495**(1-2): p. 71-6.
16. Al-Jiboury, H. and J.D. Kaunitz, *Gastroduodenal mucosal defense*. Curr Opin Gastroenterol, 2012. **28**(6): p. 594-601.
17. Burke, A.J., et al., *The yin and yang of nitric oxide in cancer progression*. Carcinogenesis, 2013. **34**(3): p. 503-12.
18. Franco, L. and G. Talamini, *Cross-talk between inducible nitric oxide synthase and cyclooxygenase in Helicobacter-pylori-induced gastritis*. Med Princ Pract, 2009. **18**(6): p. 477-81.
19. Hernandez-Ramirez, R.U., et al., *Dietary intake of polyphenols, nitrate and nitrite and gastric cancer risk in Mexico City*. Int J Cancer, 2009. **125**(6): p. 1424-30.
20. Shao, Z.M., W.J. Radziszewski, and S.H. Barsky, *Tamoxifen enhances myoepithelial cell suppression of human breast carcinoma progression in vitro by two different effector mechanisms*. Cancer Lett, 2000. **157**(2): p. 133-44.

CHAPTER 5: CONCLUSIONS AND FUTURE DIRECTIONS

Conclusions

The goal of my thesis has been to understand mechanisms that regulate gastric epithelial stem cell proliferation during normal homeostasis and preneoplastic metaplasia. The main predisposing factor for developing gastric metaplasia and cancer is infection with *Helicobacter pylori*. *H. pylori* infection leads to parietal cell atrophy and an associated expansion in progenitor cells. However, there is a large amount of inflammation associated with infection, which makes it difficult to separate the individual signals responsible for atrophy and increase in proliferation respectively. Hence, to analyze different signaling pathways that are induced early following atrophy of parietal cells, we first identified a model for inducing atrophy in a rapid and synchronous manner, without a substantial inflammatory component.

In Chapter 2, we showed that a single injection with a high dose of the breast cancer chemotherapeutic drug, tamoxifen, induces rapid parietal cell atrophy within three days of administration [1]. Moreover, tamoxifen induced atrophy is not accompanied by substantial inflammation but does cause an expansion in the proliferative progenitor cell compartment, along with dedifferentiation of zymogenic cells [1]. Parietal cell loss is reversible within two weeks of cessation of tamoxifen treatment [1]. Although the mechanism of tamoxifen toxicity on parietal cells is unknown, treatment with the proton pump inhibitor, omeprazole, partially rescues atrophy; suggesting that tamoxifen may act by disrupting the proton gradient [1].

In Chapter 3, we utilized the ability of tamoxifen to kill parietal cells and remodel the gastric epithelium to determine mechanisms that modulate progenitor cell expansion. We found that the proliferating isthmal cells label with the cell surface receptor, CD44 [2]. CD44 is normally expressed in the immune cells and mesenchyme, but also labels small, undifferentiated isthmal

cells in the normal, uninjured gastric epithelium [2]. Upon treatment with tamoxifen, CD44⁺ cells from the isthmus start expanding towards the base of the unit until day 3 of the treatment, when all cells in the gastric unit label with CD44 [2]. We found that loss of CD44, either by deletion of the *Cd44* gene or by blocking its activation using PEP-1, reduced the number of proliferating cells at baseline when compared to wildtype controls [2]. Accordingly, *Cd44*^{-/-} and PEP-1 treated mice were unable to dramatically increase proliferation when challenged with tamoxifen. Conversely, when CD44 was activated by treating mice with its ligand hyaluronan, there was an increase in proliferation [2]. Thus, CD44 interaction with its normal extracellular matrix binding partner is necessary and sufficient for proliferation under normal and injury conditions. We then determined the mechanism by which CD44 regulates proliferation. We found that CD44 binds to pSTAT3 and regulates the transcription of the proliferation gene, CyclinD1 [2, [3]. When STAT3 activation is blocked pharmacologically and challenged with tamoxifen, there is a dampening of the proliferative response and expression of CyclinD1 [2]. Therefore, CD44 enhances progenitor cell proliferation following injury by binding to STAT3 and controlling the expression of CyclinD1. Since we found CD44 is induced at the transcriptional level, we then determined which signaling pathway might induce *Cd44* gene expression. We found that ERK was activated by phosphorylation early upon treatment with tamoxifen, and blocking of ERK activation inhibited proliferation and *Cd44* expression [2]. Hence, we concluded that atrophy-induced CD44 expansion depends on pERK, which, accordingly, also labels the proliferating isthmal cells that respond to atrophy.

We have shown that even though we inject mice systemically with tamoxifen, the stomach is specifically sensitive to injury when compared to other organs [1]. Therefore, in Chapter 4, we

analyzed signals from the circulation, which could cause parietal cell death and increased proliferation. We found that mice that were treated with tamoxifen showed a dramatic increase in IL-6 in their sera. Since IL-6 is generally secreted by T-cells and macrophages, we looked for the presence of these cells in the stomachs of mice treated with tamoxifen. While control mice did not show cells labeling with the macrophage specific marker, F4/80, we found scant F4/80⁺ macrophages in the mesenchymes of tamoxifen treated stomachs. When cultured and treated with tamoxifen, peritoneal macrophages showed an increase in the expression of *Il-6*. Depletion of macrophages with clodronate not only reduced the proliferative response to tamoxifen, but also blocked atrophy of parietal cells. Therefore, we next identified the signal from the macrophages to the parietal cells that causes atrophy upon tamoxifen treatment.

iNOS expression is increased in parietal cells upon treatment with tamoxifen and in humans with intestinal metaplasia. When treated with nitric oxide donors, the mice showed parietal cell damage and a concomitant increase in proliferation, reminiscent of tamoxifen treatment. Blocking of iNOS with its pharmacological inhibitor or scavenging of nitric oxide rescued the increase in proliferation. Hence, we conclude that factors secreted by macrophages upon tamoxifen challenge are sufficient to induce parietal cell atrophy by increasing the expression of iNOS. Nitric oxide (NO) is a diffusible gas that can signal to cells locally. Depending upon the concentration of NO, it is capable of inducing proliferation in stem cells via the MAPK pathway independent of EGFR [4]. Furthermore, NO causes dedifferentiation of articular chondrocytes by increasing ERK signaling and inhibiting p38MAPK [5]. Therefore, NO serves as an ideal signaling intermediate released by PCs during injury that can signal to adjacent stem cells to proliferate and zymogenic cells to dedifferentiate and re-enter the cell cycle.

In conclusion, in this thesis, we have outlined a tamoxifen induced mechanism by which parietal cells undergo atrophy and initiate the development of metaplasia. Metaplasia is associated with an expansion in stem cell proliferation brought about by an ERK→CD44→STAT3→cyclin D1 signaling cascade. Once challenged with tamoxifen, macrophages secrete cytokines that induce parietal cell death, in a mechanism that depends on parietal cell induction of iNOS, and stem cell proliferation, through the activation of ERK signaling.

Future Directions

- 1) *Determining the role of the CD44 ligand, hyaluronan, in regulating CD44 expression and proliferation of isthmal cells*

Hyaluronan (HA) is a component of the extracellular matrix and is found in connective, epithelial and neural tissues, forming large networks in the extracellular compartment [6]. Each HA molecule consists of on average 10,000 repeating disaccharide units of D-glucuronic acid and N-acetylglucosamine, synthesized by the action of three HA synthesizing enzymes (HAS1, 2 and 3) [6]. HA accumulates at sites of inflammation and tumor progression [6]. Although HA accumulation is not a universal characteristic of all tumors, many cancers contain increased amounts of HA compared to normal tissues [7]. It is also believed that HA surrounding cancer cells helps in increasing their spread and migration [8]. The stroma surrounding gastric tumors shows increased staining of HA relative to normal gastric mesenchyme [7]. We found that HA staining was found in the mesenchyme surrounding the gastric unit in normal wildtype mice [2]. However, there was also an increase in HA in the mesenchyme of tamoxifen treated mice (Chapter 3 [2]). The expression of HA synthesizing enzymes, HAS1 and HAS2 was also increased (Chapter 3 [2]). Fig. 5.1 (adapted from Chapter 3) shows the expression of HA and HAS1, 2 in normal and tamoxifen treated mice.

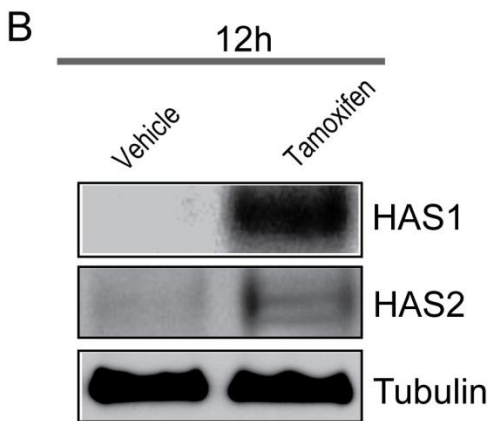
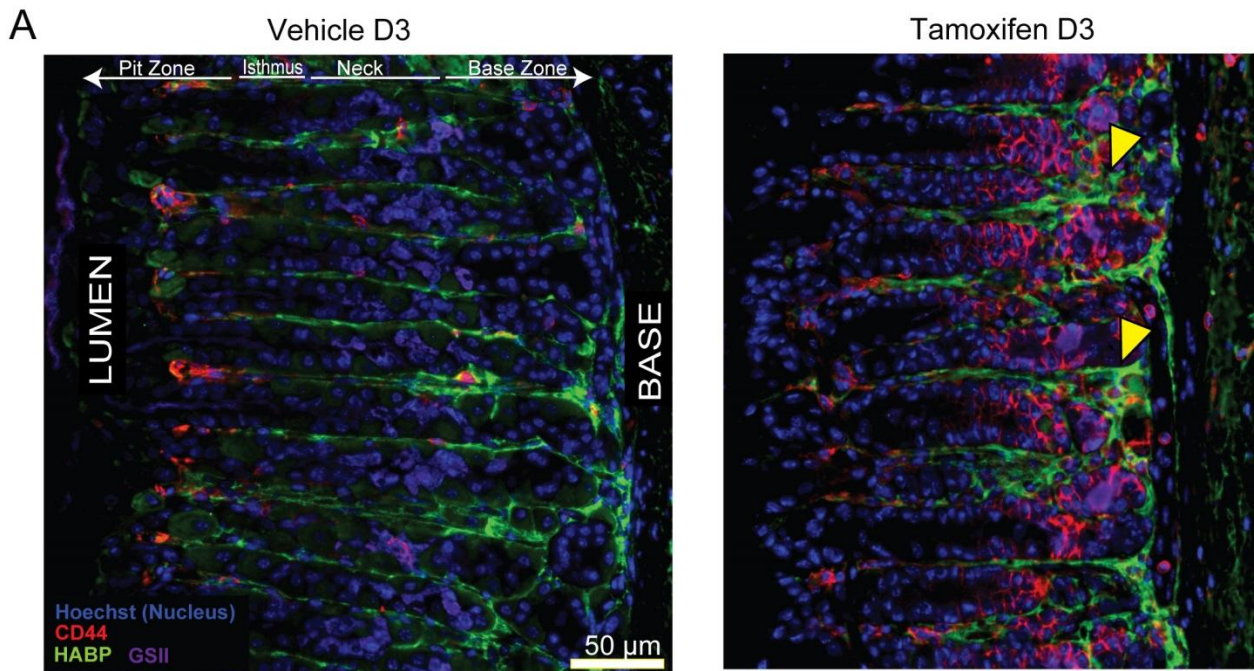


Fig. 5.1: Hyaluronic acid (HA), a ligand of CD44, was increased upon atrophic injury with tamoxifen. HA (stained using Hyaluronan-binding protein; in green) and CD44 (red) were increased in expression towards the base of the gastric unit during tamoxifen induced metaplasia (A, arrowheads). HAS1 and HAS2, enzymes that synthesizes HA, were also increased by 12h of tamoxifen treatment (B).

Moreover, we observed an increase in HA staining in human biopsies of patients who had developed intestinal metaplasia (Fig. 5.2). In normal human stomachs, HA stained the mesenchymes in between gastric units; however, in humans with intestinal metaplasia, these regions of HA staining in the mesenchyme were greatly expanded (Fig. 5.2).

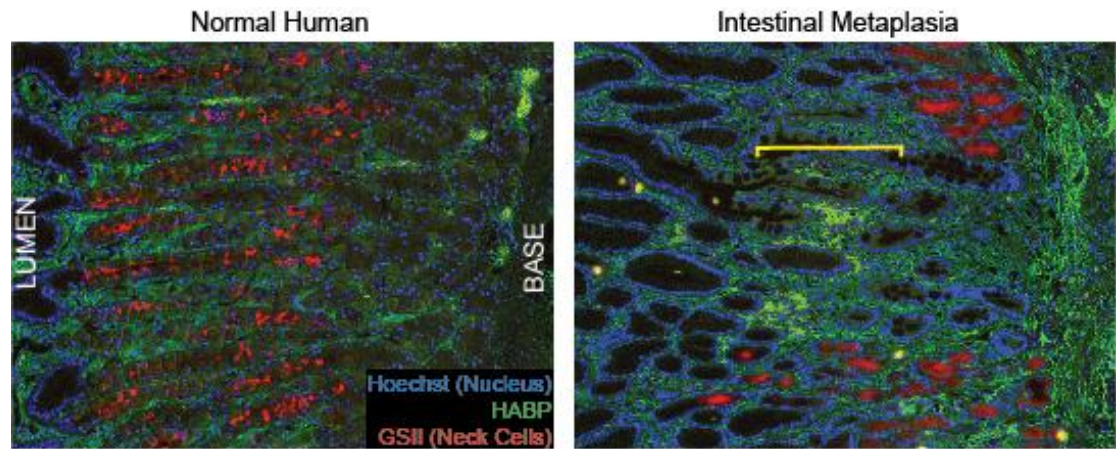


Fig. 5.2: Hyaluronic acid (HA) is increased in human patients with gastritis and intestinal metaplasia. HA (stained using Hyaluronan-binding protein; in green) and GSII (red) were increased in expression in the mesenchyme surrounding the gastric unit during intestinal metaplasia (yellow bracket).

Since atrophy and metaplasia are accompanied by a surge in proliferation that are regulated by the HA receptor, CD44 (Chapter 3), we next looked at whether HA was sufficient to induce proliferation. We injected 3-week old mice with HA twice a week for 5 weeks and found that they had increased proliferation, with increased pit cell census (Chapter 3) compared to wildtype controls. Since the mouse gastric epithelium continues to develop and differentiate for a few weeks after birth, our data show that HA is an important regulator of proliferation during this developmental period. To assess whether HA is involved in adult gastric epithelial proliferation, we injected adult wildtype mice with HA every day for 3 days and 10 days and found a significant increase in proliferation (Fig. 5.3).

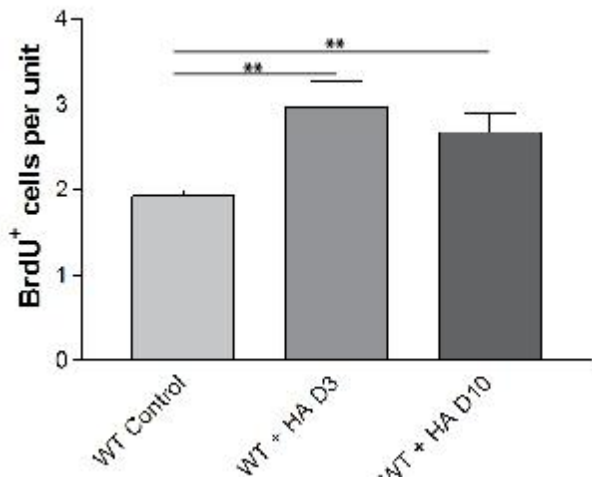


Fig. 5.3: HA is sufficient to induce expansion of stem cell proliferation.

Mice treated every day with HA for 3 days and 10 days showed significant increase in proliferation, stained with BrdU, compared to vehicle treated control mice.

We then tested for sufficiency of HA in inducing proliferation, by blocking the interaction of HA with its receptors using the peptide PEP-1 (Fig. 5.4 and Chapter 3).

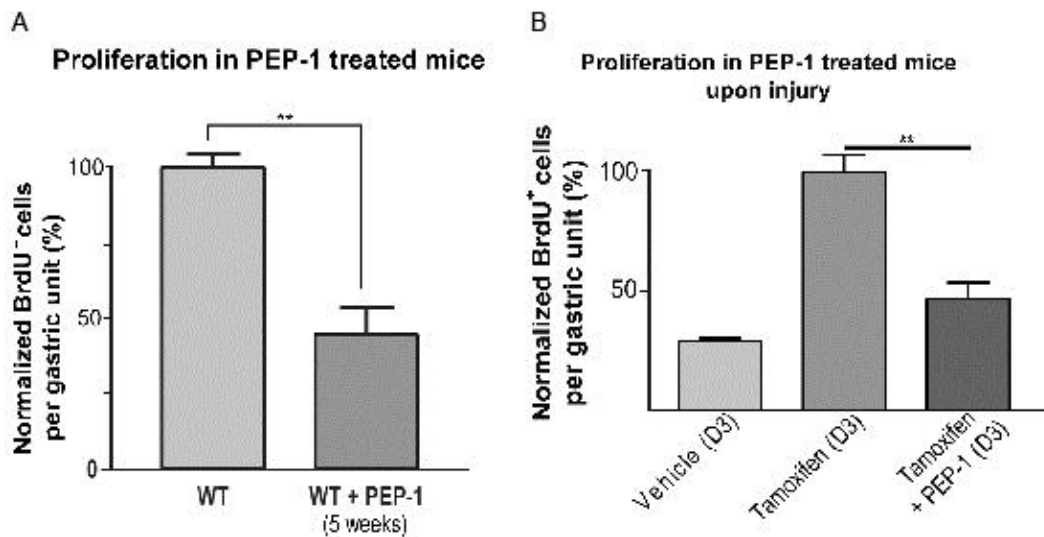


Fig. 5.4. HA is necessary for normal and injury induced expansion of proliferation. Mice treated with the HA blocking peptide, PEP-1, for 5 weeks showed half the number of proliferating cells compared to wildtype controls (A). When PEP-1 treated mice were injected with tamoxifen, they were able to expand proliferation to only half of that of mice treated with tamoxifen alone (B).

Since HA is necessary and sufficient for inducing proliferation but does not lead to parietal cell death or zymogenic cell dedifferentiation (data not shown), stem cell proliferation must be uncouplable from parietal cell death. While pERK induced CD44 expansion and interaction with HA appears to be the mechanism adopted by injured stem cells to increase proliferation, HA induced proliferation even in the absence of pERK can modulate normal proliferation in the gastric epithelium. Thus, if we can understand the mechanisms that regulate HA synthesis, we should have a strong foothold into the pathways that feed into both normal cell turnover and atrophy induced expansion of gastric stem cells.

II) Determining the factors secreted by activated macrophages that lead to parietal cell atrophy and proliferation expansion

We have shown in Chapter 4 that macrophages secrete IL-6, among other factors, which increase parietal cell death and associated expansion of proliferation. However, it is unlikely that IL-6 is the only factor responsible for rescuing the metaplastic changes in the epithelium during injury. Our collaborative work with Dr. Richard DiPaolo, as well as the work of others [9], has shown that IL-11 is involved in inducing PC injury during autoimmune gastritis, along with IL-6 [10]. Moreover, loss of EBI3, which forms have the heterodimeric cytokines IL-27 and IL-35, accelerates the development of metaplasia in mice with autoimmune gastritis (DiPaolo lab, unpublished data). To identify factors responsible for PC atrophy and stem cell proliferation, we will first determine whether macrophage secreted factors are sufficient for development of metaplasia. For this, we will isolate peritoneal macrophages, culture and treat them with tamoxifen, and then adoptively transfer them into clodronate treated or irradiated mice and assess whether the recipient mice develop metaplasia. Once we have established sufficiency, we can determine which proteins and cytokines have higher expression in tamoxifen treated macrophage

cultures using qRT-PCR. Finally, we can test sufficiency of individual factors by injecting recombinant versions of these factors into mice or transducing them using adenovirus vectors and assessing whether they undergo PC atrophy or expansion in proliferation or ZC dedifferentiation or all of the aforementioned processes.

III) Determining the mechanism by which zymogenic cells undergo dedifferentiation following parietal cell atrophy

Along with proliferation expansion, another epithelial remodeling process associated with parietal cell death is the dedifferentiation of zymogenic cells. Zymogenic cells are largely post-mitotic and normally do nothing but their physiological duty of elaborating enzymes critical for digestion. Upon parietal cell atrophy, zymogenic cells start re-expressing markers of their precursors, i.e. neck cells, such as TFF-2, represented by GSII in Figure 5.5 [1].

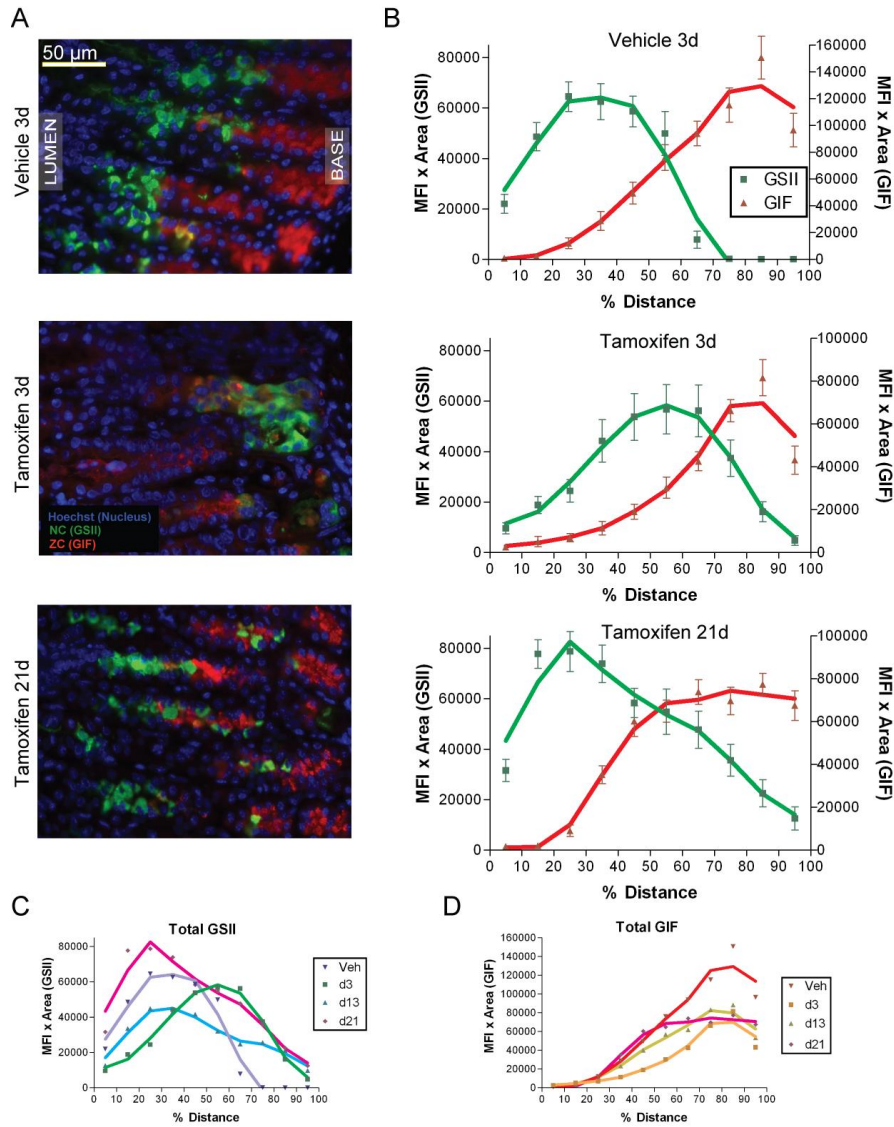


Fig. 5.5 Tamoxifen induces spasmolytic polypeptide-expressing metaplasia (SPEM). *A*: photomicrographs of basal and neck zones of gastric units with mucous neck cells (green, GS-II lectin) and zymogenic cells (red, GIF) taken 3 days after vehicle treatment (above); 3 days (middle) and 21 days (below) after tamoxifen treatment. *B*: Neck and base zones of gastric units were analyzed for expression of neck and zymogenic cell markers as a function of distance (0=first cell positive for neck/zymogenic markers; 100 = basal-most neck/zymogenic cell). For each unit, distance was normalized into bins representing 10% of total distance. Plotted are the products of the mean fluorescent intensity and the total area that is either GS-II (neck cell) or

GIF (zymogenic cell) positive (means±SD, across all gastric units). Note how normal neck cell differentiation peaks, then falls off toward the base, whereas, zymogenic cells are found in the base and not the neck. Tamoxifen treatment causes neck cell marker expression in the base. The changes in neck cell (C) and zymogenic cell (D) markers for all conditions are plotted on the same axes.

Blocking of PC atrophy inhibits the dedifferentiation of ZCs. This could be caused by one of three mechanisms:

- i. Healthy PCs constantly engage in homeostatic signaling with ZCs, the loss of which during atrophy leads to ZC dedifferentiation
- ii. Injured PCs release stress signals that cause ZCs to dedifferentiate
- iii. A common upstream stress signal leads to death of PCs and dedifferentiation of ZCs

While the nature of signaling between PCs and ZCs is not extensively elucidated, our data with blocking iNOS and macrophage activation show that either the PC stress signals or common activators or both might be involved in orchestrating epithelial remodeling during injury. Whatever the nature of the PC to ZC signaling might be during atrophy, it results in ZC dedifferentiation. We observe an increase in CD44⁺ cells at the base of the gastric units during atrophy (Fig. 3.1). These CD44⁺ cells could either originate from CD44⁺ isthmal cells that proliferate and occupy the base and/or from the dedifferentiation of ZCs which causes them to reduce their size, express the stem cell marker, CD44, and enter the cell-cycle. It is technically challenging to establish the relative contribution to the CD44-positive cells from expanded isthmal stem cells vs. dedifferentiating ZCs. Once CD44 is expressed, it imparts the ZCs with

proliferative (and potentially stem/progenitor) cell capabilities, because it has been well established that ZCs act as cryptic progenitors during atrophy and give rise to metaplastic cells [11].

An important developmental pathway that regulates dedifferentiation is the Hippo pathway [12]. Inactivation of the *hpo* kinase cascade in drosophila larval eye imaginal discs increases the rate of cell duplication, protects cells from apoptosis, and delays the cell cycle exit of the uncommitted cells [13]. The Hippo pathway restricts organ growth and size by phosphorylating and inactivating the transcription factor YAP (Yes-Associated Protein). Inactivation of the tumor suppressors of the Hippo pathway or activation of the oncogene YAP results in massive tissue overgrowth characterized by increased cell proliferation and diminished cell death [14]. YAP1 dephosphorylation is a reliable metric for assessing Hippo activation. Hence, we determined the status of YAP1 phosphorylation in our model of tamoxifen induced atrophy in Figure 5.6. We found a decrease in pYAP1 at Day 3 of tamoxifen treatment, which coincides with the highest number of proliferating cells during tamoxifen induced atrophy, as well as the appearance of proliferating ZCs [1]. Therefore, to reiterate, we find an increase in YAP1 activation and Hippo signaling coinciding with increased proliferation and ZC dedifferentiation in our model of tamoxifen induced atrophy.

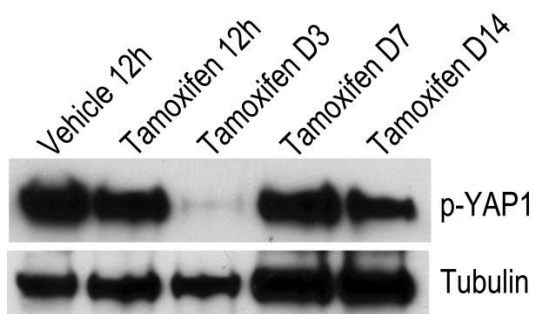


Fig. 5.6. YAP1 is activated upon treatment with tamoxifen. Phosphorylation of YAP1, which deactivates it, is decreased 3 days after treatment with tamoxifen, which coincides with maximum parietal cell atrophy and CD44 expression

CD44 has been shown to interact with merlin, a product of the *Nf-2* gene, which is a component of the Hippo tumor suppressor pathway and interacts with cytoskeletal components [15]. In schwannoma cells, merlin binds to the cytoplasmic tail of CD44 and this binding inhibits the association between CD44 and HA [15]. It will be interesting to determine whether CD44 increase in ZCs during atrophy causes ZC dedifferentiation and proliferation via the Hippo pathway. This can be studied using null mutants of the Hippo kinases *Mst1* and *Mst2*. *Pdx1-Cre* driven *Mst1*^{-/-} X *Mst2*^{fl/fl} mice have shown to cause dedifferentiation in pancreatic acinar cells [9]. In order to adapt these mice to our system, we can generate *β-actin-Cre; Mst1*^{-/-}/*Mst2*^{fl/fl} mice or *Mist1-Cre; Mst1*^{-/-}/*Mst2*^{fl/fl} mice which should over-activate the Hippo pathway in the entire epithelium or zymogenic cells, respectively. If these mice show dedifferentiation of zymogenic cells and increase their proliferation, it will confirm the role of Hippo in developing metaplasia.

A recent study in *Drosophila* larval imaginal discs showed a link between Hedgehog (Hh) signaling and the Hippo pathway in regulating cell proliferation [16]. The authors showed that the Hh inhibitory receptor, Patched (PTCH1) acts as a tumor suppressor, and loss of *Ptch1* leads to hyperactivation of YAP1, resulting in excess proliferation [16]. In humans, PTCH1 is highly expressed in the gastric epithelium and especially in the membrane compartment of ZCs (Human Protein Atlas). In the stomach, *Shh* is expressed highly, though recent studies using *Shh-Cre* lineage tracing have shown that all major corpus lineages express *Shh* [17]. Hedgehog signaling is frequently associated with advanced gastric adenocarcinomas [18]. Although, during metaplasia there is a loss of *Shh* due to death of parietal cells, there is an increase in the expression of the Hh target, *Gli1*, when compared to controls (data not shown). This indicates

that either other cell lineages increase expression of *Shh* during PC atrophy or that Shh molecules are released by dying PCs which enables signaling to other cells in the unit, including ZCs. Increased *Gli1* expression is a readout of increased Shh signaling and mirrors the result of loss of *Ptch1*. I hypothesize that increased Hh signaling results in hyperactivation of YAP1 and increased proliferation via the Hippo pathway. This is an unexplored area of research and can be beneficial in understanding mechanisms that lead to ZC dedifferentiation and entry into the cell cycle.

VII. Determining the role of CD44 in Helicobacter pylori niche establishment

Helicobacter pylori infection in humans is the major risk factor for developing gastric cancer [19]. Once *H. pylori* colonizes the stomach, it persists for the lifetime of the host. Although infection is associated with inflammation, it typically does not clear the bacteria [19]. In mice, the CagA⁺ strain of *H. pylori*, PMSS1, colonizes the antrum of the stomach [20], which is devoid of acid secreting parietal cells. This enables *H. pylori* to evade the harsh acidic environment of the stomach corpus and phenocopies the way infection is thought to occur in humans. The bacteria survive as two major populations: first, freely swimming in the mucus gel and using its motility, chemotaxis and stress responses to survive and swim towards the shelter of the epithelium; and second, adhered to epithelial cell surface through various adhesins [20]. Howitt et. al. [21] found that *H. pylori* utilizes a novel family of chemotactic proteins called ChePep for colonizing the stomach. ChePep is necessary for *H. pylori* flagellar rotation, which enables it to evade acidic regions within the stomach, which act as chemorepellants [21]. ChePep also regulates its ability to colonize deeper into antral glands [21]. Thus, *H. pylori* is presumably attracted to some moiety on the surface of gastric epithelial cells, eventually attaches to the cell

surface and establishes a colony. *H. pylori* preferentially adhere to intercellular junctions between epithelial cells [20]. Tan et. al. found that the bacteria adhered to the intercellular junctions were able to undergo several rounds of replication while being adhered to their original point of attachment [20]. Moreover, *H. pylori* colonization is typically adjacent to a dividing cell (Manuel Amieva, Stanford University; personal communication). It is unclear whether bacterial attachment promotes epithelial cell proliferation or whether *H. pylori* is chemically attracted to dividing cells within the gastric unit. Either scenario presents interesting, addressable questions in order to understand the nature of host-pathogen interactions.

Once attached to the host cell, *H. pylori* deliver the cytotoxin-associated gene A (CagA) protein into the host cell [22]. CagA is one of the most important links between infection and development of gastric cancer [22]. Once inside the host cell, CagA localizes to the plasma membrane and interacts with host cell junctional complex machinery, such as ZO-1, Jam and E-cadherin [22]. Moreover, kinases from the host cell, such as c-Src/Lyn and Abl, phosphorylate tyrosines on the CagA protein and activate a receptor tyrosine kinase signaling cascade [22]. These events lead to loss of host cell polarity and increased invasiveness [22]. Recent studies have shown that in an attempt to protect host cells from the infection, intracellular CagA is degraded by autophagy induced by accumulation of reactive oxygen species (ROS) [23]. The accumulation of CagA is restricted to cells deficient in autophagy [23]. Tsugawa et. al. found that cells expressing CD44 (specifically, the variant CD44v9) were resistant to ROS and, therefore, deficient in autophagic degradation of CagA [23]. This observation is important in understanding the relation between *H. pylori* infection and CD44 in gastric metaplasia, since presence of both leads to gastric cancer.

We have shown in Chapter 3 that CD44 labels proliferating cells, normally and during parietal cell atrophy by tamoxifen and *H. pylori* infection [2]. The human Cd44 gene contains 20 exons [24]. Exons 1-5 and 16-20 are typically spliced together to form standard CD44 or sCD44, which forms a 37kDa protein and is ubiquitously expressed [24]. Exons 6-15 can be variably spliced into the standard exons to give rise to CD44 variants in the N-terminal extracellular domain [24]. Certain CD44 isoforms, such as CD44v6 and CD44v9, are overexpressed in gastric cancer [25]. As mentioned before, CD44v9 enables resistance to ROS and promotes *H. pylori* infection in hosts [23].

These observations raise a number of interesting questions:

1. Is *H. pylori* chemically attracted to CD44⁺ cells in the normal gastric epithelium, by virtue of specific sugar moieties on the CD44 extracellular domain?
2. Does attachment of *H. pylori* to potentially CD44⁺ stem cells lead to an increase in stem cell proliferation?
3. Does *H. pylori* attachment selectively increase expression of CD44v9 over CD44s?
4. Are *Cd44*^{-/-} mice resistant to *H. pylori* colonization and persistence?
5. Is ROS induction sufficient to induce CD44⁺ stem cell proliferation?

Addressing these questions will provide key insights into the mechanisms by which *H. pylori* modulates the host epithelium to establish its niche. Moreover, since host cell changes persist after eradication of the bacterium, understanding the role of CD44 will facilitate devising therapeutic strategies post *H. pylori* clearance in patients.

References

1. Huh, W.J., et al., *Tamoxifen induces rapid, reversible atrophy, and metaplasia in mouse stomach*. *Gastroenterology*, 2012. **142**(1): p. 21-24 e7.
2. Khurana, S.S., et al., *The hyaluronic acid receptor CD44 coordinates normal and metaplastic gastric epithelial progenitor cell proliferation*. *J Biol Chem*, 2013. **288**(22): p. 16085-97.
3. Lee, J.L., M.J. Wang, and J.Y. Chen, *Acetylation and activation of STAT3 mediated by nuclear translocation of CD44*. *J Cell Biol*, 2009. **185**(6): p. 949-57.
4. Carreira, B.P., et al., *Nitric oxide stimulates the proliferation of neural stem cells bypassing the epidermal growth factor receptor*. *Stem Cells*, 2010. **28**(7): p. 1219-30.
5. Yoon, J.B., et al., *Non-steroidal anti-inflammatory drugs inhibit nitric oxide-induced apoptosis and dedifferentiation of articular chondrocytes independent of cyclooxygenase activity*. *J Biol Chem*, 2003. **278**(17): p. 15319-25.
6. Heldin, P., et al., *Importance of hyaluronan-CD44 interactions in inflammation and tumorigenesis*. *Connect Tissue Res*, 2008. **49**(3): p. 215-8.
7. Wang, C., et al., *Hyaluronan distribution in the normal epithelium of esophagus, stomach, and colon and their cancers*. *Am J Pathol*, 1996. **148**(6): p. 1861-9.
8. Tammi, R.H., et al., *Hyaluronan in human tumors: pathobiological and prognostic messages from cell-associated and stromal hyaluronan*. *Semin Cancer Biol*, 2008. **18**(4): p. 288-95.
9. Howlett, M., et al., *Differential regulation of gastric tumor growth by cytokines that signal exclusively through the coreceptor gp130*. *Gastroenterology*, 2005. **129**(3): p. 1005-18.
10. Nguyen, T.L., et al., *Autoimmune gastritis mediated by CD4+ T cells promotes the development of gastric cancer*. *Cancer Res*, 2013. **73**(7): p. 2117-26.
11. Nam, K.T., et al., *Mature chief cells are cryptic progenitors for metaplasia in the stomach*. *Gastroenterology*, 2010. **139**(6): p. 2028-2037 e9.
12. Edgar, B.A., *From cell structure to transcription: Hippo forges a new path*. *Cell*, 2006. **124**(2): p. 267-73.
13. Pantalacci, S., N. Tapon, and P. Leopold, *The Salvador partner Hippo promotes apoptosis and cell-cycle exit in Drosophila*. *Nat Cell Biol*, 2003. **5**(10): p. 921-7.
14. Dong, J., et al., *Elucidation of a universal size-control mechanism in Drosophila and mammals*. *Cell*, 2007. **130**(6): p. 1120-33.
15. Bai, Y., et al., *Inhibition of the hyaluronan-CD44 interaction by merlin contributes to the tumor-suppressor activity of merlin*. *Oncogene*, 2007. **26**(6): p. 836-50.
16. Kagey, J.D., J.A. Brown, and K.H. Moberg, *Regulation of Yorkie activity in Drosophila imaginal discs by the Hedgehog receptor gene patched*. *Mech Dev*, 2012. **129**(9-12): p. 339-49.
17. Sherman, A.E. and Y. Zavros, *Role of Sonic Hedgehog signaling during progression from inflammation to cancer in the stomach*. *World J Gastrointest Pathophysiol*, 2011. **2**(6): p. 103-8.
18. Ma, X., et al., *Frequent activation of the hedgehog pathway in advanced gastric adenocarcinomas*. *Carcinogenesis*, 2005. **26**(10): p. 1698-705.
19. Wroblewski, L.E., R.M. Peek, Jr., and K.T. Wilson, *Helicobacter pylori and gastric cancer: factors that modulate disease risk*. *Clin Microbiol Rev*, 2010. **23**(4): p. 713-39.

20. Tan, S., L.S. Tompkins, and M.R. Amieva, *Helicobacter pylori* usurps cell polarity to turn the cell surface into a replicative niche. PLoS Pathog, 2009. **5**(5): p. e1000407.
21. Howitt, M.R., et al., *ChePep* controls *Helicobacter pylori* Infection of the gastric glands and chemotaxis in the *Epsilonproteobacteria*. MBio, 2011. **2**(4).
22. Buti, L., et al., *Helicobacter pylori* cytotoxin-associated gene A (*CagA*) subverts the apoptosis-stimulating protein of p53 (*ASPP2*) tumor suppressor pathway of the host. Proc Natl Acad Sci U S A, 2011. **108**(22): p. 9238-43.
23. Tsugawa, H., et al., Reactive oxygen species-induced autophagic degradation of *Helicobacter pylori* *CagA* is specifically suppressed in cancer stem-like cells. Cell Host Microbe, 2012. **12**(6): p. 764-77.
24. Goodison, S., V. Urquidi, and D. Tarin, *CD44* cell adhesion molecules. Mol Pathol, 1999. **52**(4): p. 189-96.
25. da Cunha, C.B., et al., *De novo* expression of *CD44* variants in sporadic and hereditary gastric cancer. Lab Invest, 2010. **90**(11): p. 1604-14.

APPENDIX 1: The Gastric Mucosa: Development and Differentiation

Abstract

The development and differentiation of the gastric mucosa are controlled by a complex interplay of signaling proteins and transcriptional regulators. This process is complicated by the fact that the stomach is derived from two germ layers, the endoderm and the mesoderm, with the first giving rise to the mature epithelium and the latter contributing the smooth muscle required for peristalsis. Reciprocal epithelial–mesenchymal interactions dictate the formation of the stomach during fetal development, and also contribute to its continuous regeneration and differentiation throughout adult life. In this chapter, we discuss the discoveries that have been made in different model systems, from zebrafish to human, which show that the Hedgehog, Wnt, Notch, bone morphogenetic protein, and fibroblast growth factor (FGF) signaling systems play essential roles during various stages of stomach development.

Introduction

Evolutionarily, the stomach as a functional organ, with its acid and digestive enzyme-secreting properties, emerged well after the development of the intestine, and was more or less concomitant with the evolution of jaws. Its final, adult form is similarly slow to develop, occurring, for example, several weeks after birth, in rodents. Like the rest of the epithelium of the luminal gastrointestinal (GI) tract, the gastric epithelium exhibits continual cell loss throughout adult life [1]. To replace the lost cells, resident stem cells continually differentiate into multiple cell lineages. Thus, in terms of cell fate specification decisions, developmental processes never stop in the stomach. In this chapter, we examine the embryonic specification of the stomach from the luminal GI tract, its subsequent development into a mature organ, and, finally, the differentiation processes that continue into adulthood. More specifically, we examine the development of cell lineages and the role of signaling pathways at each step.

I. Early Foregut Development

We first briefly review early development, to put the emergence of the stomach in its proper context. In the mouse embryo, gastrulation begins at E6.25, with the formation of a thickening on the posterior side of the epiblast, called the “primitive streak”. Epiblast cells ingress through the primitive streak and the node, and undergo an epithelial-to-mesenchymal transition (EMT) to gradually form the endoderm and the mesoderm. During the formation of the vertebrate GI tract, the endoderm and mesoderm undergo extensive regionalization and elongation to give rise to organs with specific structures and functions. The vertebrate embryonic GI tract consists of an endodermally derived epithelium and a mesodermally derived mesenchyme. Eventually, the gut tube is patterned along the anterior–hindgut (which forms the distal transverse, descending, and

rectosigmoid segments of the colon) [2]. After this initial patterning, the fate of the endoderm, although broadly determined, is still only partially specified and depends on patterning factors secreted by the underlying mesoderm. As we will discuss, the fact that factors from the mesenchyme direct epithelial fate decisions remains relevant, to some degree, throughout adult life. Key regulatory pathways that are developmentally critical, such as the Hedgehog, Wnt, bone morphogenetic protein (BMP), and FGF systems, send signals across the epithelial–mesenchymal boundaries throughout the nascent luminal GI tract and thus contribute toward patterning of the gut tube along the left–right, A–P, dorsal–ventral, and radial axes.

II. Specification of the Stomach as a Separate Organ: An Overview

Following gastrulation, the primitive gut tube is formed from the endoderm, and it encircles the inner leaflet of the lateral plate mesoderm, which then forms the visceral mesoderm [2]. The formation of a solid gut tube at the dorsal midline by the convergent-extension of the sheet of endodermal cells requires both the vascular endothelial growth factor (VEGF) and Wnt/PCP (planar cell polarity) pathways, as studied in zebrafish [3]. The transcription factor HNF1b/Tcf2 aids in the formation of a single gut tube lumen by inducing genes whose expression results in apical fluid secretion into the developing luminal space [4]. The primitive gut tube endoderm is broadly partitioned antero-posteriorly, with the anterior half of the embryo expressing the transcription factors Hhex, Sox2, and Foxa2 and the posterior half expressing Cdx1, 2, and 4 [5]. The anterior half forms the foregut while the posterior half forms the hindgut. Between E8.0 and E9.5, broad foregut and hindgut territories become divided into organ-specific zones and lineages in the mouse embryo. Gastric epithelial cytodifferentiation is initiated around E13.5. Unlike humans—who have entirely glandular stomachs—mice have a stomach in which the

proximal third is lined by a stratified, keratinized squamous epithelium (the region known as the forestomach). By E16.5, the morphological differences between the forestomach and glandular epithelia are evident in mice. Recombination experiments have shown that the presumptive stomach endoderm might have some plasticity until E11.5/E12.5, but at E14.5, the endoderm no longer requires mesenchymal instructive signals for its A–P patterning [6]. This finding is corroborated by studies in the chick, which also show that most of the endoderm is capable of self-differentiation even from the early stages of development and that it does not require mesodermal inputs to do so. However, mesodermal signals are crucial for early specification and patterning [7].

III. Morphogenetic Codes Involved in Stomach Specification

In the 1960s, Lewis Wolpert hypothesized that molecules could affect target tissues by traveling over distances in a gradient, much like the color gradients on the French Flag (thus called the French Flag model). Morphogens are such molecules, which originate in a specific tissue, and travel over some distance to act on specific receptors with progressively decreasing signal strength. The dose or strength of the ligand molecule binding to its receptor determines the output of gene expression in the target tissue, and it is, therefore, the decisive factor in establishing positional information. A limited number of morphogenetic signaling pathways that play crucial roles in determining the different axes during development of an organ have been identified. The four principal signaling pathways are the Hedgehog, Wnt, transforming growth factor (TGF), and receptor tyrosine kinase (such as fibroblast growth factor (FGF), epithelial growth factor (EGF), and platelet derived growth factor (PDGF)) systems. These four pathways

coordinate the spatiotemporal expression of transcription factors that impart foregut or hindgut identity to the GI tract [5].

A. The Hedgehog Signaling Pathway – Early Events

1. Left-Right Axis Formation

Correct patterning of the left-right axis is essential for the proper development of gut-derived organs such as the pancreas and liver and for leftward looping of the gut tube. During gastrulation, a group of ciliated cells at the anterior end of the primitive streak form a notch called the node, which is believed to regulate left-right axis formation of the gut, by generating a leftward flow of the extraembryonic fluid [8]. Hedgehog signaling is involved in gut tube formation as Smo and Shh/Ihh mutant mice fail to close the midgut, probably due to leftward gut malrotation [9]. Shh is expressed at E7.75 in the anterior endoderm [10, [11] and later expands to the posterior part of the gut, whereas Ihh is expressed in the posterior endoderm and spreads anteriorly [12, [13]. Shh and Ihh play redundant roles in left-right axis formation, and both mutants lack Nodal expression in the left lateral plate mesoderm and fail to specify the left side program. It has been proposed that hedgehog has an indirect role in this process in that it becomes distributed asymmetrically to one side of the embryo secondary to impaired nodal flow [13, [14]. This asymmetrical flow of Hh is thought to be dependent on FGF signaling [14].

2. Anterior-Posterior Endodermal Patterning in the Gut

Patterning of the endoderm along the A-P axis occurs after gastrulation, as early as E6.7. The first endodermal cells to exit the primitive streak move anteriorly and express the Hex gene, whereas later-exiting endodermal cells express FoxA2 (Hnf3 β), and those exiting last form the posterior endoderm and express Cdx2 [15, [16]. However, the timing of the exit of cells from the

primitive streak is not the only determinant early of A-P patterning. At this stage, patterning factors secreted by the mesenchyme are essential to provide hindgut. Hex, FoxA2 and Sox2 are required for foregut development, while Cdx1, 2 and 4 are required for hindgut development and defining the foregut-hindgut boundary [5, [17]. At later stages of development, the endoderm plays an instructive role in patterning the mesoderm [18].

3. Hedgehog in Stomach Development

Shh is expressed at high levels in the forestomach epithelium and at low levels in the glandular part of the stomach epithelium from E11.5 to 15.5 [19]. Ihh has a reciprocal expression pattern to that of Shh, in that it is highly expressed in the glandular stomach and to a lesser extent in the forestomach [20]. The expression of Ptc1, which is both the receptor for and a target of Hedgehog signaling, in the underlying mesenchyme closely follows the expression of Shh [20]. Ihh mutants do not show any gross abnormalities in glandular stomach development [9], which suggests that in spite of high amounts of message in the glandular stomach, Ihh might not be translated or active, or may be compensated by Shh. Ihh expression in the hindstomach depends on the mesenchymal/epithelial signaling brought about by FGF10 binding to the FGFR2b receptor (Spencer-Dene et al., 2006). Inhibition of Shh signal in the glandular epithelium in these earlier stages is blocked by FGF10 through Gata4 [18, [20]. At later stages of development, i.e. E18.5, Shh expression expands to include the glandular stomach epithelium and results in signaling within the epithelium itself and to the mesenchyme [9]. Shh null mice display a small, malformed forestomach which is in accordance with its early expression pattern. Shh apparently does not play a major role in governing development of gastric epithelial cell lineages, and glands form normally in the posterior stomach, though with reduced gland branching [18]. Shh

and *Ihh* double null embryos arrest shortly post-gastrulation, and as *Shh* and *Ihh* may have redundant functions, single null alleles do not yield an accurate analysis of overall Hh signaling during gastrointestinal morphogenesis. To fully understand the function of Hedgehog signaling in the developing GI tract, Mao and coworkers [21] used conditional gene targeting to ablate both *Shh* and *Ihh* at E9.5, and found that Hh signaling plays a critical role in promoting the survival and proliferation of mesenchymal progenitors underlying the gastric epithelium.

B. The Wnt Signaling Pathway

Wnt ligands are secreted glycoproteins and have been shown to govern important developmental processes such as cell fate determination, tissue patterning, cell proliferation and morphogenesis [22]. Wnt signaling occurs by two pathways, the canonical Wnt/ β -catenin signaling pathway (Wnt1, 3 and 8) which brings about activation and nuclear translocation of β -catenin, and the non-canonical Wnt/ Ca^{2+} and Wnt/Fz planar cell polarity pathways (Wnt 5a and 11). Wnt signaling is also regulated by various secreted Wnt antagonists, the Soluble Frizzled Related Proteins (Sfrps), which bind to and block Wnt ligands from binding to Frizzled receptors [23], the WIF-1 protein, which has a similar mechanism of action as SFRPs but is structurally different and has been studied extensively in *Drosophila* and *Xenopus* [24], and Cerberus, a Wnt antagonist similar to SFRP and WIF-1 that has been studied principally in *Xenopus*. At present, it is not clear whether the mouse Cerberus like protein, mCer1, functions as a true orthologue of Cerberus [25]. Finally, there are the Dickkopf (Dkk1-4) proteins that act by binding to the Wnt co-receptors LRP5/6 rather than by interacting with the Wnt ligands directly [21, [26, [27].

At stage E12.5 of mouse embryonic development, Wnt4, 5a and 11 exhibit specific and partially overlapping expression patterns in the stomach: Wnt1 expression is strong in the esophageal-

pyloric junction and in part of the forestomach around the lesser curvature; Wnt5a is expressed in the entire forestomach and part of the corpus; Wnt4 expression is confined to the pyloric region of the stomach epithelium and is weakly present in the esophagus. Wnt5b and 6 might be expressed in the esophageal epithelium at this stage as well [28]. The non-canonical Wnt5a is diffusely expressed in the mesenchyme at E12.5 and more specifically in the ectomesenchyme just underlying the epithelium at E14.5. Decreasing Wnt5a expression results in repression of the intestinal marker Cdx2 and posterior expansion of Sox2, the foregut marker [29]. In the chick embryo, Wnt5a is expressed in the presumptive stomach mesenchyme, and overexpression of Wnt5a causes increased and ectopic expression of some of the marker genes of the luminal and glandular epithelial cells, the former characterized by the expression of Spasmolytic Polypeptide and thus analogous to neck cells in the mammalian gastric corpus, and the latter marked by the expression of pepsinogen, analogous to the zymogenic or chief cells in mammals. In particular, the overexpression of Wnt5a markedly enhances the expression of ECPg (Embryonic Chicken Pepsinogen), indicating its role as a mesenchymal factor that regulates the differentiation of the proventricular epithelium [30]. Wnt/ β -catenin signaling is necessary and sufficient to promote hindgut development of the endoderm and repress foregut formation in frog and zebrafish embryos [31].

Given the interdependence of Wnts and their receptors, it is also important to understand the spatio-temporal expression of Sfrps and other inhibitors when evaluating Wnt signaling in the developing stomach. Recent studies have shown that Sfrp1, Sfrp2 and Sfrp5 are redundant in function and required for forestomach morphogenesis [22]. Sfrp1 expression starts in the splanchnic mesoderm around E10.5, extending from the caudal region of the presumptive stomach up to the midgut. Sfrp1 and 2 are targets of Barx1, a homeodomain transcription

factor, which is specifically expressed in the presumptive stomach mesenchyme from E9 until E15, with a peak at E13.5 [32]. Barx1 acts by inhibiting the canonical Wnt pathway in the stomach. Using TOP-GAL reporter mice, the authors showed that canonical Wnt signaling is active in the presumptive intestine but not the presumptive stomach endoderm. Wnt signaling initiates around E9.5, persists through E12.5, and is attenuated by E14. Barx1 upregulates the expression of Sfrp1 and 2 in the mesoderm, which in turn compete with the Wnt ligands, blocking signaling to the epithelium. The attenuation of Wnt is required for specification of the stomach-specific program in the epithelium. Since Barx1 is not expressed in the intestinal mesenchyme, Wnt signaling in the intestinal epithelium is not attenuated and the epithelium continues to follow the default intestinal specific program [32]. That the intestinal program is in fact, the default pathway, has also been suggested by studies in chick embryos [33]; although in these studies, Wnt involvement was not specifically addressed. Barx1 also regulates the expression of Bapx1 (Nkx3.2) in the mesenchyme, which is required for the formation of the pyloric sphincter [34]. Overall, the literature indicates that Wnt signaling promotes posterior fates in the gut endoderm, with inhibition of Wnt promoting foregut marker expression posteriorly and overexpression leading to intestinal differentiation (posteriorization) of the stomach.

C. The FGF pathway:

FGFs (through FGF receptors) have been shown to signal across epithelial-mesenchymal borders to promote cell proliferation, migration, and differentiation during the development of the lung, intestine, and stomach [35, [36, [37]. The mouse and human FGF families consist of 23 members that are structurally related and are either secreted or act as intracellular ligands. Nyeng and

colleagues analyzed the expression of all 23 FGF ligands in later stages of the developing stomach (E14.5-E18.5) on the messenger RNA level and found that FGF1-3, FGF7, FGF9 and FGF10 were expressed above a baseline control gene [36]. Earlier, Bhushan and coworkers [38] had shown that FGF10 was expressed in the posterior part of the stomach mesenchyme at E11.5, before cytodifferentiation had occurred. FGF10 is a ligand for FGFR2-IIIb, which is expressed on the epithelium. During these later stages of embryonic gastric morphogenesis, FGFR2b expression in the corpus and antrum was more or less constant over time with a slight increase at E15.5, coinciding with the timing of the highest expression of FGF10 and, interestingly, was more prominent in newly forming glands.

In chick embryos, overexpression of FGF10 in the presumptive stomach mesenchyme results in excessive cell proliferation of the overlying epithelium and affects its differentiation, leading to the expression of cSP (spasmolytic polypeptide – luminal marker) as well as Smad8 (a glandular marker) in epithelial cells [7]. In mouse and chick embryos, FGF4 is expressed in the mesoderm, and signals to the endoderm to promote the expression of Cdx genes in the presumptive hindgut region and to repress the expression of Hhex and Foxa2 in the presumptive foregut [39, [40, [41].

D. The BMP/TGF Signaling pathway

Bone morphogenetic proteins (BMPs) are multi-functional growth factors that belong to the transforming growth factor beta (TGF β) superfamily. BMPs have been shown to play critical roles in heart, neural, cartilage, postnatal bone development and other organs such as kidney, lung, liver, limb, amnion, eye, teeth, pituitary, and testes. Smad1, 5 and 8 are the immediate downstream signaling molecules of BMP receptors. BMP signaling promotes posterior endoderm development [5]. Danesh and colleagues studied the expression patterns of different

BMP ligands in the early developing murine embryo (E7.25-E10.5) (Danesh et al., 2009). They found that BMP2 is absent from the gut tube at this time. At E8.25, BMP4 is expressed in the posterior lateral plate mesoderm; whereas at E10.5, it extends to dorsal gut mesoderm [42]. BMP7 is expressed at low levels in the foregut endoderm at E8.75, and by E10.5, its expression in the posterior stomach is highly intensified. BMP2 is expressed in the mesenchyme of the developing proventricular mesenchyme of the chick. Overexpression of BMP2 leads to an increase in the number of glands expressing ECPg (embryonic chicken pepsinogen), whereas overexpression of Noggin (a BMP antagonist) completely inhibits gland formation [7]. On the other hand, overexpression of BMP4 does not lead to any change in gland formation [7].

E. The Retinoic Acid Signaling pathway

Retinoic Acid (RA), the active derivative of Vitamin A, is a diffusible embryonic signaling molecule that has a wide array of target molecules in a variety of different organs. In the GI tract, RA signaling is important in establishing the foregut-hindgut boundary [5]. Retinoic Acid activity depends on the RA-synthesizing enzyme, retinaldehyde dehydrogenase (RALDH). Raldh1 is weakly expressed in the stomach epithelium at E12.4-14.5; whereas Raldh2 has a stronger expression in the stomach mesenchyme at E10.5-E12.5 [43]. Raldh2^{-/-} mouse fetuses exhibit a smaller, rudimentary stomach than wild type littermates, with a columnar epithelium lacking squamous or glandular differentiation [44]. These knockout mice have lower FGF10 expression in the mesenchyme, but Hoxa5 expression is unaffected. It has been proposed [45] that Hoxa5 regulates FGF10 expression, but the above results indicate that there might be other upstream players controlling FGF10.

F. The Notch Signaling System

While Notch signaling has been shown to play important roles in controlling cell fate decisions during development of various tissues, including the intestinal epithelium, its role in the development of the mammalian stomach has not been fully explored, although it has been shown that the differentiation of multiple enteroendocrine cell lineages in the stomach is dependent on the transcription factor Ngn3, and important effector of the pathway [46]. In the developing chicken proventricular epithelium, Notch signaling acts as a binary switch between choosing the luminal (cSP expressing) or glandular (Smad8/ECPg expressing) cell fate [47]. Nyeng and colleagues [36] studied the cross talk between Notch and FGF signaling in the mouse embryonic gut development and found Notch1, its downstream bHLH transcription factor Hes1, and its ligand Jagged2 to be expressed in the gastric epithelium in the corpus and antrum at high levels. and in the forestomach at a basal level from E14.5 through E18.5 [36]. They also found that Hes1 expression was upregulated in response to FGF10, thus implying that FGF10 positively regulates Notch signaling in the developing stomach epithelium [36].

IV. Transcription Factors

In an attempt to identify marker genes for the development of each organ of the GI tract in chicks, Yasugi and Mizuno identified groups of genes expressed in the epithelium at different times around gland formation, i.e. when the epithelium invaginates into the mesenchyme to form gastric glands [7]. The first group includes genes which are expressed prior to and during gland formation, i.e. *foxa2*, *cSox3*, *cfos* and *junD*. The second group of genes, *cSox2*, *Shh*, *cSP*, and *PPAR γ* , are expressed prior to but not after gland formation. The last set of genes is expressed

specifically after gland formation, i.e. *Smad8* and *Gata5*. *Delta* and *Notch* are expressed sporadically. *ECPg* is expressed after gland formation and specifically in the gland epithelium.

A. The Hox Genes

The Hox transcription factors share a common DNA-binding motif called the homeodomain. These proteins are involved in regional specification along the A–P axis during embryonic development and are expressed in lateral plate mesoderm.⁴⁸ As the gut derivatives are locally specified along the A–P axis, it is expected that the Hox genes will play a role in establishing regional identities. Kawazoe and coworkers⁴⁸ examined the expression of the different Hox genes in the developing GI tract at E12.5. Among the HoxA cluster, in situ hybridization studies showed that *Hoxa-4* and *Hoxa-5* were expressed in the distal part of the stomach, whereas *Hoxa-6* is expressed in the entire stomach mesenchyme. *Hoxb-4* also has a distal stomach expression pattern, whereas *Hoxb-5* and *Hoxb-7* are expressed over the entire stomach. No expression of *Hoxc-4*, *Hoxc-5* and *Hoxd-4* was observed in the stomach at E12.5. The authors hypothesize that a different Hox code exists in different regions of the gut, which regulates regional specification, with the HoxA cluster predominating the foregut domain. *Hoxa-5* is expressed as early as E9.0 in the caudal segment of the foregut and by E15.5 its expression follows a gradient, with highest levels in the hindstomach mesenchyme. *Hoxa-5* expression vanishes after birth, around P15 in mice. *Hoxa5*^{-/-} mice, at age P15, display a thinner stomach epithelium and hypertrophied submucosa. Aubin and colleagues proposed that *Hox5a* acts by negatively regulating *Fgf10* expression in the hindstomach mesenchyme, which then decreases *Ihh* in the hindstomach epithelium and increases *Shh* in the forestomach epithelium [45]. *Hoxa5* also increases *Tgfb1* and *Tgfb3* in the mesenchyme. Overall, *Hoxa5* appears to provide a posteriorization signal to the

gastric epithelium and mesenchyme. Finally, a study on *Hoxb1* expression in the gut mesenchyme revealed that it is regulated by retinoic acid signaling [48].

B. COUP-TFII

COUP-TFs (COUP-TFI or NR2F1 and COUP-TFII or NR2F2) are highly conserved nuclear orphan receptors that are expressed in the mouse embryonic stomach mesenchyme [49]. At E12.5, COUP-TFII is expressed in the mesenchyme adjacent to the endoderm but not distally, and regulates radial and A-P patterning of the stomach [50]. Ablation of *COUP-TFII* specifically in the mesenchyme leads to the formation of a thicker epithelium, an anterior shift of the limiting ridge that divides the fore- and hind-stomach, reduction in the size of the forestomach, and expansion of the hindstomach. COUP-TFII may be regulated by Hh signaling from the overlying epithelium and it, in turn, might regulate the expression of *Bmp4* in the mesenchyme [50]. Since COUP-TFII may be downstream of *Shh*, it acts as an anteriorization signal like *Shh*. In the adult, COUP-TFII is expressed in the gastric epithelium, specifically in the parietal cells and the base of the gastric unit [50].

C. Sox2

Sox2 is a transcription factor that is important to maintain pluripotency of the epiblast and embryonic stem cells. At E9.5 in the mouse embryo, *Sox2* is expressed in the endoderm of the entire foregut. However, its expression is gradually localized to the esophageal endoderm as the embryo develops. In the stomach, *Sox2* is initially expressed in the stomach epithelium as distally as the pylorus but is later downregulated in the glandular corpus and antrum and expressed only in the forestomach by E18.5 (Que et. al., 2007). Hypermorphic *Sox2* allele expression causes the forestomach epithelium to resemble that of the glandular stomach due to

the expression of mucin and trefoil factor genes [51]. This suggests that Sox2 might act in the developing fetus by inhibiting the expression of the hindstomach genes in the forestomach.

D. Barx1:

Barx1 is a mouse homeodomain transcription factor, a member of the Bar subclass of transcription factors, which is expressed in restricted areas of the head and neck mesenchyme and that of the developing stomach from E9.5 to E16.5 [52]. Kim and coworkers [32] observed that Barx1 had a high enrichment of RNA message in the stomach mesenchyme as compared to the intestine in E12 mouse embryos. Inbred Barx1^{-/-} embryos and outbred Barx1^{-/-} neonates (since inbred Barx1^{-/-} embryos die at E12.5) show stomach defects, with much smaller stomachs than wild type littermates and lack of leftward rotation [32, [53]. Moreover, the mucosa is highly thickened and disorganized and the posterior 3rd of the Barx1^{-/-} neonate stomach undergoes intestinal homeotic transformation, showing expression of intestinal markers and true villus morphology [53]. As outlined above, Barx1 acts by upregulating the expression of soluble Wnt antagonists Sfrp1 and Sfrp2, which in turn bind to Wnt ligands and limit their availability to engage Frizzled receptors on endodermal cells of the presumptive stomach. Since Barx1 is not expressed in the presumptive intestinal mesenchyme, Wnt signaling is not inhibited in this region and it follows an intestinal specific program [53]. Thus, Barx1 acts as an anteriorizing signal and in its absence, the gastro-duodenal boundary are shifted anteriorly.

E. Bapx1

Bapx1 is a homeodomain transcription factor that specifies gut smooth muscle in *Drosophila* [54]. In the chick embryo, Bapx1 is expressed in the gizzard mesenchyme and inhibits the expression of Bmp4 and Wnt5a [55]. Bapx1 is presumed to be regulated by Shh and controls the patterning of the gizzard [55]. Studies in mouse embryos show Bapx1 to be activated at E8.5 in

the lateral plate mesoderm adjacent to the endoderm [34]. Embryos lacking *Bapx1* show a defect in the expansion and morphogenesis of the antral-pyloric segment, rendering it an important factor for pyloric sphincter development [34].

F. Forkhead-box (FOX) family:

Forkhead transcription factors belong to the winged helix family of factors and are so named due to the appearance of their DNA binding motifs when bound to DNA [56]. Kaestner and colleagues [57] identified *Fkh6* (forkhead homologue 6, now termed *FoxL1*) as being specifically expressed in the gastrointestinal mesoderm just underlying the endoderm. *FoxL1*^{-/-} mice show an expanded glandular epithelium, extensive branching within the mucosa and vacuolated pit cells [57]. Absence of *FoxL1* caused decreased *Bmp2* and *Bmp4* expression. The phenotype implies a role for *FoxL1* in epithelial proliferation [57]. Another interesting study done by Fukamachi and colleagues [58] suggested a role for *FoxL1* in the differentiation of oxynticopeptic cells (which are cells combining the separate roles of parietal cells and zymogenic cells that characterize mammalian stomachs) into parietal cells, since eliminating *FoxL1* in mice caused parietal cells to stain positively for pepsinogen.

In evolution, the first species to display two different cell types, i.e. the parietal cell and zymogenic cell, for the secretion of hydrochloric acid and digestive enzymes may be found in the elasmobranch *Hexanchus griseus*, but the molecular mechanism governing this lineage differentiation (e.g., whether a *FoxL1* ortholog plays a role) during evolution is unknown [59]. Loss of *FoxL1* severely abrogates basal and histamine-stimulated gastric acid secretion without affecting the cellular canaliculi architecture [58]. A related transcription factor, *FoxF1*, is co-expressed with *FoxL1* in the developing gut mesoderm, and both are direct targets of Hedgehog signaling through *Gli2* and *Gli3* [60]. In the adult, *FoxL1* indirectly targets *Wnt/β-catenin*

signaling by upregulating extracellular matrix heparin sulfate proteoglycans, which in turn increase the local concentration of Wnt ligand for binding to Frizzled receptors which are expressed in the epithelium [61]. Wnt signaling provides a positive signal for cell proliferation, suggesting that FoxL1 may have opposing roles in the fetus and the adult.

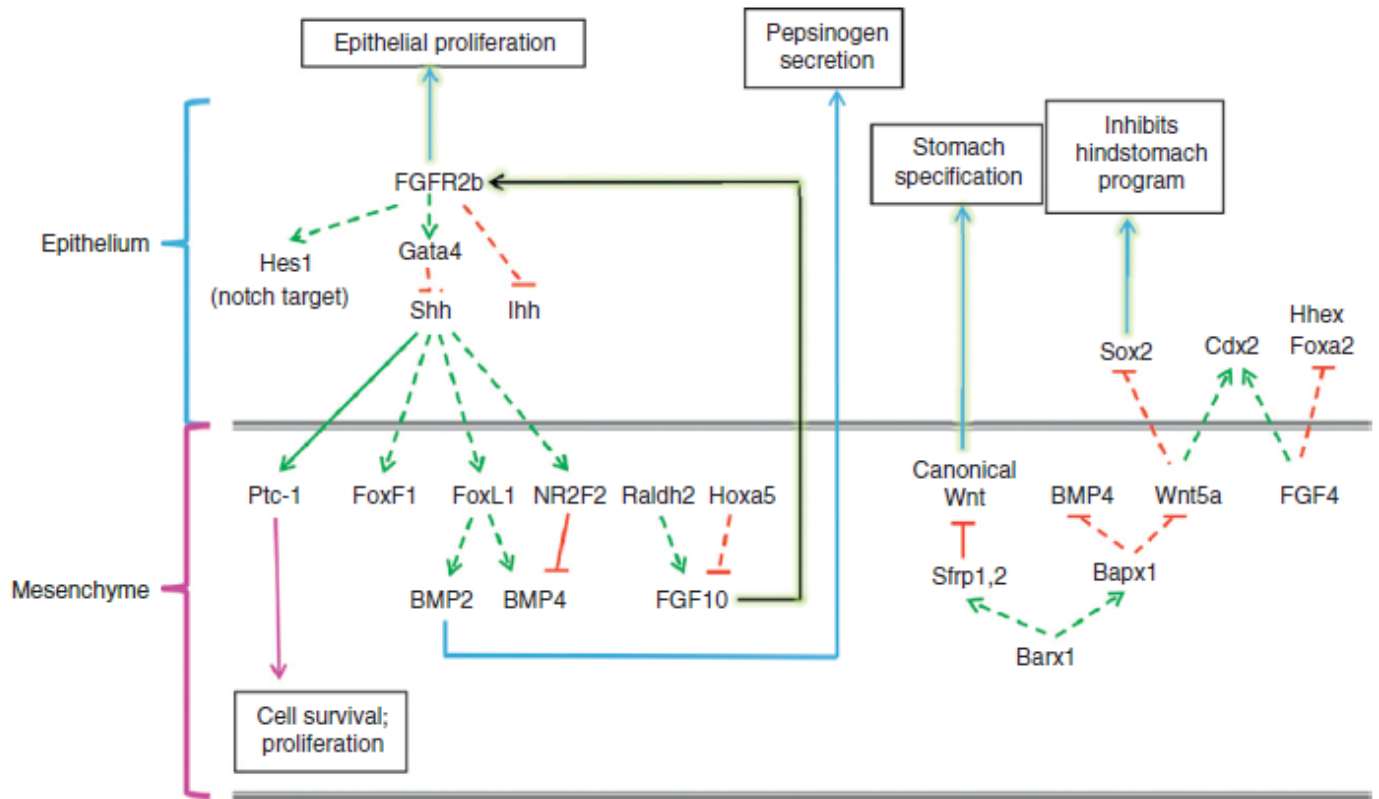


Fig. A1.1. Epithelial-mesenchymal interactions during early foregut/stomach development in the embryo. The gut tube is formed by the juxtaposition of an endodermally derived epithelial later and a mesodermally derived mesenchymal later. Post-gastrulation, important signaling interactions occur bidirectional across the epithelial-mesenchymal boundary, which help in specifying the different organs of the gut tube along the different axes. Depicted is a schematic of the cross talk occurring between the two tissue layers during the specification of the stomach.

V. Postnatal Gastric Development

The source of nutrients for an embryo is obviously different from that of a neonate. Until birth, the developing embryo procures its nourishment from the placenta and substances from swallowed amniotic fluid, which also might contain factors that aid in development [62]. As the newborn develops, maturation and gland formation of the gastrointestinal tract continue, peaking its rate of growth at around three weeks in rodents. The stomach grows at a more rapid rate just after birth as compared to the rest of the body [63]. Gastric epithelial cells differentiate into and establish different lineages – the pit, zymogenic, enteroendocrine and parietal cell lineage [64]. At birth, gastric acid secretion capacity is low, but it rapidly increases about three-fold during the first three days post partum [65], coupled with a proportionate increase in the number of parietal cells per unit volume of gastric mucosa (Xu et. al., 1992). The low pH of the stomach immediately after birth equips the neonates with the first line of defense against ingested microorganisms as the pups change their environment from a sterile to an open one [66]. Gastric acid secretion is responsive to levels of the hormone gastrin (secreted by G-cells of the antrum). Gastrin expression increases shortly after birth, in correlation with the observed increase in acid. Gastrin gene expression responds to EGF via cAMP activation [67]. Interestingly, there is >1,000 times more EGF in colostrum and milk consumed by neonates as compared to plasma levels, and ingested EGF might act as the trigger for gastrin release, subsequent parietal cell proliferation, and acid secretion immediately after birth [68].

Studies in neonatal rats have shown that changes in suckling of new born pups, such as weaning, have an impact on proliferation of gastric mucosal cells [69]. Gama and Alvarez showed that if pups are early-weaned, the basal proliferation in the gastric mucosa is higher, suggesting that milk plays an important role in maintaining the desired proliferative rate and homeostasis.

Indeed, the mitogen TGF β is found in rat milk and its concentration decreases towards weaning [70]. TGF β receptors I and II are also expressed in the gastric epithelial cells at E20 until weaning [71]. This timing coincides with the proliferation of the cells in the developing gastric unit. Post-weaning, the proliferative zone of the unit is restricted to the isthmus region where the stem cell is believed to reside.

Ghrelin is a growth-hormone-releasing peptide released by the endocrine cells of the rat fetal stomach from E18 onward, and its expression peaks during the second and third weeks after birth [72]. Ghrelin is also released by other tissues in the pregnant mother (such as the brain, hypothalamus, pituitary, immune cells, ovary, placenta and others), in the fetus during development (such as in the stomach, intestine, pancreas, lungs), and in the neonate (such as the stomach and lungs) [73]. For the newborn, the sources of circulating ghrelin include secretion by the stomach mucosa and the maternal contribution in colostrum and milk [74]. Ghrelin may play a role in postnatal gut development as it leads to an increase in total body weight and the weight of the stomach (Hayashida et. al., 2002).

VI. Adult Gastric Homeostasis

The gastric epithelium undergoes continuous renewal throughout the life span of the animal [1]. This renewal occurs due to the proliferation and differentiation of multipotent stem cells that are present in the isthmus region of the adult gastric unit. The stem cell gives rise to precursors that move bidirectionally (towards the lumen and towards the base) in the unit, giving rise to three main lineages with eleven cell types, i.e.

1. **Pit (also known as surface-associated/foveolar) cell lineage** – Pre-pit cell precursors, Pre-pit cells, Pit cells

2. **Zymogenic cell lineage** – Pre-neck cell precursors, Pre-neck cells, Neck cells, Pre-zymogenic cells, Zymogenic cells

3. **Parietal cell lineage** - Pre-parietal cell precursors, Pre-parietal cells, Parietal cells

In addition to these lineages, endocrine cells are also scattered throughout the gastric unit. Even though there is emerging literature on the mechanisms by which the different cell types are formed, many gaps remain. For example, even though the location of the stem cell within the gastric corpus has been well established by ultrastructure and turnover analysis, its molecular identity has not been well characterized (Huh et. al., 2006).

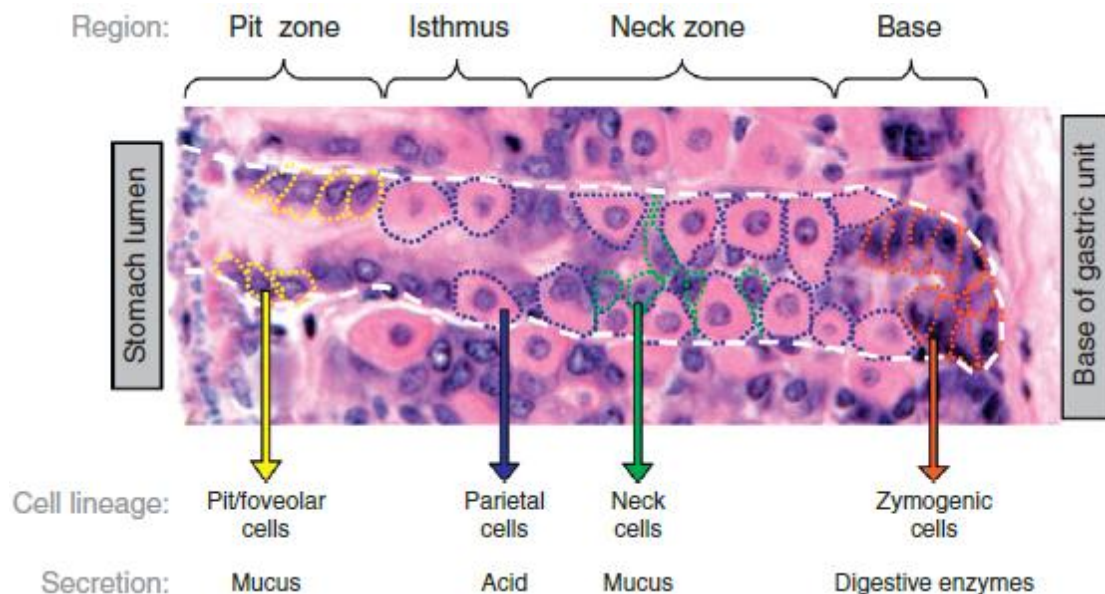


Fig. A1.2. Normal architecture and organization of different cell types in the gastric unit of the adult mouse. The corpus (body) of the adult stomach consists of repeating invaginations called gastric units, each of which can be divided into four regions characterized by the presence of specific cell types in each region. Depicted is an H&E stained slide of the adult mouse stomach showing a single gastric unit outlined in white, with each region labeled: 1, Pit region, which lines the stomach lumen, consists of mucus-secreting pit aka foveolar cells, and narrows

deeper in the unit into the isthmus region; 2, the isthmus region, characterized by the presence of multipotent gastric stem cell; 3, neck region, where mucus-secreting neck cells and most of the acid-secreting parietal cells reside; and 4, base region, where enzyme producing zymogenic cells are present.

1. The Pit cell lineage: The stem cell in the isthmus region gives rise to a pit cell precursor, which is devoid of secretory granules. The precursor then differentiates into pre-pit and ultimately into pit cells, which migrate into the pit region. Pit cells contain mucous granules (characterized by Muc5AC, Gkn1, Tff1) and degenerate upon reaching the luminal surface. This entire process takes place over three days [75, [76, [77, [78]. Verzi and colleagues showed that the forkhead transcription factor FoxQ1 is expressed specifically in the stomach in the adult GI tract and within the stomach, its expression is limited to pit cells [79]. However, this finding is controversial as another report claims that FoxQ1 is expressed exclusively in parietal cells [80]. Verzi and coworkers find that FoxQ1 is required for the expression of Muc5AC but not Gkn1 in pit cells [79]. FoxQ1 mutant stomachs also have dysregulation of genes involved in assembly and function of membranous organelles, such as Rpgrip, Sec22 and Stk25, suggesting that it may play a crucial role not only in the expression of Muc5AC, but also in imparting this cell with its specific architecture [79]. Gastrin has been implicated in increasing proliferation of pit cells, leading to an extended pit region [81]. Ihh may also play a role in pit cell differentiation and maintenance [82].

2. The Zymogenic cell lineage: The pre-neck cell precursors that arise from the stem cell in the isthmus give rise to mucus-secreting neck cells, which eventually mature to form

enzyme-secreting zymogenic cells (ZC), which occupy the base of the unit. Neck cells are characterized by the expression of TFF2 (also known as spasmolytic polypeptide) and the expression of TFF2 is expanded during SPEM (spasmolytic polypeptide expressing metaplasia) [83]. The journey of the neck cell to the base to form zymogenic cells takes around 14 days, and zymogenic cells at the base of the gland have a half life of 194 days [84]. The improbability of a terminally differentiated, post-mitotic mucus secreting neck cell maturing into an enzyme secreting zymogenic cells was highlighted by Hanby and colleagues [85]. However, Ramsey and co-workers presented the first molecular evidence that zymogenic cells, in fact, arise from neck cells, and that this maturation is controlled by the bHLH transcription factor, Mist1 [86]. Recent studies by Tian and colleagues show that Mist1 facilitates structural maturation of zymogenic cells in part by regulating the expression of Rab proteins, which control the formation of serous secretory granules [87]. Another pathway that expands the zymogenic cell population is the retinoic acid pathway [88].

3. **The Parietal cell lineage:** Parietal cells (PCs) arise from pre-parietal cells in the isthmus region, function in acid secretion, and contain a highly dense canalicular network [89]. Aside from their acid secretion function, parietal cells also produce growth factors that maintain normal patterns of cell differentiation and proliferation within the gastric unit [90]. Most of the PC transcriptional machinery is centered around regulating the expression of genes that keep the cell functional, such as *Arf1*, *Sod2*, *Mucdhl*, *Fads1*, and *Calm2* [90]. The PC also elaborates growth factors such as *Igfbp2* and *Pthlh* that can have an effect on the differentiation and proliferation status of other cell types in the

gastric unit [90, [91]. The aforementioned transcription factor FoxQ1 appears to be unique in that it controls gastric acid secretion, but not the development of parietal cells, and FoxQ1^{-/-} mice show a defect in the development of canaliculi and are less responsive to gastrin [80].

Hormonal regulation of gastric acid secretion is performed by peptides such as gastrin (secreted by the G-cells of the antrum), ghrelin (produced by Gr cells), natriuretic peptides (produced in the central nervous system), orexins (neuropeptides), histamine and others, either alone or in combination [92]. Gastrin is the main stimulant for acid secretion after a meal, and its mechanism of action is via the activation of the CCK-2 (cholecystokinin) receptor, which in turn activates the PLC and/or MAPK pathways, causing the release of histamine from ECL cells (endocrine cells) of the stomach [93]. Histamine diffuses to parietal cells, where it binds to H-2 receptors and activates cAMP production, ultimately resulting in the recruitment of the H⁺/K⁺ATPase to the canalicular membrane to enable acid secretion [94].

VII. Morphogenetic pathways in maintaining adult gastric homeostasis:

A. The Hedgehog Pathway

Studies by Van den Brink and colleagues first catalogued Shh expression in the adult gastric fundus [95]. Ptc-1, a target of hedgehog signaling, is also expressed in parietal cells and epithelial cells at the base of the unit. There are contrasting observations relating to the expression of Shh in the pit region, and it is not yet certain if Shh is, in fact, expressed in these cells [96]. Within the epithelium, the targets of hedgehog signaling are parietal cells at the cellular level and FoxA2, Isl-1, the H⁺/K⁺ATPase, and BMP4 at the molecular level [18, [95, [97]. Shh is in turn regulated by EGF signaling [97]. While FoxA2, Isl-1 and H/KATPase are

expressed in the epithelium, BMP4 is expressed in the interstitial myofibroblast like cells [95]. However, studies by Fukaya and coworkers showed that Ptc-1 expression was absent from the isthmus region suggesting that hedgehog does not act directly on stem/progenitor cells [82]. In contrast, Ihh is expressed in differentiated pit cells and may play a role in the differentiation and maintenance of this lineage [18, [82].

B. The BMP signaling system

As discussed earlier, BMP4, but not BMP2, is a target of Shh in the stomach. Nitsche and coworkers showed that BMP4 regulates the expression of H⁺/K⁺ATPase- α subunit, through the activation of Smad-1, in an isolated canine parietal cell culture system [98]. There are contrasting observations regarding the cellular identity of BMP4-producing cells. Van den Brink and colleagues found BMP4 solely in fibroblasts *in-vivo* [95], whereas, Nitsche and coworkers recently showed that it is also expressed in parietal cells *in-vitro* [98]. EGF acts by inhibiting H⁺/K⁺ATPase expression in parietal cells and this effect can be reversed by BMP4 [98]. Therefore, BMP4 may be a crucial regulator of differentiation and functional maturation in parietal cells. Indeed, inducible ablation of the Bmp4 gene in mice leads to hyperplastic polyp formation in the antral mucosa, indicative of a sustained role for BMP4 in suppressing antral proliferative response [99, [100].

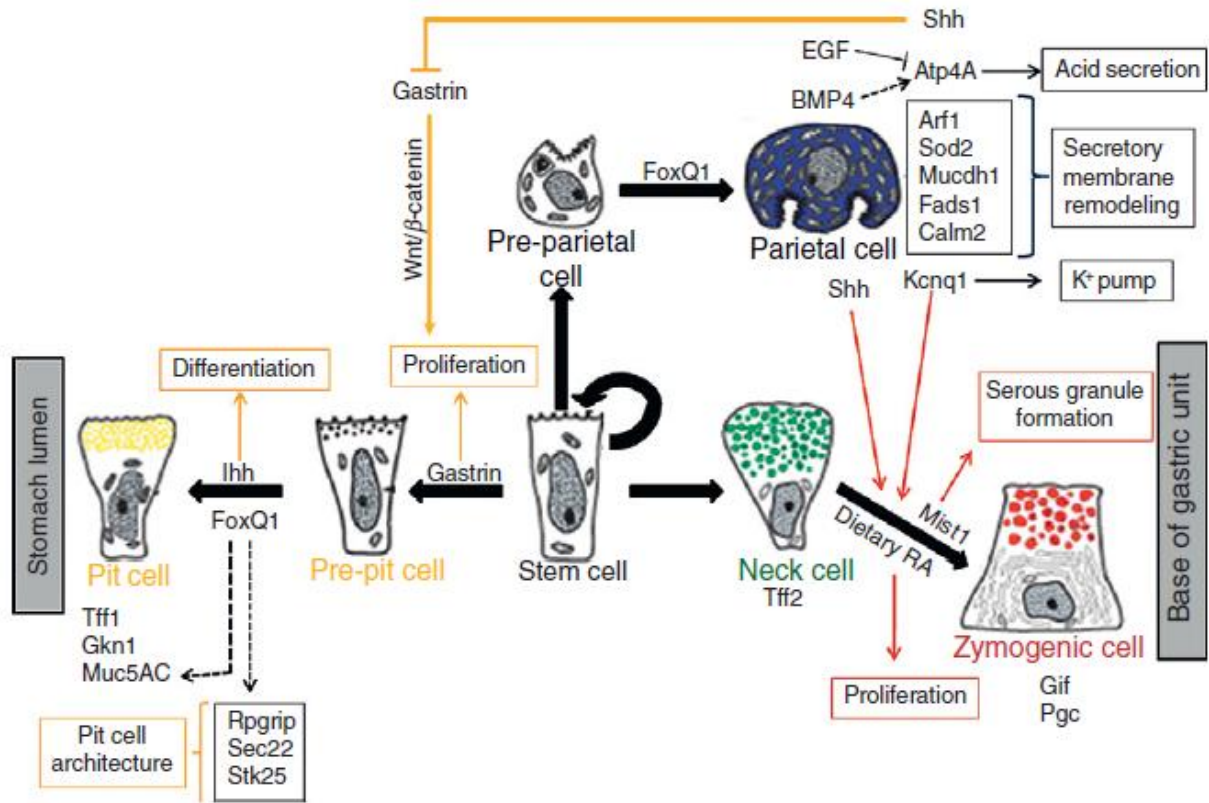


Fig. A1.3. Interplay between developmental signaling pathways coordinating differentiation and maintenance of different cell lineages within the gastric unit. The gastric epithelium is constantly renewing which requires replenishment of the various differentiated cell types (each having a different life span), from multipotent stem cells. The schematic shows signaling intermediates involved in the maintenance of cell lineage homeostasis and physiology in the gastric unit.

Conclusion

In conclusion, multiple transcriptional regulators and spatially controlled signaling pathways contribute to the development of the stomach during fetal life, and to the continuing

differentiation of the gastric mucosa throughout adult life. The relatively recent evolutionary appearance of a separate stomach provides an interesting model system to study mesenchymal/epithelial signaling, which may provide information on similar processes elsewhere in the body. Given the high incidence and mortality of gastric cancer, discussed in detail elsewhere in this volume, an understanding of how these factors control epithelial biology is a prerequisite for improving diagnosis and treatment.

References

1. Stevens, C.E. and C.P. Leblond, *Renewal of the mucous cells in the gastric mucosa of the rat*. *Anat Rec*, 1953. **115**(2): p. 231-45.
2. McLin, V.A., S.J. Henning, and M. Jamrich, *The role of the visceral mesoderm in the development of the gastrointestinal tract*. *Gastroenterology*, 2009. **136**(7): p. 2074-91.
3. Matsui, T., et al., *Noncanonical Wnt signaling regulates midline convergence of organ primordia during zebrafish development*. *Genes Dev*, 2005. **19**(1): p. 164-75.
4. Bagnat, M., et al., *Genetic control of single lumen formation in the zebrafish gut*. *Nat Cell Biol*, 2007. **9**(8): p. 954-60.
5. Zorn, A.M. and J.M. Wells, *Vertebrate endoderm development and organ formation*. *Annu Rev Cell Dev Biol*, 2009. **25**: p. 221-51.
6. Fukamachi, H., T. Mizuno, and S. Takayama, *Epithelial-mesenchymal interactions in differentiation of stomach epithelium in fetal mice*. *Anat Embryol (Berl)*, 1979. **157**(2): p. 151-60.
7. Yasugi, S. and T. Mizuno, *Molecular analysis of endoderm regionalization*. *Dev Growth Differ*, 2008. **50 Suppl 1**: p. S79-96.
8. Hirokawa, N., et al., *Nodal flow and the generation of left-right asymmetry*. *Cell*, 2006. **125**(1): p. 33-45.
9. Ramalho-Santos, M., D.A. Melton, and A.P. McMahon, *Hedgehog signals regulate multiple aspects of gastrointestinal development*. *Development*, 2000. **127**(12): p. 2763-72.
10. Echelard, Y., et al., *Sonic hedgehog, a member of a family of putative signaling molecules, is implicated in the regulation of CNS polarity*. *Cell*, 1993. **75**(7): p. 1417-30.
11. Zhang, X.M., M. Ramalho-Santos, and A.P. McMahon, *Smoothed mutants reveal redundant roles for Shh and Ihh signaling including regulation of L/R asymmetry by the mouse node*. *Cell*, 2001. **105**(6): p. 781-92.
12. Farrington, S.M., M. Belaousoff, and M.H. Baron, *Winged-helix, Hedgehog and Bmp genes are differentially expressed in distinct cell layers of the murine yolk sac*. *Mech Dev*, 1997. **62**(2): p. 197-211.

13. Zhang, X.M., M. Ramalho-Santos, and A.P. McMahon, *Smoothed mutants reveal redundant roles for Shh and Ihh signaling including regulation of L/R symmetry by the mouse node*. Cell, 2001. **106**(2): p. 781-92.
14. Tanaka, Y., Y. Okada, and N. Hirokawa, *FGF-induced vesicular release of Sonic hedgehog and retinoic acid in leftward nodal flow is critical for left-right determination*. Nature, 2005. **435**(7039): p. 172-7.
15. Beck, F., et al., *Expression of Cdx-2 in the mouse embryo and placenta: possible role in patterning of the extra-embryonic membranes*. Dev Dyn, 1995. **204**(3): p. 219-27.
16. Thomas, P.Q., A. Brown, and R.S. Beddington, *Hex: a homeobox gene revealing peri-implantation asymmetry in the mouse embryo and an early transient marker of endothelial cell precursors*. Development, 1998. **125**(1): p. 85-94.
17. Gao, N. and K.H. Kaestner, *Cdx2 regulates endo-lysosomal function and epithelial cell polarity*. Genes Dev, 2010. **24**(12): p. 1295-305.
18. van den Brink, G.R., *Hedgehog signaling in development and homeostasis of the gastrointestinal tract*. Physiol Rev, 2007. **87**(4): p. 1343-75.
19. Bitgood, M.J. and A.P. McMahon, *Hedgehog and Bmp genes are coexpressed at many diverse sites of cell-cell interaction in the mouse embryo*. Dev Biol, 1995. **172**(1): p. 126-38.
20. Spencer-Dene, B., et al., *Stomach development is dependent on fibroblast growth factor 10/fibroblast growth factor receptor 2b-mediated signaling*. Gastroenterology, 2006. **130**(4): p. 1233-44.
21. Mao, B., et al., *LDL-receptor-related protein 6 is a receptor for Dickkopf proteins*. Nature, 2001. **411**(6835): p. 321-5.
22. Matsuyama, M., S. Aizawa, and A. Shimono, *Sfrp controls apicobasal polarity and oriented cell division in developing gut epithelium*. PLoS Genet, 2009. **5**(3): p. e1000427.
23. Jones, S.E. and C. Jomary, *Secreted Frizzled-related proteins: searching for relationships and patterns*. Bioessays, 2002. **24**(9): p. 811-20.
24. Hsieh, J.C., et al., *A new secreted protein that binds to Wnt proteins and inhibits their activities*. Nature, 1999. **398**(6726): p. 431-6.
25. Belo, J.A., et al., *Cerberus-like is a secreted BMP and nodal antagonist not essential for mouse development*. Genesis, 2000. **26**(4): p. 265-70.
26. Bafico, A., et al., *Novel mechanism of Wnt signalling inhibition mediated by Dickkopf-1 interaction with LRP6/Arrow*. Nat Cell Biol, 2001. **3**(7): p. 683-6.
27. Semenov, M.V., et al., *Head inducer Dickkopf-1 is a ligand for Wnt coreceptor LRP6*. Curr Biol, 2001. **11**(12): p. 951-61.
28. Lickert, H., et al., *Expression patterns of Wnt genes in mouse gut development*. Mech Dev, 2001. **105**(1-2): p. 181-4.
29. Cervantes, S., T.P. Yamaguchi, and M. Hebrok, *Wnt5a is essential for intestinal elongation in mice*. Dev Biol, 2009. **326**(2): p. 285-94.
30. Listyorini, D. and S. Yasugi, *Expression and function of Wnt5a in the development of the glandular stomach in the chicken embryo*. Dev Growth Differ, 2006. **48**(4): p. 243-52.
31. Zorn, A.M., K. Butler, and J.B. Gurdon, *Anterior endomesoderm specification in Xenopus by Wnt/beta-catenin and TGF-beta signalling pathways*. Dev Biol, 1999. **209**(2): p. 282-97.
32. Kim, B.M., et al., *The stomach mesenchymal transcription factor Barx1 specifies gastric epithelial identity through inhibition of transient Wnt signaling*. Dev Cell, 2005. **8**(4): p. 611-22.

33. Masui, T., *Differentiation of the yolk-sac endoderm under the influence of the digestive-tract mesenchyme*. J Embryol Exp Morphol, 1981. **62**: p. 277-89.
34. Verzi, M.P., et al., *Role of the homeodomain transcription factor Bapx1 in mouse distal stomach development*. Gastroenterology, 2009. **136**(5): p. 1701-10.
35. Geske, M.J., et al., *Fgf9 signaling regulates small intestinal elongation and mesenchymal development*. Development, 2008. **135**(17): p. 2959-68.
36. Nyeng, P., et al., *FGF10 signaling controls stomach morphogenesis*. Dev Biol, 2007. **303**(1): p. 295-310.
37. Yin, Y., et al., *An FGF-WNT gene regulatory network controls lung mesenchyme development*. Dev Biol, 2008. **319**(2): p. 426-36.
38. Bhushan, A., et al., *Fgf10 is essential for maintaining the proliferative capacity of epithelial progenitor cells during early pancreatic organogenesis*. Development, 2001. **128**(24): p. 5109-17.
39. Dessimoz, J., et al., *FGF signaling is necessary for establishing gut tube domains along the anterior-posterior axis in vivo*. Mech Dev, 2006. **123**(1): p. 42-55.
40. Haremake, T., et al., *Integration of multiple signal transducing pathways on Fgf response elements of the Xenopus caudal homologue Xcad3*. Development, 2003. **130**(20): p. 4907-17.
41. Wells, J.M. and D.A. Melton, *Early mouse endoderm is patterned by soluble factors from adjacent germ layers*. Development, 2000. **127**(8): p. 1563-72.
42. Danesh, S.M., et al., *BMP and BMP receptor expression during murine organogenesis*. Gene Expr Patterns, 2009. **9**(5): p. 255-65.
43. Niederreither, K., et al., *Differential expression of retinoic acid-synthesizing (RALDH) enzymes during fetal development and organ differentiation in the mouse*. Mech Dev, 2002. **110**(1-2): p. 165-71.
44. Wang, Z., et al., *Retinoic acid regulates morphogenesis and patterning of posterior foregut derivatives*. Dev Biol, 2006. **297**(2): p. 433-45.
45. Aubin, J., et al., *Stomach regional specification requires Hoxa5-driven mesenchymal-epithelial signaling*. Development, 2002. **129**(17): p. 4075-87.
46. Lee, C.S., et al., *Neurogenin 3 is essential for the proper specification of gastric enteroendocrine cells and the maintenance of gastric epithelial cell identity*. Genes Dev, 2002. **16**(12): p. 1488-97.
47. Matsuda, Y., et al., *Notch signaling functions as a binary switch for the determination of glandular and luminal fates of endodermal epithelium during chicken stomach development*. Development, 2005. **132**(12): p. 2783-93.
48. Huang, D., S.W. Chen, and L.J. Gudas, *Analysis of two distinct retinoic acid response elements in the homeobox gene Hoxb1 in transgenic mice*. Dev Dyn, 2002. **223**(3): p. 353-70.
49. Tsai, S.Y. and M.J. Tsai, *Chick ovalbumin upstream promoter-transcription factors (COUP-TFs): coming of age*. Endocr Rev, 1997. **18**(2): p. 229-40.
50. Takamoto, N., et al., *COUP-TFII is essential for radial and anteroposterior patterning of the stomach*. Development, 2005. **132**(9): p. 2179-89.
51. Que, J., et al., *Multiple dose-dependent roles for Sox2 in the patterning and differentiation of anterior foregut endoderm*. Development, 2007. **134**(13): p. 2521-31.
52. Tissier-Seta, J.P., et al., *Barx1, a new mouse homeodomain transcription factor expressed in cranio-facial ectomesenchyme and the stomach*. Mech Dev, 1995. **51**(1): p. 3-15.
53. Kim, B.M., et al., *Independent functions and mechanisms for homeobox gene Barx1 in patterning mouse stomach and spleen*. Development, 2007. **134**(20): p. 3603-13.

54. Azpiazu, N. and M. Frasch, *tinman and bagpipe: two homeo box genes that determine cell fates in the dorsal mesoderm of Drosophila*. *Genes Dev*, 1993. **7**(7B): p. 1325-40.
55. Nielsen, C., et al., *Gizzard formation and the role of Bapx1*. *Dev Biol*, 2001. **231**(1): p. 164-74.
56. Clark, K.L., et al., *Co-crystal structure of the HNF-3/fork head DNA-recognition motif resembles histone H5*. *Nature*, 1993. **364**(6436): p. 412-20.
57. Kaestner, K.H., et al., *The mesenchymal winged helix transcription factor Fkh6 is required for the control of gastrointestinal proliferation and differentiation*. *Genes Dev*, 1997. **11**(12): p. 1583-95.
58. Fukamachi, H., et al., *Mesenchymal transcription factor Fkh6 is essential for the development and differentiation of parietal cells*. *Biochem Biophys Res Commun*, 2001. **280**(4): p. 1069-76.
59. Michelangeli, F., et al., *Mammalian-like differentiation of gastric cells in the shark *Hexanchus griseus**. *Cell Tissue Res*, 1988. **251**(1): p. 225-7.
60. Madison, B.B., et al., *FoxF1 and FoxL1 link hedgehog signaling and the control of epithelial proliferation in the developing stomach and intestine*. *J Biol Chem*, 2009. **284**(9): p. 5936-44.
61. Perreault, N., et al., *Foxl1 controls the Wnt/beta-catenin pathway by modulating the expression of proteoglycans in the gut*. *J Biol Chem*, 2001. **276**(46): p. 43328-33.
62. Trahair, J.F. and R. Harding, *Ultrastructural anomalies in the fetal small intestine indicate that fetal swallowing is important for normal development: an experimental study*. *Virchows Arch A Pathol Anat Histopathol*, 1992. **420**(4): p. 305-12.
63. Widdowson, E.M., *Cellular growth and function*. *Proc Nutr Soc*, 1976. **35**(3): p. 357-62.
64. Karam, S.M., *Lineage commitment and maturation of epithelial cells in the gut*. *Front Biosci*, 1999. **4**: p. D286-98.
65. Xu, R.J. and P.D. Cranwell, *Development of gastric acid secretion in pigs from birth to thirty six days of age: the response to pentagastrin*. *J Dev Physiol*, 1990. **13**(6): p. 315-26.
66. Johnson, L.R., *Functional development of the stomach*. *Annu Rev Physiol*, 1985. **47**: p. 199-215.
67. Shiotani, A. and J.L. Merchant, *cAMP regulates gastrin gene expression*. *Am J Physiol*, 1995. **269**(3 Pt 1): p. G458-64.
68. Kverka, M., et al., *Cytokine profiling in human colostrum and milk by protein array*. *Clin Chem*, 2007. **53**(5): p. 955-62.
69. Gama, P. and E.P. Alvares, *Early weaning and prolonged nursing induce changes in cell proliferation in the gastric epithelium of developing rats*. *J Nutr*, 2000. **130**(10): p. 2594-8.
70. Penttila, I.A., et al., *Transforming growth factor-beta levels in maternal milk and expression in postnatal rat duodenum and ileum*. *Pediatr Res*, 1998. **44**(4): p. 524-31.
71. de Andrade Sa, E.R., et al., *Ontogenic expression of TGFbeta 1, 2, and 3 and its receptors in the rat gastric mucosa*. *Dev Dyn*, 2003. **227**(3): p. 450-7.
72. Lee, H.M., et al., *Ghrelin, a new gastrointestinal endocrine peptide that stimulates insulin secretion: enteric distribution, ontogeny, influence of endocrine, and dietary manipulations*. *Endocrinology*, 2002. **143**(1): p. 185-90.
73. Kotunia, A. and R. Zabielski, *Ghrelin in the postnatal development of the gastrointestinal tract*. *J Physiol Pharmacol*, 2006. **57 Suppl 5**: p. 97-111.
74. Aydin, S., et al., *Ghrelin is present in human colostrum, transitional and mature milk*. *Peptides*, 2006. **27**(4): p. 878-82.

75. Karam, S.M. and C.P. Leblond, *Dynamics of epithelial cells in the corpus of the mouse stomach. II. Outward migration of pit cells.* Anat Rec, 1993. **236**(2): p. 280-96.
76. Lee, H.S., et al., *MUC1, MUC2, MUC5AC, and MUC6 expressions in gastric carcinomas: their roles as prognostic indicators.* Cancer, 2001. **92**(6): p. 1427-34.
77. Longman, R.J., et al., *Coordinated localisation of mucins and trefoil peptides in the ulcer associated cell lineage and the gastrointestinal mucosa.* Gut, 2000. **47**(6): p. 792-800.
78. Oien, K.A., et al., *Gastrokine 1 is abundantly and specifically expressed in superficial gastric epithelium, down-regulated in gastric carcinoma, and shows high evolutionary conservation.* J Pathol, 2004. **203**(3): p. 789-97.
79. Verzi, M.P., et al., *Transcription factor foxq1 controls mucin gene expression and granule content in mouse stomach surface mucous cells.* Gastroenterology, 2008. **135**(2): p. 591-600.
80. Goering, W., et al., *Impairment of gastric acid secretion and increase of embryonic lethality in Foxq1-deficient mice.* Cytogenet Genome Res, 2008. **121**(2): p. 88-95.
81. Nakajima, T., et al., *Gastrin stimulates the growth of gastric pit cell precursors by inducing its own receptors.* Am J Physiol Gastrointest Liver Physiol, 2002. **282**(2): p. G359-66.
82. Fukaya, M., et al., *Hedgehog signal activation in gastric pit cell and in diffuse-type gastric cancer.* Gastroenterology, 2006. **131**(1): p. 14-29.
83. Nozaki, K., et al., *A molecular signature of gastric metaplasia arising in response to acute parietal cell loss.* Gastroenterology, 2008. **134**(2): p. 511-22.
84. Karam, S.M. and C.P. Leblond, *Dynamics of epithelial cells in the corpus of the mouse stomach. III. Inward migration of neck cells followed by progressive transformation into zymogenic cells.* Anat Rec, 1993. **236**(2): p. 297-313.
85. Hanby, A.M., et al., *The mucous neck cell in the human gastric corpus: a distinctive, functional cell lineage.* J Pathol, 1999. **187**(3): p. 331-7.
86. Ramsey, V.G., et al., *The maturation of mucus-secreting gastric epithelial progenitors into digestive-enzyme secreting zymogenic cells requires Mist1.* Development, 2007. **134**(1): p. 211-22.
87. Tian, X., et al., *RAB26 and RAB3D are direct transcriptional targets of MIST1 that regulate exocrine granule maturation.* Mol Cell Biol, 2010. **30**(5): p. 1269-84.
88. Karam, S.M., et al., *Retinoic acid stimulates the dynamics of mouse gastric epithelial progenitors.* Stem Cells, 2005. **23**(3): p. 433-41.
89. Karam, S.M., et al., *Defining epithelial cell progenitors in the human oxyntic mucosa.* Stem Cells, 2003. **21**(3): p. 322-36.
90. Capoccia, B.J., W.J. Huh, and J.C. Mills, *How form follows functional genomics: gene expression profiling gastric epithelial cells with a particular discourse on the parietal cell.* Physiol Genomics, 2009. **37**(2): p. 67-78.
91. Mills, J.C., et al., *A molecular profile of the mouse gastric parietal cell with and without exposure to Helicobacter pylori.* Proc Natl Acad Sci U S A, 2001. **98**(24): p. 13687-92.
92. von Rosenvinge, E.C. and J.P. Raufman, *Gastrointestinal peptides and regulation of gastric acid secretion.* Curr Opin Endocrinol Diabetes Obes. **17**(1): p. 40-3.
93. Schubert, M.L., *Hormonal regulation of gastric acid secretion.* Curr Gastroenterol Rep, 2008. **10**(6): p. 523-7.
94. Mettler, S.E., et al., *Modulatory role of phosphoinositide 3-kinase in gastric acid secretion.* Am J Physiol Gastrointest Liver Physiol, 2007. **293**(3): p. G532-43.

95. van den Brink, G.R., et al., *Sonic hedgehog regulates gastric gland morphogenesis in man and mouse*. Gastroenterology, 2001. **121**(2): p. 317-28.
96. Zavros, Y., et al., *Sonic hedgehog is associated with H⁺-K⁺-ATPase-containing membranes in gastric parietal cells and secreted with histamine stimulation*. Am J Physiol Gastrointest Liver Physiol, 2008. **295**(1): p. G99-G111.
97. Stepan, V., et al., *Regulation and function of the sonic hedgehog signal transduction pathway in isolated gastric parietal cells*. J Biol Chem, 2005. **280**(16): p. 15700-8.
98. Nitsche, H., et al., *Functional role of bone morphogenetic protein-4 in isolated canine parietal cells*. Am J Physiol Gastrointest Liver Physiol, 2007. **293**(3): p. G607-14.
99. Bleuming, S.A., et al., *Bone morphogenetic protein signaling suppresses tumorigenesis at gastric epithelial transition zones in mice*. Cancer Res, 2007. **67**(17): p. 8149-55.
100. Huh, W.J., I.U. Mysorekar, and J.C. Mills, *Inducible activation of Cre recombinase in adult mice causes gastric epithelial atrophy, metaplasia and regenerative changes in the absence of "floxed" alleles*. Am J Physiol Gastrointest Liver Physiol.

APPENDIX 2: Autoimmune gastritis mediated by CD4⁺ T cells promotes the development of gastric cancer.

This appendix was published in Cancer Research

Autoimmune gastritis mediated by CD4⁺ T cells promotes the development of gastric cancer

Nguyen TL, Khurana SS, Bellone CJ, Capoccia BJ, Sagartz JE, Kesman RA Jr, Mills JC,

DiPaolo RJ.

Cancer Research 2013 Apr 1;73(7):2117-26. doi: 10.1158/0008-5472.CAN-12-3957. Epub 2013

Feb 1

PMID: 23378345

Abstract

Chronic inflammation is a risk factor for cancer, including gastric and other gastrointestinal cancers. For example, chronic inflammation caused by Autoimmune Gastritis is associated with an increased risk of gastric polyps, gastric carcinoid tumors, and possibly adenocarcinomas. This study details the progression of gastric cancer in a mouse model of Autoimmune Gastritis (AIG). Disease is caused by CD4⁺ T cells which express a transgenic T cell receptor specific for a peptide from the H⁺/K⁺ ATPase proton pump, a protein expressed by parietal cells in the stomach. Here, we show that autoimmune gastritis causes epithelial cell aberrations that mimic most of those seen during progression to gastric cancer in humans. These include: chronic gastritis followed by oxyntic atrophy, mucous neck cell hyperplasia, spasmolytic polypeptide-expressing metaplasia (SPEM), dysplasia, and ultimately gastric intraepithelial neoplasias (GIN). These studies provide direct evidence that autoimmune gastritis supports the development of gastric neoplasias. This AIG model should be useful for studying inflammation induced gastric cancer.

Introduction

Autoimmune gastritis (AIG) is one of the most common autoimmune conditions in humans, and is caused when the adaptive immune system (T and B cells) targets self-antigens expressed by parietal cells and chief cells in the gastric mucosa. AIG may persist in an asymptomatic form for many years. A subset of individuals will eventually develop Pernicious Anemia (PA). PA is the major cause of vitamin B12 deficiency. AIG and PA have respective prevalence of 2 and 0.15–1% in the general population [1, [2], which is increased 3- to 5-fold in individuals with other, concomitant autoimmune diseases, such as type 1 diabetes [3, [4] and autoimmune thyroid disease [5, [6]. Gastric carcinoid tumors, evolving from enterochromaffine-like (ECL) cell hyper/dysplasia induced by hypergastrinemia, develop in 4–9% of patients with AIG/PA [7, [8, [9]. Gastric carcinoid tumors are relatively benign lesions, metastasizing in less than 10% of cases [10]. Several studies have examined whether individuals with AIG/PA also have a higher risk of developing gastric adenocarcinomas, which is the second leading cause of cancer related deaths in the world. Two recent studies, one with 4.5 million retired male veterans in the USA and the other with included 9 million individuals from Sweden, reported that individuals with PA had an increased risk of developing not only gastrointestinal carcinoids, but also stomach adenocarcinomas, small intestinal adenocarcinomas, squamous cell carcinomas (SCC), and esophageal SCCs [11, [12].

Gastric cancer is the fourth most common cancer and the second most deadly malignant neoplasia in the world. A model, referred to as the Correa pathway, describes the development of gastric adenocarcinomas in humans from a histological perspective [13]. This model details the progression of gastric cancer through a series of pathological steps the epithelium undergoes starting with chronic inflammation (gastritis), followed by atrophy (especially loss of parietal

cells), metaplasia, dysplasia, and eventually neoplasia. A better understanding of how inflammation induces gastric epithelial cell changes could provide potential therapeutic strategies for diagnosing and preventing gastric cancer [14]. To gain a better understanding of the progression of gastric cancer from a cellular and molecular perspective, numerous groups have developed animal models, mouse models in particular, to study gastric carcinogenesis. Such strategies have included chronic infection with *Helicobacter* [15], chemical depletion of parietal cells [16, [17], and several different lines of genetically modified mice. While these models have increased our understanding of the roles of infection, parietal cell loss, and genes involved in regulating epithelial cell biology, none have directly examined the role of chronic inflammation as the primary inducer of epithelial cell change, which would be useful for understanding the roles of cytokines and immune cells in promoting gastric cancer and for addressing the potential link between AIG and gastric cancer.

We investigated the potential link between AIG and gastric cancer using a T cell receptor (TCR) transgenic mouse model of AIG [18]. These transgenic CD4⁺ T cells recognizes a peptide from the parietal cell specific antigen H⁺/K⁺ ATPase, which is also the major autoantigen targeted by the immune system in humans with AIG/PA [19]. All mice developed chronic gastritis that resulted from large numbers of CD4⁺ T cells that infiltrated the gastric mucosa and produced large amounts of IFN- γ and smaller amounts of IL-17. Mice developed severe oxyntic atrophy and metaplasia by 2 to 4 months of age. At this stage of disease, mice also developed several molecular features associated with the progression of gastric cancer in humans, including spasmolytic polypeptide expressing metaplasia (SPEM), increased levels of mRNA for gastric cancer biomarkers (HE4, OLFM4, TFF2), and increased levels of phosphorylated STAT3 compared to non-transgenic control mice. Finally, by 12 months of age, all mice with AIG

developed high grade dysplasia consistent with gastric intraepithelial neoplasia (GIN). In summary, we report a new mouse model demonstrating that inflammation associated with AIG induces many of the pathologic and molecule features of gastric carcinogenesis, including the development of severe dysplasia/GIN. These studies support a link between AIG and gastric cancer and highlight the importance of localized inflammation in the development of stomach cancer. This new, immune-system-induced model of gastric cancer will be useful for studying important host factors that influence inflammation induced adenocarcinomas.

Material and Methods

Mice - TxA23 TCR transgenic mice have been previously described, and have been bred >15 generations onto the BALB/c background [18]. The BALB/c control mice described in these experiments are TCR transgene negative littermates that were co-housed with the TxA23 TCR transgenic mice. All mice were maintained under specific pathogen-free conditions and cared for in our animal facility in accordance with institutional guidelines. Our colony tested negative by PCR for the following: *Helicobacter bilis*, *Helicobacter hepaticus*, *Helicobacter rodentium*, *Helicobacter sp.*, *Helicobacter trogontum*, and *Helicobacter typhlonius*.

Histopathology - Stomachs were removed from mice, rinsed in saline, immersion fixed in 10% neutral-buffered formalin (Thermo Scientific), paraffin embedded, sectioned, and stained with hematoxylin and eosin. Pathology scores were assigned using methods modified from Rogers et al. [20]. Slides were blinded and sections from individual mice were assigned scores between 0 (absent) and 4 (severe) to indicate the severity of inflammation, oxyntic atrophy, mucinous

hyperplasia/metaplasia, and dysplasia. Scores were validated by an independent second pathologist blinded to experimental conditions.

Immunofluorescence - Stomachs were fixed for 20 minutes with methacarn (60% methanol, 30% chloroform and 10% glacial acetic acid (all from Fisher)), washed with 70% ethanol, embedded in paraffin and sectioned into 0.5 μ m thick sections. Slides were deparaffinized, rehydrated, stained, and imaged using methods modified from Ramsey et. al. [21]. The primary antibodies used for immunostaining were rabbit anti-human gastric intrinsic factor (gifts of Dr. David Alpers, Washington University), rabbit anti-Ki67 (Abcam), and mouse anti-Ecadherin (BD Bioscience). Secondary antibodies and GSII lectin (Molecular Probes) labeling were as described [21].

A gastric unit is defined as an invagination of the gastric mucosa that is lined by a single layer of columnar epithelium. Each gastric unit is lined by foveolar cells at the luminal end and zymogenic cells at the base. Ki67 staining was quantified by counting each Ki67+ nucleus per gastric unit for >50 units per mouse and classified into <10, 10-20 and >20 positive nuclei per unit. Percentages were calculated by dividing the number of gastric units in each category by total number of gastric units analyzed in that mouse stomach sample.

Immunohistochemistry - Tissue was deparaffinized and rehydrated. Endogenous peroxidase was blocked using a 0.3% H₂O₂ in methanol for 15 minutes. Antigen retrieval was done in a pressure cooker with Diva (Biocare: DV2004MX). Avidin/biotin kit (Biocare) was used to block endogenous biotin. The antibody pStat3 (D3A7) from Cell Signaling was diluted in Davinci (Biocare) and incubated over night at 4°C. The secondary antibody, biotinylated goat anti-rabbit and streptavidin-HRP from Jackson Labs were each applied for 1 hour at room temperature.

Visualization was done with Biocare's Betaziod DAB and slides were counterstained in hematoxylin.

Immunoblot - A section from the stomach was homogenized with an electric pestle tissue homogenizer. Cells were then lysed in .5 ml of lysis buffer (20 mM Tris-HCl pH 7.5, 150 mM NaCl, 1 mM Na₂EDTA, 1 mM EGTA, 1% Triton, 2.5 mM sodium pyrophosphate, 1 mM beta-glycerophosphate, 1 mM Na₃VO₄, 1 µg/ml leupeptin (Cell Signaling) and a protease inhibitor cocktail (Sigma)). Lysates were vortexed for 1 minute and sonicated for 15 seconds followed by centrifugation for 10 min at 4°C. Lysates were ran on a NuPAGE 4-12% BIS-TRIS gradient gel (Novex) and transferred to a nitrocellulose membrane. Membrane was blocked for 1 hour with 5% non-fat dairy milk. Primary antibodies (all from Cell Signaling) were stained for 1 hour (rabbit mAB-β-Actin-and rabbit mAB-STAT3) or overnight (rabbit mAB-Phospho-STAT 3) in 5% bovine serum albumin in 4°C. HRP-Linked secondary antibody (anti-rabbit IgG) was stained for 1 hours at room temperature in 5% non-fat dairy milk. Protein was detected by chemiluminescence using LumiGLO (Cell Signaling) on CL-Xposure X-Ray film (Fisher).

Flow cytometry - Cell surface staining was performed according to standard procedures using monoclonal antibodies against CD4, CD19, CD11b and Ly6G. Intracellular cytokine staining was performed using monoclonal antibodies against IFN γ and IL-17A. All antibodies were purchased from BD Pharmingen. All flow cytometry was performed on a BD LSRII or BD FACSCalibur and analyzed using FlowJo (TreeStar). For intracellular cytokine staining, cells were stimulated with PMA (Calbiochem) and Ionomycin (Calbiochem) for 4 hours at 37°C. Golgi-stop (BD Bioscience) was added after 1 hour. Cells were then washed, fixed in 4% formyl saline, washed, and permeabilized (0.5% BSA, 0.1% Triton, and 2mM EDTA in PBS) for 1 hr at

room temperature. After washing, cells were incubated overnight with the anti-cytokine antibodies, washed and analyzed by flow cytometry.

Isolation of cells from the gastric lymph nodes and gastric mucosa - The method for isolating cells from the stomach tissue has been described previously [22, [23]. Briefly, the gastric lymph nodes (gLN) were removed from the stomachs, homogenized, and passed through a 40- μ M pore nylon filter. Stomachs were opened with an incision from the antrum to the fundus, and rinsed in PBS to remove food. Cells were flushed from the gastric mucosa using a syringe with a 25 gauge needle. PBS containing 5% FCS and penicillin/streptomycin (Sigma) was repeatedly injected within the mucosa causing the tissue to swell and rupture. Single cell suspensions were collected, gently vortexed, and passed through a 40- μ M nylon filter. Cells were counted, stained with antibodies, and analyzed by flow cytometry. To detect secreted cytokines, 1×10^6 cells were culture *in vitro* in 24 well plates containing 2 mL of supplemented RPMI. Supernatants from cell cultures were collected after 48 hours and cytokines and chemokines were measured using Milliplex (Millipore).

Quantitative Real Time PCR - Total RNA was prepared using the RNeasy Mini Kit system (Qiagen). The quantity and quality of RNA was determined using a NanoDrop 2000 spectrophotometer (Thermo Scientific) and 0.5 μ g of the RNA was used to generate a first strand cDNA copy according to the manufacturer's instruction (High Capacity cDNA Reverse Transcription Kit, Applied Biosystems). Quantitative PCR was performed using TaqMan® Gene Expression Assays systems (Applied Biosystems). GAPDH served as an internal reference standard. PCR was ran on the 7500 Real-Time PCR System (Applied Biosystems).

Statistical Analysis - Data are expressed as means of individual determinations +/- standard error. Statistical analysis was performed using the Mann-Whitney Test (*P<.05; **P<.01; ***P<.001) using GraphPad Prism 5.

Results:

Inflammation in TxA23 mice is characterized by CD4⁺ T cells secreting IFN- γ and IL-17. Our first goal was to characterize the cell types and cytokines of TxA23 mice. Cells were isolated from the gastric mucosa and gastric lymph nodes of 2 month old mice and analyzed by flow cytometry. The majority (>85%) of the hematopoietic derived cells isolated were either CD4⁺ T cells or CD19⁺ B cells (Figure 1A). As expected, the majority of the CD4⁺ T cells that infiltrated the stomach expressed the transgenic TCR (TCRV α 2/TCRV β 2) specific for the H⁺/K⁺ ATPase peptide (Figure 1B). Macrophages (CD11b⁺Ly6G⁻) and neutrophils (CD11b⁺Ly6G⁺) and a subset of dendritic cells (CD11b⁺CD11c⁺, data not shown) comprised the rest of the cells found in the gastric mucosa (Figure 1C). Next, cells were re-stimulated and cytokine production by CD4⁺ T cells was determined by intracellular cytokine staining. The majority of cytokine producing CD4⁺ T cells isolated from the stomachs and gastric lymph node produced IFN- γ , and fewer produced IL-2, and IL-17. IL-4 secretion by CD4⁺ T cells was not detected (Figure 1D). Finally, total cells isolated from the gastric lymph node were cultured immediately after isolation. The amounts of several cytokines secreted into the supernatants were determined after 48 hours. The most abundant cytokines secreted by cells were IFN- γ and IL-17 (Figure 1E). Lower levels of IL-6, IL-2, IL-10, and IL-4 were also detected. Thus the inflammatory cell infiltrate within the gastric mucosa consists primarily of a mixture of Th1 (IFN- γ ⁺) and Th17 (IL-17⁺) CD4⁺ T cells,

and B cells. This type of inflammation is consistent with the types of inflammation described in humans infected with *H. Pylori* and with autoimmune gastritis [24, [25].

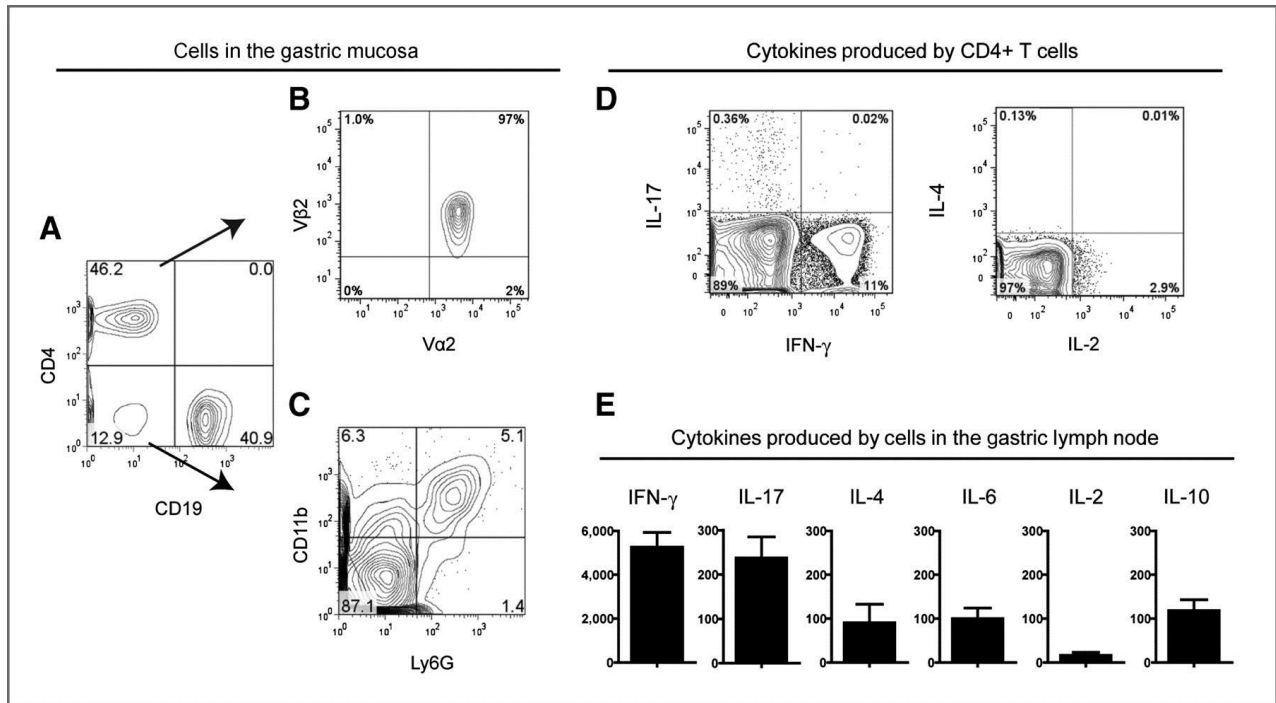
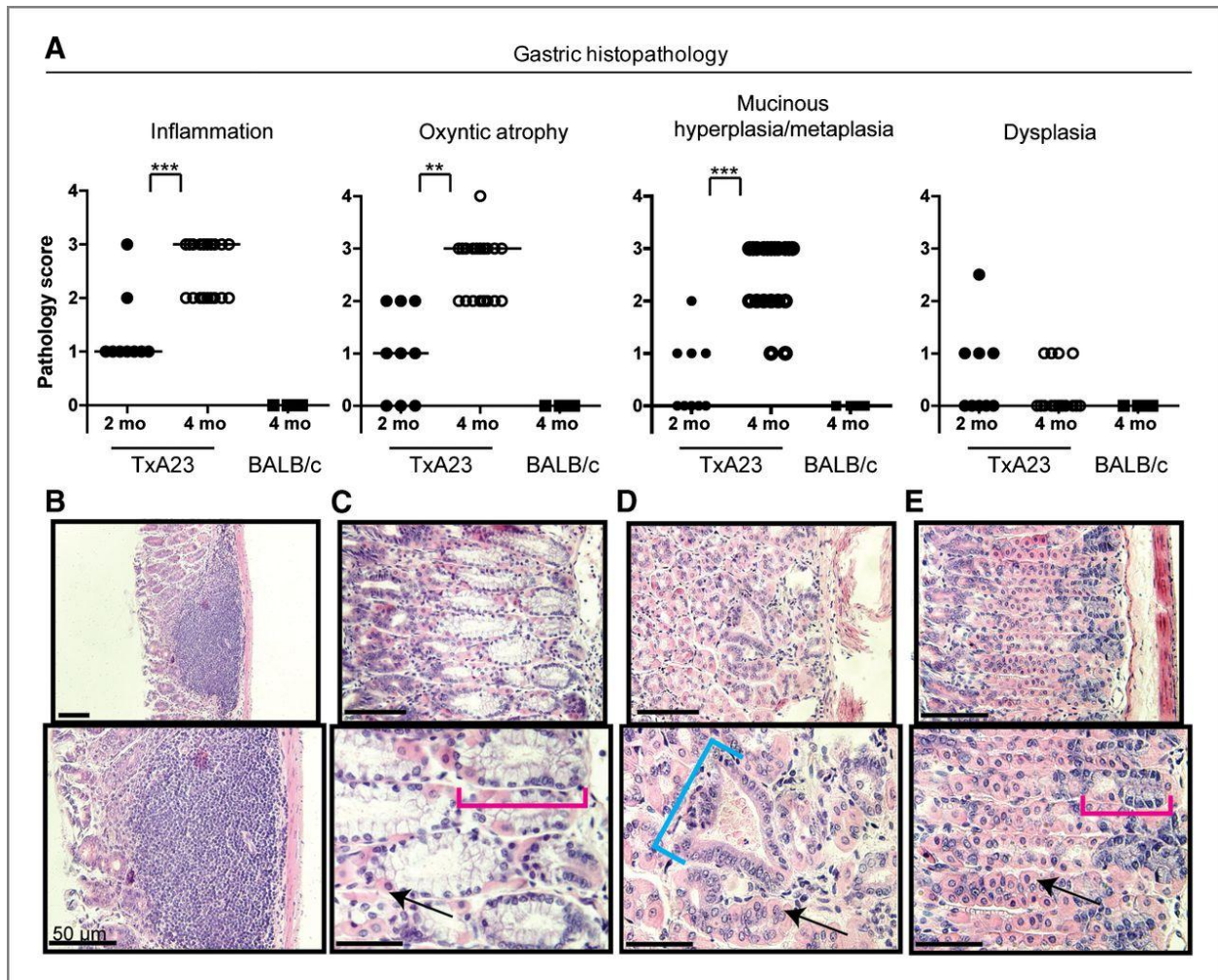


Fig. A.2.1. Inflammation in TxA23 mice. Representative flow cytometric plots of cell types and cytokines from a TxA23 mice ($n = 21$). A, flow cytometry was used to identify T cells (CD4+) and B cells (CD19+). B, the majority of CD4+-gated T cells express the transgenic TCR (TCRVa2/TCRVβ2) that recognizes a peptide from H+/K+ ATPase. C, macrophages (CD11b+Ly6G-) and neutrophils (CD11b+Ly6G+) make up a large proportion of the remaining cells. D, intracellular cytokine staining showing IL-17, IFN-γ, IL-2, and IL-4 production by CD4+ T cells combined from the gastric mucosa and lymph node. E, cytokines secreted by cells isolated from the gastric lymph nodes of TxA23 mice were measured by bead-based ELISA. Data are the mean ± SE of 7 mice from 3 independent experiments.

TxA23 progress through a series of pathological changes associated with the development of gastric cancer.

In humans, the progression of intestinal-type gastric cancer is thought to evolve through a series of discrete steps known as the Correa pathway [13]. The first step in this pathway is inflammation (gastritis), then loss of parietal cells (oxyntic atrophy) and the development of mucinous metaplasia, followed by dysplasia and finally cancer. We examined the pathological features of gastric disease in TxA23 mice. At 2 months of age, TxA23 mice had moderate degrees of inflammation, oxyntic atrophy and mucosal hyperplasia/metaplasia, but little or no evidence of dysplasia (Figure 2A). By 4 months of age, inflammation, oxyntic atrophy, and mucosal hyperplasia/metaplasia were significantly more severe compared to 2 month old mice (Figure 2A). Lesions in the stomachs of 4 month old TxA23 mice comprised large areas in which parietal cells were either reduced in number or absent from the gastric units, and the remaining mucosa was dominated by large, hyperplastic mucus-containing cells that expanded to the bases of gastric units (Figure 2B-C). Four of the 19 mice had developed mild focal dysplasia (Figure 2D). For comparison, Figure 2E is representative of the normal pathology observed in 11 individual control mouse, which are transgene negative BALB/c mice that were co-housed with TxA23 littermates. Disease severity was similar in male and female mice at all ages. These data demonstrate that chronic inflammation resulting from autoimmune gastritis induced the development of preneoplastic lesions in the gastric mucosa of TxA23 mice with many pathological features in common with the Correa pathway.



*Fig. A.2.2. Preneoplastic lesions in TxA23 mice. A, pathology scores of stomach sections from 2-month-old ($n = 9$) and 4-month-old TxA23 mice ($n = 19$). B–D, representative images of pathology observed in TxA23 mice illustrating inflammation, oxyntic atrophy, and mucosal hyperplasia (B). C, extensive parietal cell loss accompanied by moderate levels of mucinous metaplasia (red bracket). D, focal regions of mild dysplasia (blue bracket). E, normal morphology in a BALB/c control mouse with healthy parietal cells and basal nonmetaplastic zymogenic chief cells at base of unit (red bracket, base region). Arrows point to healthy parietal cells. Statistics were conducted using the Mann–Whitney U test (**, $P < 0.01$; ***, $P < 0.001$).*

Increased epithelial cell proliferation, phosphorylated STAT3, IL-6, and expression of gastric cancer-associated biomarkers in TxA23 mice. Next, we used immunofluorescence to compare the extent of gastric epithelial cell proliferation in 2 and 4 month old TxA23 mice compared to BALB/c control mice (Figure 3A-C). In wild type BALB/c mice, the number of proliferating (marked by Ki67⁺ immunoreactivity) epithelial cells (marked by E-cadherin⁺) per individual gastric unit was always less than 10. However, in TxA23 mice almost 70% of 2-month old gastric units had 10 or more proliferating cells, and by 4 months, more than 75% had more than 10 with about a third of those having 20 or more (Figure 3D).

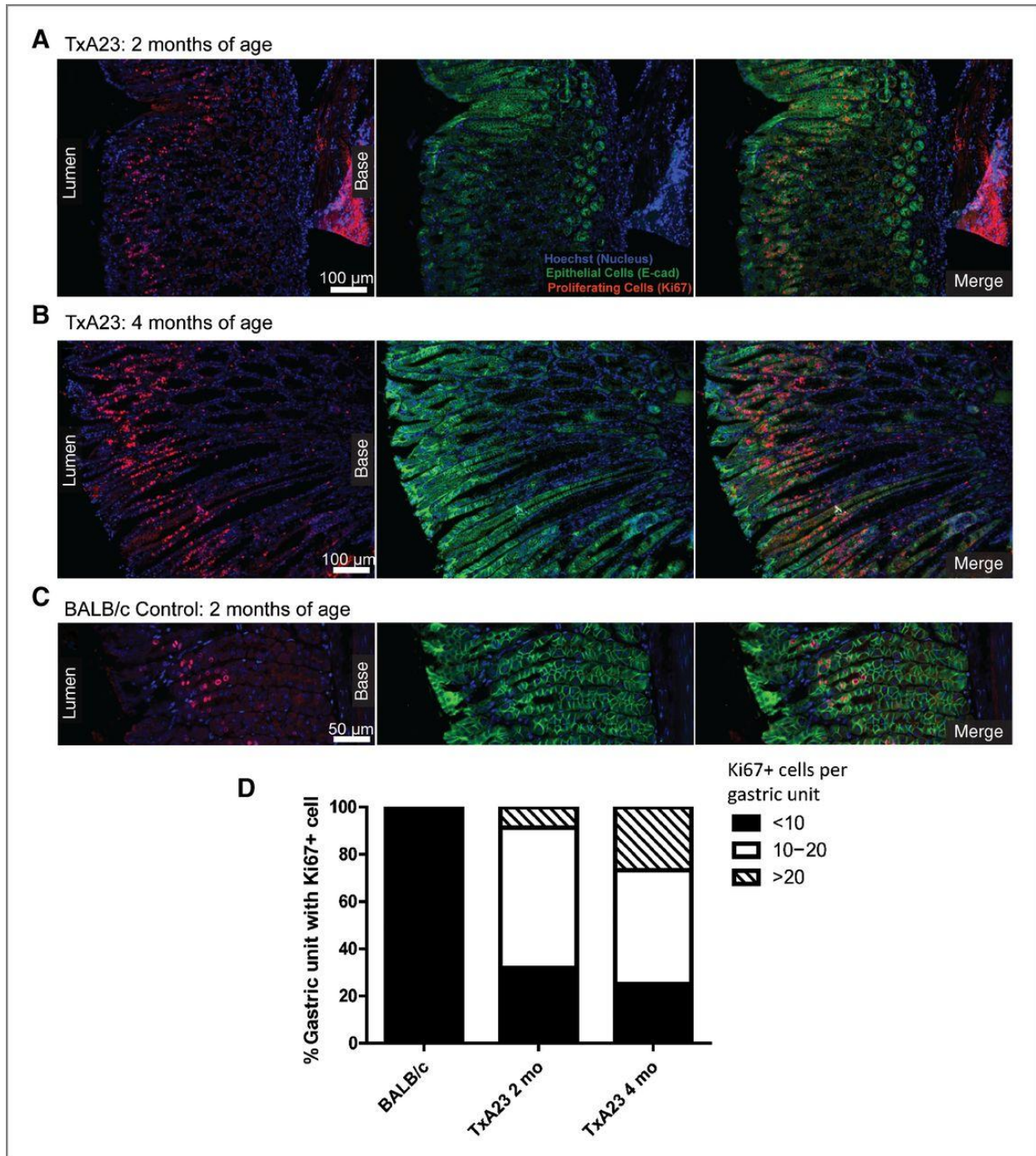


Fig. A.2.3. Increased epithelial cell proliferation in the gastric mucosa of TxA23 mice. A–C, images are representative of 2-month-old (A) and 4-month old (B) TxA23 mice and 4-month-old (C) BALB/c stomach sections. E-Cadherin (green) stains epithelial cells, Ki67 (red) stains proliferating cells, and Hoechst (blue) was used to stain nuclei. D, a quantitative analysis of the

percentage of gastric units containing proliferating epithelial cells (E-cadherin+Ki67+) in BALB/c and 2- and 4-month-old TxA23 mice.

Increased levels of the active (phosphorylated) signal transducer and activator of transcription 3 (pSTAT3) was involved in cellular transformation in numerous cancers of epithelial origin, including gastric cancer [26]. A recent study suggested that pSTAT3 is a significant prognostic factor in gastric cancer in humans [27]. To determine whether the level of pSTAT3 was increased in the stomachs of TxA23 mice, we performed western blots on gastric tissue lysates between age matched TxA23 and healthy BALB/c control mice. Compared to BALB/c mice, TxA23 mice expressed slightly higher levels of total STAT3 and a much higher level of pSTAT3 (Figure 4A). Immunohistochemical analysis revealed a large number of pSTAT3 positive epithelial cells present in the gastric mucosa of TxA23 mice, and nearly undetectable levels in gastric tissue from BALB/c controls (Figure 4B), in agreement with the results observed by Western blot.

Several members of the IL-6 cytokine family, including IL-6 and IL-11, activate STAT3 [28]. IL-6 and IL-11 have important roles in maintaining gastric homeostasis by regulating mucosal proliferation, inflammation, angiogenesis, and apoptosis [29, [30]. We performed quantitative real time PCR analysis using mRNA isolated from gastric tissue from 2 month old TxA23 and BALB/c mice to measure the relative levels of IL-6 and IL-11. The levels of IL-11 mRNA were equivalent between the two genotypes; however, the levels of IL-6 mRNA were ~40 fold higher in TxA23 mice compared to BALB/c mice (Figure 4C).

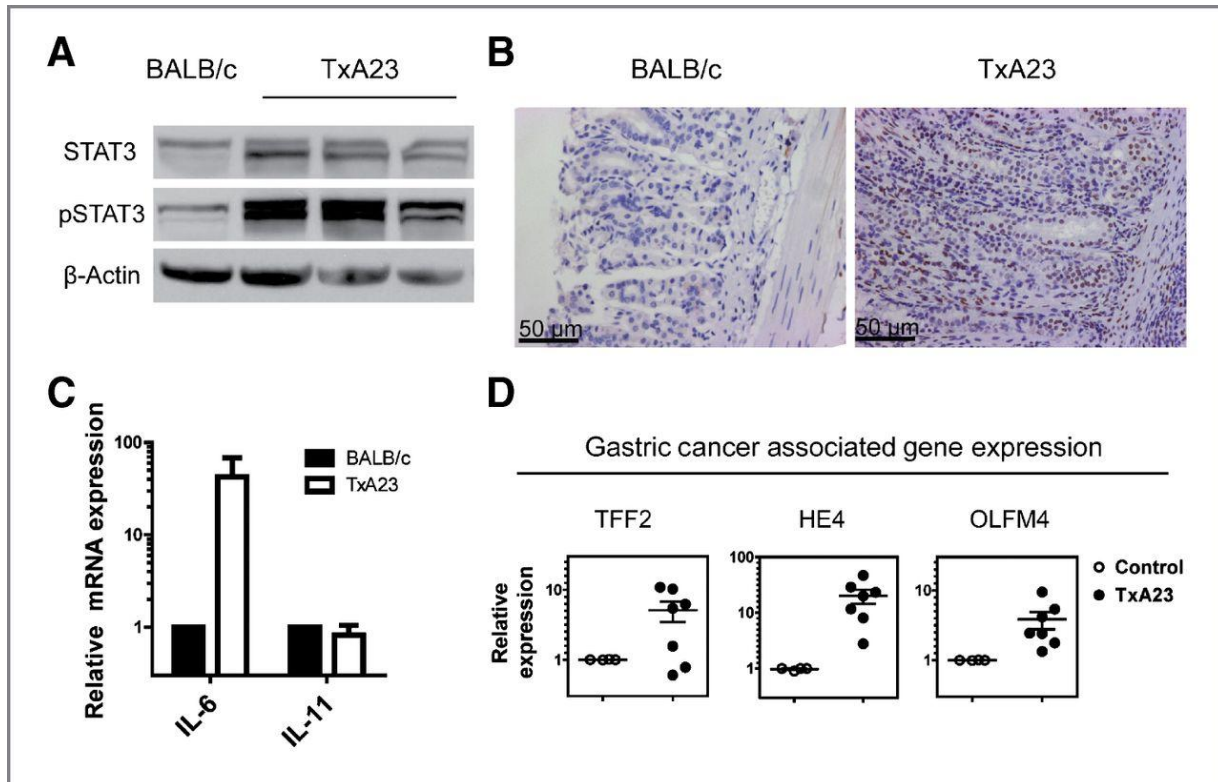


Fig. A.2.4 Increased levels of cancer associated markers in TxA23 mice. A, representative Western blotting of STAT3, pSTAT3 and β -actin on whole stomach lysates of 2-month-old TxA23 ($n = 9$) and BALB/c mice. B, immunohistochemistry staining for pSTAT3 in gastric pits of BALB/c and TxA23 stomachs (magnification, $\times 20$). C, the relative expression of IL-6 and IL-11 in mRNA extracted from the stomachs of TxA23 and BALB/c mice. D, the relative expression of genes (HE4, TFF2, and OLFM4) that serves as biomarkers for the SPEM and preneoplastic progress was compared between mRNA isolated from the stomachs of TxA23 mice and BALB/c controls.

A number of genes have been described as biomarkers for precursor lesions like SPEM that are predisposing for gastric cancer. Some of these genes include Human Epididymis 4 (HE4) [16], Trefoil Factor 2 (TFF2) and Olfactomedin 4 (OLFM4) [31]. HE4 is absent in normal stomach

and expressed in humans and mice with SPEM [16]. Increased levels of OLFM4, also known as GW112, have been observed in gastric cancers, including 58% of stage III/IV gastric cancers [31]. TFF2 is also known as spasmolytic polypeptide, and, by definition, increases when SPEM is present. We performed quantitative real time PCR analysis using mRNA isolated from sections taken from the body of the stomachs of TxA23 mice. All of the TxA23 mice expressed higher levels of HE4 and OLFM4, and a majority, 5 out of 7 mice, expressed higher levels of TFF2 compared to age-matched BALB/c control mice (Figure 4D). Together these data demonstrate that disease in TxA23 mice shares many of the molecular features of gastric cancer that have been reported in humans, including increased epithelial cell proliferation, increased levels of pSTAT3 protein, and higher levels of IL-6, HE4, OLFM4, and TFF2 mRNA.

SPEM is present in the gastric mucosa of TxA23 mice. Intestinal-type gastric cancer predominantly develops in the setting of oxyntic atrophy and mucous cell metaplasia [13]. Spasmolytic polypeptide-expressing metaplasia (SPEM), is a metaplasia in the gastric fundus resembling deep antral gland cells, and recent studies have indicated that SPEM may be directly linked to gastric neoplasia [25, [32]. We used immunohistochemistry to determine whether 4 month old TxA23 mice developed SPEM. A representative section from a TxA23 mouse is shown in figure 5A. In gastric units in which parietal cells have not yet been destroyed, chief cells are found at the base of the unit and are identified by staining with antibodies to gastric intrinsic factor (GIF). Of note, the antrum/pyloris of TxA23 mice were indistinguishable from BALB/c control mice. In the corpus region, neck cells are found above and identified by lectin GSII staining (Figure 5B). However, we also observed multiple gastric units in which the majority or all of the parietal cells had been lost (Figure 5B, C). In these parietal cell depleted

units, there was an expansion of GSII-positive cells (mucous neck cell hyperplasia) and an emergence of cells expressing both neck cell specific and chief cell specific markers (GIF) in the base of the units, whereas in regions with parietal cell preservation, the normal basal marker expression pattern was maintained (Figure 5D). Thus, GSII-positive GIF-positive cells in the base of gastric units that lack parietal cells also stained positive for TFF2 (data not shown), demonstrating¹³ that TxA23 mice developed regions of SPEM by 4 months of age.

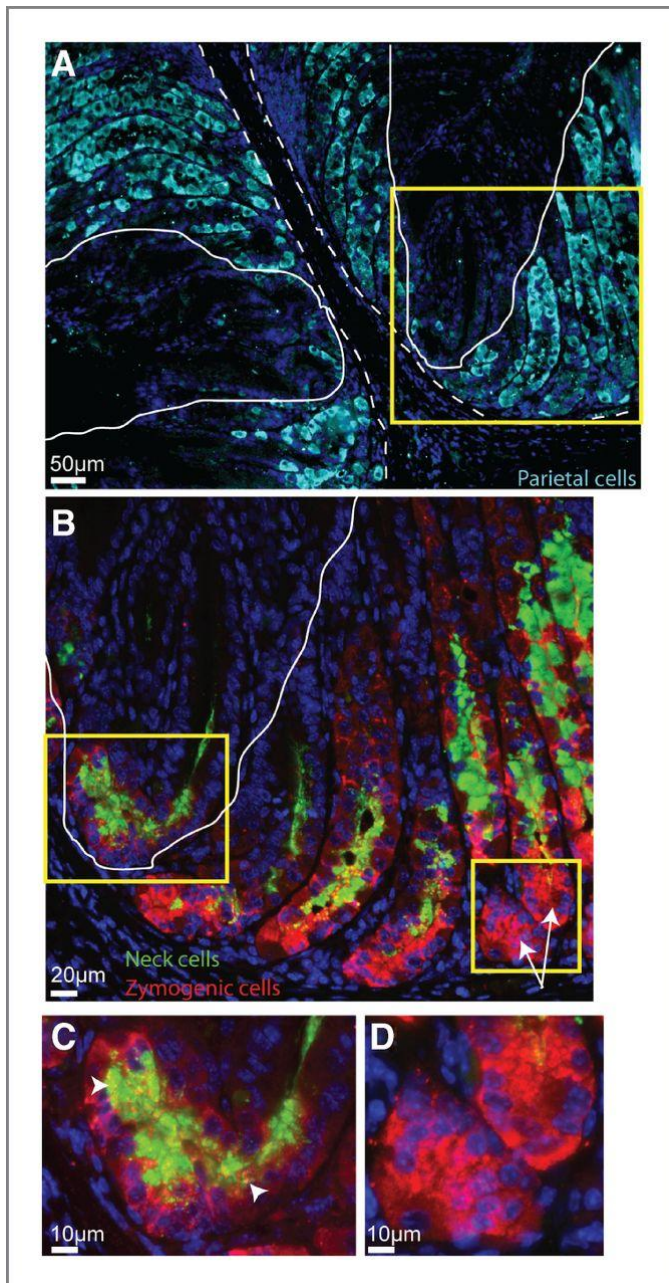


Fig. A.2.5. TxA23 mice have distinct regions of parietal cell loss coupled with the emergence SPEM. Representative immunostains of the corpus region of the stomach of TxA23 transgenic mice. A, the lamina propria is separated from the glandular mucosa by the white dotted lines wherein parietal cells are stained with VEGFB (teal) and nuclei with Hoechst (blue). Note the distinct regions of parietal cell loss as highlighted by solid white lines. B, the area highlighted by the yellow box in A was stained with GSII (green, neck cells), GIF (red, ZC), and Hoechst (blue, nuclei). The yellow box on the left indicates a region of SPEM where cells co-express GSII and GIF (white arrowheads).

This region of the stomach has shown considerable parietal cell destruction. Higher magnification of this region is shown in C. White arrows indicate areas of relatively normal gastric epithelial cell differentiation that correlate with regions where parietal cell numbers are normal. Further magnification of this region is shown in D.

TxA23 Mice Develop Gastric Intraepithelial Neoplasia (GIN). In the next set of experiments we allowed a cohort of TxA23 mice to age, and performed histopathological evaluations to determine whether disease in TxA23 mice progressed beyond SPEM to dysplasia. Sections from stomachs of 4 and 12 month old mice were examined by a pathologist using a murine gastric histopathology scoring paradigm described previously [20] (Figure 6A). The analysis of mice at 4 months of age revealed that 15 of 19 had dysplasia scores of 0, and 4 of 19 mice had dysplasia scores of 1, indicating focal irregularly shaped gastric glands, including elongated, slit, trident, and back to back forms (Figure 6B). By 12 months of age, disease progressed to the point at which 7 of 8 mice developed severe dysplasia, indicated by scores of 3.5. In this scoring system a score of 3 is used to indicate severe loss of gland organization and columnar orientation, marked cell atypia, visible mitoses, gastric intraepithelial neoplasia (GIN), and 0.5 is added for carcinoma in situ or invasion without frank malignancy. We observed both focal and wide spread dysplasia, and most cases involved pseudoinvasion into the submucosa and/or serosa (Figure 6C-E). We also observed the formation of irregular glandular forms on the adventitial surface of the stomach, some of which contained papillary projections of atypical epithelium (Figure 6F). These data demonstrates that precancerous lesions observed in 4 month old TxA23 mice ultimately progressed to neoplastic disease.

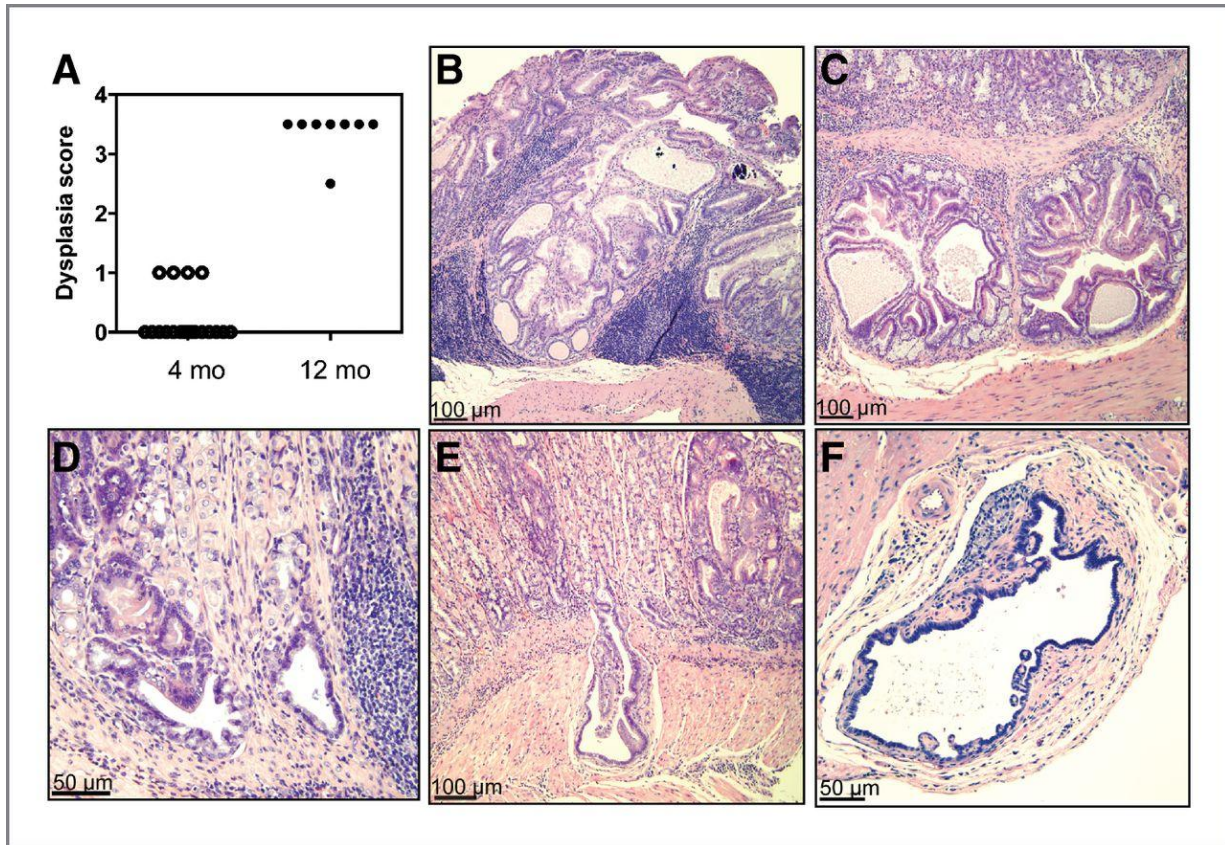


Fig. A.2.6. TxA23 mice develop masses with dysplastic foci as they age. A, dysplasia scores (where 1 = irregular glad forms, 3 = severe loss of glands and of columnar orientation of epithelium with regions of cellular atypia, increased mitotic figures, and 0.5 added when invasion of muscle or carcinoma in situ was identified) for sections at given ages. Each point represents an individual mouse. B, section of a mouse at 10 months of age (magnification, $\times 10$). Note to formation of mass with abundant, dense chronic inflammatory infiltrates. C–F, images of stomach sections that represent pathology observed in 12-month-old mice with various degrees of pseudoinvasion of irregular glands into the submucosa. C, section showing submucosal focus of irregular gland formations (magnification, $\times 10$). D, section showing focus of irregular glands in submucosal tissue with surrounding chronic inflammation (magnification, $\times 20$). E, section showing deep submucosal pseudoinvasion by an irregular gland (magnification, $\times 10$). F, irregular glandular form on the adventitial surface of the stomach (magnification, $\times 20$).

Discussion

Although chronic atrophic gastritis is believed to be important in initiating gastric carcinogenesis, the precise role(s) of inflammation in the complex changes in gastric epithelial cells during the progression of gastric cancer are not understood. Furthermore, the relationship between AIG/PA and gastric cancer has been controversial and requires further investigation. In this study we describe a new mouse model demonstrating that autoimmune gastritis induces precancerous lesions similar to those that precede gastric cancer in humans. Mice with chronic inflammation caused by H⁺/K⁺ ATPase-specific CD4⁺ T cells developed severe oxyntic atrophy coupled with metaplasia, including SPEM by 4 months of age. Similar to *H. pylori* infection and AIG in humans, inflammation in TxA23 mice contained CD4⁺ T cells of the Th1 (IFN- γ ⁺) and Th17 (IL-17⁺) phenotype [33, [34]. Consistent with the Correa pathway that describes the progression of gastric cancer in humans, TxA23 mice progressed through a series of stages that included inflammation, atrophic gastritis, mucous neck cell hyperplasia, SPEM, which over time progressed to dysplasia, and neoplasia. These data indicate that the TxA23 model system is unique in that it allows for the study of the development and regulation of gastric carcinogenesis in a setting where chronic inflammation, in the absence of infection, toxins, and drugs, is the primary upstream instigator. Our findings of carcinogenesis in our mouse model are consistent with reports that humans with AIG/PA are 3- to 6- times more likely to develop gastric adenocarcinoma and other cancers [35, [36]. It has been reported that a subset of individuals contain T cells and antibodies specific for H⁺/K⁺ ATPase after they are infected with *H. pylori* [37, [38, [39, [40]. It is possible that individuals that develop autoimmune responses during *H. pylori* infection may remain at risk for gastric cancer even if they are treated for *H. pylori* infection. Studies have shown that the eradication of *H. pylori* reduces risk for subsequent

gastric cancer by about 25% [40, [41, [42]. Strategies to reduce inflammation in addition to eradicating *H. pylori* may further reduce the risk of gastric cancer.

With the two recent studies reporting that individuals with Pernicious Anemia developed gastrointestinal cancers at a higher than expected rate, animal models that mimic AIG are likely to be useful for understanding the link between AIG and GI cancers. There is no doubt that infection with *H. pylori* is an important, prerequisite risk factor for gastric cancer; however, the vast majority of infected patients do not develop cancer. Therefore, it may be the types of chronic inflammation in the gastric mucosa that is triggered by *H. pylori* that are downstream adjuvants or causes of actual cancer. The TxA23 mouse model described here mimics the human disease and demonstrates the progression of AIG to the development of SPEM and eventually severe to dysplasia. Other genetically engineered mouse models have been useful for studying factors that influence the development of gastric cancer independently of *Helicobacter* infection. For example, mice expressing gastrin under the insulin promoter [43], mice deficient in: TFF1 [44], Smad4 [45], and Hip1r [46], and mice expressing a mutated form of the IL-6 family co-receptor gp130 [47] all develop forms of gastric metaplasia and some cases dysplasia. Our model specifically focuses on the immune response to H^+/K^+ ATPase and its role in promoting SPEM with progression to severe dysplasia. By inducing severe dysplasia in the absence of infection, this model will allow for a direct examination of the mechanisms whereby inflammation influences gastric epithelial cell biology. For example, when examining disease in cytokine knockout mice, using our model, we do not have to be concerned with the potential indirect effects of the importance of the cytokine in modulating *Helicobacter* infection itself. Our model will be also useful for evaluating the importance of immune cells, such as regulatory T cells and how they influence changes in gastric epithelial cells that are associated with the

progression of gastric cancer. Finally, future studies using this model will address how various host factors, especially immune-related genes, influence the risk of developing gastric cancer.

References

1. Jacobson, D.L., et al., *Epidemiology and estimated population burden of selected autoimmune diseases in the United States*. Clin Immunol Immunopathol, 1997. **84**(3): p. 223-43.
2. Carmel, R., *Prevalence of undiagnosed pernicious anemia in the elderly*. Arch Intern Med, 1996. **156**(10): p. 1097-100.
3. Riley, W.J., et al., *Predictive value of gastric parietal cell autoantibodies as a marker for gastric and hematologic abnormalities associated with insulin-dependent diabetes*. Diabetes, 1982. **31**(12): p. 1051-5.
4. De Block, C.E., I.H. De Leeuw, and L.F. Van Gaal, *High prevalence of manifestations of gastric autoimmunity in parietal cell antibody-positive type 1 (insulin-dependent) diabetic patients. The Belgian Diabetes Registry*. J Clin Endocrinol Metab, 1999. **84**(11): p. 4062-7.
5. Centanni, M., et al., *Atrophic body gastritis in patients with autoimmune thyroid disease: an underdiagnosed association*. Arch Intern Med, 1999. **159**(15): p. 1726-30.
6. Irvine, W.J., et al., *Thyroid and gastric autoimmunity in patients with diabetes mellitus*. Lancet, 1970. **2**(7665): p. 163-8.
7. Kokkola, A., et al., *The risk of gastric carcinoma and carcinoid tumours in patients with pernicious anaemia. A prospective follow-up study*. Scand J Gastroenterol, 1998. **33**(1): p. 88-92.
8. Armbrecht, U., et al., *Development of gastric dysplasia in pernicious anaemia: a clinical and endoscopic follow up study of 80 patients*. Gut, 1990. **31**(10): p. 1105-9.
9. Borch, K., H. Renvall, and G. Liedberg, *Gastric endocrine cell hyperplasia and carcinoid tumors in pernicious anemia*. Gastroenterology, 1985. **88**(3): p. 638-48.
10. Modlin, I.M., et al., *Current status of gastrointestinal carcinoids*. Gastroenterology, 2005. **128**(6): p. 1717-51.
11. Landgren, A.M., et al., *Autoimmune disease and subsequent risk of developing alimentary tract cancers among 4.5 million US male veterans*. Cancer, 2011. **117**(6): p. 1163-71.
12. Hemminki, K., et al., *Effect of autoimmune diseases on mortality and survival in subsequent digestive tract cancers*. Ann Oncol, 2012. **23**(8): p. 2179-84.
13. Correa, P., *A human model of gastric carcinogenesis*. Cancer Res, 1988. **48**(13): p. 3554-60.
14. Goldenring, J.R., et al., *Spasmolytic polypeptide-expressing metaplasia and intestinal metaplasia: time for reevaluation of metaplasias and the origins of gastric cancer*. Gastroenterology, 2010. **138**(7): p. 2207-10, 2210 e1.

15. Fox, J.G., et al., *Hypertrophic gastropathy in Helicobacter felis-infected wild-type C57BL/6 mice and p53 hemizygous transgenic mice*. Gastroenterology, 1996. **110**(1): p. 155-66.
16. Nozaki, K., et al., *A molecular signature of gastric metaplasia arising in response to acute parietal cell loss*. Gastroenterology, 2008. **134**(2): p. 511-22.
17. Huh, W.J., et al., *Tamoxifen induces rapid, reversible atrophy, and metaplasia in mouse stomach*. Gastroenterology, 2012. **142**(1): p. 21-24 e7.
18. McHugh, R.S., et al., *A T cell receptor transgenic model of severe, spontaneous organ-specific autoimmunity*. Eur J Immunol, 2001. **31**(7): p. 2094-103.
19. Callaghan, J.M., et al., *Alpha and beta subunits of the gastric H⁺/K⁺-ATPase are concordantly targeted by parietal cell autoantibodies associated with autoimmune gastritis*. Autoimmunity, 1993. **16**(4): p. 289-95.
20. Rogers, A.B., et al., *Helicobacter pylori but not high salt induces gastric intraepithelial neoplasia in B6129 mice*. Cancer Res, 2005. **65**(23): p. 10709-15.
21. Ramsey, V.G., et al., *The maturation of mucus-secreting gastric epithelial progenitors into digestive-enzyme secreting zymogenic cells requires Mist1*. Development, 2007. **134**(1): p. 211-22.
22. Alderuccio, F., et al., *A novel method for isolating mononuclear cells from the stomachs of mice with experimental autoimmune gastritis*. Autoimmunity, 1995. **21**(3): p. 215-21.
23. DiPaolo, R.J., et al., *CD4⁺CD25⁺ T cells prevent the development of organ-specific autoimmune disease by inhibiting the differentiation of autoreactive effector T cells*. J Immunol, 2005. **175**(11): p. 7135-42.
24. Shi, Y., et al., *Helicobacter pylori-induced Th17 responses modulate Th1 cell responses, benefit bacterial growth, and contribute to pathology in mice*. J Immunol. **184**(9): p. 5121-9.
25. Lopez-Diaz, L., et al., *Parietal cell hyperstimulation and autoimmune gastritis in cholera toxin transgenic mice*. Am J Physiol Gastrointest Liver Physiol, 2006. **290**(5): p. G970-9.
26. Gong, W., et al., *Expression of activated signal transducer and activator of transcription 3 predicts expression of vascular endothelial growth factor in and angiogenic phenotype of human gastric cancer*. Clin Cancer Res, 2005. **11**(4): p. 1386-93.
27. Xiong, H., et al., *Constitutive activation of STAT3 is predictive of poor prognosis in human gastric cancer*. J Mol Med (Berl), 2012. **90**(9): p. 1037-46.
28. Silver, J.S. and C.A. Hunter, *gp130 at the nexus of inflammation, autoimmunity, and cancer*. J Leukoc Biol. **88**(6): p. 1145-56.
29. Jackson, C.B., et al., *Augmented gp130-mediated cytokine signalling accompanies human gastric cancer progression*. J Pathol, 2007. **213**(2): p. 140-51.
30. Giraud, A.S., et al., *Differentiation of the Gastric Mucosa IV. Role of trefoil peptides and IL-6 cytokine family signaling in gastric homeostasis*. Am J Physiol Gastrointest Liver Physiol, 2007. **292**(1): p. G1-5.
31. Oue, N., et al., *Serum olfactomedin 4 (GW112, hGC-1) in combination with Reg IV is a highly sensitive biomarker for gastric cancer patients*. Int J Cancer, 2009. **125**(10): p. 2383-92.
32. Lennerz, J.K., et al., *The transcription factor MIST1 is a novel human gastric chief cell marker whose expression is lost in metaplasia, dysplasia, and carcinoma*. Am J Pathol, 2010. **177**(3): p. 1514-33.

33. Mohammadi, M., et al., *Helicobacter-specific cell-mediated immune responses display a predominant Th1 phenotype and promote a delayed-type hypersensitivity response in the stomachs of mice*. J Immunol, 1996. **156**(12): p. 4729-38.
34. Smythies, L.E., et al., *Helicobacter pylori-induced mucosal inflammation is Th1 mediated and exacerbated in IL-4, but not IFN-gamma, gene-deficient mice*. J Immunol, 2000. **165**(2): p. 1022-9.
35. Hsing, A.W., et al., *Pernicious anemia and subsequent cancer. A population-based cohort study*. Cancer, 1993. **71**(3): p. 745-50.
36. Brinton, L.A., et al., *Cancer risk following pernicious anaemia*. Br J Cancer, 1989. **59**(5): p. 810-3.
37. Ito, M., et al., *Role of anti-parietal cell antibody in Helicobacter pylori-associated atrophic gastritis: evaluation in a country of high prevalence of atrophic gastritis*. Scand J Gastroenterol, 2002. **37**(3): p. 287-93.
38. Claeys, D., et al., *The gastric H⁺,K⁺-ATPase is a major autoantigen in chronic Helicobacter pylori gastritis with body mucosa atrophy*. Gastroenterology, 1998. **115**(2): p. 340-7.
39. Amedei, A., et al., *Molecular mimicry between Helicobacter pylori antigens and H⁺, K⁺--adenosine triphosphatase in human gastric autoimmunity*. J Exp Med, 2003. **198**(8): p. 1147-56.
40. D'Elis, M.M., et al., *Molecular specificity and functional properties of autoreactive T-cell response in human gastric autoimmunity*. Int Rev Immunol, 2005. **24**(1-2): p. 111-22.
41. de Vries, A.C., E.J. Kuipers, and E.A. Rauws, *Helicobacter pylori eradication and gastric cancer: when is the horse out of the barn?* Am J Gastroenterol, 2009. **104**(6): p. 1342-5.
42. Wong, B.C., et al., *Helicobacter pylori eradication to prevent gastric cancer in a high-risk region of China: a randomized controlled trial*. JAMA, 2004. **291**(2): p. 187-94.
43. Wang, T.C., et al., *Synergistic interaction between hypergastrinemia and Helicobacter infection in a mouse model of gastric cancer*. Gastroenterology, 2000. **118**(1): p. 36-47.
44. Lefebvre, O., et al., *Gastric mucosa abnormalities and tumorigenesis in mice lacking the pS2 trefoil protein*. Science, 1996. **274**(5285): p. 259-62.
45. Xu, X., et al., *Haploid loss of the tumor suppressor Smad4/Dpc4 initiates gastric polyposis and cancer in mice*. Oncogene, 2000. **19**(15): p. 1868-74.
46. Jain, R.N., et al., *Hip1r is expressed in gastric parietal cells and is required for tubulovesicle formation and cell survival in mice*. J Clin Invest, 2008. **118**(7): p. 2459-70.
47. Judd, L.M., et al., *Gastric cancer development in mice lacking the SHP2 binding site on the IL-6 family co-receptor gp130*. Gastroenterology, 2004. **126**(1): p. 196-207.

Curriculum Vitae – Shradha S. Khurana

Graduate Research Assistant, Washington University School of Medicine

Department of Medicine – Division of Gastroenterology
Washington University School of Medicine
660 S. Euclid Ave., Campus Box 8124, St. Louis MO 63110

EDUCATION

- 2013 Ph.D. Candidate; Developmental, Regenerative and Stem Cell Biology
Washington University School of Medicine, St. Louis, MO
- 2006 M.S. Biotechnology
Indian Institute of Technology (IIT) Roorkee, India
- 2004 B.S. Zoology
Fergusson College, University of Pune, India
-

EMPLOYMENT

- 2008 – 2013 Doctoral Student, Department of Medicine – Division of Gastroenterology
Washington University School of Medicine, St. Louis, MO
- 2009 Teaching Assistant, Fundamentals of Biology
Washington University in St. Louis
- 2006 – 2007 Research Fellow, Immunology Lab., National Center for Cell Science, India
- 2006 Research Assistant, Protein Biochemistry Lab.,
Indian Institute of Technology (IIT) Roorkee, India
- 2005 Summer Intern, Diabetes Lab., National Center for Cell Science, India
-

HONORS AND AWARDS

- 2013 Oral Presentation and Travel Award, FASEB Summer Research Conferences
Gastrointestinal Tract XV: Epithelia, Microbes, Inflammation and Cancer
Steamboat Springs, CO
- 2013 Viktor Hamburger Award for Best Student Oral Presentation
Washington University School of Medicine, St. Louis, MO
- 2012 Oral Presentation and Travel Award, AGA
Freston Single Topic Conference: Gastrointestinal Stem Cell Biology and
Pathobiology. Chicago, IL
- 2012 Outstanding Predoctoral Poster Presentation Award, APS
Experimental Biology Conference. San Diego, CA

2010 – 2012 Siteman Cancer Center – Cancer Biology Pathway Award
2011 Rita Levi-Montalcini Award for Best Student Poster Presentation
Washington University School of Medicine, St. Louis, MO
2006 Junior Research Fellowship, Council of Scientific and Industrial Research
Government of India
2004 National Scholarships Scheme, First Rank in the University of Pune, India

INVITED PRESENTATIONS

August 2013 Oral Presentation, FASEB Summer Research Conferences
Gastrointestinal Tract XV: Epithelia, Microbes, Inflammation and Cancer
Steamboat Springs, CO
May 2013 Oral Presentation, Developmental Biology Retreat
Washington University School of Medicine, St. Louis, MO
August 2012 Oral Presentation, Freston Single Topic Conference: Gastrointestinal Stem
Cell Biology and Pathobiology. Chicago, IL
February 2012 Oral Presentation, Developmental Biology Research Forum
Washington University School of Medicine, St. Louis, MO

PEER REVIEWED PUBLICATIONS

1. **Shradha S. Khurana**, Terrence E. Riehl, Benjamin D. Moore, Matteo Fassan, Massimo Rugge, Judith Romero-Gallo, Jennifer Noto, Richard M. Peek, Jr, William F. Stenson and Jason C. Mills. CD44 signaling is required for proliferation of gastric corpus progenitors during homeostasis and metaplasia. *J Biol Chem.* 2013 May 31;288(22):16085-97.
2. Huh WJ*, **Khurana SS***, Geahlen JH, Kohli K, Waller RA, Mills JC. Tamoxifen induces rapid, reversible atrophy, and metaplasia in mouse stomach. *Gastroenterology* 2012 Jan;142(1):21-24. (*denotes equal contribution).
3. **Khurana S**, Mills JC. The gastric mucosa development and differentiation. *Prog Mol Biol Transl Sci.* 2010;96:93-115.
4. Thanh-Long M. Nguyen, **Shradha S. Khurana**, Clifford J. Bellone, Benjamin J. Capoccia, John E. Sagartz, Russell A. Kesman Jr., Jason C. Mills, and Richard J. DiPaolo. Autoimmune gastritis mediated by CD4+ T-cells promotes the development of gastric cancer. *Cancer Res.* 2013 Mar 27.
5. Jennifer M. Noto; Tinatin Khizanishvili; M. Blanca Piazuolo; Rupesh Chaturvedi; Judith Romero-Gallo; Alberto G. Delgado; **Shradha S. Khurana**; Johanna C. Sierra; Uma S. Krishna; Giovanni Suarez; Anne E. Powell; James R. Goldenring; Robert J. Coffey; Vincent W. Yang; Pelayo Correa; Jason C. Mills; Keith T. Wilson; Richard

M. Peek. *Helicobacter pylori* promotes the expression of Krüppel-like factor 5, a mediator of carcinogenesis, in vitro and in vivo. *PLoS One*. 2013;8(1):e54344.

6. Jessica Geahlen, Carlo Lapid, Kaisa Thorell, Igor Nikolskiy, Won Huh, Edward Oates, Jochen Lennerz, Xiaolin Tian, Victoria Weis, **Shradha Khurana**, Samuel Lundin, Alan Templeton, and Jason Mills. Evolution of the Human Gastroke Locus and Confounding Factors Regarding the Pseudogenicity of Gkn3. *Physiol Genomics*. 2013 Aug 1;45(15):667-83.
7. Chang Mo Moon, Seok-Hyung Kim, Sang Kil Lee, Jiyeon Hyeon, Ja Seung Koo, Sangheun Lee, Jean S. Wang, Won Jae Huh, **Shradha S. Khurana**, and Jason C. Mills. Chronic tamoxifen use is associated with a decreased risk of intestinal metaplasia in human gastric epithelium (*Dig. Dis. Sci.*, Under Revision).

PUBLISHED ABSTRACTS

Khurana, Shradha, et al. "The presumptive gastric corpus stem cell population is CD44-positive and expands during metaplasia via increased ERK-MAPK signaling." *FASEB JOURNAL*. Vol. 26. 9650 ROCKVILLE PIKE, BETHESDA, MD 20814-3998 USA: FEDERATION AMER SOC EXP BIOL, 2012.

Nguyen, Thanh-Long M., et al. "874 EB13 (IL-27/IL-35) Regulates the Progression From Atrophic Gastritis to Gastric Cancer." *Gastroenterology* 144.5 (2013): S-153.
